



University
of Glasgow

<https://theses.gla.ac.uk/>

Theses Digitisation:

<https://www.gla.ac.uk/myglasgow/research/enlighten/theses/digitisation/>

This is a digitised version of the original print thesis.

Copyright and moral rights for this work are retained by the author

A copy can be downloaded for personal non-commercial research or study,
without prior permission or charge

This work cannot be reproduced or quoted extensively from without first
obtaining permission in writing from the author

The content must not be changed in any way or sold commercially in any
format or medium without the formal permission of the author

When referring to this work, full bibliographic details including the author,
title, awarding institution and date of the thesis must be given

Enlighten: Theses

<https://theses.gla.ac.uk/>
research-enlighten@glasgow.ac.uk

Construction of Fully Equivalent Neuronal Cables: An Analysis of Neuron Morphology

by

James M. Ogden

A thesis submitted to
the Faculty of Science
at the University of Glasgow
for the degree of
Doctor of Philosophy

©James Ogden, January 1999.

ProQuest Number: 10391440

All rights reserved

INFORMATION TO ALL USERS

The quality of this reproduction is dependent upon the quality of the copy submitted.

In the unlikely event that the author did not send a complete manuscript and there are missing pages, these will be noted. Also, if material had to be removed, a note will indicate the deletion.



ProQuest 10391440

Published by ProQuest LLC (2017). Copyright of the Dissertation is held by the Author.

All rights reserved.

This work is protected against unauthorized copying under Title 17, United States Code
Microform Edition © ProQuest LLC.

ProQuest LLC.
789 East Eisenhower Parkway
P.O. Box 1346
Ann Arbor, MI 48106 – 1346



11621 (copy 2)

Summary

Neuronal dendritic trees exhibit a huge variety of morphologies, and their information processing capabilities are, for the most part, poorly understood. The fundamental difficulty stems from the fact that dendrites can be bewilderingly complicated and appear to operate at a global level; an event in one location potentially influences the entire tree. At first sight, it would seem that the entire tree must be analysed as a single entity unless conceptual simplifications can be introduced.

This thesis presents procedures for reducing passive neuronal dendritic tree models to fully equivalent unbranched non-uniform cables. A fully equivalent cable is equivalent in a mathematical sense to the original tree model and capable of reproducing the same physiological behaviour. An understanding of the construction procedures, as well as the results they produce, gives new, and general, insight into the local and global signal processing capabilities conferred on passive dendritic trees by their geometry.

Chapter One (*Neurophysiological Background and Dendritic Function*) outlines the basic neurophysiology of relevance to this thesis. The major neuronal components, i.e. dendritic trees, soma, axon, neuronal membrane, and synaptic connections, are introduced. The electrochemical basis of membrane excitability, manifest as a changing transmembrane electrical potential, is described. We consider how ion channels allow specific ion species (K^+ , Na^+ , Ca^{2+} , Cl^-) to pass across the membrane, and how equilibrium is sought as transmembrane electrostatic forces balance with transmembrane chemical gradients to establish a resting transmembrane potential. Equivalent cable construction is particularly concerned with dendritic trees and so their signal processing role is considered, from the generally accepted signal integration mechanisms that follow almost inevitably for such branching excitable structures, to some theoretical and speculative possibilities that have not so far been verifiable due to the lack of appropriate experimental techniques, but could possibly have a significant role in certain aspects of real neuron operation.

Chapter Two (*Cable Theory and the Multiple Segment Dendritic Tree Model*) details a generalisation of the one dimensional cable theory commonly used to describe electrical activity in neuronal structures. The derivation follows from fundamental principles such as charge conservation and from the nature of membrane constitutive properties. Other

than the one-dimensional and ohmic electrical properties of the dendritic cytoplasm, few assumptions are made about electrical and geometrical properties. The resulting cable equation is valid for segments of dendrite with non-uniform cross-sectional profiles and can incorporate arbitrary types and densities of ion channels and synaptic inputs. Following this, the assumptions which must be made to yield the passive linear cable equation — which is the basis of equivalent cable construction — are explained. By assuming the existence of a steady resting transmembrane potential, the transmembrane currents can be quite naturally expressed as a sum of linear and non-linear contributions. The linear cable equation is obtained by assuming the non-linear component is zero. The standard dimensionless (electrotonic) form of this equation is then formulated, along with joining and terminal boundary conditions for the multiple segment dendritic tree model. The multi-cylinder specialisations of the general equations are also given since these will be used in later chapters to derive the methods of equivalent cable construction. For the passive tree model to be valid for equivalent cable construction, the membrane time constant must be a constant over the entire tree, and only cut (zero potential) and current injection (specified potential gradient) boundary conditions may be applied at terminals.

Chapter Three (*Equivalent Cables*) outlines the equivalent cable concept as it has developed over the years. An equivalent cable is basically an unbranched dendrite model which is, in some sense, “equivalent” to a dendritic tree model. We start with a detailed examination of the first major result concerning equivalence, i.e. Rall’s equivalent cylinder, then proceed with an outline of the empirically derived and geometrically and/or electrically restrictive cables that have been inspired by Rall’s model. We then move to a thorough description of the new fully equivalent cables that are the concern of the rest of this thesis, describing important structural properties such as the existence of disconnected cable sections, and conserved quantities, such as electrotonic length and steady-state input conductance. Of major importance is the definition of equivalence. Unlike previous models, fully equivalent cables satisfy a rigorous mathematical definition of equivalence which demands the existence of a bijective electrical mapping that specifies a unique relationship between configurations of electrical activity on the tree model and those on its equivalent cable. Whereas previous models have been developed mainly as an aid for neuron electrical parameter estimation, the new fully equivalent cable model must be regarded as a fundamentally different, and more powerful mathematical object. They have implications for the understanding of local and global signal processing functions that arise as a consequence of dendritic geometry, and introduce several new ideas such as passive coincidence detection and characteristic distributions of tree activity. Much emphasis is placed on the transformation of basic singly branched structure. Any tree may be transformed to an equivalent cable by successive reduction of such Y-junctions.

Chapter Four (*Matrix Methods for Constructing Fully Equivalent Cables*) describes a matrix formalism for transforming passive dendritic tree models into their fully equivalent cables. The matrix methods employ a finite difference scheme to build a nearly tri-diagonal matrix representation of a dendritic tree. This matrix is then tri-diagonalised, and the resulting matrix represents the fully equivalent cable. Two methods, requiring specific implementations of Lanczos tri-diagonalisation and Householder tri-diagonalisation, have been found suitable. We show how the original tree matrix structure guarantees that essential equivalent cable matrix structure is preserved. Computer algorithms are given for both methods, and aspects such as efficiency and storage are discussed. Algebraic examples of each method are given. By employing numerical procedures, these methods obscure details of the underlying construction mechanism, and we conclude that the theoretical foundation of fully equivalent cable construction must follow from a more fundamental analysis of the passive linear cable equation. This theoretical foundation is developed in Chapters Five, Six and Seven.

The full set of analytical construction rules exhibit a high level of algebraic complexity. In order to present the basic cable construction ideas, and avoid too much technical detail, we start in Chapter Five (*Foundations of Equivalent Cable Construction*) by introducing all the required concepts via specific and reasonably simple examples. General solutions of the Laplace transformed passive cable equation are employed as part of a loosely defined first-principles algorithm for cable construction. This first-principles approach indicates that cable construction is actually an iterative two-stage procedure. Firstly, electrical continuity, i.e. voltage continuity and current conservation, must be guaranteed between the cylinders that form a fully equivalent cable. We state several of the “electrical continuity” rules that are developed in full in Chapter Six. However, it turns out that these rules do not uniquely determine equivalent cable structure, i.e. cylinder diameters are not fixed. The necessary constraints for determining the final, and unique, cable structure, and simultaneously ensuring eventual termination, are imposed by an “isolation condition”, which we also state. This condition ensures that a dendritic sub-tree may be transformed without concerning oneself with the structure to which it is connected. Although the electrical continuity rules are obtained in the Laplace domain, properties of the construction rules are such that these rules are equally valid in the physical (electrotonic) domain.

Chapter Six (*The General Analytical Construction Rules*) contains the technical derivation of the analytical construction rules for a singly branched tree. Firstly, the general electrical continuity rules are obtained using the first-principles approach given in Chapter Five. These rules are applied to an expression for the potential in one cylinder in order to generate an expression for the potential in the next cylinder. Only a “framework” potential is generated however, since cable cylinder diameters are not determined

at this stage. The necessary constraints for determining the final cable structure, and simultaneously ensuring eventual termination, are imposed by a set of self-reinforcing isolation-termination rules, of which the “isolation condition” is the simplest and most fundamental. Ensuring that dendritic sub-structure may be transformed in isolation from the rest of the tree corresponds to ensuring that the isolation condition is always satisfied. Prior to construction, equivalent cable section lengths and boundary conditions may be predicted using results from this chapter. There are indications in the analytical method of a deeper mathematical structure that has yet to be fully determined.

Chapter Seven (*An Analysis of Cable Structure Using Branch Shifting*) takes a more in depth look at simple Y-junctions — singly branched structure where each branch is formed from a single uniform dendritic segment. Their fully equivalent cables may be constructed rapidly using a method that follows straightforwardly from the simplest analytical construction rules. This method, referred to as branch-shifting, involves producing an equivalent cable by passing through a set of equivalent Y-junctions, the final member of which transforms to the fully equivalent cable. The analytical expressions given by this method for a fully equivalent cable’s geometry and electrical mapping give very useful insights into overall trends in cable structure. These insights are also valid for more general Y-junctions, and may be simply stated as “sealed terminals promote narrow cable diameters, strong voltage mappings and weak current mapping”, and “cut terminals promote large cable diameters, weak voltage mappings, and strong current mappings”.

Chapter Eight (*Discussion, Conclusions, and Future Work*) provides an overview of the nature of fully equivalent cables and their implications. We briefly review the construction methods, and discuss, in physiological terms, and with illustrated examples, revelations from previous chapters concerning fully equivalent cable structure. To link the construction techniques with reality, cables created using data for several real motoneuron dendrites are also illustrated. Mathematical equivalence of fully equivalent cables permits an exhaustive, and novel, analysis of the properties of passive dendritic geometry that goes beyond the capabilities of previous “quasi-equivalent” cable models, or numerical simulation. It is significant that this method reveals signal integration properties that arise solely as a consequence of dendritic geometry. We discuss the relationship between dendritic geometry and dendritic function in this new light. Limitations of the passive model are balanced with the insight gained, and we consider the implications for more generally realistic active models. Possible applications and future extensions of this work are discussed.

Acknowledgments

Firstly, I would like to thank my supervisors, Jay Rosenberg in the Division of Neuroscience and Biomedical Systems, Ken Lindsay in the Department of Mathematics, and Rex Whitehead in the Department of Physics and Astronomy. I am very grateful to Rex for giving me the opportunity to work in the field of "theoretical neurophysics". I was introduced to Rex by Jim Hough, also from the Physics department, and I would like to thank him too. The perfect combination of Jay's encouragement and Neurophysiological knowledge, and Ken's mathematical insight and technical know-how, has ensured that working for this thesis has been an enjoyable experience.

I am grateful for the generous support of The Wellcome Trust during my four year Mathematical Biology Research Training Studentship (041314/Z/94/Z).

I would like to thank Doug Junge and Janice Goldhaber, who were generous hosts and good friends during my visit to Los Angeles and UCLA in June 1997. Many thanks also go to Bob Burke at the NINDS, National Institutes of Health in Bethesda, Maryland, for the supply of motoneurone morphological data, and his generous hospitality during my visit to his lab, also in the summer of 1997.

Finally, I would like to thank my family and dedicate this thesis to them.

Contents

1. Neurophysiological Background and Dendritic Function	16
1.1. Introduction	16
1.2. Neuron Structure and Connections	18
1.3. The Nature of Electrical Excitability in Neurons	22
1.4. The Signal Processing Role of Dendritic Geometry	28
2. Cable Theory and the Multiple Segment Dendritic Tree Model	32
2.1. Introduction	32
2.2. General Model of a Dendritic Segment	33
2.2.1. Fundamental Model Assumptions	33
2.2.2. Derivation of the General Cable Equation	37
2.2.3. Specification of the Membrane Currents	39
2.2.4. Constraints on Geometry	42
2.2.5. Constraints on Constitutive Membrane Properties	43
2.3. The Passive Linear Cable Equation	45
2.4. The Dimensionless Linear Cable Equation	46
2.4.1. Electrotropic Units	46
2.5. The Multiple Segment Model of a Dendritic Tree	51
2.5.1. Introduction	51
2.5.2. Modelling Using Real Data	52
2.5.3. Obtaining Solutions for a System of Cable Equations	53
2.5.4. Tree Structure Terminology	54
2.5.5. Initial and Boundary Conditions	55
2.5.6. The Passive Multi-Segment Tree Model	58
2.5.7. The Passive Multi-Cylinder Tree Model	60
2.5.8. Typical Electrical Parameters in a 'Tree'	60
2.5.9. The Tree Model Surface Area	60
2.6. Electrical Activity in Simple Passive Structures	61

2.6.1	Passive Signal Propagation	61
2.6.2	Impedance Matching	61
2.6.3	Steady State Solutions of the Cable Equation	62
2.6.4	Steady-State Input Conductance	63
2.6.5	Uniform Voltage Decay	63
2.7	Requirements for Equivalent Cable Construction	64
3	Equivalent Cables	65
3.1	Introduction	65
3.2	The Various Cable Models	66
3.3	Rall's Equivalent Cylinder	67
3.3.1	Proof	69
3.3.2	Mapping Electrical Activity Between Tree and Cylinder	71
3.3.3	A Hint of Full Equivalence	73
3.3.4	Application of Rall's Equivalent Cylinder	76
3.4	Continuous Tapering Models	77
3.5	Empirical Cable Models	78
3.6	Fully Equivalent Cables	80
3.6.1	A Definition of Equivalence	80
3.6.2	The Cable Origin	81
3.6.3	Introduction to Fully Equivalent cables	81
3.6.4	Equivalent Cables for Basic Branching Structure	84
3.6.5	Complicated Branching Structure	90
3.6.6	Equivalent Cable Structure is Robust	92
3.6.7	Trees With Identical Connected Sections	93
3.6.8	Methods of Construction	95
3.6.9	Construction and Pre-programming of Artificial Dendritic Trees . .	95
3.7	Discussion	96
4	Matrix Methods for Constructing Fully Equivalent Cables	98
4.1	Introduction	98
4.2	The Matrix Representation of a Dendritic Tree	99
4.2.1	Discretisation Nodes and Terminology	100
4.2.2	Discrete Cable Equations	103
4.2.3	The Matrix Representation of a Dendritic Tree	111
4.3	Transforming a Tree Matrix to a Cable Matrix Equivalent Cable Construction	119

4.3.1	Introduction and Outline Theory	119
4.3.2	Some Properties of Tree and Cable Matrices	121
4.3.3	The Symmetric Tree Matrix	126
4.3.4	Lanczos Tri-diagonalisation	128
4.3.5	Householder Tri-diagonalisation	137
4.3.6	Extracting the Equivalent Cable	143
4.3.7	Further Computational Considerations	147
4.4	Algebraic Examples of the Matrix Methods	148
4.4.1	The Lanczos Method	148
4.4.2	The Householder Method	152
4.5	Observations and Discussion of Matrix Methods	155
5	Foundations of Equivalent Cable Construction	157
5.1	Introduction	157
5.2	The Multi-cylinder Tree Model in the Laplace Domain	159
5.2.1	The Laplace Transform	159
5.2.2	The Cable Equation	160
5.2.3	Boundary Conditions	160
5.2.4	Solutions of the Laplace Transformed Cable Equation	161
5.3	The Strategy for Equivalent Cable Construction	162
5.4	Examples of Cable Construction from First Principles	164
5.4.1	Example One	164
5.4.2	Example Two	170
5.5	An Introduction to the Construction Rules	175
5.5.1	Potential Function Components and Component Diagrams	175
5.5.2	The Electrical Continuity Rules	175
5.6	Example One Using the Analytical Construction Rules	178
5.7	Discussion	180
6	The General Analytical Construction Rules	181
6.1	Introduction	181
6.2	Notation and Terminology for the General Y-junction	182
6.2.1	Electrical and Physical Properties of Tree and Cable Cylinders	182
6.2.2	Framework Potentials and Uniquely Defined Potentials	185
6.2.3	Potential Function Components and Component Diagrams	185
6.3	The Electrical Continuity Rules	186
6.3.1	Derivation of General Reflection–Transmission Rules	186
6.3.2	General Observations Concerning the Electrical Continuity Rules	192

6.3.3	Reflection and Transmission at Specific Geometrical Structure	196
6.3.4	Electrical Continuity Rules in the General Y-junction	199
6.4	The Isolation-Termination Rules	200
6.4.1	Cable Cylinders “1” to “3”	202
6.4.2	The Piecewise Generalisation of Rall’s Equivalent Cylinder	208
6.4.3	Cable Cylinder k — Prior to Left and Right Branch Termination	211
6.4.4	Cable cylinder k — Approaching the Left Branch Termination: $k = m_L$ and $k = m_L + 1$	226
6.4.5	Cable cylinder k — Including the Left Branch Termination	228
6.4.6	Cable Cylinder k — Beyond Both Left and Right Terminals	234
6.4.7	Full Isolation-Termination Rules Summary ($m_L, m_R \geq 2$)	236
6.4.8	Termination and Disconnected Sections	241
6.5	A Matrix Formalism for Analytical Results	253
6.6	Future Analytical Work	254
7	An Analysis of Cable Structure Using Branch-shifting	256
7.1	Introduction	256
7.2	The Symmetric Y-junction	258
7.2.1	Rall Symmetric Y-junction	258
7.2.2	Non-Rall Symmetric Y-junction	259
7.3	Short Cylinder has a Cut Terminal	259
7.4	Short Cylinder has a Sealed Terminal	262
7.4.1	Long Branch is at Least Twice as Long as Short Branch ($n > m$)	263
7.4.2	Long Cylinder Has a Sealed End and is Less Than Twice the Length of the Short Cylinder ($n \leq m$).	265
7.4.3	Long Cylinder Has a Cut End and is Less Than Twice the Length of the Short Cylinder ($n \leq m$).	268
7.5	Discussion	273
8	Discussion, Conclusions, and Future Work	274
8.1	Introduction	274
8.2	Fully Equivalent Cable Construction	275
8.3	Fully Equivalent Cable Structure and Tree Function	277
8.3.1	The Influence of Boundary Conditions	278
8.3.2	Signal Loss and Signal Reflection	279

8.3.3	Implications of "Fuzzy" Tree Data	284
8.3.4	Complicated Dendritic Geometry	284
8.3.5	Consequences for Parameter Estimation	285
8.3.6	Local and Global Processing	287
8.3.7	Tree Classification	288
8.4	Concluding Remarks and Future Perspectives	288

List of Figures

1.1	Idealistic representation of a neuron.	18
1.2	Examples of real neurons.	21
1.3	Equilibrium state for membrane permeable to a single ion species.	24
1.4	Equilibrium state for sodium and potassium ions in solution either side of a membrane permeable only to these two ion species.	25
1.5	Shape and strength of neuronal electrical signals.	27
2.1	A non-uniform segment of dendrite.	34
2.2	Uniform segment of core medium.	36
2.3	Special cases of dendritic structure described by simplified cable equations.	42
2.4	Electrical compactness of a semi infinite nerve cylinder.	48
2.5	Dendritic tree model terminology.	55
2.6	Steady state response in two connected semi-infinite cylinders.	63
3.1	Singly branched binary Rall tree and its equivalent cylinder.	68
3.2	Successive reduction of Rall Y-junctions at the tips of more complicated Rall trees, to transform a complicated Rall tree to its equivalent cylinder. .	71
3.3	The electrical mapping from Rall cylinder to tree is not unique.	72
3.4	The mapping between a Rall Y-junction and its fully equivalent cable is unique.	73
3.5	The Y-junction by Y-junction reduction of a Rall tree into its fully equivalent cable.	75
3.6	Electrotomographic dendrogram representation of a dendritic tree and its corresponding lambda cable.	78
3.7	Any point over a tree may be chosen as the origin, provided the appropriate conditions for transformation to an equivalent cable are satisfied with respect to this point.	81
3.8	A selection of simple trees and their equivalent cables.	83
3.9	The general Y-junction and its equivalent cable.	85

3.10	Mapping electrical activity between a dendritic tree and its fully equivalent cable.	87
3.11	Passive coincidence detection in dendritic trees.	88
3.12	The Y-junction by Y-junction reduction of a dendritic tree to its fully equivalent cable.	90
3.13	Equivalent cable structure is robust. 1 — deviations from completely symmetric sealed Rall Y-junction.	92
3.14	Equivalent cable structure is robust. 2 — deviations from cut Rall Y-junction.	94
3.15	Identical fully equivalent cable connected sections implies electrical equivalence, with respect to the soma, of different trees.	94
4.1	Discretisation of a dendritic tree.	102
4.2	Some simple structures illustrating node connectivity in discrete cable equations.	108
4.3	Problems encountered with discrete cable equations if describing short cable structure when $z = 1$.	111
4.4	Branched trees, unbranched cables and their tree matrix representation.	115
4.5	Simple examples of discretised dendritic trees.	116
4.6	Schematic of a general Y-junction.	118
4.7	Schematic of the Householder tri-diagonalisation procedure applied to the tree matrix for a general Y-junction.	139
4.8	The equivalent cable for the Lanczos example in section 4.4.	151
5.1	Fully equivalent cable construction from first principles for a general Y-junction.	163
5.2	A simple Y-junction and its equivalent cable, determined from first principles.	169
5.3	The Y-junction and its fully equivalent cable for first-principles example two.	173
5.4	Component diagrams for the cable potential functions generated for a simple Y-junction with both terminals sealed.	176
6.1	The general Y-junction.	183
6.2	Component diagrams illustrating the electrical continuity rules at the general branch point, where $n + 1$ cylinders meet.	191
6.3	Reflection and Transmission at (a) binary branch point and (b) diameter step.	195
6.4	Component diagram illustrating reflection of origin bound components in a Y-junction, provided the isolation condition holds.	197

6.5	Component diagrams for component structure relevant to the general Y-junction.	201
6.6	Component diagrams for the first three equivalent cable cylinders (1-3) for the general Y-junction.	203
6.7	Examples of non-uniform generalised Rall trees.	210
6.8	Component diagrams for the k^{th} and $(k + 1)^{th}$ cable cylinder potential functions, prior to termination of either left or right branch.	214
6.9	Interaction between voltage rule coefficients.	223
6.10	Rule reinforcement in potential functions.	225
6.11	Component diagrams for the cable cylinder potential function $k = m_L$ and $k = m_L + 1$	227
6.12	Component diagrams for the cable cylinder potential functions with $k > m_L$	230
6.13	Component diagrams for the cable cylinder potential functions with $k > m_L, m_R$	235
6.14	The component structure for the final cylinder of the connected section for all non-degenerate Y-junctions.	247
6.15	Unit length disconnected section component structure.	249
6.16	Predicted Equivalent cable structure when each Y-junction limb is an even number of basic length units.	250
6.17	Predicted Equivalent cable structure when each Y-junction limb is an odd number of basic length units.	251
6.18	Predicted Equivalent cable structure when one Y-junction limb is an even number of basic length units, and the other is an odd number of basic length units.	252
7.1	The branch-shifting operations for symmetric Y-junctions.	258
7.2	The branch-shifting operation when the short branch has a cut terminal.	262
7.3	The branch-shifting operation when the short branch has a sealed terminal and $n > m$	265
7.4	The branch-shifting operation when both Y-junction terminals are sealed and $n < m$	267
7.5	The branch-shifting operation when the short cylinder terminal is sealed, the long terminal is cut and $n < m$	271
7.6	Example 1, illustrating the branch-shifting process.	272
7.7	Example 2, illustrating the branch-shifting process.	272
8.1	Features of fully equivalent cable structure and the construction methods.	276

8.2	A selection of cables for simple Y-junctions with the same surface area but different left and right branch lengths; both tree terminals are sealed.	280
8.3	A selection of cables for simple Y-junctions with the same surface area but different left and right branch lengths; one tree terminal is sealed, while the other is cut.	281
8.4	Examples of electrical mappings in Y-junction dendritic trees where the electrotonic lengths of child branches are unequal.	283
8.5	Equivalent cables generated from data for motoneuron cell M43/5.	286

List of Tables

Chapter 1

Neurophysiological Background and Dendritic Function

1.1 Introduction

Formed from billions of interconnected neurons, the human nervous system is an incredibly complicated structure. The level of physical intricacy is often bewildering, from the molecular to the single neuron, through the local networks they form, to the larger networks associated with distinct functional regions of the brain. When one also considers the range of electrical and biochemical processes through which neurons are able to interact and adapt, and the range of time scales over which these processes take place, it becomes even clearer why it has been difficult to obtain a detailed understanding of most aspects of nervous system function. Evolution has enabled coherent function to emerge from the interaction of all these processes.

Neuron structure and interconnectedness seems to confer upon the brain its ability to perform an impressive array of mechanical, regulatory and cognitive functions; through various electrical and chemical processes, the brain is able to receive, encode, decode, transmit and retain, vast quantities of information. The way in which information is represented and processed by neurons and their networks is only understood in limited detail. Many advances have been made where work has concentrated on functions that are well-specified and do not present too much difficulty for experimental access, e.g. some aspects of the visual and motor systems. Properties of the nervous system that underlie less directly accessible functions such as memory, and other cognitive aspects of brain function, are not as well understood. However, with the introduction and widespread use of powerful visualisation tools such as functional magnetic resonance imaging, it is possible to observe (large scale) regional changes in brain activity associated with specific

cognitive functions, enabling improved understanding of higher brain function. There have also been advances at the molecular level, concerning, for example, the development and the genetic basis of the nervous system. It is a major challenge, however, to gain a detailed understanding of the intermediate functional levels of the single neuron and the neural network.

Advances in understanding neuron function are contributed primarily by experiment, although theoretical and mathematical modelling approaches play a significant role in attempts to explain and predict the electro-chemical behaviour that underlies experimentally observed phenomena. Neuronal models and signal analysis techniques are also used to investigate how information might be coded in the electrical signals that are input to and output from real neurons and their networks, and how this information is transformed. Many signal processing operations that real neurons might perform have been postulated, for example simple logic operations, input coincidence detection, and Hebbian learning (see McKenna *et al.*, 1992, for an overview of several possibilities). The fact that neurons process information in some way often motivates a description of neuron function in terms of "computation". However, since signal processing in complicated real neurons is not well understood (in contrast with digital computation), the term is presently used fairly vaguely, encompassing broad possibilities of neuron operation. Interesting discussions on the nature of computation for real neurons can be found in Schwartz (1990).

Ever since the wealth of dendritic structure was revealed by Ramon y Cajal (1911), the observed complexity and variety of single neuron morphology has raised many questions concerning the role that geometry might play in neuronal signal processing. Unfortunately, an extensively branched tree does not generally lend itself to mathematical or experimental analysis which might reveal subtle and important function associated with specific neuronal shapes. However, the fully equivalent cables that are the subject of this thesis allow one to extract previously unobtainable information about the way dendritic geometry can influence the full range of electrical activity that arises in a particular class of tree models (electrically passive models). These equivalent cables are the first such tool to allow this type of analysis for dendritic trees.

The purpose of this chapter is to introduce some basic neurophysiology, describing the nature of electrical activity in neurons and covering briefly the role of dendritic trees in neuron function. The detail given here should be sufficient for an understanding of the mathematical models and methods described in later chapters.

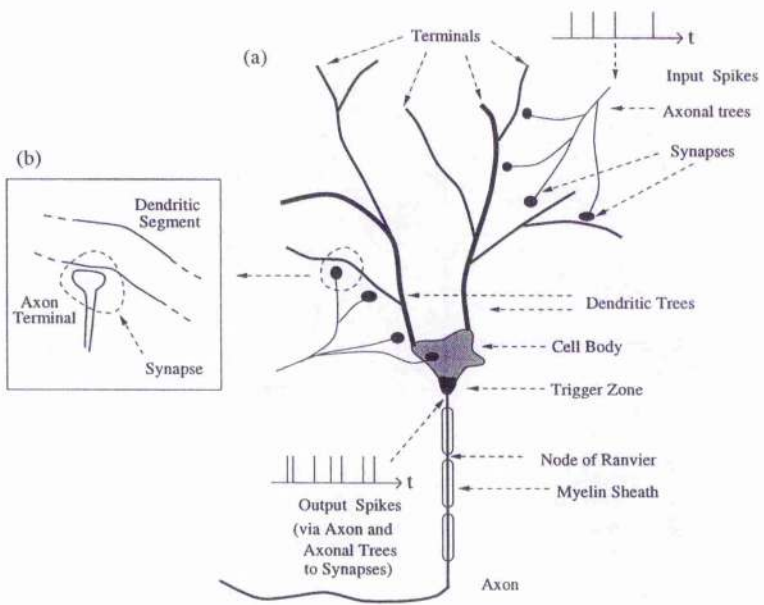


Figure 1.1: Idealistic representation of a neuron. (a) The main anatomical components of a neuron are illustrated: the cell body, dendritic trees, and axon. (b) Cells influence one another via synaptic connections. See discussion in text for more details.

1.2 Neuron Structure and Connections

Figure 1.1 illustrates the main physical features of a neuron in an idealised representation. Not all neurons share these features, while some exhibit additional structure. The *cell body*, or *soma*, is usually a distinct bulk, from which several long, thin, and usually branching, cable-like appendages may emerge — the *dendritic trees* (or *dendrites*), of which there can be several, are traditionally regarded as gatherers of electrical input, while the single *axon* is the path of electrical output. Electrical activity at the soma (or more specifically, at a trigger zone on, or near, the soma), which is due to the combined effects of inputs on the dendritic trees and the soma itself, will determine if an output is generated at any point in time.

The axon branches to form synaptic connections with other cells, often forming many connections on each target cell. *Local neurons* form connections with other neurons in the immediate vicinity of the output-generating cell, while the axons of *projection neurons* are longer and sheathed in myelin, allowing signals to travel significant distances rapidly and with little degradation to more distant target cells. The myelin sheath is broken at regular intervals, known as *nodes of Ranvier*, where output signals are reinforced.

This division of function among the main components of a neuron is a useful generalisation for many purposes, but there is great scope within the dendritic trees and axonal

trees for more complex roles. Dendritic trees, for example, because of their branched structure and electrical properties, are possibly capable of localised signal processing (e.g. Koch *et al.*, 1982; Woolf *et al.*, 1991). Section 1.4 discusses general dendritic function in greater detail.

Of course, a self-contained system of neuron to neuron input-output is not of much practical use to a living creature: some neurons (in the peripheral nervous system, rather than the central nervous system) must gather information about the outside world, and others must control functions of the body. Apart from the most prevalent *interneurons* which connect to other neurons, there are specialised *sensory neurons* which receive, for example, visual, and auditory information; *motoneurons* control muscle.

Each neuron is bounded entirely by a thin membrane (width approximately 2.3 nm), separating the intracellular fluid (cytoplasm) from the extracellular space. The membrane exhibits a capacitive effect, and is capable of retaining a charge density on the membrane-intracellular and membrane-extracellular interfaces (the membrane capacitance per unit area is often approximated as $1.0 \mu\text{F}/\text{cm}^2$). The intracellular medium is an ionic solution which contains sub-cellular components that perform essential metabolic processes; the soma contains the cell's nucleus. Immediately extracellular to a neuron is another ionic solution that forms a narrow region (roughly 20 nm) between cells; segments of other dendrites and axons may lie close by, perhaps receiving input from or sending input to the same sources, perhaps not. Also present are cells generally associated with regulatory brain functions, known collectively as *glial cells*.

A distribution of *ion channels* lies across the membrane, allowing specific ionic species (in particular sodium, potassium, calcium and chloride ions) that are in solution either side of the membrane to pass across it. Section 1.3 explains how the type and density of ion channels distributed over the neuron membrane, combined with intracellular and extracellular ion concentrations, determines the range of excitable electrical phenomena that can be produced when the neuron is subject to synaptic input.

A *synapse* is a junction between two cells, where *pre-synaptic* structure (usually an axon terminal) influences *post-synaptic* structure (usually the dendrites or soma). The majority of synapses are chemical synapses, where the cells are not directly connected. Instead a neurotransmitter substance is released at the axon terminal of the pre-synaptic cell in response to electrical activity (more specifically, an increase in intracellular calcium concentration). The neurotransmitter diffuses across the small gap between cells (the *synaptic cleft*, approximately 20–40 nm in width) and binds to receptors on the post-synaptic cell membrane, thus initiating electrical activity (sometimes through a secondary process) by opening specialised ion channels and allowing specific ions to flow more easily across the membrane. Chemical synapses are either excitatory, in which case, when activated, they

increase the likelihood of an output signal being generated by the post-synaptic cell, or inhibitory, in which case the likelihood is decreased. There are also electrical synapses where the two cells are directly connected by a small membrane *gap-junction* which allows electrical activity to spread between cells in the same manner as it spreads within a cell. These connections are often associated with synchronisation of activity between populations of neurons. Electrical synapses are given no further consideration in this thesis. Synaptic organisation in the brain is discussed in great detail in Shepherd (1990).

Depending on the neuron type, synapses may be located at many thousands, tens of thousands, or even hundreds of thousands, of sites over the dendritic trees and soma. In addition to the *axo-dendritic* (axon to dendrite) and *axo-somatic* (axon to soma) connections described above, there exist *axo-axonic* (axon to axon) synaptic connections where output from one neuron can directly influence the output of another by connecting in the region of an axon terminal. Less common, though not necessarily less important, are the *dendro-dendritic* synapses, where a dendrite of one cell forms a synaptic connection with the dendrite of another cell.

It is useful to consider typical dimensions of the often studied motoneuron, to get an idea of the sizes of the objects under consideration, though it should be noted there can be significant variation between neuron types. (source of following data: Tuckwell, 1988a). The dendritic membrane surface area is usually much larger than that of the cell body. For example, the ratio of dendritic to somatic surface area for the motoneuron is of the order 10, with a total combined surface area averaging $145,000 \mu\text{m}^2$; the density of synaptic connections over the membrane is around 10-20 synapses per $100 \mu\text{m}^2$, but varies over the cell body and dendrites. The roughly spherical motoneuron soma has diameter of approximately $80\mu\text{m}$, while dendritic diameters range from around $10\mu\text{m}$, narrowing with distance from the soma. The dendrites of a single cell are typically long compared to the soma and dendrite diameters, reaching up to $500\mu\text{m}$ or more in length from the cell body. Local neurons output to cells within a few millimeters of the cell body, while projection neurons can reach many centimeters.

Dendritic Structure

Neuronal dendritic trees exhibit a wide variety of observably distinct branching patterns, as shown by Ramon y Cajal (1911). Figure 1.2 illustrates several of the many neuron types familiar to neurophysiologists. The major geometrical differences between neurons can be characterised by the number of trees that emerge from the soma, the number of branches and branch points, branch lengths and diameters, and the three-dimensional orientation of the branches.

Some dendritic trees, for example those of Purkinje cells (Figure 1.2a), are highly

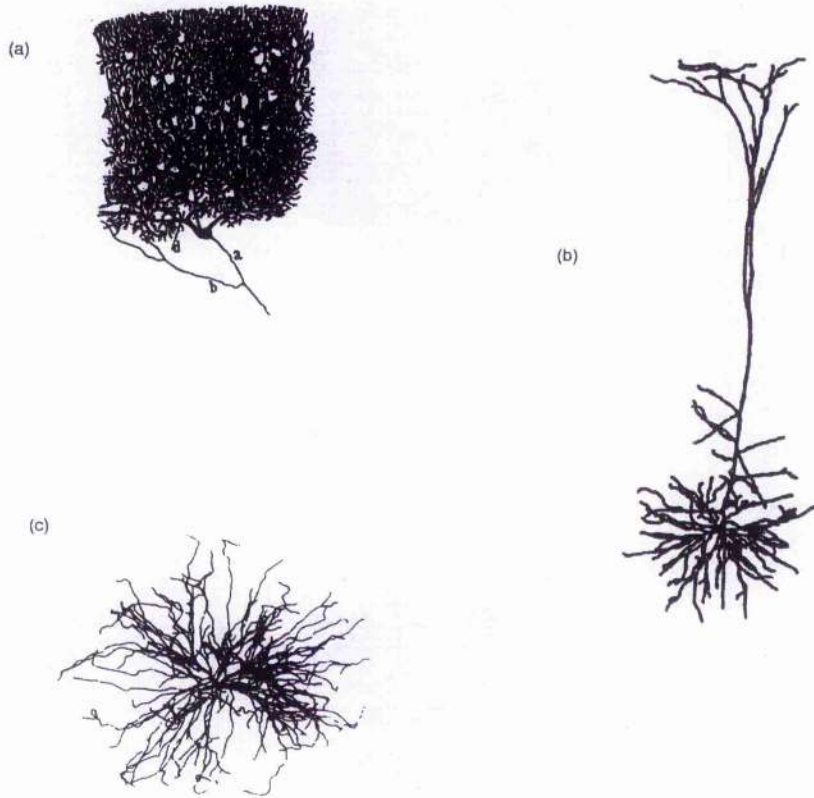


Figure 1.2: Examples of real neurons. (a) Purkinje cell. (b) Pyramidal cell. (c) Motoneuron.

branched, with branches tightly packed together in a two dimensional planar orientation; it is estimated that as many as two hundred thousand synapses may form on these cells. Others, such as the pyramidal cell (Figure 1.2a), have less packed branching and, in this particular cell, there are two distinct dendritic components: the apical dendrites emerge from a long dendritic trunk, while the basal dendrites branch closer to the cell body. Both types of branching exhibit a three dimensional distribution.

The dendritic trees of certain neuronal types (e.g. Purkinje cells, pyramidal cells) may, at least in part, be covered in *dendritic spines* which are tiny protrusions from the surface (in a sense tiny branches) still ensheathed in membrane to preserve the continuous boundary of the cell. Spines may take several distinct shapes, from the short stubby type, to mushroom shaped, and elongated types (see e.g. Rall and Segev, 1990). If a dendritic segment is covered in spines, synapses are usually associated with the spines rather than the main shaft of a dendritic branch segment. One physical advantage of spines is that they protrude through materials that closely surround the neuron, perhaps allowing synaptic connections to form more easily. However, it is the role of spines in synaptic plasticity that may be significant for learning and memory (see, e.g. Brown *et al.*, 1992). Dendritic spines are narrow, with typical widths in the range 0.1–0.5 μm , much wider than the cell membrane. Typical lengths are in the range 1–2 μm .

Extensive illustration and discussion of central and peripheral nervous system organisation, neuron morphologies, the chemical make-up of the membrane, glial cells, and general cellular mechanisms can be found in e.g. Kandel *et al.* (1991).

1.3 The Nature of Electrical Excitability in Neurons

Membrane Ion Channels

The following is a brief discussion of the nature of ion channels and the vital role they play in nerve cell excitation. Certain aspects of the electro-chemical processes are presented in a slightly simplified manner or in limited detail to highlight the most important features for the mathematical models developed later. Hille (1984) gives a detailed account of membrane ion channel properties and a historical background to the theory and experiment surrounding their discovery. More extensive discussion of the material outlined below can also be found in this book, and also in Shepherd (1990).

Ionic species that are mobile in the intracellular and extracellular solutions, most significantly the cations potassium (K^+), sodium (Na^+), and calcium (Ca^{2+}), and the anion chloride (Cl^-), can permeate the membrane through a distribution of ion channels.

Significantly, extracellular and intracellular solutions contain different concentrations

of the various ion species. For example, the ratio of intracellular to extracellular K⁺ concentrations is generally very high (a typical ratio may be 30:1), while for Na⁺ and Cl⁻, the extracellular to intracellular concentration ratio is high (a typical ratio may be 10:1 in each case). As diffusive and electrical processes act to move ions across the membrane, and also cause them to disperse intracellularly, a spatio-temporally varying transmembrane electrical potential distribution is established.

Ion channels are either *non-gated* or *gated*. Non-gated channels are a permanently open two-way route for ionic currents. Gated ion channels are opened in response to either electrical (voltage gated channels) or chemical (chemically gated channels) stimuli.

Ion channels are often highly selective for just one ion species, i.e. primarily ions of that type are able to pass, though they may display limited permeability to other major species. There are also ion channel types that are significantly permeable to more than one of the main ion species. Ion channel types that differ physically (in their chemical structure) may also be associated with the same ion species.

It is possible to identify, experimentally, many distinct ionic currents, the time courses of which are determined by differing channel *activation* and *inactivation* characteristics; these characteristics are controlled by underlying molecular kinetics and so can depend on the chemical structure of the channel, local membrane electrical activity, the concentrations of specific ion species, and neurotransmitter substances. It is through combinations and interactions of these various currents that a specific neuron displays its characteristic electrical behaviour. Ion channel types and densities can vary significantly over a single neuron's membrane, and between different neuron types. By employing different types and distributions of ion channels, two classes of neuron can exhibit markedly different electrical behaviour. A multitude of different ionic currents and channel types have been discovered in recent years (Sejnowski, 1997). Hille (1984) gives an account of activation and inactivation kinetics. See McCormick (1990) for a useful overview of many different types of ion currents and their activation/inactivation characteristics.

Ion channels are pores, and, when open, essentially form holes in the membrane. The size of an ion species (more specifically its hydrated form in solution) will determine whether it can pass through a specific channel. When open, a single ion channel allows rapid movement of ions across the membrane, with rates typically of the order 10⁵–10⁷ ions per second. The conductance of a single ion channel typically lies at some point in the range 1–150 pS. The low density of ion channels (of the order 1 per μm, though increased at synaptic sites and other “hot spots” of activity such as nodes of Ranvier and the action potential initiation site; they typically occupy less than one percent of the total membrane), is capable of producing transmembrane currents strong enough for typical levels of cell excitation (source of data: Hille, 1984).

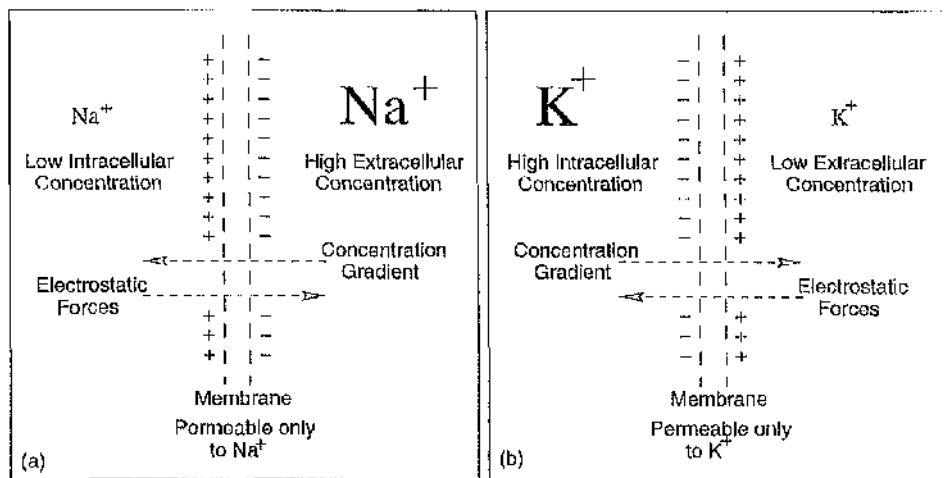


Figure 1.3: Equilibrium states for membrane permeable to a single ion species. (a) Equilibrium state for sodium ions in solution either side of a membrane permeable only to sodium ions. Extracellular concentration is higher, so diffusive and electrical forces balance when transmembrane potential is positive. (b) Equilibrium state for potassium ions in solution either side of a membrane permeable only to potassium. Intracellular concentration is higher, so diffusive and electrical forces balance when transmembrane potential is negative.

The Equilibrium Potential

By convention, transmembrane potential is internal potential minus external potential. Consider a single ion species, Na^+ , with extracellular concentration higher than intracellular concentration, and a membrane permeable only to this ion. If the potential difference across the membrane is initially zero, i.e. the solutions on each side of the membrane are electrically neutral, then Na^+ ions will diffuse down the concentration gradient, from extracellular to intracellular medium. The quantity of ions that traverse the membrane is assumed to have negligible effect on the ion concentrations — this is generally true unless the activity is maintained for long periods, or excited structure is small, such as a spine or narrow dendrite, where significant changes in concentration of certain ions may occur. A positive transmembrane potential develops since there is a greater number of positive ions intracellularly, and the anions that ensure total overall electrical neutrality cannot pass across the membrane. The resulting electric field across the membrane acts to resist the movement of additional positive charge until eventually, at equilibrium, the diffusive and electrical forces are balanced. There is no net flow of ions and so no current flows. Figure 1.3 illustrates the balance of forces for both Na^+ and K^+ ions individually.

The equilibrium transmembrane potential (or *Nernst potential*), for a single ion species,

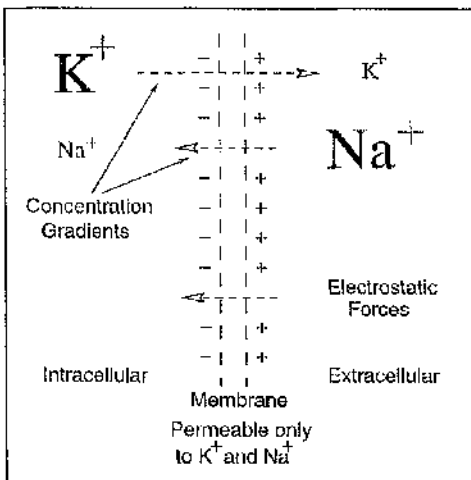


Figure 1.4: Equilibrium state for sodium and potassium ions in solution either side of a membrane permeable only to these two ion species. Potassium permeability is higher than sodium permeability of the membrane so concentration gradients and electrostatic forces balance when transmembrane potential is negative.

k say, is defined as the potential at which electrical forces balance diffusive forces. It is denoted E_k and given by the *Nernst equation*,

$$E_k = \frac{RT}{zF} \ln \frac{[k]_o}{[k]_i}, \quad (1.1)$$

where R is the gas constant ($8.314 \text{ Jmol}^{-1}\text{K}^{-1}$), T is Kelvin temperature (K), F is the Faraday constant ($9.648 \times 10^4 \text{ Cmol}^{-1}$), z is the valency of the ionic species, and $[k]_o$, $[k]_i$ are respectively the extracellular and intracellular concentration of ion species k . A derivation of this equation is given in Tuckwell (1988a). The equilibrium potential for potassium is typically negative (around -80mV to -100mV); and for sodium it is positive (around $+40\text{mV}$ to $+60\text{mV}$).

The equilibrium potential for a single ion species is independent of the level of permeability of the membrane to the ion species and so, if the transmembrane potential is at the Nernst potential, opening any additional ion channels selective for species k will not induce any current flow. If the transmembrane potential is less than the equilibrium potential, ions of species k flow outward across the membrane to the extracellular solution (if k is negatively charged) or inward (if k is positively charged) to restore the equilibrium. The converse is true if the transmembrane potential is above the equilibrium potential.

When more than one ion species is involved, there are now multiple concentration gradients (assumed independent) to be considered. The equilibrium potential in the presence

of n ion species, assuming they all have the same valency, is

$$E_{eq} = \frac{RT}{zF} \ln \left[\frac{\sum_{k=1}^n P_k [k]_o}{\sum_{k=1}^n P_k [k]_i} \right]; \quad (1.2)$$

where P_k is the *permeability coefficient* of the membrane for ion species k , which is simply a measure of how easily those ions will pass across the membrane. The value of P_k will depend on the density of open ion channels selective for each species and the rate at which each ion channel allows ions to pass. The sum is taken over all ion species to which the membrane is permeable. This is a special case of the more general Goldman formula derived by assuming a constant electric field through the membrane (Goldman, 1943; see also Hille, 1984; Tuckwell, 1988a). Figure 1.4 illustrates the situation for membrane permeable to just sodium and potassium ions (with constant P_{Na+} and P_{K+}).

When membrane is permeable to multiple ion species and the membrane potential is at the corresponding equilibrium potential, no net current will flow. This potential is in general different from the equilibrium potential for any one specific ion species, and so ions of all relevant species must be continually flowing across the membrane via channels. Inevitably, there must eventually be a change in intracellular and extracellular ion concentrations, and a consequent alteration in the individual ion equilibrium potentials, unless processes act to maintain the ion concentrations. These processes are the *active transport*, or *pumping* mechanisms. Ions are exchanged between intracellular and extracellular solutions by *carrier* molecules which are embedded in the membrane. Most notably, the Na-K pump which exchanges sodium and potassium ions (three Na^+ for each K^+ , so there is a net pumping current in this case), moving sodium outwards and potassium inwards. Discussion of active transport processes can be found in Hille (1984) and references therein.

For many neurons, the overall equilibrium, or *resting*, potential due ion channel and pumping currents, is roughly -70 mV, between the sodium and potassium Nernst potentials, but much closer to the potassium potential since at rest there are more potassium channels open.

The derivation of these equations assumes ionic independence, i.e. the ion solutions are dilute enough that the probability of an ion crossing the membrane is independent of the presence of other ions. The general mathematical representation of ionic currents is given in Chapter 2.

Overview of Electrical Input, Integration, and Output

It is useful to give an overview of the process of signal input, integration and output within a neuron, in the light of the previous discussion of membrane ion channels. Figure 1.5

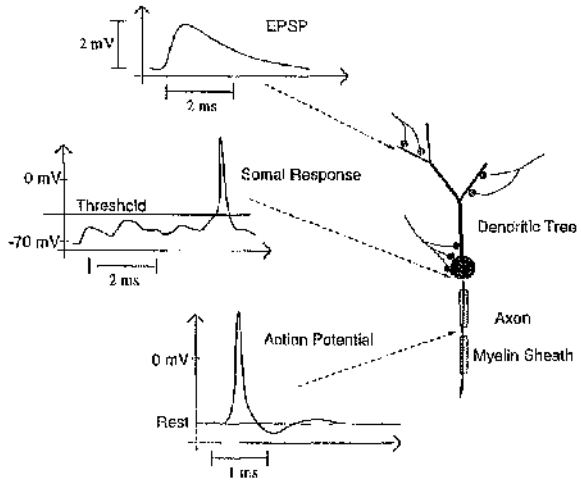


Figure 1.5: Shape and strength of neuronal electrical signals. Synaptic potentials on dendrites and soma combine spatially and temporally. If the total effect at the soma (trigger zone) reaches a threshold value then an action potential is initiated which flows along the axon.

illustrates the strength and shape of typical input and output potentials.

Membrane is *depolarised* when the potential becomes less negative than the resting potential. The membrane is *hyperpolarised* when the potential becomes more negative than the resting potential.

Electrical activity is initiated when ion channels open briefly to allow influx or efflux of specific ion species at synaptic sites; the channels then inactivate and are closed (eventually reactivating so that it is once more possible for them to open). The time scale of a typical synaptic event is in the millisecond range (though there are important exceptions, such as long term potentiation, see e.g. Brown *et al.*, 1992). The activity spreads from the synaptic site as charge disperses intracellularly within the dendritic and somatic cytoplasm. As this charge disperses, it can leak across the membrane, and may also initiate additional activity by causing voltage-gated ion channels away from the initiation site to open. As a neuron is bombarded with spatio-temporal patterns of thousands of synaptic inputs, the resulting distribution of excitation through a neuron can be extremely complicated.

Excitatory synaptic input causes a depolarisation of the membrane at the synaptic site by temporarily increasing the number of channels open to ions with equilibrium potentials greater than the resting potential (sodium ions and calcium ions). This causes charge to briefly seek an equilibrium potential that is temporarily raised. The membrane voltage disturbance initiated in the post-synaptic cell by an excitatory synapse is known as the *excitatory post-synaptic potential* or EPSP.

Inhibitory synaptic input acts to prevent membrane excitation by opening channels

selective for ions with equilibrium potentials less than or perhaps close to the resting potential (chlorine and potassium ions). In the former case, the membrane is hyperpolarised. In the latter case, there will be no discernible influence on electrical activity unless the membrane is already excited away from rest; this is known as *shunting inhibition*. A membrane voltage disturbance initiated in the post-synaptic cell by an inhibitory synapse is known as the *inhibitory post-synaptic potential*, or IPSP.

Individual synaptic inputs typically alter the local membrane polarisation by a few millivolts. Synaptic input on the soma will have an immediate influence on the likelihood of an output being generated, causing a sharp brief change in the local potential. By contrast, input on distant sections of a dendritic tree will take time to exert their full influence on the soma. As charge spreads within the tree, the voltage distribution is typically smoothed and attenuated, with a weaker, graded, and longer lasting impact at the soma. If the total depolarisation at the soma is sufficiently strong, i.e. the membrane potential reaches a threshold value, then an output spike (action potential) will be generated. Differing spatio-temporal relationships between inputs can have markedly different combined effect on the soma.

Note that, in contrast with dendrites, most axons have very similar ionic properties, with action potentials controlled by Na^+ and K^+ ion channels. The sharp local depolarisation of membrane when a threshold potential is reached is due to sudden opening of voltage-gated sodium channels and an in-rush of Na^+ , turning the membrane potential positive. This influx quickly inactivates and a slower efflux of potassium ions restores the membrane to equilibrium after a small hyperpolarisation. The signal can move along the axon, regenerated by the opening of sodium channels as the signal progresses, eventually influencing potentially many hundreds, or even thousands, more neurons.

Action potentials can also be initiated in dendrites, but are usually associated with Ca^{2+} currents. They have been found in, for example, Purkinje and pyramidal cells.

1.4 The Signal Processing Role of Dendritic Geometry

This thesis is concerned with dendritic signal processing function, in particular how electrical activity interacts in the presence of these complicated branched structures and how to analyse this interaction. What follows is a brief overview of some fairly general and widely accepted aspects of signal processing in dendritic trees, and, in addition, we speculate about the possible significance of differing geometries. Some aspects of dendritic function have been investigated in modelling studies, however most suggestions that have been made are, at present, difficult to confirm by experiment. For much more extensive discussion of neuron function, and experimentally observed phenomena in particular

neuronal types (primarily motoneurons, Purkinje cells, and pyramidal cells), see, for example, Mel (1994), McKenna *et al.* (1992), Segev *et al.* (1995), Koch (1997), Koch and Segev (1989), and Rugg (1997). Segev and Rall (1998) discuss recent experimental results obtained using optical recording techniques.

The formation in the nervous system of networks, neurons, and their dendritic trees is due to a combination of genetic pre-specification and learning or adaptation mechanisms involving structural or synaptic modification. Some basic neural framework within which function may take place must be pre-defined, while learning mechanisms will adapt the individual neuron structure and connections over time to fine tune their eventual function. The two mechanisms may have contrasting significance for different neuron types.

Neuron to neuron communication largely takes the form of spike trains. Information is encoded in the temporal pattern of the spikes, since the spikes themselves are essentially indistinguishable. This is of course a vital component of neuron processing, however, here the focus is on the processes that occur within dendritic trees, though the two are inevitably strongly linked.

The number and branching patterns of dendrites can vary widely between different neuron types and it is a natural question to query the significance of a specific neuron morphology. What functional advantages (if any), for example, does the shape of a motoneuron dendrite offer over dendrites of, say, pyramidal or Purkinje cells, so that the whole cell might perform its assigned task optimally? It is likely that the characteristic shape of a specific class of dendritic trees is optimised specifically for the task the neurons are involved in. Ideally, one wants tools to investigate, quantitatively, the effect dendritic geometry has on the integration of the full range of complex spatio-temporal patterns of synaptic input, with a view to understanding the nature of any signal processing operations being performed, and perhaps determining the synaptic distributions that might be involved.

The dendritic tree has a fairly general and loosely defined role as an integrator of, and physical framework for, distributed synaptic activity. Dendrites essentially funnel excitation towards the cell body, but also allow each point on the tree to potentially influence every other. Considering the complicated spatio-temporal patterns of synaptic input they receive, and adding to this mechanisms for synaptic and structural modifications (e.g. dendritic spines are thought to be involved in synaptic plasticity), then it is reasonable to believe that dendritic trees may be powerful signal processing units.

In terms of enhanced signal processing capability, a branched structure has several advantages over an unbranched structure, although branching is not essential for providing the necessary surface area for all synaptic connections. There must be other reasons that neurons can have such a wide field of reception. Branching that takes of advantage of three

dimensional space allows a neuron to receive inputs more easily from sources originating from numerous directions. Branching can support complex patterns of spatio-temporally distributed input, and allows a division of synaptic input into regions of a dendritic tree which are themselves electrically remote from each other or the soma — in other words, branching may support extensive local signal processing (Koch *et al.* 1982; Woolf *et al.*, 1991; Mel, 1994). Branching allows input from numerous sources to connect at distributed points which are equally significant, electrically, with respect to the soma, or with respect to other points on the tree.

There is also important variation in synapse types, aside from the fundamental differences that makes them inhibitory or excitatory. The membrane potentials they induce can vary in strength and time-course, features that may depend on the neurotransmitters involved, the local potential at the point and time of initiation, and on the presence of other chemicals. Yet more variation can be found in the different membrane channels, and consequent form of the ionic currents — a single neuron may exhibit varying types and densities over its surface, and the types may change from neuron to neuron. In conjunction with dendritic geometry, a suitable arrangement of synapses and ion channels with particular voltage-dependent characteristics is possibly a vital feature for certain processing operations. Perhaps “hot-spots” of ion channels that initiate strong activity play an important role in controlling this structure-signal interaction. Results in this thesis suggest that processing properties can arise solely as a consequence of specific geometry. It may also be beneficial for a robust nervous system if a neuron has multiple ways of performing, or taking part in, the same signal processing operation; this idea of electrical degeneracy, or redundancy, as a consequence of branching, is also introduced in this thesis within the formal mathematical framework of the fully equivalent cable.

The initiation of an output spike or spike train depends on the input patterns over the dendritic trees. Can single neurons, or groups of neurons, represent information¹, different aspects of which are accessed (in some sense) and transmitted as output, depending on the input pattern. Does a different input configuration mean that a different operation is performed on this information, or maybe that different information is accessed altogether. Basically, it is possible there are several modes of operation a single neuron may be in, depending on outside influences (see e.g. Bernander *et al.*, 1994; Bernander *et al.*, 1991; Holmes and Woody, 1989). Perhaps changes between modes are permanent, temporary, or transient. It may be that short term modifications are part of a processing operation, while long term changes mark an alteration in processing capabilities. For example, synchronisation of synaptic activity has been investigated by Bernander *et al.* (1994) and Rapp *et al.* (1992).

¹The term “information” here is not used in any formal sense.

In conclusion, it is easy to speculate about possible dendritic function, and difficult to determine the precise relationship between neuron function and dendritic structure. For experimental reasons it is difficult to establish whether or not real neurons perform in many of the ways that have been suggested (here and elsewhere).

This thesis outlines a method for completely analysing the role geometry plays in signal integration within a specific type of tree model, i.e. the passive tree model. New and extensive insight into passive signal integration in neurons can be gained using this technique. This is by no means the most realistic model, but it can capture well the sub-threshold behaviour of some neurons. One cannot hope to understand in any great depth the role of geometry in more complicated models until the simpler models on which they are based are fully understood.

Chapter 2

Cable Theory and the Multiple Segment Dendritic Tree Model

2.1 Introduction

Within the context of neuronal modelling the term “cable theory” refers to a range of non-linear and linear models that may be used to describe the behaviour of electrical activity in arbitrarily branched dendritic trees, axons, and axonal trees, where physical and electrical properties of the cell are represented to varying degrees of biophysical realism. Cable theory was initially developed by Kelvin (1855) to describe electrical transmission in submarine cables. See Rall (1977) and Segev *et al.* (1995) for historical overviews.

Initially, we formulate a general non-linear cable equation that describes a non-uniform segment of (unbranched) dendrite, for example that illustrated in Figure 2.1. Here, non-uniformity implies that the cross-sectional area and perimeter may vary continuously. This model can incorporate arbitrary synaptic inputs and distributions of gated and non-gated ion channels. The derivation follows simply from charge conservation and a direct analysis of the currents that are allowed to flow, given model assumptions about constitutive properties of the dendritic segment.

Starting with the non-linear cable equation, which is significantly more general than cable equations normally used for modelling purposes, we make simplifying assumptions about the geometrical and electrical properties of the segment, progressively yielding several equations more typical of those used in simulations. In particular, cylindrical geometry is often assumed, as is the existence of a resting state. We show how the latter allows a separation of the term due to transmembrane ionic currents into linear and non-linear components. To highlight the progression from the non-linear equation to the passive linear equation that is eventually required, we briefly discuss how the assumption

of voltage-independence of the ion channel currents leads to a general linear cable equation incorporating ionic equilibrium potentials.

Eventually we obtain the linear cable equation for a uniform *electrically passive* dendritic segment, in both dimensional and convenient non-dimensional forms. The validity of the corresponding simplifying assumptions is considered. Here, uniformity implies a constant cross-sectional area along the length of the segment, and also a constant perimeter. The common assumption of a circular cross-section (e.g. Jack *et al.*, 1983; Tuckwell, 1988a) need not be made. The given equations will usually be expressed in terms of bulk electrical parameters that are independent of geometrical structure, however, to provide a link with previous representations of the cable equation, commonly used geometry-dependent parameters are also included.

A dendritic tree model is then derived. It is formed from connected segments, each represented by a general cable equation and linked or terminated by appropriate boundary conditions. The non-dimensional linear cable equation is the basis of the passive dendritic tree model used for constructing the fully equivalent cables described in the remaining chapters of this thesis. Important electrical properties of some simple passive structures are illustrated and discussed.

2.2 General Model of a Dendritic Segment

The model has three main components: the *intracellular medium*, ensheathed in a uniformly thin *membrane*, forms the dendritic segment; the segment is immersed in a perfectly conducting *extracellular medium*. The membrane is highly resistive, and also acts, in part, as a capacitor, retaining charge on the membrane-liquid interfaces. Charge can accumulate within the dendrite, moving across the membrane through a distribution of ion channels, and dispersing longitudinally, establishing a time- and space-dependent transmembrane voltage distribution. We assume the whole system is isothermal, so the temperature dependence of relevant chemical interactions can be ignored.

2.2.1 Fundamental Model Assumptions

Intra-cellular Medium — Ohmic Core Conductor

The cross-sectional dimensions of the core medium are small compared to the length of a dendritic segment. Assuming an isotropic core, potential gradients over the cross-sectional surface are small compared to those longitudinally, i.e. for our purposes the cross-section is effectively equipotential (a perfect conductor radially!).

These assumptions conveniently permit a one-dimensional treatment of the core; the

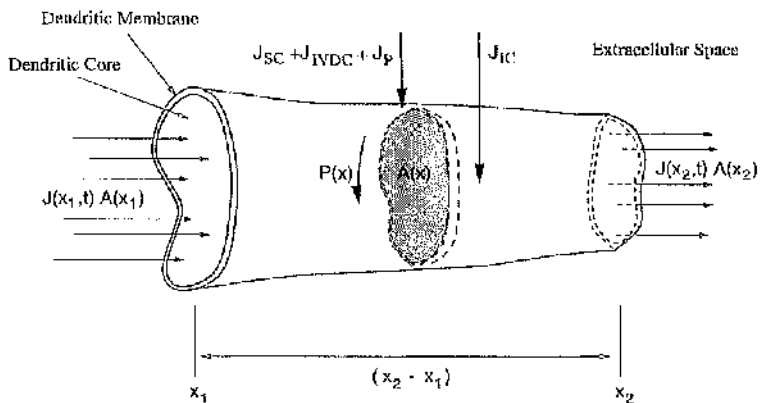


Figure 2.1: A non-uniform segment of dendrite. The cross-sectional area profile of the intracellular medium is $A(x)$, while the perimeter profile is $P(x)$. If J is the axial current density, axial current flowing into the segment at point x_1 is $J(x_1, t)A(x_1)$, while current leaving the segment at point x_2 is $J(x_2, t)A(x_2)$. Membrane current densities are synaptic, J_{SC} , intrinsic and voltage dependent, J_{IVDC} , and active transport, J_P , while J_{IC} is injected current.

only spatial dimension that is of explicit interest is denoted x and measured axially along the length of dendritic segments. Only spatial variation of the transmembrane potential with x is of concern. The cross-sectional profile of the dendritic segment must have a shape that does not invalidate these assumptions. The imperfect, but roughly circular, or elliptical, cross-sections of real dendrites are perfectly acceptable, though they are normally treated as circular.

For cylindrical segments, a three-dimensional analysis of intracellular current flow has been performed by Rall (1969b), and also Eisenberg and Johnson (1970), justifying the one dimensional treatment, except perhaps in the vicinity of a point current source in the core, where cross-sectional potential gradients may be significant.

Extra-cellular Medium — External Conductor

The extracellular solution forms a very narrow region between neighbouring cells. However, for many modelling purposes, it can be regarded as a very good conductor compared to the highly resistive membrane. It is commonly treated as a perfect conductor, and we follow this approach; charge that leaks from the dendritic segment is instantly incorporated into what is regarded as an isopotential extracellular ion pool. Consequently, at the membrane-extracellular interface there is no potential gradient to drive extracellular currents, and this interface is isopotential. Branching angles, or curvature in dendritic segments may also conveniently be ignored since there are no complicated three-dimensional

patterns of current flows to account for in this model.

The cable equation derivation that follows later may be easily adapted to incorporate an external longitudinal resistivity to current flow, whereby currents flow in the extracellular medium flow parallel to the segment axis (see, for example, Tuckwell, 1988a, for details).

Transmembrane Potential

Denote the internal (core) potential by $v_i(x, t)$. The spatially uniform extracellular potential is denoted v_e , but can be arbitrarily fixed, and so is usually taken to be zero. The potential difference between internal and external media is called the *transmembrane potential*, and denoted v_m , where

$$v_m(x, t) = v_i(x, t) - v_e. \quad (2.1)$$

Note that, by convention, x increases along dendrites away from the soma.

Axial Core Current and Axial Resistivity

The resistance to axial current flow presented by the core conductor is assumed to be ohmic. If J denotes the axial current density (axial current flow per unit cross-sectional surface area) in the direction of increasing x , then Ohm's law (for one dimension) is

$$J(x, t) = -\frac{1}{\rho_i} \frac{\partial v_m(x, t)}{\partial x}, \quad (2.2)$$

where ρ_i is the axial resistivity of the core, and is assumed to be constant. If the cross-sectional area of the dendritic segment is denoted $A(x)$, then the axial current, $i_a(x, t)$, is given by

$$i_a(x, t) = A(x)J(x, t). \quad (2.3)$$

By convention, axial current is positive where there is a net flow of positive charge in the direction of increasing x .

Consider a uniform slab of core material with cross-sectional area A and length l , as illustrated in Figure 2.2. Ohm's law (2.2) can be integrated to give $V = IR$ where V is the potential across the segment, I is the axial current flowing through the segment, and R is the total resistance this slab presents to axial current flow, so that

$$R = \frac{\rho_i l}{A}. \quad (2.4)$$

Thus the resistance per unit length of this segment, denoted r_i , is

$$r_i = \frac{R}{l} = \frac{\rho_i}{A}. \quad (2.5)$$

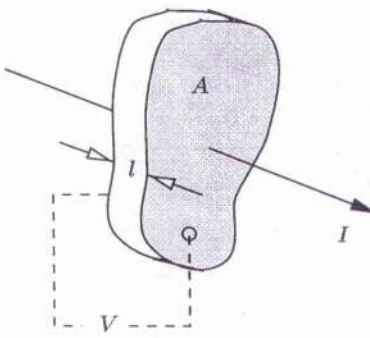


Figure 2.2: Uniform segment of core medium. Segment has surface area A , length l . Axial current is I , while potential difference across segment is V .

If cross-sectional area varies axially, then so will the resistance per unit length,

$$r_i(x) = \frac{\rho_i}{A(x)}. \quad (2.6)$$

Using equations (2.2), (2.3), and (2.6), the axial current may be written

$$i_a(x, t) = -\frac{1}{r_i} \frac{\partial v_m}{\partial x}, \quad (2.7)$$

The above equations can be adapted for spatially varying ρ_i , however experimental evidence for such variation is limited (see Rall *et al.*, 1992, for an overview). The final model we develop will require core homogeneity.

Cell Membrane

The membrane is permeable to the ion species relevant to cell excitation at sparsely distributed ion channels, as discussed in Chapter 1 (see also Hille, 1984). Associated with each ionic species that contributes to electrical activity within the dendritic cylinder are channels that permit only ions of that type to pass across the membrane. Ion channel density may vary over a segment of dendrite. A proportion of channels are *non-gated*, i.e. permanently open, and always allow ionic currents to flow. The remaining channels may be voltage-gated and chemically-gated. Ion channels are modelled as parallel transmembrane conductances. Although channels are located at discrete points over the membrane, they can be effectively modelled as a continuum. The full model representation of the corresponding ionic currents will be left until the general cable equation has been derived. For the moment, we just consider the term $J_T(x, t)$, which is a total current density (current per unit area of membrane) that has contributions from all possible sources of transmembrane currents. This includes gated and non-gated membrane ion channel currents, exogenous injected currents, synaptic currents and current due to active transport

mechanisms. It does not include capacitive currents. We follow the convention that the membrane current is positive when net positive charge flows *outwards* from the core. Consequently, $-J_T$ gives the current flowing *into* the core across the membrane. Note that only the spatio-temporal variation of J_T is explicitly indicated; contributions to J_T may also have explicit voltage dependence, as well as dependence on variables describing the molecular kinetics of the underlying mechanisms that allow current flow. For simplicity, such dependencies may be assumed acceptable unless we state otherwise.

Membrane Capacitance

Let C_M be the capacitance per unit surface area of membrane. It is assumed uniform over the dendritic segment, although the cable equation derivation that follows allows spatial (axial) variation. The current density (per unit area) due to capacitive effects, denoted J_C , is then

$$J_C(x, t) = C_M \frac{\partial v_m(x, t)}{\partial t}. \quad (2.8)$$

The membrane capacitance per unit length of segment, c_m , is also commonly used. If $P(x)$ describes the non-uniform segment perimeter (Figure 2.1) then

$$c_m(x) = C_M P(x). \quad (2.9)$$

2.2.2 Derivation of the General Cable Equation

Consider the dendritic segment illustrated in Figure 2.1. It has non-uniform cross-section and non-uniform perimeter, and the two ends of the segment are at points x_1 and x_2 , where $x_2 > x_1$. Using equation (2.3), the total current flowing *into* the segment at time t must be

$$A(x_1)J(x_1, t) - A(x_2)J(x_2, t) - \int_{x_1}^{x_2} J_T(x, t)P(x) dx. \quad (2.10)$$

So, during the time interval $[t_1, t_2]$, the total charge flowing into the segment is

$$\int_{t_1}^{t_2} [A(x_1)J(x_1, t) - A(x_2)J(x_2, t)] dt - \int_{t_1}^{t_2} \int_{x_1}^{x_2} J_T(x, t)P(x) dx dt. \quad (2.11)$$

This additional charge is stored on the dendritic membrane, which has capacitance C_M per unit area. The charge stored in the segment over time interval $[t_1, t_2]$ must be

$$\int_{x_1}^{x_2} C_M P(x)v_m(x, t_2) dx - \int_{x_1}^{x_2} C_M P(x)v_m(x, t_1) dx. \quad (2.12)$$

Conservation of charge requires that equations (2.11) and (2.12) are equal, so

$$\begin{aligned} & \int_{x_1}^{x_2} C_M P(x) [v_m(x, t_2) - v_m(x, t_1)] dx = \\ & \int_{t_1}^{t_2} [A(x_1)J(x_1, t) - A(x_2)J(x_2, t)] dt - \int_{t_1}^{t_2} \int_{x_1}^{x_2} J_T(x, t)P(x) dx dt. \end{aligned} \quad (2.13)$$

This is the fundamental equation describing the temporal and spatial evolution of the membrane potential $v_m(x, t)$. Provided v_m is a sufficiently differentiable function of space and time, then by dividing equation (2.13) by $(t_2 - t_1)$ and subsequently letting $t_1, t_2 \rightarrow t$, it follows that

$$\int_{x_1}^{x_2} C_M P(x) \frac{\partial v_m(x, t)}{\partial t} dx = [A(x_1) J(x_1, t) - A(x_2) J(x_2, t)] - \int_{x_1}^{x_2} J_T(x, t) P(x) dx. \quad (2.14)$$

Similarly, now divide by $(x_2 - x_1)$ and take the limit $x_1, x_2 \rightarrow x$, revealing that $v_m(x, t)$ satisfies the partial differential equation

$$C_M \frac{\partial v_m(x, t)}{\partial t} = -\frac{1}{P(x)} \frac{\partial (A(x) J(x, t))}{\partial x} - J_T(x, t). \quad (2.15)$$

This equation is entirely a consequence of charge conservation, and the initial assumptions ensuring only axial core current flow. At this point we assume the core is a homogeneous ohmic resistance, and substitute for axial current density J using equation (2.2), giving

$$C_M \frac{\partial v_m(x, t)}{\partial t} = \frac{1}{P(x)} \frac{\partial}{\partial x} \left(\frac{A(x)}{\rho_i} \frac{\partial v_m(x, t)}{\partial x} \right) - J_T(x, t). \quad (2.16)$$

This equation will subsequently be referred to as the *general cable equation*. A second order partial differential equation, it describes the non-linear diffusion of the transmembrane voltage over a segment of dendrite. Capacitive currents (the term on the left), diffusive currents (the second order term) and membrane currents must all balance. As charge moves axially in the core and radially across the membrane, an equilibrium state is continually sought (whether or not it is ever actually reached depends on the properties of the membrane and the associated transmembrane currents). Many commonly used cable equations can be obtained from this general form.

The next section completes the description of a dendritic segment by specifying general forms for the transmembrane currents J_T . For details of the representation of specific currents in various models, see e.g. Poznanski (1999), Tuckwell (1988b), Koch and Segev (1989), and McKenna *et al.* (1992). Subsequent subsections detail how assumptions concerning geometrical and membrane constitutive properties give rise to various non-linear and linear models. In section 2.5 we move to a complete tree where segments must be linked at branch points by voltage continuity and current conservation boundary conditions, assigned appropriate terminal boundary conditions, and the trunk of the tree should be linked to a representation of the cell body.

The Non-dimensionalised Non-linear Cable Equation

The general cable equation may be expressed in a non-dimensional form, by an appropriate change of variables from x and t . Full details of the non-dimensionalisation procedure are given in section 2.4, where it is applied to the passive linear cable equation.

2.2.3 Specification of the Membrane Currents

Assume the membrane current density, J_T , consists of four main components,

$$J_T = J_{IVDC} + J_{SC} + J_P - J_{IC}, \quad (2.17)$$

where J_{IVDC} represents Intrinsic and Voltage Dependent Currents, that is, currents through all gated and non-gated ion channels, except those currents through chemically-gated channels opened during synaptic events; J_{SC} represents all Synaptic Currents; J_P represents Pump currents due to active transport mechanisms. These first three currents are determined by the constitutive properties of the membrane. The convention for direction of current flow used for J_{IVDC} , J_{SC} and J_P is the same as for J_T . The fourth contribution, J_{IC} , represents exogenous current density (Injected Current, which is strictly injected directly into the core medium, but is straightforwardly treated as a membrane current density), however this current is assumed positive when positive charge is injected *into* the core, hence the minus sign in equation (2.17).

Modelling Ion Channel Currents

The flow of ions through ion channels, and the resulting theory of equilibrium and resting potentials was discussed in Chapter 1. Denote the current density (current per unit area) flowing due to ionic species k by $J^{(k)}$ (the k -current). It is modelled by

$$J^{(k)} = g^{(k)}(v_m - E_k), \quad (2.18)$$

where $g^{(k)}$ is the conductance per unit area of membrane, and E_k is the equilibrium potential (1.1) for ion species k . There is zero k -current when $v_m = E_k$, as should be expected when diffusive and electrical forces are balanced and provided the ion species flow essentially independently of each other. The conductance $g^{(k)}$ is generally non-linear, following from the underlying kinetic processes that determine the activation/inactivation characteristics of the ion channels; it is a function of time, often of voltage (if not explicitly, then in terms of kinetic variables that are themselves voltage dependent in some way), and may also contain explicit spatial variation if there is an inhomogeneous density of ion channels (there is already implicit spatial variation).

The total ion channel current is then given by

$$J_{IVDC} = \sum_k g^{(k)}(v_m - E_k). \quad (2.19)$$

where the sum is over all the relevant ion species.

Conductances can be determined experimentally using techniques such as voltage-clamp (for details see Jack *et al.*, 1983; Hille, 1984); patch-clamp techniques allow currents

through single ion channels to be recorded (Hamill *et al.*, 1981; Sakmann and Neher, 1983). For example, the original Hodgkin-Huxley equations describing the squid giant axon (Hodgkin and Huxley, 1952) identify one sodium current, and one potassium current, both with non-linear conductances which describe the activation and inactivation characteristic of the currents. The sodium current is rapid, quickly depolarising the membrane, and then quickly inactivating after a millisecond or so. The potassium current, which develops more slowly, then takes over, repolarising the membrane and after a brief hyperpolarisation returning the membrane to rest. Their model required another current referred to as the leak current which is not associated with any one particular ion type but is necessary to complete the model description of the experimental observations. The leak current is effectively modelled with a constant leak conductance and a constant leak equilibrium potential. More detail can be found in, e.g. Tuckwell (1988b).

At this point, it would be possible to introduce additional equations to account for varying intracellular and extracellular ion concentrations, so that equilibrium potentials are not constant. However, we now assume constant concentrations since this is often realistic, simpler to deal with, and essential for the final model that will be developed.

Modelling Synaptic Inputs

The synaptic current, J_{SC} , which describes all inhibitory and excitatory synaptic events, are due to a temporary opening of specific chemically-gated ion channels. Again, they can be modelled by a conductance change at the synaptic site. If synapse j is located at point x_j , for $j = 1, 2, \dots, N$, and initiated at times t_{ij} then

$$J_{SC}(x, t) = \sum_{i=1}^{\infty} \sum_{j=1}^N \sum_k g_{syn}^{(k)}(t - t_{ij}^k) [v_m(x_j, t) - E_k] \delta(x - x_j) \quad (2.20)$$

where $t_{1j}^k, t_{2j}^k, \dots$ are the times at which ionic current k associated with synapse j becomes active, while $g_{syn}^{(k)}(t)$ models the conductance associated with this current, and $\delta(x - x_j)$ is the Dirac delta function at $x = x_j$ (see below, equation 2.26). The profile of the conductance $g_{syn}^{(k)}(t)$ is a consequence of the kinetics of the neurotransmitter binding to receptors and any other processes involved in opening ion channels. However, it is often modelled using the time dependent *alpha function* (Jack *et al.*, 1983),

$$g_{syn}^{(k)}(t) = g_*^{(k)} t e^{-\alpha t}, \quad (2.21)$$

where $g_*^{(k)}$ and α are constants.

Modelling Active Transport Mechanisms

In cable theory, active transport currents are not often modelled explicitly. The corresponding currents are typically relatively small over the time scales typical of neuronal signals. They may be assumed to contribute a constant current or they could be dependent upon the membrane potential and ion concentrations.

Modelling Applied Currents

Current sources are assumed to inject charge directly into the core medium. The resulting axial core currents have uniform flux density through the cross-section, (the injected charge at x may be regarded as applied uniformly over the cross-section at x because of the effectively zero radial resistance in the core). The distribution of applied current over a dendritic segment can be expressed as a current line density (current per unit axial length), $i_d(x, t)$, where

$$i_d(x, t) = J_{IC}(x, t)P(x). \quad (2.22)$$

So, if $i_A(x_1, x_2, t)$ denotes the total charge injected between points x_1 and x_2 on the segment, where $x_1 < x_2$, then

$$i_A(x_1, x_2, t) = \int_{x_1}^{x_2} i_d(x, t) dx. \quad (2.23)$$

It is also convenient to define

$$i_A(x, t) = i_A(0, x, t). \quad (2.24)$$

A single point source of current, $i_A(t)$, injected at some point $x = a$ along the segment has current density

$$i_d(x, t) = i_A(t)\delta(x - a), \quad (2.25)$$

where $\delta(x)$ is the Dirac delta function, satisfying

$$\int_{-\epsilon}^{+\epsilon} \delta(x) dx = 1, \quad (2.26)$$

for any $\epsilon > 0$. If f is function of x then,

$$\int_{-\infty}^{+\infty} f(x)\delta(x - a) dx = f(a). \quad (2.27)$$

The applied current density (per unit length) may be expressed in terms of the charge injected into the dendritic segment. If $q_A(x, t)$ represents the total charge introduced over dendritic segment $[0, x]$ over time interval $[0, t]$, then, by definition

$$i_A(x, t) = \frac{\partial q_A(x, t)}{\partial t}, \quad (2.28)$$

so that

$$i_d(x, t) = \frac{\partial^2 q_A(x, t)}{\partial x \partial t}. \quad (2.29)$$

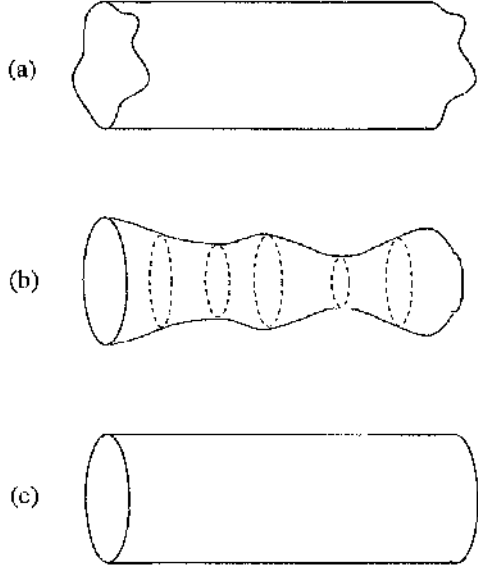


Figure 2.3: Special cases of dendritic structure described by simplified cable equations. (a) Uniform dendritic segment with irregular cross-section. (b) Non-uniform dendritic segment with cylindrical cross-section. (c) Uniform cylindrical dendritic segment.

2.2.4 Constraints on Geometry

Consider now how constraints on geometrical structure simplify the form of the general cable equation.

Tapering Cylindrical Dendrite

If the core cross-section is circular, as is widely assumed, with continuous diameter profile $d(x)$, as Figure 2.3b illustrates, then the cross-sectional surface area and cross-section perimeter are given by

$$A(x) = \frac{\pi d^2(x)}{4} \quad \text{and} \quad P(x) = \pi d(x). \quad (2.30)$$

The general cable equation (2.16) can be rearranged to give

$$C_M \frac{\partial v_m}{\partial t} = \frac{1}{4d} \frac{\partial}{\partial x} \left(\frac{d^2}{\rho_i} \frac{\partial v_m}{\partial x} \right) - J_T. \quad (2.31)$$

Using equations (2.6) and (2.9), note that the membrane capacitance per unit length of dendrite and the intracellular resistance per unit length are given by

$$c_m(x) = C_M \pi d(x) \quad \text{and} \quad r_i(x) = \frac{4\rho_i}{\pi d^2(x)}. \quad (2.32)$$

Uniform Segments of Dendrite

For uniform dendritic segments (not necessarily cylindrical), for example Figure 2.3a, the cross-sectional area, A , and the perimeter, P , are constant, so from equations (2.6) and (2.9),

$$c_m = C_M P \quad \text{and} \quad r_i = \rho_i / A \quad (2.33)$$

are constant. Rewrite the cable equation (2.31) as

$$c_m \frac{\partial v_m}{\partial t} = \frac{1}{r_i} \frac{\partial^2 v_m}{\partial x^2} - P J_T. \quad (2.34)$$

Uniform Cylindrical Segments of Dendrite

For the special case of uniform cylindrical dendritic segments, with constant diameter d , e.g. Figure 2.3c, then

$$P = \pi d, \quad A = \frac{\pi d^2}{4}, \quad c_m = C_M \pi d, \quad r_i = \frac{4\rho_i}{\pi d^2}. \quad (2.35)$$

Assumptions about current flow in the cylinder ensure that the rotational symmetry (invariance under rotation about axis) of the cylinder holds for electrical activity as well as physical structure.

2.2.5 Constraints on Constitutive Membrane Properties

Linear and Non-linear Contributions to Ionic Currents

Consider again the general cable equation describing a non-uniform dendritic segment. We now suppose the segment can be in a resting state, i.e. when no net current flows across the membrane. At rest there is no axial current flow in the segment, no current may be injected, and there are no synaptic events, so $J_{IC} = J_{SC} = 0$; no net transmembrane current must flow so $J_P + J_{IVDC} = 0$. All ionic channel and pumping currents that flow across the membrane are balanced. The corresponding resting potential, denoted v_R , is uniform over the segment membrane. External and internal ion concentrations for the various ion species are maintained.

Denote the current density due to ion channels and active transport by J_M , so

$$J_M = J_P + J_{IVDC}. \quad (2.36)$$

Since at rest this must be zero, we can write, without loss of generality,

$$J_M = C(v_m) - C(v_R), \quad (2.37)$$

where C is a constitutive function of membrane potential. Assuming that C is a suitably differentiable function of v_m , the *mean value theorem* states that

$$J_M = \frac{dC(v^*)}{dv_m} (v_m - v_R) = g(v^*) (v_m - v_R), \quad (2.38)$$

where $v^* = v^*(v_m, v_R)$ is a potential between v_m and v_R , and $g(v^*)$ may be regarded as a non-linear conductance (per unit area). Similarly, the mean value theorem applied to $g(v^*)$ yields

$$g(v^*) = g(v_R) + \frac{dg(v^{**})}{dv^*} (v^* - v_R) = g_M + g_{NL}, \quad (2.39)$$

where $g_M = g(v_R)$ is a constant membrane conductance per unit area, $v^{**} = v^{**}(v^*, v_R)$ is a potential between v^* and v_R (and consequently between v_m and v_R) and g_{NL} defines a non-linear conductance per unit area. Note that g_{NL} is implicitly a function of v_m and is zero when $v_m = v_R$. Thus, equations (2.38) and (2.39) combined give

$$J_M = g_M (v_m - v_R) + g_{NL} (v_m - v_R), \quad (2.40)$$

which neatly separates the linear contribution to membrane potential from the non-linear contribution. The constant conductance per unit area, g_M , can be associated with non-gated ion channels (or at least those that are open at rest), and resting state pumping currents, while g_{NL} can be associated with voltage-gated ionic currents and activity-dependent transport processes. The dendritic segment membrane is said to be *passive* if $g_{NL} = 0$, otherwise it is *active*. Conductance g_{NL} may also be referred to as the active conductance.

The general cable equation (2.16) can be re-written using equations (2.17), (2.36) and (2.40), to give

$$C_M \frac{\partial v_m(x, t)}{\partial t} = \frac{1}{P(x)} \frac{\partial}{\partial x} \left(\frac{A(x)}{\rho_i} \frac{\partial v_m(x, t)}{\partial x} \right) - g_M (v_m - v_R) - g_{NL} (v_m - v_R) - J_{SC} + J_{IC}. \quad (2.41)$$

It is convenient to work with the potential relative to the resting potential, v , given by

$$v(x, t) = v_m(x, t) - v_R, \quad (2.42)$$

so that, if the dendritic membrane is in a resting state then $v = 0$. Since v_R has been assumed constant, the cable equation (2.41) now becomes

$$C_M \frac{\partial v(x, t)}{\partial t} = \frac{1}{P(x)} \frac{\partial}{\partial x} \left(\frac{A(x)}{\rho_i} \frac{\partial v(x, t)}{\partial x} \right) - g_M v(x, t) - g_{NL} v(x, t) - J_{SC} + J_{IC}. \quad (2.43)$$

From equations (2.7) and (2.42), and noting again that v_R is constant, the axial current can be written in terms of the deviation from resting potential,

$$i_a = -\frac{1}{r_i} \frac{\partial v}{\partial x}. \quad (2.44)$$

The General Linear Cable Equation

Returning to the general cable equation, one can obtain the most general form for a linear cable equation by assuming that all sources of transmembrane current only exhibit spatial and temporal dependence. Basically, ion channel conductances, $g^{(k)}(x, t)$, are voltage independent so that the contribution from the ion channel currents maintain the linearity of the differential operator. Similarly, synaptic conductances, $g_{syn}^{(k)}$, and consequently synaptic currents must maintain the linearity of the differential operator (e.g. the alpha function), as must pumping currents and, as usual, injected currents.

While the resulting equation is strictly linear, it is not considered passive since membrane properties may still vary. The equation traditionally thought of as *the* cable equation is a simplified version, with $g_{NL} = 0$, and additional geometrical constraints, as shown below. It is much more easily solved.

2.3 The Passive Linear Cable Equation

The linear cable equation for a uniform segment of passive dendrite is obtained from the cable equation (2.43), with the relevant geometrical simplifications given by equation (2.33)¹. There are no synaptic currents ($J_{SC} = 0$), the non-linear contribution to membrane conductance is zero ($g_{NL} = 0$), and applied currents are expressed as a line density, using equation (2.22). Thus, after a slight rearrangement,

$$c_m \frac{\partial v(x, t)}{\partial t} = \frac{1}{r_i} \frac{\partial^2 v(x, t)}{\partial x^2} - Pg_M v(x, t) + i_d(x, t). \quad (2.45)$$

This expression is strictly only valid where $|g_{NL}| \ll |g_M|$, that is, when the transmembrane potential does not deviate far enough from rest to open significant numbers of voltage gated channels. The validity of the expression for a particular neuron, or dendritic segment, depends entirely on the nature of any active conductances, and the threshold potentials at which they are strongly activated. The linear cable equation effectively describes sub-threshold neuronal activity, although it should be noted that some active conductances, i.e. significant non-linearities, may be activated very rapidly at low threshold.

In its own right, the linear cable equation describes membrane where the ionic currents flow through a constant population of open ion channels; any pumping mechanisms contribute a constant current. At the resting membrane potential, these currents are balanced. Synaptic input currents must now only be modelled using the linear exogenous current injection term, i_d , and not as conductance changes.

Note again that the segment has not been assumed cylindrical, as is conventional. Such

¹A passive non-uniform segment would be described if the assumption of uniformity had not been made.

a condition is unnecessary, as the equations are of the same fundamental form whether the cross-section is circular or not.

Another Form of the Linear Cable Equation

The membrane conductance is often expressed as a conductance per unit axial length of segment, g_m , where

$$g_m = g_M P = \frac{1}{r_m}, \quad (2.46)$$

and r_m is the membrane resistance of a unit (axial) length of cylinder.

Finally, the linear cable equation (2.45) for a uniform dendritic segment of length l can be multiplied through by r_m , and reformulated as

$$\frac{r_m}{r_i} \frac{\partial^2 v(x, t)}{\partial x^2} = r_m c_m \frac{\partial v(x, t)}{\partial t} + v(x, t) - r_m i_d(x, t), \quad 0 < x < l, \quad t > 0, \quad (2.47)$$

where, to re-cap, at position x and time t , $v(x, t)$ is the transmembrane potential with respect to the segment's uniform resting potential, $i_d(x, t)$ is a current line density applied directly into the core medium, r_m is the membrane resistance of a unit length of segment, r_i is the resistance of the intracellular medium per unit length of segment, c_m is the membrane capacitance per unit length of segment. To summarise, the three important electrical parameters are given by

$$r_i = \frac{\rho_i}{A}, \quad r_m = \frac{1}{g_M P}, \quad c_m = C_M P. \quad (2.48)$$

Circuit Analogy

The linear cable equation (2.47) is traditionally derived by considering a circuit diagram. The membrane is treated as a discrete network of parallel capacitance and resistance connecting the isopotential extracellular compartment to the resistive core compartment. Current is conserved in the segment of infinitesimal length Δx , and the limit is taken. For details see, for example, Tuckwell (1988a).

2.4 The Dimensionless Linear Cable Equation

2.4.1 Electrotonic Units

The linear cable equation (2.47) can be simplified even further by rewriting it in terms of dimensionless, or *electrotonic* units, which are measures of space and time that characterise the steady-state electrical properties of a passive uniform segment.

Electrotonic Length

Axial resistance is expressed *per unit length* by r_i , while membrane resistance is expressed *times unit length* by r_m . Consider the length of segment, denoted λ , for which the core axial resistance is matched to the membrane resistance,

$$r_i\lambda = \frac{r_m}{\lambda} \quad (2.49)$$

so that, using equations (2.48),

$$\lambda = \sqrt{\frac{r_m}{r_i}} = \sqrt{\frac{A}{g_M \rho_i P}}. \quad (2.50)$$

This characteristic length, determined by electrical and geometrical properties of both core and membrane, is known as the *electrotonic space constant*, though significantly it actually varies with the cross-sectional profile.

Electrotonic length is essentially a measure of the electrical compactness of a uniform dendritic segment. This is better illustrated by considering steady-state solutions of the cable equation. The steady-state cable equation is obtained by setting the time derivative to zero in the linear cable equation (2.47), and ignoring the time dependence, thus

$$\frac{r_m}{r_i} \frac{\partial^2 v(x)}{\partial x^2} = v(x). \quad (2.51)$$

Take a semi-infinite cylinder with diameter d and apply a constant current boundary condition, $i_a(0, t) = i_0$, at terminal $x = 0$ for a time long enough so that a steady state is achieved, and a constant potential v_0 is evolved. Let $v(x) \rightarrow 0$ as $x \rightarrow \infty$ be the second boundary condition (boundary conditions are considered in more detail in section 2.5). The steady-state solution is of the form

$$v(x) = v_0 e^{-x/\lambda}. \quad (2.52)$$

At $x = \lambda$, i.e. one space constant, the potential has decayed to $1/e$ of its value at $x = 0$.

Consider, for example, the two semi-infinite cylinders, with different diameters, illustrated in Figure 2.4. For cylindrical geometry, $A/P = d/4$, thus

$$\lambda = \frac{1}{2} \sqrt{\frac{d}{g_M \rho_i}}, \quad (2.53)$$

so the space constant varies with the square root of diameter. Other specific electrical properties being equal, a larger diameter implies a larger space constant so that, at the same physical distance from the terminal, the potential on the narrower cable experiences greater attenuation, and is considered more compact electrotonically.

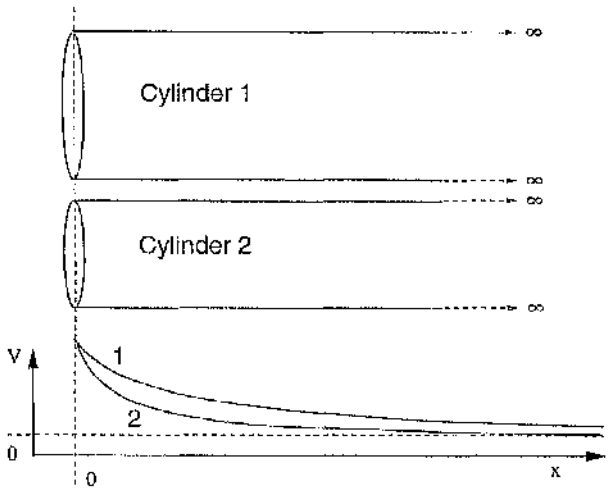


Figure 2.4: Electrical compactness of a semi infinite nerve cylinder.

Electrotonic Time

Consider a uniform segment of dendrite with passive membrane and transmembrane potential $v(x, t) = v(t)$ that is ensured uniform over the segment. There are no applied currents and the potential is initially non-zero, such that $v(0) = v_0$. This segment is described by the space-independent (space-clamped) cable equation,

$$r_m c_m \frac{\partial v(t)}{\partial t} = -v(t), \quad (2.54)$$

with solution,

$$v(t) = v_0 e^{-t/\tau_m c_m}. \quad (2.55)$$

The segment may be regarded as a capacitor that is discharging through the membrane. Current flows only radially as charge leaks across the membrane in such a way that the potential has decayed to $1/e$ of its initial value after characteristic time, τ , given by

$$\tau = r_m c_m = \frac{C_M}{g_M}. \quad (2.56)$$

This is the *membrane time constant*, determined entirely by properties of the membrane, not the core.

Re-expressing the Linear Cable Equation

Dimensionless electrotonic length, X , and time, T , are given in units of the space constant and time constant, respectively

$$X = \frac{x}{\lambda}, \quad T = \frac{t}{\tau}. \quad (2.57)$$

All electrical quantities can be re-expressed in terms of electrotonic units, and are written in upper case in this chapter to distinguish them from their dimensional counterparts. The transmembrane potential (with respect to the resting potential), is

$$V(X, T) = v(x, t). \quad (2.58)$$

In terms of units and magnitude, V and v are identical. Note the following transformations,

$$\frac{\partial v}{\partial t} = \frac{\partial V}{\partial T} \frac{dT}{dt} = \frac{1}{\tau} \frac{\partial V}{\partial T}, \quad (2.59)$$

$$\frac{\partial v}{\partial x} = \frac{\partial V}{\partial X} \frac{dx}{dx} = \frac{1}{\lambda} \frac{\partial V}{\partial X}, \quad (2.60)$$

$$\frac{\partial^2 v}{\partial x^2} = \frac{1}{\lambda^2} \frac{\partial^2 V}{\partial X^2}. \quad (2.61)$$

Re-expressed in electrotonic units, using equations (2.48) and (2.50), axial current, equation (2.44), becomes

$$I_a(X, T) = -\frac{1}{r_i} \frac{\partial V(X, T)}{\partial X} \frac{dX}{dx} = -\frac{1}{\lambda r_i} \frac{\partial V(X, T)}{\partial X} = -U \frac{\partial V(X, T)}{\partial X}, \quad (2.62)$$

where U , referred to as the *u-value* (with units ohm^{-1} , i.e. a conductance), is a product of electrical (E) and geometrical (G) parameters, i.e. $U = EG$, where

$$E = \sqrt{\frac{g_M}{\rho_i}}, \quad \text{and} \quad G = \sqrt{AP}. \quad (2.63)$$

Re-expressed in electrotonic units, charge injected into dendritic segment $[0, X]$ over time interval $[0, T]$ is given by

$$Q_A(X, T) = q_A(x, t). \quad (2.64)$$

From equation (2.29), the applied current line density may be rewritten

$$i_d(x, t) = \frac{\partial^2 Q_A(X, T)}{\partial X \partial T} \frac{dX}{dx} \frac{dT}{dt} = \frac{1}{\lambda \tau} \frac{\partial^2 Q_A(X, T)}{\partial X \partial T}. \quad (2.65)$$

It is convenient to define an electrotonic current density which has no geometry dependence,

$$I_d(X, T) = \frac{\partial^2 Q_A(X, T)}{\partial X \partial T}, \quad (2.66)$$

since, as will emerge later, its behaviour can be directly related to that of the actual applied currents. A point current source, $i_A(t)$, injected at some point along the segment, can be written

$$I_A(T) = i_A(t). \quad (2.67)$$

Finally, substitute for x , t , $v(x, t)$ and $i_d(x, t)$ in the cable equation (2.47) using equations (2.59) and (2.61) to alter the derivatives, (2.58) to alter the voltage, then (2.65) and (2.66) to alter the applied current term. This yields the dimensionless cable equation for a uniform segment, with time constant τ and space constant λ , and electrotonic length $L = l/\lambda$,

$$\frac{\partial^2 V(X, T)}{\partial X^2} = \frac{\partial V(X, T)}{\partial T} + V(X, T) - \frac{I_d(X, T)}{\tau U}, \quad 0 < X < L, \quad T > 0, \quad (2.68)$$

where, to re-cap, at electrotonic length X and electrotonic time T , $V(X, T)$ is the transmembrane potential with respect to the resting potential, $I_d(X, T)$ is an electrotonic current density (charge applied per unit electrotonic length per unit electrotonic time), and U is a constant for the uniform segment.

Uniform Segments or Uniform Cylinders?

In neuronal modelling, cable theory is almost invariably used just to describe cylindrical dendritic segments. For a cylinder with diameter d ,

$$G = \frac{\pi d^{3/2}}{2}, \quad (2.69)$$

and the dimensionless cable equation can be written

$$\frac{\partial^2 V(X, T)}{\partial X^2} = \frac{\partial V(X, T)}{\partial T} + V(X, T) - \Omega \frac{I_d(X, T)}{c}, \quad (2.70)$$

where

$$\Omega = \frac{2}{\pi \tau E}. \quad (2.71)$$

For convenience, an alternative geometrical parameter is used, i.e. the three halves power of diameter which is commonly encountered term when dealing with passive cylinders,

$$c = d^{3/2}, \quad (2.72)$$

where c will be referred to as the *c-value* (terminology introduced in Ogden *et al.*, 1999).

In this case, the segment electrical parameters may be written

$$r_i = \frac{4\rho_i}{\pi d^2}, \quad r_m = \frac{1}{g_M \pi d}, \quad c_m = C_M \pi d, \quad \lambda = \frac{1}{2} (g_M \rho_i)^{-\frac{1}{2}} \sqrt{d}, \quad \tau = \frac{C_M}{g_M}. \quad (2.73)$$

Note the diameter dependence of all parameters except the time constant.

It should be noted that all results and methods that have been developed over the years for the cylindrical case are equally valid, perhaps with very slight modifications, for the more general uniform segment case.

The general form is also valid for equivalent cable construction, however, although the spatial structure of a dendritic tree is collapsed, the methods used require that the temporal properties of the membrane, embodied in τ , are constant for all segments used to represent a complete dendritic tree.

2.5 The Multiple Segment Model of a Dendritic Tree

2.5.1 Introduction

A dendritic tree can be represented by a number of non-uniform segments, enough to connect all branch points and mark all terminals. However, it is much more common to find that a multi-cylinder representation is used. An arbitrary number of these uniform cylinder building blocks, generally with different diameters, can be placed together to form features such as tapering and branching. As a consequence, rather than a particular branch being modelled by a single general cable equation (2.16), it is described by a set of cylinders that are each described by a geometrically simplified cable equation (2.34). Each model branch therefore has a piecewise uniform, rather than continuous, diameter profile.

Computer modelling of dendritic trees was pioneered by Rall (1964), who adapted *compartmental modelling*. With compartmental models, a tree is essentially represented by an arbitrary number of cylinders. However, instead of modelling each cylinder with a cable equation, they are assumed to be isopotential compartments linked by axial resistances. Each compartment is described by the space-clamped cable equation (2.54) (with additional synaptic, ionic, injected currents), a first order ordinary differential equation. The model is integrated in time using finite difference schemes. (For details of compartmental models see, e.g. Perkel and Mulloney, 1978a, 1978b; Edwards and Mulloney, 1984; Hines, 1984; Segev *et al.*, 1989; Lindsay *et al.*, in press).

In the limit, as compartment size decreases and the number of compartments increases, the compartmental model tends to produce the same results as the cable model. However, compartmental modelling (which is regularly used) is distinguished from *cable modelling* (rarely used for numerical purposes) because if a limited number of isopotential compartments are used, the tree geometry is not well represented. If each cylinder is modelled by a cable equation, the full influence of geometry can be accounted for. It is in fact perfectly feasible to perform computer simulations of the non-uniform cable model using spectral methods (e.g. Lindsay *et al.*, in press; Canuto *et al.*, 1990) which have numerical properties that are far superior to those of the traditional finite difference schemes employed in compartmental modelling (e.g. Mascagni, 1989).

2.5.2 Modelling Using Real Data

When morphological data, typically consisting of branch lengths and diameters (plus branching angles and three-dimensional orientation in some circumstances, though this information is not required here), obtained by sampling the real tree at a suitable number of points, is acquired from a real neuron and used to build a model tree, it is given to some level of resolution dependent upon the experimental measuring procedure. Dimensional constraints have thus automatically been placed on the model, so that any variation in branch lengths and diameters within a certain bound cannot really be considered alterations at the level of the model. However, at the level of resolution typically obtained, it is reasonable to suspect that the essential morphological variation is well represented by the data.

There are additional constraints on the electrical properties of the model. While it is possible to examine a neuron at the single channel level to obtain local information about the membrane properties, it is difficult to determine accurately how membrane properties vary over the whole neuron membrane. A lot of assumptions must be made about ion channel densities, and distribution of synaptic inputs.

There is also the question of how to represent terminals, and what sort of terminal boundary conditions to apply. Should a terminal be represented by a narrowing chain of short segments, or a single abrupt terminal cylinder (and does it really matter given the model resolution). Does the terminal leak a significant current, or can it be considered leak-free.

Model detail (physical structure, membrane properties, numerical accuracy) must eventually balance with computational cost (time, storage) when it comes to actually running computer simulations.

When dealing with a computer model of a dendritic tree, whether for simulation or equivalent cable construction purposes, it is necessary to replace the real data with approximations suitable for computer implementations. Suppose the physical lengths of the segments that make up the original tree data are denoted l_1, l_2, \dots, l_n . The corresponding electrotonic lengths are denoted L_1, L_2, \dots, L_n . Associated with each electrotonic length, L_j is an error ϵ_j which embodies errors in measuring the length and the cross-sectional profile of the dendritic segment. We want to choose a suitably small quantum length L such that

$$|L_k - m_k L| \leq \epsilon_k, \quad 1 \leq k \leq n, \quad (2.74)$$

where m_1, m_2, \dots, m_n are integers. Each measured electrotonic length, L_k , can therefore be replaced by a model electrotonic length, $m_k L$, that is an integral multiple of the quantum length. The two lengths are identical within the level of resolution afforded by the

data. More details are given in Lindsay *et al* (in press).

Incorporating Spines

If a segment of dendritic tree is covered in spines, the spines will contribute significantly to the electrotonic properties of the tree. Spines can be modelled explicitly as small branches; alternatively, physical or electrical properties of dendritic segments can be adjusted to account for the membrane surface area of spines (Stratford *et al.*, 1989; Holmes, 1986; Holmes and Woody, 1989; Rall *et al.*, 1992 summarise the methods). This thesis is not concerned with the non-passive properties of spines.

2.5.3 Obtaining Solutions for a System of Cable Equations

This thesis is not concerned directly with solving a set of cable equations for an arbitrarily branched tree. Many methods are available for this task, and many computer modelling suites implement numerical procedures.

In particular, there are several analytical methods now available for solving the linear cable equations that describe a multi-cylinder passive tree model. The steady state system was solved by Rall (1959). For the time-dependent problem, Butz and Cowan (1974) introduced a graphical method based on Laplace transforms that could handle arbitrary geometry; this approach was extended by Horwitz (1981, 1983); Kawato and Tsukabara (1983) adapted it for dendrites with spines. Tuckwell (1988a) has presented several steady-state and time-dependent solutions to cable equations. Abbot *et al.* (1991), introduced a path integral approach (see also Abbot, 1992; Cau and Abbot, 1993).

There are many recent papers that present analytically derived series solutions in terms of eigenfunctions of the system. The various papers deal with different boundary and initial conditions and tree geometries: Major (1993); Major *et al.* (1993a); Major *et al.* (1993b); Major and Evans (1994); Evans and Kember (1998); Evans *et al.* (1992); Evans *et al.* (1995); Kember and Evans (1995).

Numerical procedures are generally of more practical use, since they are not restricted to the linear cable model. Several computer programs are available that have either been written specifically with neuron simulation in mind, or can be adapted for such use (e.g. NEURON, NODUS, Genesis, SPICE). De Schutter (1992) provides an overview of this software. (Note, however, that simulation using spectral methods is superior to compartmental modelling in most respects and should become more prevalent as the modelling community becomes more familiar with them; see Lindsay *et al.*, in press).

Despite the variety of methods now available, the large number of possible input configurations for any one simulation mean it is difficult to use these methods to get any

insight into how geometry shapes the full range of electrical activity over a neuron.

2.5.4 Tree Structure Terminology

Here we define the terminology used to describe features of multi-cylinder dendritic structure. This should help to avoid any possible confusion, though most terms are fairly obvious in their meaning. Figures 2.5a–b illustrate the use of terms that are not specific to the multi-cylinder model, i.e. that can describe features of any tree, while Figure 2.5c describes features characteristic of the multi-cylinder model.

A complete dendritic tree, formed from a set of cylinders (or uniform segments) of various lengths and diameters is often referred to simply as a *tree*. Several trees may connect to a single neuron's soma. Note that the distance between two points on a tree is measured along the shortest, non-recursive, axial path within the tree. Furthermore, physical length (and consequently electrotonic length) is measured along such a path, always increasing away from the soma.

A point on a tree where three or more cylinders meet is called a *branch point* or *junction*; a three cylinder junction is called a *binary branch point*. Of the cylinders that meet at the branch point, that nearest the soma is the *parent cylinder*, the others are known as *child cylinders*. The point where two cylinders meet is called a *diameter step*. A point that marks the end of one cylinder, and is not associated with any other cylinders, is called a *terminal*.

The term *branch* itself refers to a segment of tree that connects one branch point to another or one branch point to a terminal. Of the branches that meet at a branch point, that nearest the soma is the *parent branch*, the others are called *child branches*. It is possible that a cylinder constitutes an entire branch.

Each tree has a *branching order* defined as the maximum number of branch points encountered in a non-recursive path starting at the soma, and ending on a terminal, moving away from the soma at all times. An unbranched structure therefore has branching order 0. Each branch or cylinder in a tree can also be assigned a branching order, i.e. the number of branch points that are encountered on a direct path from soma to the branch or cylinder. A structure with branching order one, the single branch point being binary, is called a *Y-junction*. It consists of a parent branch (optional) connected to two child branches, usually referred to as *left* and *right*.

Take any branch and isolate a cylinder on it. This cylinder plus the entire section of the tree connected to it, and further from the cell body than it, is called a *sub-tree*, or *dendritic sub-structure*. Any two cylinders in a sub-tree are linked by path along a subset of the cylinders that form the sub-tree. The tree branch that connects to the cell body is called the *trunk*. The branch at the root of a sub-tree is referred to as the trunk of that

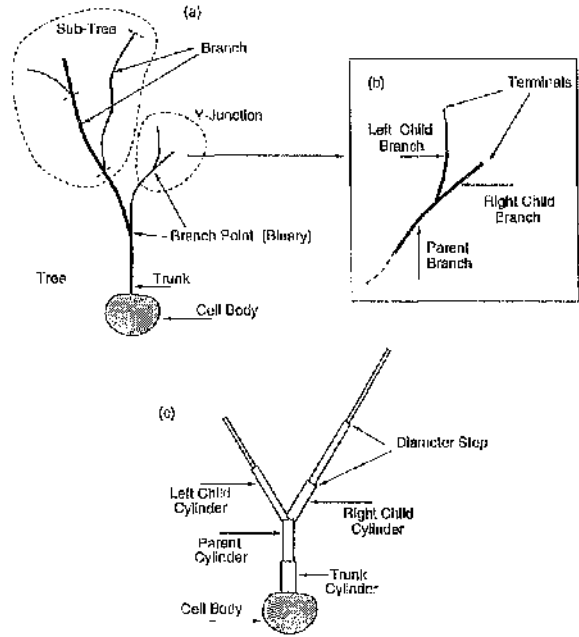


Figure 2.5: Dendritic tree model terminology. (a) General tree terminology. (b) Y-junction terminology (c) Multi-cylinder terminology. See text for full details.

sub-tree. Similarly, there will be trunk cylinders, and sub-tree trunk cylinders.

2.5.5 Initial and Boundary Conditions

If one's aim is to solve the set of cable equations describing a complete tree, the initial electrical state of the segments must be specified, as must the physical boundaries and the nature of the electrical activity at these boundaries. Voltage continuity and currents conservation conditions must be applied where dendritic segments connect, i.e. at branch points, or where diameter is discontinuous. It will become clear in later chapters that equivalent cable construction, on the other hand, only requires knowledge of boundary conditions (even then no representation of the soma is usually required, and only the general type of terminal need be known).

The following conditions are given in physical units. For the passive tree model, electrotonic forms of the conditions acceptable for equivalent cable construction are given later.

Initial Conditions

Initial conditions constitute a specified transmembrane potential distribution,

$$v(x, 0) = v_0(x). \quad (2.75)$$

General Terminal Condition

Consider a dendritic segment with length l , terminated at $x = 0$ and $x = l$. The trans-membrane potential at the terminal is $v_m(l, t)$; a current $i_A(t)$ is also injected. The total current flow out from the terminal must be $i_a(l, t) + i_A(t)$. This current is assumed to be driven, by deviations from the resting potential, $v(l, t)$, across a terminal with leakage conductance g_T , thus

$$i_a(l, t) + i_A(t) = g_T v(l, t). \quad (2.76)$$

Rewriting the axial current contribution using equation (2.44) gives an alternative form of this boundary condition,

$$\frac{1}{r_i} \frac{\partial v(l, t)}{\partial x} + g_T v(l, t) = i_A(t). \quad (2.77)$$

If a similar condition is imposed at $x = 0$ then, because of conventions for the direction of current flow, the current leaking from the terminal is $-i_a(0, t) + i_A(t)$, thus

$$-i_a(0, t) + i_A(t) = g_T v(0, t), \quad (2.78)$$

and so

$$-\frac{1}{r_i} \frac{\partial v(0, t)}{\partial x} + g_T v(0, t) = i_A(t). \quad (2.79)$$

Under certain assumptions this general boundary condition collapses to the following more commonly used conditions.

General Current Injection Condition

If a generally time-dependent axial current is specified at segment boundary $x = l$, and no current may leak from the terminal, so that $g_T = 0$ in equation (2.76), then

$$i_a(l, t) = -\frac{1}{r_i} \frac{\partial v(l, t)}{\partial x} = -i_A(t). \quad (2.80)$$

The minus sign appears because injected current is constrained to flow in the direction of decreasing x . Similarly, at $x = 0$, equation (2.78) gives

$$i_a(0, t) = -\frac{1}{r_i} \frac{\partial v(0, t)}{\partial x} = +i_A(t). \quad (2.81)$$

In this case injected current is constrained to flow in the direction of increasing x .

A zero terminal conductance is equivalent to an infinite terminal resistance to axial current flow. Thus, from equation (2.6), this condition is equivalent to a sudden drop in cross-sectional surface area to zero.

Sealed End Condition

The sealed end condition is the special case of the general current injection condition (2.80) or (2.81) where no current is actually applied,

$$i_A(t) = 0, \quad (2.82)$$

so that

$$i_a(l, t) = 0 \quad \text{or} \quad i_a(0, t) = 0, \quad (2.83)$$

This is often taken as the natural terminal condition for dendritic tips. Essentially, no current leaks from the terminal.

Cut End Condition

The cut end (or killed end) condition is obtained from (2.76) by letting $g_T \rightarrow \infty$, thus

$$v(l, t) = 0 \quad \text{or} \quad v(0, t) = 0, \quad (2.84)$$

depending on the terminal subject to the boundary condition. The transmembrane potential at the terminal is equal to the segment's resting potential.

This is not strictly a short circuit across the membrane, in which case the actual transmembrane potential at the terminal would be zero. However, there is essentially no axial resistance to currents that would move the potential at the terminal away from rest. Equation (2.6) suggests that a cut terminal may be regarded as a point where the segment surface area jumps abruptly to infinity.

Joining Conditions

If the parent segment (p) has length l_p and is connected to n child segments (c_1, \dots, c_n) then the voltage continuity condition at the branch point can be expressed

$$v_p(l_p, t) = v_{c_k}(0, t), \quad (2.85)$$

for all child cylinders $1 \leq k \leq n$. Denote axial current in segment j by $i_{a,j}$. Conventions for direction of axial and exogenous injected currents requires that at the branch point

$$i_{a,p}(l_p, t) + i_A(t) = \sum_{k=1}^n i_{a,c_k}(0, t), \quad (2.86)$$

where $i_A(t)$ is current injected into the junction and the sum is over all child segments.

The Soma Boundary Condition

To complete the model (ignoring the axon), it is necessary to attach the dendritic tree to a representation of the soma. Most commonly, a point representation is used. The soma membrane has surface area A_S , capacitance per unit area C_S , and transmembrane potential v_S .

Suppose that m dendritic trees segments are attached to the soma. Segment j has transmembrane potential $v_j(x)$ and cross-sectional area $A_j(x)$. Voltage continuity requires that $v_S(t) = v_1(0, t) = v_2(0, t) = \dots = v_m(0, t)$. The axial current in segment j is denoted $i_{a,j}$. Suppose also that J_S is the total current density (per unit area) flowing *out from* the soma across the membrane. The total amount of charge then flowing *into* the soma is

$$-J_S A_S - \sum_{j=1}^m i_a^{(j)}(0, t) = -J_S A_S + \sum_{j=1}^m \frac{A_j(0)}{\rho_i} \frac{\partial v_j(0, t)}{\partial x}. \quad (2.87)$$

This must balance the somal capacitive current, so

$$A_S C_S \frac{\partial v_S(t)}{\partial t} = -J_S A_S + \sum_{j=1}^m \frac{A_j(0)}{\rho_i} \frac{\partial v_j(0, t)}{\partial x}. \quad (2.88)$$

The current density J_S may consist of voltage dependent ionic currents, synaptic currents, pumping currents and exogenous injected currents. It can be expressed in a similar manner to the segment transmembrane current J_T , with synaptic, injected, ionic and pumping components. The reduction in soma surface area where dendrites connect has not been accounted for, but is easily done so by replacing A_S with $A_S - \sum_j A_j(0)$.

2.5.6 The Passive Multi-Segment Tree Model

The passive multi-segment tree model, valid for the construction of fully equivalent cables, is now summarised.

A tree is represented by an arbitrary number of uniform segments. Associated with each cylinder j is a surface area, A_j , a perimeter P_j , a space constant λ_j , a physical length l_j , a potential V_j , an applied current density $I_{d,j}$, and electrotonic length $L_j = l_j/\lambda_j$. Furthermore, there is a u-value $U_j = E_j G_j$.

From equation (2.70), the electrical characteristics of cylinder j are described by the dimensionless linear cable equation,

$$\frac{\partial^2 V_j(X, T)}{\partial X^2} = \frac{\partial V_j(X, T)}{\partial T} + V_j(X, T) - \frac{I_{d,j}(X, T)}{\tau U_j}, \quad 0 < X < L_j, \quad T > 0. \quad (2.89)$$

Axial current for cylinder j is denoted $I_{a,j}(x, t)$, so equation (2.62) is

$$I_{a,j}(X, T) = -U_j \frac{\partial V_j(X, T)}{\partial X}. \quad (2.90)$$

Only the following boundary conditions are valid for equivalent cable construction.

General Current Injection Condition

The current injection condition, equation (2.80), becomes

$$I_a(L, T) = -U \frac{\partial V(L, T)}{\partial X} = -I_A(T). \quad (2.91)$$

Similarly, at $x = 0$, equation (2.81) becomes

$$I_a(0, T) = -U \frac{\partial V(0, T)}{\partial X} = I_A(T). \quad (2.92)$$

Sealed End Condition

The sealed end condition, equation (2.83), is the special case of the general current injection condition (2.91) where no current is actually applied,

$$I_a(L, T) = 0 \quad \text{or} \quad I_a(0, T) = 0, \quad (2.93)$$

depending on the terminal subject to the boundary condition.

Cut End Condition

In electrotonic units, the cut end condition (2.84) is

$$V(L, T) = 0 \quad \text{or} \quad V(0, T) = 0, \quad (2.94)$$

depending on the terminal subject to the boundary condition.

Joining Conditions

If the parent cylinder (p) is connected to n child cylinders (c_1, \dots, c_n), then the voltage continuity condition in electrotonic form is

$$V_p(L_p, T) = V_{c_k}(0, T), \quad (2.95)$$

for all k where $1 \leq k \leq n$.

Conventions for the direction of axial and exogenous injected currents requires that at the branch point

$$I_{a,p}(L_p, T) + I_A(T) = \sum_{k=1}^n I_{a,k}(0, T), \quad (2.96)$$

where $I_A(t)$ is current injected into the junction and the sum is over all child cylinders k that meet parent cylinder p at the junction.

To ensure that this passive tree model is suitable for equivalent cable construction, it is only necessary to insist that τ is constant over the whole tree, i.e. the quantity C_A/g_M

is constant over the tree. Cylinder c -values ($3/2$ power of diameter), which have a more immediate physical interpretation than the u -values. Thus we shall formulate the passive multi-cylinder model with homogeneous specific electrical parameters.

2.5.7 The Passive Multi-Cylinder Tree Model

We assume that the specific electrical constants for dendritic cylinders, g_M , ρ_i , and C_M , are identical for each cylinder used to represent the tree. Consequently, τ must be constant, as must E . It has already been shown in equation (2.48) that c_m , r_m , r_i , and λ_i equation only have a diameter dependence over the tree.

From equation (2.70), the electrical characteristics of cylinder j are described by the dimensionless linear cable equation,

$$\frac{\partial^2 V_j(X, T)}{\partial X^2} = \frac{\partial V_j(X, T)}{\partial T} + V_j(X, T) - \Omega \frac{I_{d,j}(X, T)}{c_j}, \quad 0 < X < L_i, \quad T > 0. \quad (2.97)$$

Axial current for cylinder j is

$$I_{a,j}(X, T) = -K c_j \frac{\partial V_j(X, T)}{\partial X}, \quad (2.98)$$

where

$$K = \frac{1}{\Omega \tau} = \frac{\pi}{2} \sqrt{\frac{g_M}{\rho_i}}. \quad (2.99)$$

2.5.8 Typical Electrical Parameters in a Tree

The membrane capacitance per unit area, C_M , is usually assumed to be $1.0 \mu\text{Fcm}^{-2}$. Intracellular resistivity, ρ_i , may range around $50\text{--}100 \Omega/\text{cm}$. Membrane resistance per unit surface area ($1/g_M$) is not easily determined accurately, but typically is assumed to fall within the range 5,000 to 100,000 Ωcm^2 . Rall *et al.* (1992) outline methods for parameter estimation.

2.5.9 The Tree Model Surface Area

The membrane surface area of uniform dendritic segment j , with length l_j and perimeter P_j , is

$$s_j = P_j l_j. \quad (2.100)$$

In terms of electrotonic length, where $L_j = l_j/\lambda_j$, this becomes

$$s_j = P_j \lambda_j L_j. \quad (2.101)$$

The total surface area, S_ξ of tree ξ , is

$$S_\xi = \sum_j s_j, \quad (2.102)$$

where the sum is over all segments used to represent the tree.

Now, suppose all segments have the same physical length, l , the total surface area is given by

$$S_\xi = l \sum_j P_j. \quad (2.103)$$

If all segments have the same electrotonic length, L , total surface area is given by

$$S_\xi = L \sum_j P_j \lambda_j. \quad (2.104)$$

If the uniform segment is cylindrical, and electrical properties are constants for the tree, then $P_j \lambda_j = \pi c_j / 2\sqrt{g_M \rho_i}$, and

$$S_\xi = \frac{\pi}{2\sqrt{g_M \rho_i}} \sum_j c_j. \quad (2.105)$$

Essentially, the surface area of a unit electrotonic length of segment is proportional to its c-value. The sum of the c-values can be used as a measure of tree membrane surface area.

2.6 Electrical Activity in Simple Passive Structures

2.6.1 Passive Signal Propagation

Electrical input on a passive dendritic tree will, geometry permitting, induce changes in the membrane potential at structure nearer and further from the soma than the input site. These effects are carried by charges spreading axially as equilibrium is sought. A transient current input, for example, causes a transient change in membrane potential at the input location. The magnitude of this effect decays in time, as charge moves both across the membrane (radially) and through the branching tree system (axially), causing changes in the membrane potential at all points in the tree. The distance of a point on the tree from the input site, as well as overall tree geometry and the electrical properties of tree membrane and core, determine the strength and time course of the response at this point. Dendritic geometry and terminal boundary conditions can have a major influence on the spread of charge at points such as terminals, branch points and changes in diameter. Recall again that a general current injection condition is analogous to a drop in diameter to zero, while a cut condition is analogous to a sudden jump of diameter to infinity — charge may flow unhindered from the terminal.

2.6.2 Impedance Matching

Impedance matching is a useful concept. Two adjacent structures on a dendritic tree are impedance matched if a charge imbalance that has accumulated at the contact point

disperses equally into both. Essentially, there is equal immediate (local) impedance to current flow into both structures.

For example, any point on a uniform infinite cylinder represents an impedance matched structure and consequently an electrical input generates a voltage distribution that is symmetric about the input site. Impedances are not matched at terminals and abrupt diameter changes. At branch points, where more than two cylinder meet, it is possible that subsets of the cylinders are impedance matched. Where impedances are not matched, which is likely in real neurons, structures with lower impedances (larger diameters) receive more of the accumulated charge.

2.6.3 Steady State Solutions of the Cable Equation

It is helpful to illustrate impedance matching by considering the steady state solution for constant current injected at the point where two semi-infinite cylinders connect. In Figure 2.6a, two such cylinders are illustrated. Figure 2.6b shows that the voltage response in physical space is unsymmetric about the contact point. If x is measured increasing away from the discontinuity for both cylinders, the solutions in each cylinder are,

$$v_1(x) = v_0 e^{-x/\lambda_1} \quad \text{and} \quad v_2(x) = v_0 e^{-x/\lambda_2}. \quad (2.106)$$

The voltage decays with a shorter space constant in the narrower cylinder. However, if the response is drawn in electrotonic space, Figure 2.4c, it is symmetric about the contact point, since

$$V_1(X) = V_2(X) = V_0 e^{-X}. \quad (2.107)$$

Current conservation at the discontinuity means that

$$I_A(T) = -Kc_1 \left. \frac{\partial V_1}{\partial X} \right|_{x=0} - Kc_2 \left. \frac{\partial V_1}{\partial X} \right|_{x=0}. \quad (2.108)$$

Since K is constant and the voltage response profiles are identical in electrotonic space, then the ratio of the currents flowing into each cylinder is the ratio of c -values. (This generalises to the u -values for uniform segments with different electrical and geometrical properties.)

Now consider a binary branch point where three semi-infinite cylinders (denoted parent, left and right) connect. In each cylinder, x increases away from the branch point. Again, the voltage responses in each cylinder are identical in electrotonic space (though in physical space they will depend on the diameter). The ratio of current flowing into any two cylinders depends on their relative c -values. Thus, the same amount of current flowing into the left and right cylinders will equal that flowing into the parent only when $c_P = c_L + c_R$.

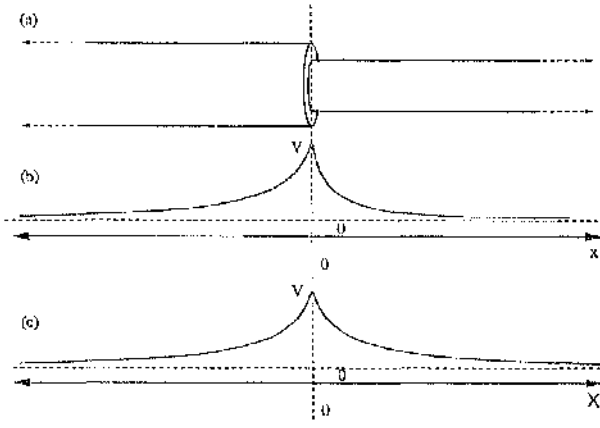


Figure 2.6: Steady state response in two connected semi-infinite cylinders.

Consider a set of connected cylinders. One sub-set of these cylinders is impedance matched with the remaining sub-set if the sum of c -values for each sub-set is equal.

2.6.4 Steady-State Input Conductance

The *steady-state input conductance*, G_{in} with respect to a specific point on a branched tree structure, is the ratio of steady input current (i_0) at the input site to the steady potential (v_0) evolved at the input site, thus

$$G_{in} = \frac{i_0}{v_0}. \quad (2.109)$$

For example, in the case of a semi-infinite cylinder, equations (2.44) and (2.55) give

$$G_{in} = \frac{1}{r_i \lambda} = \frac{1}{\sqrt{r_m r_i}}. \quad (2.110)$$

Rall (1959) gives a recursive procedure for evaluating G_{in} for any multi-cylinder passive tree.

2.6.5 Uniform Voltage Decay

Consider a complete multi-segment dendritic tree with arbitrary geometry but all terminals sealed. The tree is isopotential so that no axial currents flow. A similar analysis to that for the single dendritic segment (Section 2.4.1) reveals that this voltage decays with characteristic time constant τ . The total capacitive discharge current flow is

$$C_M \frac{\partial v(t)}{\partial t} \sum_i P_i l_i = C_M \frac{\partial v(t)}{\partial t} \sum_i s_i. \quad (2.111)$$

where the sum is over all dendritic segments that form the tree. The current is proportional to the surface area.

2.7 Requirements for Equivalent Cable Construction

Although cable construction theory is valid for passive uniform segments (provided the membrane time constant is actually a constant for the whole tree), the rest of this thesis is developed from just the dimensionless passive linear cable equation for cylindrical geometry (2.97), the corresponding equation for axial current (2.98), expressions for cut and current injection terminal boundary conditions (2.91, 2.93, and 2.94), plus voltage continuity and current conservation joining conditions (2.95 and 2.96). Bulk electrical parameters C_M , g_M and ρ_i are taken to be constant.

If required, cable results could be extended quite naturally from cylinders to segments, with u -values replacing c -values. Thus there is some flexibility in the choice of electrical parameters g_M , ρ_i , and C_M , and geometrical parameters A and P which may vary between segments provided a constant membrane time constant (C_M/g_M) is maintained.

The measures of surface area, steady-state input conductance, and the idea of a uniform potential over a completely sealed tree decaying uniformly, are introduced because they are significant whole-tree properties that must be conserved during equivalent cable construction for all, or important classes of, model trees.

Chapter 3

Equivalent Cables

3.1 Introduction

Within the context of neuronal modelling, the term “equivalent cable” has been used to describe a variety of unbranched, and often non-uniform, *reduced models* which are “electrically equivalent”, in some sense, to an original dendritic tree model (or perhaps axonal tree model), and can thus be used to analyse its electrical properties and signal processing function. The motivation for developing these models has been the success of the original *equivalent cylinder* result (Rall, 1962b), which we describe in detail in section 3.3. In principle, the electrical properties of an unbranched structure can be analysed more easily than the original tree. If one can construct an unbranched structure that preserves many of the tree’s electrical properties, then it may be easier to gain some insight into its function, or estimate important electrical parameters. Rall showed how this could be done for a limited class of tree, and subsequent efforts have attempted to generalise his result.

Here we describe and compare the different cable models that have been proposed, then comment briefly on how they are constructed, and how they are used, i.e. primarily whole-cell electrical parameter estimation. We emphasise the fact that these cable models cannot be equivalent to the original tree model in a mathematical sense. We subsequently state a precise definition of equivalence that has a rigorous mathematical basis, and then describe the fully equivalent cables that were discovered by Whitehead and Rosenberg (1993) and which satisfy this definition. True mathematical equivalence between a tree model and an unbranched cable is a very powerful concept, and we consider some of the general insights that follow from this result. Existing quasi-equivalent cable models are also compared in light of the definition of equivalence. Three different methods for constructing these cables are briefly discussed; the full details, given in Chapters 4, 5, 6 and 7 form the bulk of this thesis. Significant general features concerning the shape and

boundary conditions of fully equivalent cables are also outlined, anticipating more detailed discussion and illustration, also given in these chapters and overviewed in Chapter 8.

It is important to note that, while the results given in this chapter assume, and were originally derived for, cylindrical dendritic segments, they can be shown to be valid for general uniform segments with non-circular cross-section, as was stressed in Chapter 2. The model equations have an essentially identical form.

In this chapter, in contrast to the previous chapter, for notational convenience lower case letters are used to represent electrotonic units and quantities expressed in terms of electrotonic units.

3.2 The Various Cable Models

An equivalent unbranched structure can only be constructed and compared to the dendritic tree it is supposed to represent provided one has a working definition of what is meant by "equivalence". Previous notions of equivalence has primarily been "needs-led", e.g. the need to reproduce results with the cable model that can be identified with results of an experimental procedure, such as a transient voltage response at the soma. Equivalence is typically measured with respect to the soma, and once a cable has been generated it is attached to the soma instead of the tree (that is, the model is replaced); ideally the two structures have identical electrical properties and thus represent identical electrical loads that are indistinguishable by the soma. In practice, the perceived notion of equivalence is often either geometrically and/or electrically restrictive (Rall 1962a, 1962b; Tuckwell, 1988a; Ohme and Schierwagen, 1998), or even approximate in nature (Fleshman *et al*, 1988; Stratford *et al*, 1989; Clements and Redman, 1989; Manor *et al*, 1991). The question "What constitutes true electrical equivalence?" is often unasked. It is easy to say this with hindsight, of course. It is most likely that, given the complexity of realistic geometry, it was assumed unlikely an exactly equivalent structure existed in general. Construction procedures for quasi-equivalent cables can differ markedly, are intimately linked to the definition of equivalence, and can be classified into two general types.

- (A) *Restricted Cables*: Equivalent cables that follow directly from the mathematical model of the dendritic tree, i.e. it is possible to prove that they meet some level of "equivalence". One imposes conditions, some of which are unrealistic, or at best rarely encountered, on the geometry of, and/or the electrical activity within, a dendritic tree, until the equivalent model falls out inevitably, via mathematical analysis, from the specified mathematical description of the tree. (Note that any such conditions are in addition to the basic assumptions of the mathematical model — usually the passive multi-cylinder model described in Chapter 2.)

- (B) *Empirical Cables*: Equivalent cables that are constructed using some heuristic based on empirically observed conditions for reproducing voltage responses observed at the cell body. Given some known parameters that are characteristic of the whole tree (for example steady-state input conductance, and in certain cases membrane surface area) that one expects should be invariant in an equivalent structure, one tries to build a cable that also has these properties.

In addition, the fully equivalent cables introduced by Whitehead and Rosenberg (1993) fall into a category of their own.

- (C) *Fully Equivalent Cables*: See definition later.

Cables of both type (A) and (B) are, under certain circumstances, incomplete special cases of type (C) — significantly, they are always incomplete in a mathematical sense. Categories (A) to (C) roughly encapsulates the chronological order of the introduction of all cables, with minor exceptions.

The power of true equivalence, and the absence of geometrical and electrical restrictions, ensures that the new cables represent an analytical tool capable of giving far more insight into the signal processing properties of passive tree geometry than cables of type (A) and (B).

It should be noted that unbranched models are often used in computer simulations where one is investigating properties of neurons but is not necessarily concerned with the influence of branching structure (see, for example, Goldstein and Rall, 1974; Halliday, 1995b; Toth and Crunelli, 1998). The unbranched structure is just a convenient framework for producing the phenomena of interest. Though often similar in structure to equivalent cables, they are not intended as a replacement for a specific dendritic tree.

3.3 Rall's Equivalent Cylinder

The classic, and probably most well-known example of a reduced model is Rall's equivalent cylinder (Rall, 1962b, 1964, 1977), which is the precursor to, and inspiration for, all subsequent equivalent cable models. It falls into category (A). The desire to construct equivalent cables has arisen primarily because of the success of Rall's model for estimating passive electrical parameters of neurons (e.g. g_M , ρ_i). Its simple structure makes it more susceptible to mathematical analysis and its electrical properties are more easily visualised than those of the corresponding tree.

Given a multi-cylinder model of a passive dendritic tree, as described in Chapter 2, where uniform cylinders meet only at branch points, the tree is a *Rall tree* provided the following three conditions hold:

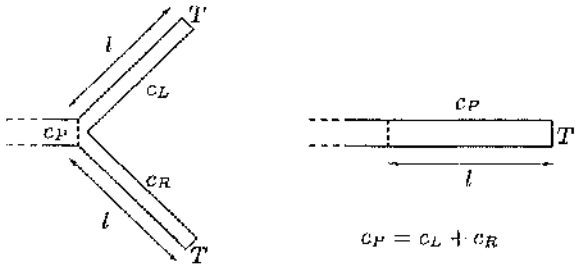


Figure 3.1: Singly branched binary Rall tree and its equivalent cylinder. Each tree limbs has electrotonic length l , as does the equivalent cylinder. Tree limbs and equivalent cylinder have the same terminal boundary condition, denoted T' .

1. All terminal boundary conditions are of the same type.
2. At any branch point the sum of child cylinder c -values (c_1, \dots, c_n) equals the c -value of the parent cylinder (p), thus $c_p = \sum c_i$. Recall from Chapter 2 that $c_k = d_k^{3/2}$, so this is Rall's 3/2 power law for dendritic cylinder diameters.
3. All dendritic terminals are located at the same electrotonic distance, L , from the soma.

We assume that condition (1) simply requires that the potential, $v_i(x, t)$, of terminating cylinder i , satisfies the boundary condition

$$\alpha v_i(l_i, t) + \beta \frac{\partial v_i(l_i, t)}{\partial x} = f_i(t), \quad (3.1)$$

where, from equation (2.76), α is a measure of leakage conductance from the terminal, β is a measure of intracellular axial conductance at the terminal, and f_i represents the (current) supply or forcing term. The quantity α/β thus measures relative amounts of leakage and axial current flow. Current injection ($\alpha = 0$) and cut ($\alpha \rightarrow \infty$) conditions are just special cases of equation (3.1). Condition (2) is essentially an impedance-matching condition between the parent cylinder and its child cylinders at each branch point.

A Rall tree may be replaced by a uniform cylinder, attached to the soma. This cylinder exhibits the same impedance matching properties as the Rall tree. It has electrotonic length L , the same type of terminal condition as the tree terminals, and c -value equal to that of the trunk cylinder, i.e. that which connects to the soma. It has total surface area equal to that of the tree.

Figure 3.1 illustrates a singly branched Rall tree and its equivalent cylinder. The equivalent cylinder result need only be proven for this simple case. The general result for multiple branching follows by successive reductions.

3.3.1 Proof

Rall originally demonstrated the foundations of his result by analysing steady state solutions of the cable equations, and determining the simplifying conditions that ensure the steady state input conductance for the tree is identical to that for a uniform cylinder (Rall, 1959; 1962b). This approach is unnecessary (though insightful) however, and the result follows simply for the time-dependent case from an elementary analysis of the partial differential equations. One need not be concerned with specific expressions for the tree cylinder potentials (e.g. steady-state solutions in terms of $\sinh x$ and $\cosh x$). All that is required are the describing equation (the cable equation) and the boundary conditions.

Consider the left (L) and right (R) cylinders of the simple symmetric Y-junction, each with electrotonic length l , and c-values c_L and c_R . The left and right potentials, $v_L(x, t)$ and $v_R(x, t)$ satisfy the dimensionless cable equation, thus

$$\frac{\partial^2 v_L}{\partial x^2} = \frac{\partial v_L}{\partial t} + v_L - \Omega \frac{i_L}{c_L}, \quad \text{and} \quad \frac{\partial^2 v_R}{\partial x^2} = \frac{\partial v_R}{\partial t} + v_R - \Omega \frac{i_R}{c_R}, \quad 0 < x < l, \quad (3.2)$$

where $i_L(x, t)$ and $i_R(x, t)$ are the electrotonic applied current densities on each branch. Recall that Ω is constant. Voltage continuity at the branch point ensures that $v_L(0, t) = v_R(0, t)$. The two terminal boundary conditions are

$$\alpha v_L(l, t) + \beta \frac{\partial v_L(l, t)}{\partial x} = f_L(t) \quad \text{and} \quad \alpha v_R(l, t) + \beta \frac{\partial v_R(l, t)}{\partial x} = f_R(t). \quad (3.3)$$

Using equation (2.98), the total axial current flowing into the two cylinders from the junction is

$$i_J = -K \left[c_L \left. \frac{\partial v_L}{\partial x} \right|_{x=0} + c_R \left. \frac{\partial v_R}{\partial x} \right|_{x=0} \right]. \quad (3.4)$$

Now consider the simple linear combination of potentials,

$$v_C(x, t) = \frac{c_L}{c_L + c_R} v_L(x, t) + \frac{c_R}{c_L + c_R} v_R(x, t). \quad (3.5)$$

The claim is that v_C represents the potential in a uniform cylinder, with c-value $c_L + c_R$, and which can be connected to the branch point instead of the Y-junction while still preserving voltage continuity and current conservation. Voltage continuity where the new cylinder connects to the junction is guaranteed, because of voltage continuity in the original Y-junction junction, i.e.

$$v_C(0, t) = \frac{c_L}{c_L + c_R} v_L(0, t) + \frac{c_R}{c_L + c_R} v_R(0, t) = v_L(0, t) = v_R(0, t). \quad (3.6)$$

Also, since

$$v_C(l, t) = \frac{c_L}{c_L + c_R} v_L(l, t) + \frac{c_R}{c_L + c_R} v_R(l, t), \quad (3.7)$$

and

$$\frac{\partial v_C(l, t)}{\partial x} = \frac{c_L}{c_L + c_R} \frac{\partial v_L(l, t)}{\partial x} + \frac{c_R}{c_L + c_R} \frac{\partial v_R(l, t)}{\partial x}, \quad (3.8)$$

then v_C satisfies the terminal condition

$$\alpha v_C(l, t) + \beta \frac{\partial v_C(l, t)}{\partial x} = f_C(t), \quad (3.9)$$

where

$$f_C(t) = \frac{c_L}{c_L + c_R} f_L(t) + \frac{c_R}{c_L + c_R} f_R(t). \quad (3.10)$$

Current conservation at the junction is guaranteed since, from equation (2.98), and using equations (3.8) and (3.4)

$$-Kc_C \frac{\partial v_C}{\partial x} \Big|_{x=0} = i_J, \quad (3.11)$$

provided $c_C = c_L + c_R$. Choosing

$$i_C(x, t) = i_L(x, t) + i_R(x, t), \quad (3.12)$$

it is easy to check that v_C satisfies

$$\frac{\partial^2 v_C}{\partial x^2} = \frac{\partial v_C}{\partial t} + v_C - \Omega \frac{i_C}{c_C}, \quad 0 < x < l. \quad (3.13)$$

The equivalent cylinder result for the Y-junction follows immediately.

The general Rall tree can be reduced Y-junction by Y-junction, with the equivalent cylinder potentials (applied currents) now being formed from nested combinations of tree cylinder potentials (applied currents) as more and more structure is transformed. If $v_j(x)$ and $i_j(x)$ represent the potential and applied current on branch j , at a distance x from the cell body, then the potential and applied current over the equivalent cylinder that represents the whole tree are given by

$$v_C(x) = \sum_j \frac{c_j}{c_C} v_j(x) \quad \text{and} \quad i_C(x) = \sum_j i_j(x), \quad (3.14)$$

where the sums are taken over all branch cylinders, j , that lie at a distance x from the cell body. The cylinder c -value, c_C , is the sum of all branch c -values that lie at any particular distance from the soma — the Rall conditions ensure this is a constant throughout the tree, from soma to tips.

Figure 3.2 illustrates the reduction of a highly symmetric Rall tree with four orders of branching. If any of the structures (b) to (e) are attached to the soma instead of the original tree (a), one cannot determine which from their individual voltage responses at the soma. Any electrical activity on tree (a) can be mapped (using equations of the form 3.5 and 3.12) to any structure (b) to (e). Note that, of course, activity only needs to be mapped from sub-structure that has been transformed. Electrical activity on untransformed structure will be identical. Resulting electrical activity observed at the cell body will be, necessarily, identical.

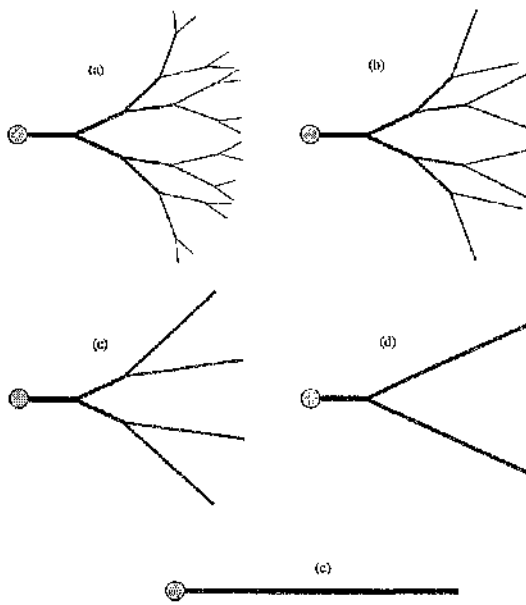


Figure 3.2: Successive reduction of Rall Y-junctions at the tips of more complicated Rall trees, to transform a complicated Rall tree to its equivalent cylinder. Reduction from (a) 4-order branching, though (b)–(d) to (e) zero orders of branching. All terminal boundary conditions are of the same type.

Note that Tuckwell (1988a) has proposed an equivalent cylinder theorem (theorem 5.2) including applied currents that attempts to formalise Rall's result, but imposes unnecessary restrictions upon v_L , v_R , i_L and i_R . His subsequent theorem (theorem 5.3) (see also Walsh and Tuckwell, 1985) is essentially the correct result. He also states that it is possible to determine the potential over the whole Rall tree using this theorem, given the potential over the cylinder. It is not however, possible to determine an *unique* configuration given the potential on the equivalent cylinder. The following discussion about mapping electrical activity should clarify this point.

3.3.2 Mapping Electrical Activity Between Tree and Cylinder

Given some configuration of electrical activity (voltage distribution and applied currents) in the Y-junction, the activity within the cylinder that generates the same response at the branch point is given by equations (3.5) and (3.12).

It is less clear how to map electrical activity back to the tree from the cylinder. Consider Figure 3.3a. A single input current, I , is mapped from the Rall Y-junction limb to the equivalent cylinder using equation (3.12). In Figure 3.3b, two currents are applied to the Y-junction, one on each branch, at the same distance from the branch point. One has magnitude rI , the other magnitude sI , where $r + s = 1$. Again the corresponding

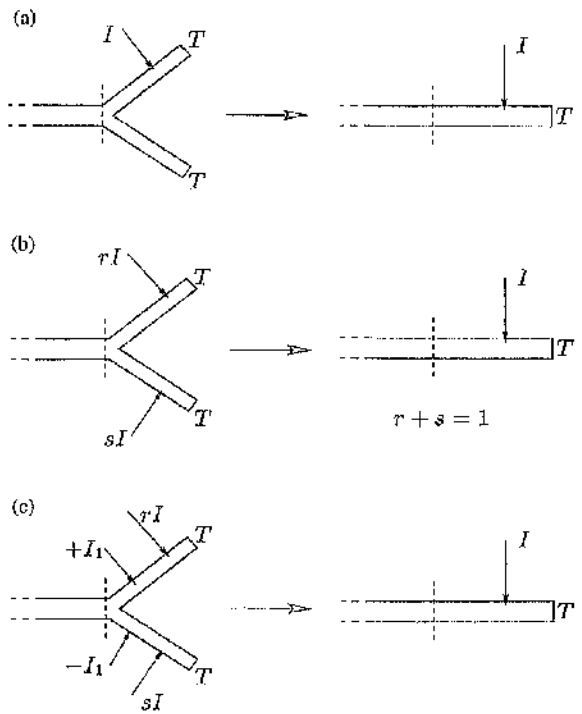


Figure 3.3: The electrical mapping from Rall cylinder to tree is not unique. Different applied currents on the trees (a)–(c) will map to the same configuration over the cable.

input current on the equivalent cylinder is I , at the same distance from the branch point. So, there is an infinite number of tree input configurations, determined by the choice of r and s , that map to the same cylinder input. Inputs need not even be located at the same distance from the soma. In Figure 3.3c, two additional currents, $+I_1$ and $-I_1$, are applied on the limbs, equidistant from the branch point. They cancel when mapped to the equivalent cylinder. The consequent non-uniqueness of the mapping from cylinder to tree is clear — to which tree configuration is the cylinder input mapped?

In mathematical terms, the mapping of electrical activity from tree to cylinder is surjective (every configuration of cable activity is associated with at least one configuration of tree activity), however it is not injective (which requires that no two tree configuration map to the same unique cable configuration), thus the mapping between cable and tree is not unique, i.e. the mapping is not bijective, which follows from surjectivity and injectivity combined.

In a different form, this non-uniqueness of the mapping between Rall tree and equivalent cylinder has been referred to as the “principle of independence of response on geometry” for Rall trees (Tuckwell, 1988a; Walsh and Tuckwell, 1985). Given the response at the soma to an input somewhere on the tree, only the electrotonic distance of the input from the soma may be inferred, not its precise location on the tree. The same current

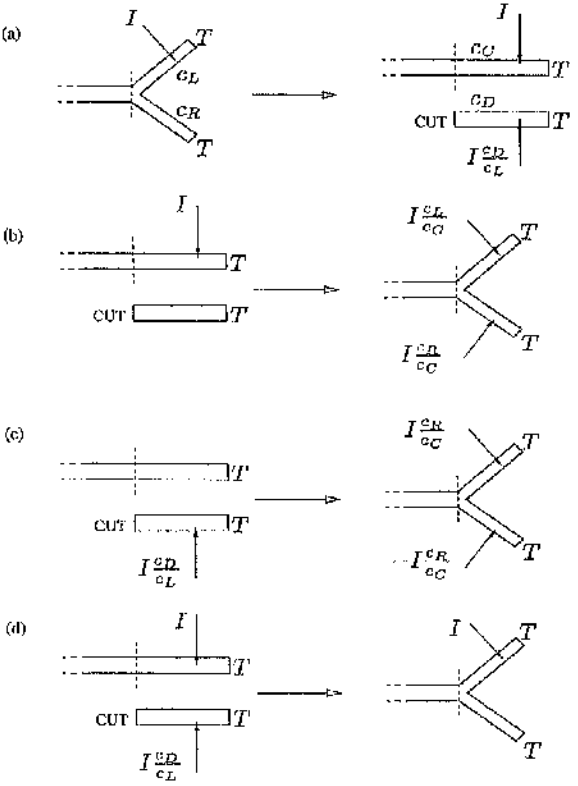


Figure 3.4: The mapping between a Rall Y-junction and its fully equivalent cable is unique. (a) A single injected current maps to the usual injected current on the cylinder plus a scaled current on the disconnected section. (b)–(c) Individually, these cable currents each map to two tree currents. (d) The mapping in (a) is unique and reversible.

input at two different locations on the tree, equidistant from the soma, will give rise to the same response at the soma. The soma cannot distinguish such inputs.

3.3.3 A Hint of Full Equivalence

It is instructive to introduce, in their simplest form, some features of fully equivalent cables. Consider the anti-symmetric combination of Rall Y-junction limb potentials (as opposed to the weighted symmetric combination v_C),

$$v_D(x, t) = v_L(x, t) - v_R(x, t), \quad (3.15)$$

and observe that v_D satisfies a cut condition at $x = 0$, i.e.

$$v_D(0, t) = v_L(0, t) - v_R(0, t) = 0, \quad (3.16)$$

in sympathy with voltage continuity at the origin. At $x = l$, v_D satisfies the boundary condition

$$\alpha v_D(l, t) + \beta \frac{\partial v_D(l, t)}{\partial x} = f_D(t), \quad (3.17)$$

where

$$f_D(t) = f_L(t) - f_R(t). \quad (3.18)$$

Taking

$$\frac{i_D(x, t)}{c_D} = \frac{i_L(x, t)}{c_L} - \frac{i_R(x, t)}{c_R}, \quad (3.19)$$

potential v_D satisfies the cable equation

$$\frac{\partial^2 v_D}{\partial x^2} = \frac{\partial v_D}{\partial t} + v_D - \Omega \frac{i_D}{c_D}, \quad 0 < x < l. \quad (3.20)$$

So, v_D is the potential in a cylinder with electrotonic length l , and c-value c_D (which has not been specified, and may take any positive value). Appropriate boundary conditions are satisfied at $x = 0$ and $x = l$, and cylinder D is not attached to the soma --- in fact it is not attached to anything. This is the *disconnected section* of a Rall Y-junction's fully equivalent cable; the equivalent cylinder is the *connected section*. In this case, the disconnected section describes the difference between the potentials on the two limbs. This is information that structure connected to the Y-junction cannot discern, hence the disconnection.

We now have two linearly independent equations describing the two potential functions on the two Y-junction limbs. The entire space of electrical activity over the Y-junction is represented by v_C and v_D . It is now possible to invert the mapping from tree to cable (equations 3.5 and 3.12), thus

$$v_L(x, t) = v_C(x, t) + \frac{c_R}{c_C} v_D(x, t), \quad v_R(x, t) = v_C(x, t) - \frac{c_L}{c_C} v_D(x, t), \quad (3.21)$$

and

$$i_L(x, t) = i_C(x, t) \frac{c_L}{c_C} + i_D(x, t) \frac{c_R c_L}{c_C c_D}, \quad i_R(x, t) = i_C(x, t) \frac{c_R}{c_C} - i_D(x, t) \frac{c_R c_L}{c_C c_D}. \quad (3.22)$$

Transformations that generate fully equivalent cables must be (electrotonic) length-preserving. By their very nature, no quasi-equivalent cable model can achieve this.

Figure 3.4 illustrates the equivalent cylinder for a singly branched binary Rall tree, and the uniqueness of the electrical mapping. Figure 3.5 illustrates the equivalent cable for the 4-order Rall tree in Figure 3.2.

Slight Relaxations of Rall's Conditions

We just briefly mention that an extension to the above analysis, using multiple cylinders for each limb, will show that if the Y-junction has branches with non-uniform (piecewise

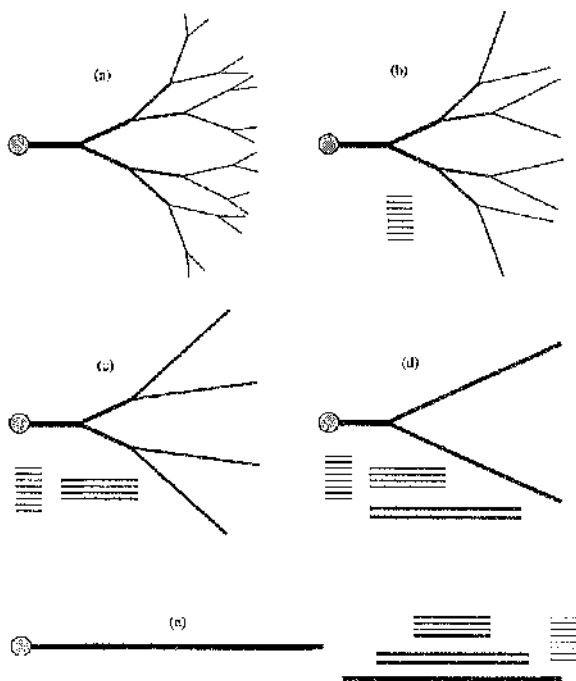


Figure 3.5: The Y-junction by Y-junction reduction of a Rall tree into its fully equivalent cable. Trees (a)–(d) are successively reduced and eventually (e) a single connected section is produced, plus $2^4 - 1$ disconnected sections. All five structures are equivalent since an electrical mapping will uniquely relate activity between any two.

uniform) diameter profiles, such that $c_L(x)/c_R(x) = r$ is a constant, but otherwise satisfies the Rall conditions (1) and (3) above, then the potential

$$v_C(x, t) = \frac{r}{1+r}v_L(x, t) + \frac{1}{1+r}v_R(x, t), \quad (3.23)$$

describes an equivalent structure with diameter profile $c_C(x) = (1+r)c_R(x)$. A disconnected section with potential

$$v_D(x, t) = v_L(x, t) - v_R(x, t) \quad (3.24)$$

has a similar diameter profile, with $c_D(x) = Fc_R(x)$, where F is an arbitrary positive constant.

Again, successive reductions may be applied to a highly branched tree provided the diameter profiles of each limb are appropriate. This result is discussed in greater detail in Chapter 6, where an alternative proof is given.

The left and right c-value profiles may in fact be continuous functions of x . This can easily be shown using a similar analysis to that above for Rall's equivalent cylinder, but using a non-uniform passive cable equation based on equation (2.16) (it must first be non-dimensionalised). Taking the arguments even further, the diameter profiles may in fact be a mixture of both continuous and discontinuous segments, again provided that the limb ratios are constant. The quantity g_M/C_M , i.e. the time constants, may even vary in each limb, provided $\tau_L(X) = \tau_R(X)$.

3.3.4 Application of Rall's Equivalent Cylinder

The equivalent cylinder concept was just one result that followed from Rall's application of passive cable theory to obtain expressions for steady-state electrical properties of neurons (details given in Rall, 1977; Rall *et al.*, 1992). Rall (1959, 1960) recognised that previous estimates of motoneuron parameters, such as steady state input conductance, and the membrane time constant, were erroneous because the significance of the electrical and geometrical properties of dendrites had been underestimated. Historical overviews can be found in Rall (1977) and Segev *et al.* (1995). This work clarified the electrical significance of dendrites, and also synaptic events that are initiated away from the cell body, and was an important step in treating the spatial complexity of these structures mathematically.

Estimating parameters is a vital component of constructing and constraining biophysically detailed models of neural activity. A typical approach to parameter estimation using the equivalent cylinder model may involve analysing recorded somatic voltage transients (generated by applying a current pulse at the soma) and comparing them, in some way, to theoretical responses corresponding to an equivalent cylinder. For example, the voltage response in a passive tree may be theoretically a sum of exponential decays. One can

estimate the largest decay time constant since it dominates the tail (late times) portion of the transient voltage response. Additional time constants are determined by "peeling", which involves subtracting the estimated exponential contribution to the transient so that the tail portion is now dominated by the next largest time constant.

The obvious limitation of the equivalent cylinder representation for realistic dendritic trees was recognised by Rall (who has cautioned against its inappropriate use), yet it has proved to be an extremely useful simplification that has helped in the understanding of the electrical characteristics of passive dendritic trees, and has been widely used in theoretical (e.g. Rall and Rinzel, 1973; Rinzel and Rall, 1974; Jack and Redman, 1971a, 1971b) and experimental (e.g. Iansek and Redman 1973; Jackson, 1992; Ulrich *et al.* 1994) studies.

The problem of parameter estimation using equivalent structures can be quite complicated, with many experimental and theoretical factors to consider, as discussed in detail in Rall *et al.* (1992). While C_M is often taken to be $1.0\mu\text{F}$, there can be great variation in the values of g_M and ρ_i that fit experimental data. Furthermore, as soon as one starts using these techniques for trees which do not satisfy Rall's conditions, then one must be careful how one should (if at all) interpret the results. Although for certain real neuronal trees Rall's conditions for an equivalent cylinder seem to be satisfied approximately, for others, and in general, this clearly isn't the case (see Rall, 1977 for discussion), and the equivalent cylinder is not an appropriate representation. Consequently, there have been several efforts to improve and extend the parameter estimation using model to dendritic trees which are not geometrically constrained by Rall's conditions.

Following from the equivalent cylinder approach is the idea that a complicated dendritic tree might have an *effective electrotonic length* — the electrotonic length of its best fit equivalent cylinder. Expressions for estimating the electrotonic length of a cylinder for various boundary conditions are given in Rall (1969a).

3.4 Continuous Tapering Models

Rall (1962a) proposed an extension to the equivalent cylinder result in an attempt to account for tapering tree geometry. This result assumes that the number of branches at a distance x from the soma is continuous function, $n(x)$, of distance from the soma, as is the radius of each branch, $r(x)$. The idea is to choose a tapering profile, r , then determine the corresponding n so that the tree can be represented by one cable equation (with generalised length parameter) that describes an equivalent cylinder. Jack *et al.* (1983) list several pairs of tapering and branching functions. These cables are of type (A) (restricted cables). Clearly, the introduction of fractional orders of dendritic branching is unphysiological. One must approximate the theoretical object with a tree that has

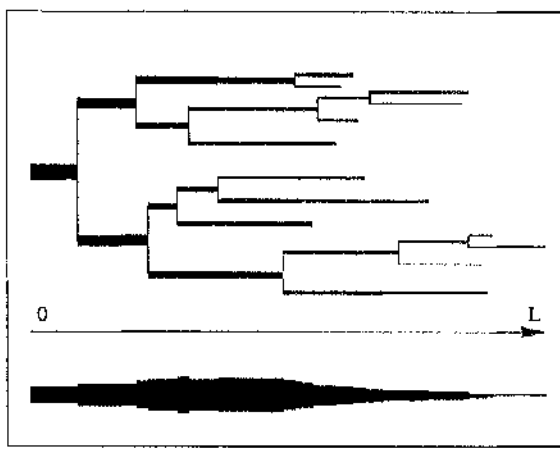


Figure 3.6: Electrotonic dendrogram representation of a dendritic tree and its corresponding lambda cable.

integral numbers of branches at any distance from the soma. Consequently, this approach is limited in its applicability, and is only remotely reasonable for trees with a high order of branching.

Poznanski (1988, 1991, 1994; Poznanski and Glenn, 1994) has used tapering cable models to estimate effective electrotonic lengths using the formulas of Rall (1969a) derived for the equivalent cylinder.

Ohme and Schierwagen (1998) have proposed continuous tapering cables which they claim justify the use of the (discontinuous) empirical cables discussed in the next section. They also claim that their result is a generalisation of Rall's equivalent cylinder to active dendrites with tapering diameter profiles. It is in fact just an extension to Tuckwell's (unnecessarily restrictive) variation on the equivalent cylinder result (Tuckwell, 1988a), with an array of imposed unrealistic geometrical and electrical conditions on the tree that are essential only in the non-linear case.

3.5 Empirical Cable Models

Empirical cables (type B) are built by marching along a dendritic tree in small steps, from soma to tips, using some measure of electrotonic architecture to determine the step size in each branch; at each step outwards from the soma, segments of tree are lumped together by preserving surface area.

The original, and most commonly used, measure of step size is electrotonic length (Clements and Redman, 1989; Fleshman *et al*, 1988). Burke (1997) refers to cables generated in this way as *lambda cables*. This approach automatically preserves surface area; when drawn in electrotonic space, the soma-to-tip surface area profile of the dendritic tree

is identical to the original tree, as Figure 3.6 illustrates using an electrotonic dendrogram. Burke (1997) has also used the "temporal delay for transient signals propagating outward from the soma" and "outward steady-state attenuation" (see also Agmon-Snir and Segev, 1993) to determine step size. The different cables, and original tree, generally have slightly different steady-state input conductances.

When compared to full branching multi-cylinder passive tree models of real motoneurons (e.g. Burke *et al.*, 1994; Burke 1997), it has been found that these cables reproduce a reasonably accurate transient voltage response (for late times, where the largest time constants dominates) at the soma when it (the soma) is subject to an exogenous current pulse, thus justifying their use in parameter estimation for these neurons.

There are no geometrical restrictions on trees that may be reduced using the empirical construction procedures, although their acceptability is in question when branches terminate at distinctly different electrotonic lengths. Although it does not seem to have been made explicit previously, all terminals must be assumed sealed. This is essential, otherwise the surface area need not be preserved. Recall that a cut terminal, for example, acts like a sudden diameter step to infinity. The important influence of boundary conditions on equivalent cable structure, and in particular on what tree properties one can expect to be preserved, becomes clearer in later chapters.

Empirical cables are of practical use in parameter estimation (Rall *et al.*, 1992) and because of their flexibility have replaced the restrictive equivalent cylinder; they have also been used in computer simulations (Manor *et al.* 1991) to dynamically reduce trees during computer simulation to improve efficiency of calculations on tree segments subject to low activity. Empirical cables are often more practical in these situations than fully equivalent cables since they can be constructed and simulated very quickly, while producing results of a suitable accuracy (Burke and Ogden, unpublished observations). This can be an important consideration when one runs repeated simulations with varying electrical parameters, or if one is repeatedly reducing and expanding portions of a tree during simulation. It should be noted, however, that parameter estimation can be done using the original tree model, and the *only* advantage an empirical equivalent cable model offers is efficiency in construction and simulation. In fact, simplified "equivalent" tree models ("cartoon representations") have also been used (Stratford *et al.*, 1989).

The principles of parameter estimation are similar to those for the equivalent cylinder. Experimentally recorded voltage transients are analysed, allowing estimation of time constants, specific electrical parameters, and effective electrotonic lengths. Holmes and Rall (1992a, 1992b) and Holmes *et al.* (1992) discuss the problem of estimating electrotonic length for trees where branches terminate at different electrotonic lengths. This problem is also considered in Chapter 8, in light of fully equivalent cable results.

An up-to-date exposition of cable theory for parameter estimation, the underlying assumptions, and the limitations of empirical cable models can be found in Rall *et al.* (1992).

3.6 Fully Equivalent Cables

3.6.1 A Definition of Equivalence

Mathematically, equivalence is really about information preservation. For dendritic trees, this involves retaining all information about electrical activity and geometrical structure at every point within the tree. The ability of the equivalent model to reproduce, exactly, somatic transients generated by the full tree model, is a natural consequence of such equivalence, not the goal.

Two models of a dendritic tree are *equivalent* provided there exists a transformation that allows one to identify every possible configuration of electrical activity over one model with a unique configuration over the other model. All geometrical and electro-chemical information described by a tree model is preserved, in some form, in the equivalent structure. Thus, all electrical phenomena permitted by the tree model must be reproducible, in some form, in the equivalent structure.

Note the generality of this definition (this is, in part, optimism that the equivalent cables of this thesis can be generalised to active models in some way); we do not restrict ourselves to one dimensional cable models, linear or otherwise, nor do we insist equivalent structure is necessarily unbranched. The important point is that a bijective relationship (an electrical mapping) can be established between equivalent structures. Determining whether or not this is possible for any particular model is the difficult part.

This definition of equivalence is certainly demanding and until Whitehead and Rosenberg (1993) introduced a new type of equivalent cable, full mathematical equivalence had not been considered. Rather than attempting to satisfy this more abstract definition, physical or somal equivalence has been the main concern. However, now these new cables have been established, a range of new applications and insights follow directly from their existence.

By giving the above definition of equivalence, there is no implication that structures not meeting its requirements are not useful. Clearly this is not the case, given the success of Rall's equivalent cylinder and its empirical extensions over the past three decades. It just seems more natural that, since our analytical tool of choice is the language of mathematics, when one talks of equivalence one should use the term in its strict mathematical sense, which brings with it notions of exactness, uniqueness, and completeness; the benefits of doing so are many fold.

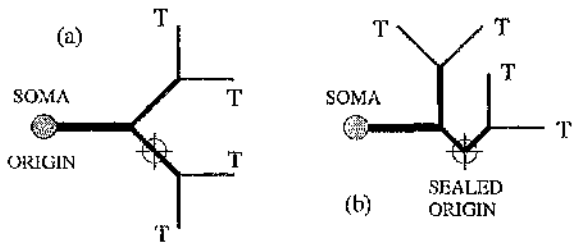


Figure 3.7: Any point over a tree may be chosen as the origin, provided the appropriate conditions for transformation to an equivalent cable are satisfied with respect to this point. (a) A Rall tree is equivalent to a cylinder when the soma is chosen as origin; the terminal condition is denoted T . (b) when a non-soma origin is chosen, the Rall conditions do not hold and the tree is not equivalent to a cylinder.

3.6.2 The Cable Origin

An equivalent cable must be equivalent with respect to some reference point, referred to here as the *origin*. In all previous cables, the origin has been taken as the point where the dendritic tree connects to the soma. The soma makes sense from a physiological point of view as it the central region of the neuron where dendritic trees exert their combined influence, and where experimental access for parameter estimation is usually gained.

The nature of the origin boundary condition doesn't affect the fully equivalent cable construction process. This is mostly true of previous cable models, though attenuation and delay cables are exceptions since the nature of the soma influences the measure of electrotonic architecture. In previous cable models, any point on the dendritic tree could have been chosen as origin, provided the appropriate geometrical and electrical conditions hold with respect to this point. For example, given a point on a Rall tree, the tree viewed from this point is not (in general) an idealised Rall tree, thus not equivalent to a cylinder, as Figure 3.7 illustrates.

The main problem when moving to a non-soma origin is that the boundary condition at the soma must now be accounted for in any equivalent cable. For empirical cables, this strictly means that an unrealistic sealed condition must be applied. A fully equivalent cable can only be constructed for a non-soma origin provided a cut or general current injection boundary condition is applied at the soma. Thus, the soma is usually chosen as origin.

3.6.3 Introduction to Fully Equivalent cables

The theoretical foundation of equivalent cable construction follows from passive linear cable theory, as presented in Chapter 2. A dendritic tree is represented by the homogeneous

multi-cylinder passive tree model. To summarise, each cylinder, j , is described by the dimensionless cable equation

$$\frac{\partial^2 v_j}{\partial x^2} = \frac{\partial v_j}{\partial t} + v_j - \Omega \frac{i_j}{c_j}, \quad 0 < x < l_j, \quad t > 0, \quad (3.25)$$

where v_j is the membrane potential, i_j represents exogenous currents, c_j is the c-value of the cylinder, l_j is its length, and x and t are, respectively, electrotonic space and time. Specific electrical parameters g_M (membrane conductance per unit area), C_M (membrane capacitance per unit area) and ρ_i (intracellular resistivity) are constant for the tree, and so is Ω .

Current conservation and voltage continuity conditions are imposed where cylinders meet, while current injection (specified potential gradient) or cut (zero potential) conditions may be imposed at terminals. Except for certain tree geometries, these are the only non-origin boundary conditions valid for equivalent cable construction. (In certain special cases, the cut boundary condition may be generalised to a non-zero voltage condition, but care must be taken when doing so. This usually involves a transformation of the potentials in the cable equations.)

Construction procedures ensure that current is conserved and voltage is continuous in an equivalent cable, and also ensure that any terminating dendritic sub-structure may be transformed in isolation from the rest of the tree. The latter is essential for allowing reduction of dendritic sub-trees. These elements of cable construction are made explicit in the analytical theory given in Chapters 5, 6 and 7, but are implicit in the matrix procedures of Chapter 4.

The fully equivalent cable is formed from passive dendritic cylinders, is generally non-uniform and has total electrotonic length equal to the total electrotonic length of all cylinders that form the original tree. It may consist of several disjoint sections, only one of which, the *connected section* is attached to the origin; the remaining are *disconnected sections*, which are isolated from the origin, each end being properly terminated. Figure 3.8 illustrates some simple artificial trees and their equivalent cables. Observe that electrotonic lengths have been expressed as integral numbers of some basic length. The physical shape of an equivalent cable section, i.e. its length and diameter profile in physical space, is completely independent of specific electrical parameters ρ_i , g_M and C_M . In electrotonic space, a change in g_M or ρ_i for example, forces a corresponding change in the actual electrotonic length of each tree and cable cylinder. However the basic shape of the cable, i.e. relative electrotonic lengths and actual diameters, is unchanged.

Construction procedures generate a bijective (thus invertible) electrical mapping that identifies every configuration of electrical activity (transmembrane voltage distribution, i.e. depolarisations and hyperpolarisations, and also applied currents) over the tree with a

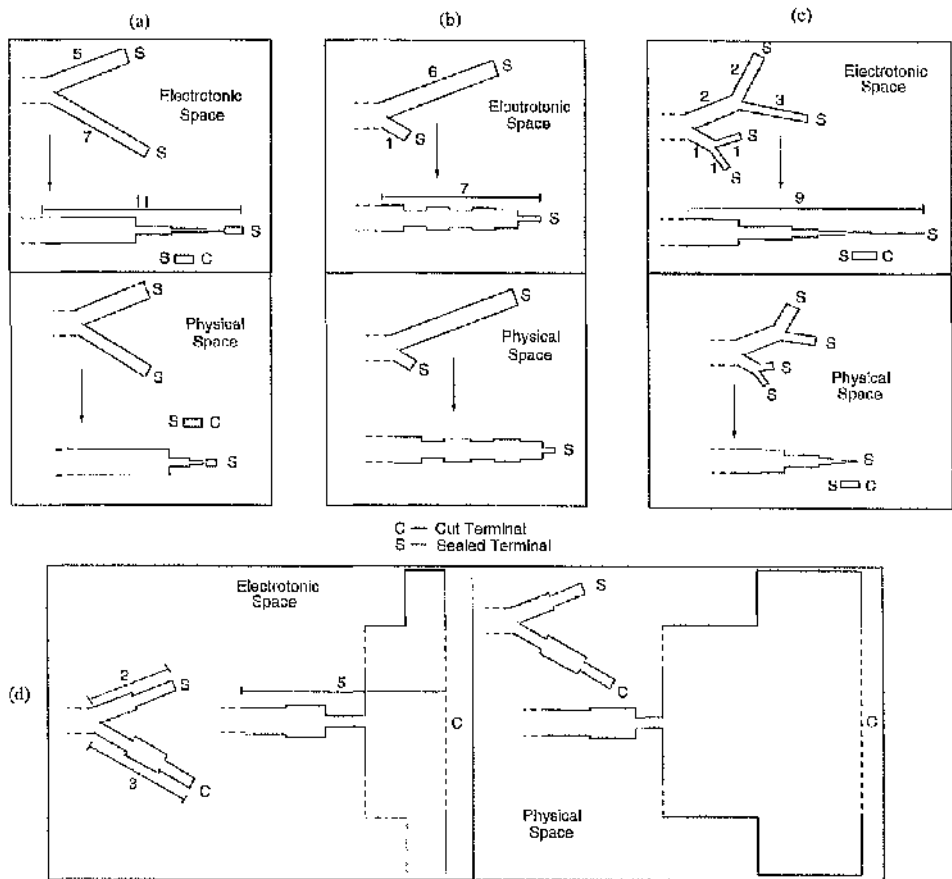


Figure 3.8: A selection of simple trees and their equivalent cables. Each tree-cable pair is shown in both electrotonic and physical space. Electrotonic lengths are integral multiples of some basic unit of electrotonic length. (a) A simple degenerate Y-junction with sealed ends. (b) Another simple Y-junction with sealed ends, this time non-degenerate, with significant length asymmetry. (c) A 2-order tree with sealed ends. Only one sub-tree is degenerate. (d) a non-uniform Y-junction with one cut terminal. The equivalent cable experiences a large increase in diameter (indicated by dotted lines).

unique configuration over the cable, and vice versa. Denote the voltage mapping by M_V , and the mapping that relates applied currents by M_I , thus

$$\mathbf{v}_C = M_V(\mathbf{v}_T) \quad \text{and} \quad \mathbf{v}_T = M_V^{-1}(\mathbf{v}_C), \quad (3.26)$$

$$\mathbf{i}_C = M_I(\mathbf{i}_T) \quad \text{and} \quad \mathbf{i}_T = M_I^{-1}(\mathbf{i}_C), \quad (3.27)$$

where \mathbf{v}_T and \mathbf{v}_C are vectors of cylinder potentials and \mathbf{i}_T and \mathbf{i}_C are vectors of cylinder applied currents for the entire tree and cable respectively. Mappings M_V and M_I are intimately linked. By reducing trees to equivalent cables, physical complexity is simply traded for complexity in the electrical mapping. Generally, electrical activity at one point in the tree is mapped to activity at many points on the cable, and vice versa.

Like the cable shape, the electrical mapping is independent of the specific whole-cell electrical parameters representative of the passive model — it always maps between the same physical points on tree and cable, while between the same relative points in electrotonic space; a cable can be constructed just by knowing the physical lengths and diameters of the tree cylinders. Altering electrical parameters merely requires a rescaling of the cable's electrotonic length and/or the membrane time constant.

Cable diameter profiles are typically discontinuous, which is inevitable for trees which do not satisfy Rall's 3/2 power law for impedance matching at branch points.

3.6.4 Equivalent Cables for Basic Branching Structure

Fully equivalent cables are best understood by considering initially the basic unit of branching structure, the *general Y-junction* (Figure 3.9a), comprising two limbs, with arbitrary lengths and diameter profiles, that meet at a branch point and satisfy appropriate boundary conditions at their respective terminals.

The equivalent cable for a general Y-junction contains a connected section plus at most one disconnected section. A Y-junction is classified as *degenerate* if its cable contains a disconnected section, otherwise it is *non-degenerate*. Figures 3.9b,c illustrate the two types schematically.

The Connected Section

The connected section always defines, via the electrical mappings M_V^{-1} and M_I^{-1} , electrical activity over the Y-junction that will influence the membrane potential at the branch point and in attached structure.

For example, a positive input current at some point along the connected section will be mapped (M_I^{-1}) to a distribution of input currents over the Y-junction limbs that, as far as the branch point and attached structure is concerned, acts like a single focussed

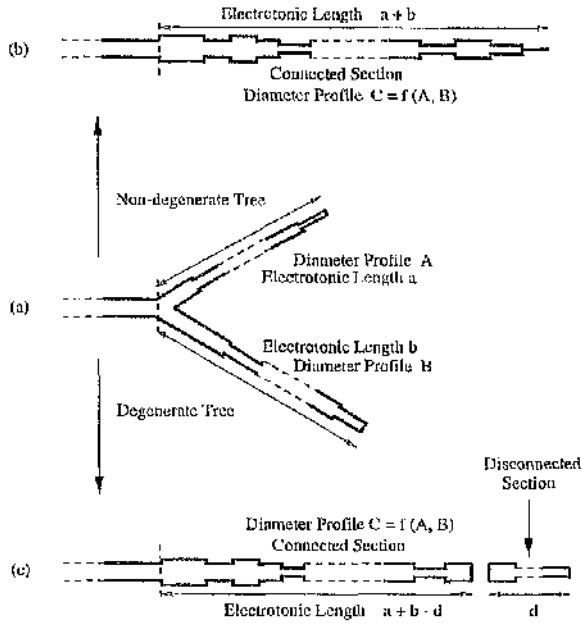


Figure 3.9: The general Y-junction and its equivalent cable. (a) Y-junctions are either non-degenerate or degenerate. (b) Non-degenerate trees are transformed to an equivalent cable consisting of just a connected section. (c) degenerate trees are transformed to equivalent cables with a connected section plus a single disconnected section.

input on an unbranched structure. The mapped activity may be a mixture of positive and negative inputs. Similarly, a depolarisation over the connected section will be mapped (M_V^{-1}) to a distribution of depolarisation and/or hyperpolarisation over the tree that will disperse passively producing the same effect at the branch point and in attached structure. A non-zero configuration of activity on a connected section must exert some influence on the electrical activity in structure connected to the Y-junction. The actual strength and shape of the voltage response at the branch point will, of course, depend on tree structure, boundary conditions and specific electrical parameters. Figure 3.10a illustrates the mapping of a current input from a Y-junction to its connected section.

As one moves along the connected section, from the cylinder that is attached to the origin (junction), to the final terminal cylinder, the corresponding electrical mappings define configurations of electrical activity over the tree that produce weaker and more graded responses at the origin (assuming the same current is injected as one moves from cylinder to cylinder).

Taking a different point of view, another aspect of connected section activity can be understood. Suppose that there is no activity initiated in the Y-junction itself, but it is still influenced by activity initiated in the structure to which it is connected, i.e. axial charge dispersal induces voltage changes in the Y-junction. This Y-junction activity, when

mapped to the cable, must be represented only in the connected section since the two are electrically identical with respect to the branch point. This activity cannot influence any disconnected section since it is not attached to the branch point. Basically, the connected section can be used to define the Y-junction voltage distributions that can be induced by activity in structure connected to the Y-junction.

The Disconnected Section

Over a degenerate Y-junction, many different configurations of electrical activity can exert the same influence on the membrane potential at the branch point, or in tree structure to which the Y-junction is attached. A disconnected section defines, via M_V^{-1} and M_I^{-1} , configurations of electrical activity that interact entirely locally, within the Y-junction, independent of the tree structure to which it is attached. For example, a configuration of current inputs over the disconnected section is mapped (M_I^{-1}) to current inputs over the Y-junction limbs which exert absolutely no influence on the potential at the branch point and in attached tree structure. Again, a similar effect is observed if one maps (M_V^{-1}) a distribution of depolarisation and hyperpolarisation over the disconnected section. The corresponding distribution of depolarisation and hyperpolarisation over the Y-junction will decay passively in a way that generates no effect at the branch point and in attached structure. Figure 3.10b illustrates a mapping between a disconnected section and a Y-junction.

Now consider electrical activity mapped from both connected and disconnected sections. Suppose an arbitrary set of input currents were simultaneously applied over the Y-junction, giving rise to a voltage transient at the Y-junction branch point. If the same configuration is re-applied, together with inputs mapped to the Y-junction from its disconnected section (not necessarily simultaneously), exactly the same response is observed — hence the degeneracy. Figure 3.10c illustrates the mappings from Figures 3.10a and 3.10b combined.

Disconnected sections are not uncommon; relative electrotonic lengths of Y-junction limbs and their terminal boundary condition types are the primary determinants of Y-junction degeneracy, and also dominate in determining the fine structure of the cable sections. The analytical results of Chapters 6 and 7 show how degeneracy can be predicted. Approximate degeneracy is also a valid concept and will be discussed later. As structure becomes more complicated, the boundaries between exact degeneracy and approximate degeneracy become more blurred, especially when one considers real neuron morphological data, and the inherent uncertainty associated with it.

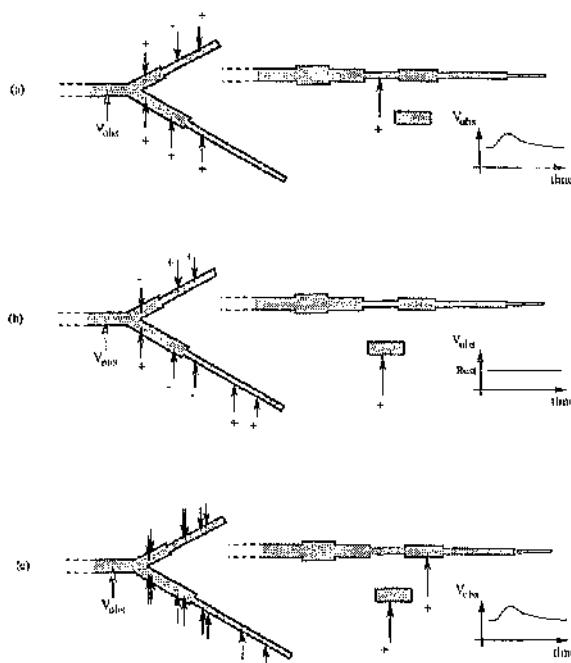


Figure 3.10: Mapping electrical activity between a dendritic tree and its fully equivalent cable. (a) Mapping electrical activity from a connected section. (b) Mapping electrical activity from a disconnected section to the original Y-junction gives a distribution of tree activity that has no effect outside the two limbs. (c) Map both previous tree inputs, and the same response is observed as for input distribution (a).

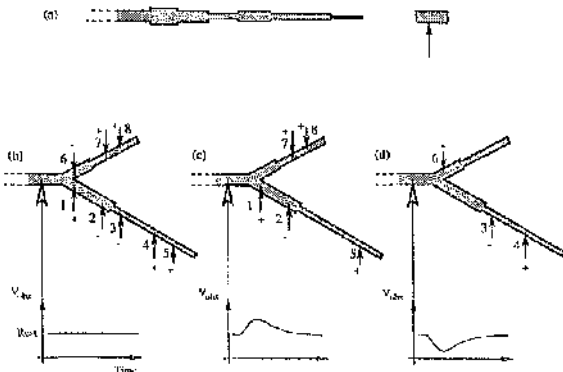


Figure 3.11: Passive coincidence detection in dendritic trees. The voltage response due to two subsets of tree activity mapped from a disconnected section. (a) Mapping electrical activity from a disconnected section to the original Y-junction gives a distribution of tree activity that has no effect outside the two limbs. (b), (c) Subsets of this activity will influence membrane outside the Y-junction, but not when applied simultaneously.

Coincidence Detection in a Y-junction

Implicit in the existence of disconnected sections is a mechanism for coincidence detection in passive trees. Activity mapped from a disconnected section to degenerate Y-junction can be divided into a number of subsets of activity, each of which could be activated by a separate source. If these subsets are activated simultaneously in the Y-junction, then their influence on attached structure is rendered ineffective. If applied asynchronously, the delay between subset activation would determine the strength of the influence of Y-junction activity.

Taking the mapped disconnected section activity from Figures 3.10, Figures 3.11c,d illustrates the voltage disturbance due to two subsets of the activity. If both configurations are applied coincidentally, no voltage disturbance is observed, Figure 3.11(a).

A degenerate Y-junction can thus act as a *passive coincidence detector* for many different subsets of activity, all defined by activity mapped from the disconnected section, which in turn is determined entirely by tree geometry and is independent of specific electrical parameters of the model.

The role of neurons as coincidence detectors has often been discussed (e.g. Abeles, 1982; Softky and Koch, 1994; Softky, 1993), but usually in terms of coincident activity increasing chances of the neuron generating an output, and not as a local operation that is a consequence of tree geometry.

General Properties of Y-junction Equivalent Cables

It is useful to summarise properties exhibited by the fully equivalent cables of general Y-junctions. Many of these feature will be explained in more detail in later chapters, either through mathematical or physical arguments, or both. Where we mention sealed end boundary conditions, the result is equally relevant for the more general current injection boundary condition.

- Total electrotonic length is preserved — the total electrotonic of all cable sections equals the combined electrotonic length of the Y-junction limbs. A (electrotonic) length-preserving transform is essential for the existence of a bijective mapping.
- The equivalent cable contains at most one disconnected section.
- Only Y-junction structure up to distance x from the branch point origin influences cable structure up to distance x from the origin. Thus if two Y-junctions have identical structure up to distance a from the origin, then so will their connected sections. If a is greater than the maximum origin-to-tip electrotonic length then the whole Y-junction influences the cable structure at this point.
- A connected section is at least as long as the longest Y-junction limb; consequently, a disconnected section is never longer than the connected section. Only in special cases (Rall Y-junctions, a slight generalisation, and a few other exceptions) will connected and disconnected sections be the same length.
- For both degenerate and non-degenerate Y-junctions, if both limbs are sealed then the connected section is sealed. If either limb is cut then the connected section is cut.
- For degenerate Y-junctions, the equivalent cable's disconnected section has at least one cut terminal. If both Y-junction limbs are sealed, so is the second disconnected section terminal. If one Y-junction terminal is cut while the other is sealed, the disconnected section is cut at one end and sealed at the other. If both Y-junction limbs are cut, so are both the disconnected section terminals. There is thus a conservation of sealed terminals for degenerate Y-junctions.
- Steady-state input conductance of the connected section equals the steady-state input conductance of the original Y-junction (with respect to the origin).
- Provided both terminals are sealed, connected section surface area equals tree surface area. Also, the total exogenous current injected into the connected section equals the total mapped exogenous current injected into the Y-junction, and vice versa.

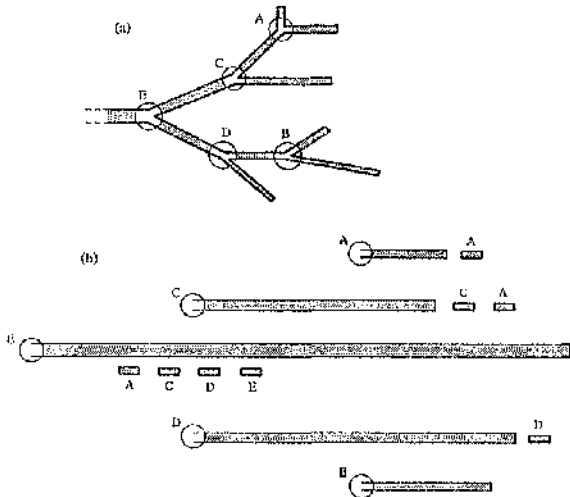


Figure 3.12: The Y-junction by Y-junction reduction of a dendritic tree to its fully equivalent cable. (a) A complex tree is reduced to its equivalent cable Y-junction by Y-junction; branch points are labelled (A)–(E). (b) The equivalent cables for each sub-tree marked by branch points (A)–(E). Disconnected sections associated with a specific tree are labelled with the same letter as the corresponding branch point. The fine structure of diameter profiles is not illustrated.

Note that a disconnected section may be regarded as an extension of the connected section. The two sections can be joined at their common boundary condition. From the point of view of the connected section, however, the disconnected sections effective diameter is either zero or infinity (depending on the connected section's terminal condition).

3.6.5 Complicated Branching Structure

The results and concepts described above for the general Y-junction extend naturally to trees that exhibit higher orders of branching. The tree is collapsed, Y-junction by Y-junction, removing branch points by successive reductions until the fully equivalent cable for the whole tree is obtained. Each Y-junction is either degenerate or non-degenerate (in which case it may be approximately degenerate — see below). A sub-tree may thus be classified as degenerate if any degenerate Y-junctions are encountered during its collapse. Initially, cable sections are associated with distal Y-junctions and define configurations of electrical activity over reasonable small, localised regions of a tree. As more structure of a complicated tree is transformed, cable sections are associated with activity distributed over wider regions of the tree — disconnected sections associated with larger sub-trees will define ineffective (at the soma) electrical activity over significant portions of the tree.

Coinciding activity in one degenerate sub-tree emphasizes the influence of activity in

the rest of the tree simply by removing the combined effect of a number of inputs. Figure 3.12 illustrates (without fine structural detail) a tree with just five branch points, and the fully equivalent cables associated with the sub-tree at each branch point. Differing geometries will exhibit different levels of degeneracy and different electrical mappings, and thus varying local processing capability. The complexity of the electrical mapping associated with a disconnected section will depend on the complexity of the Y-junction.

This notion of local signal processing — as geometry determined coincident activity associated with specific sub-structure — contrasts with other definitions (Koch *et al.*, 1982; Woolf *et al* 1991) in which *dendritic sub-units* are physical regions that are electrically isolated from the soma, according to some subjective measure of isolation based on voltage attenuation between points. However, these sub-units are insensitive to subtle morphological features, and dependent on specific electrical parameters — change ρ_t , for example, and the whole sub-unit structure may change.

Disconnected sections could be regarded as alternative, robust, and well-defined *electrical sub-units* that are independent of specific electrical parameters and determined entirely by geometry.

The results specific to each Y-junction listed above are either immediately valid for the general tree or can be extended naturally.

- Total electrotonic length is preserved
- The equivalent cable contains no more disconnected sections than the total number of Y-junctions that must be transformed to generate it.
- Only tree structure up to distance x from the branch point origin influences cable structure up to distance x from the origin. Thus if two trees have identical structure up to distance a from the origin, then so will their connected sections; if a is greater than the maximum origin-to-tip electrotonic length then the whole tree influences the cable structure.
- If all tree terminals are sealed then so is the connected section terminal. If one or more terminals is cut, so is the connected section terminal.
- Steady-state input conductance of the connected section equals the steady-state input conductance of the original tree.
- Provided all terminals are sealed (or of general injected current type), connected section surface area equals tree surface area. Also, the total exogenous current injected into the connected section equals the total mapped exogenous current injected into the tree.

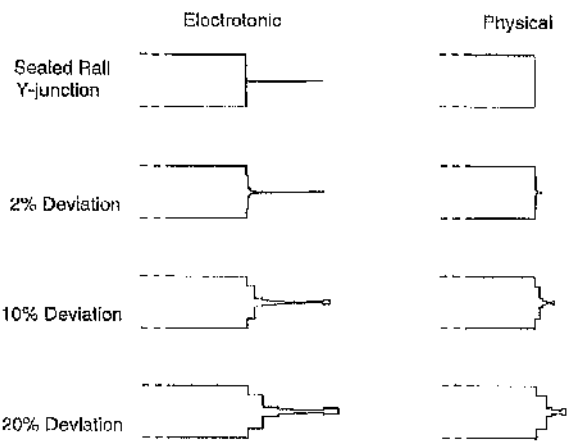


Figure 3.13: Equivalent cable structure is robust. 1 — deviations from completely symmetric sealed Rall Y-junction. The length of one limb is extended by the specified amount.

3.6.6 Equivalent Cable Structure is Robust

The discussion so far has concentrated on cables that have been constructed exactly, i.e. with algebraic precision. While equivalent cable construction procedures can be performed algebraically, computer implementations are the only practical approach in general, and there will be error associated with round-off effects, in addition to any uncertainty in measurements of the original tree data. However, equivalent cables, in particular their disconnected sections and electrical mappings, are quite robust objects, dominated by electrotonic tree symmetries (most of which are not obvious) which permit the introduction of the concept of *approximate degeneracy*.

When moving from a continuous real dendritic tree to an abstract multi-cylinder representation, one automatically imposes dimensional constraints — if the difference between two diameters is below a prescribed bound, they are essentially identical in the available model representation. Narrow cable sections within this bound can be regarded as essentially disconnected.

While exact degeneracy of a tree may disappear and reappear as one moves between slightly different model representations of the same tree data, the overall properties of the cable and electrical mapping do not change significantly.

Suppose both limbs of a degenerate Y-junction have sealed terminals. The connected section terminates with a sealed terminal, while the disconnected section has one sealed and one cut terminal. One can think of the disconnected section as attached to the connected section by joining the two sealed terminals. The disconnected section is essentially an extension, with zero diameter, to the connected section (though the disconnected section may have its own fine structure of cylinders). If the electrotonic length of one Y-junction

limb is now altered very slightly so that the new Y-junction is non-degenerate, then the equivalent cable is very similar to that previously, except that the structure at the end of the connected section narrows very rapidly, rather completely disconnecting immediately. The effect of electrical activity on such narrow sections is negligible at the soma compared to similar activity on other segments. One can make a rough measure of the significance of the change in tree structure by noting whether the change in surface area due to the change in branch length is much less than the total surface area of the Y-junction.

Consider the simple Rall Y-junction. The equivalent cable is shown in Figure 3.13. In electrotonic space the disconnected section is drawn as a thin extension to the equivalent cylinder, while in physical space it disappears (since finite zero diameter electrotonic length equal zero physical length). Also illustrated are the equivalent cables for trees which deviate from the ideal Rall situation. The electrotonic length of one branch is increased by 2%, 10% and 20%, showing how the cable structure very gradually shifts from the Rall case. At 2% deviation, the cable rapidly shrinks to very small diameters. There is very little change in overall cable structure however, with the extra surface area being accounted for in a negligible extension to the cable. The narrow section is essentially disconnected. The electrical mapping will have changed very slightly, but the strongest components form a mapping that is practically identical to that from the disconnected section.

A similar argument can be made for degenerate trees where the connected section terminates with a cut terminal. Again, the disconnected section can be regarded as attached to the connected section, except this time it represents an extension of infinite diameter. A slight alteration in the length of a Y-junction limb can be made so that a non-degenerate tree is produced. The connected section, rather than terminating early as before, will suddenly jump in diameter by an extreme amount. The increase in diameter is large enough to be regarded as approximate cut end, and the tree can be regarded as approximately degenerate.

Figure 3.14 illustrates this for the Rall Y-junction, again, this time for 2% and 20% deviations from the Rall situation. At 2% deviation, the jump is particularly massive, with the cable having a correspondingly huge physical length (indicated by arrows).

3.6.7 Trees With Identical Connected Sections

Once a tree has been reduced to its fully equivalent cable, the connected section's suitability as a tool for comparing and classifying passive trees becomes apparent. Consider the two trees illustrated in Figures 3.15a–b. Despite their obviously dissimilar morphologies, their fully equivalent cables (c) have identical connected sections. The two trees therefore have identical global properties (the soma cannot distinguish them), but different local

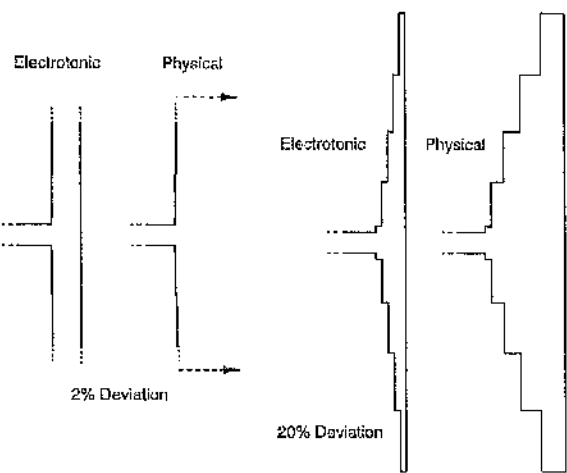


Figure 3.14: Equivalent cable structure is robust. 2 — deviations from cut Rall Y-junction.

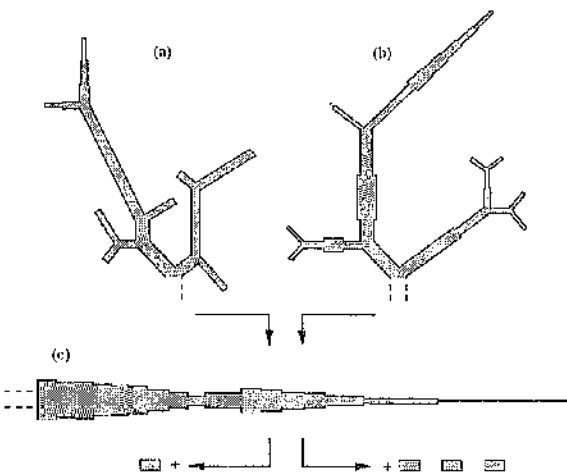


Figure 3.15: Identical fully equivalent cable connected sections implies electrical equivalence, with respect to the soma, of different trees. Two trees (a) and (b) have the same equivalent cable connected section (c), and thus global passive properties. Tree (a) has three exactly disconnected sections, while tree (b) has one. The tree has different local processing properties.

properties. A configuration of electrical activity over tree (a) may be mapped to its equivalent cable. Activity on tree (a) that will not influence the response at the soma can be mapped from cable (a)'s disconnected sections. Now map the connected section activity to tree (b) — the same response will still be observed. Again, tree (b)'s activity can be modified without effect on the soma by mapping any activity from tree (b)'s disconnected sections. Thus we can define, exhaustively, all configurations of activity on tree (a) and tree (b) that give the same response at the soma.

If two equivalent trees both have no disconnected sections, there is a unique configuration of activity on each tree that generates any specific response.

3.6.8 Methods of Construction

There are three methods described in this thesis for constructing fully equivalent cables for trees of arbitrary multi-segment geometry: two matrix procedures (Lanczos and Householder) are given in Chapter 4, and one analytical procedure is given in Chapter 6. Chapter 7 gives the optimal method for transforming simple Y-junctions.

For the Lanczos and Householder procedures, discretised cable equations are used to formulate a matrix representation of a dendritic tree (Whitehead and Rosenberg, 1993; Ogden *et al.*, 1997; Ogden *et al.* 1999; Lindsay *et al.*, in press), to implement what is essentially an algebraic transform (there is no discretisation error in the matrix procedures). Degeneracy of a Y-junction corresponds to degeneracy in the eigenvalues of the tree matrix. The analytical procedure follows from the theoretical basis of cable construction. The three procedures are intimately linked, and generate the same fully equivalent cable (within the bounds of numerical error when implemented on computer). The electrical mapping is discrete for the matrix procedure, but continuous for the analytical procedure. The continuous mapping can be inferred from the discrete mapping given an understanding of the analytical construction procedure.

The analytical theory presented in Chapter 6 provides most insight into why the cables can be constructed. It also allows one to predict exactly which general Y-junctions will be degenerate. The branch-shifting construction process developed in Chapter 7 can be used to transform simple Y-junctions, and this approach provides very useful insight into how tree lengths and boundary conditions shape equivalent cable fine structure and the electrical mapping.

3.6.9 Construction and Pre-programming of Artificial Dendritic Trees

One possible future application of the fully equivalent cable model is in the construction, in software, or possibly even in hardware, of networks of neurons with passive trees that

perform complicated signal processing operations controlled by coincidence detection of characteristic input configurations. It is straightforward to choose degenerate tree geometry so that certain activity mapped from a disconnected section consists of any specified number (greater than two) of significant inputs over the tree. The usefulness of the passive tree as a form of programmable analogue processing element needs further investigation.

3.7 Discussion

Simulation of biophysically detailed model neurons can give great insight into the electrochemical processes that underlie locally observed phenomena associated with a series of inter-related conductance changes, but are less practical as a tool for investigating the influence of complicated geometry, given the vast number of possible configurations of activity. Even passive structures have been poorly understood in this regard, as the results presented in this thesis show.

If one regards the previous quasi-equivalent cable models as representing degrees of equivalence, then they are, in one way or another, certainly less equivalent than fully equivalent cables (it is difficult to decide how one would organise previous cables in order of increasing equivalence, however). In a mathematical sense they are not equivalent at all.

For the limited geometrical structure for which it is valid, a Rall tree and its equivalent cylinder are identical electrical loads. A mapping relates tree activity to cylinder activity, but the mapping is not unique. As was shown, a disconnected section is required to complete the equivalent structure. The equivalent cylinder represents a very restricted subset of equivalent cables, with the soma taken as origin, and disconnected sections (of which there will be at least one) ignored. In fact the number of disconnected sections, as well as their electrotonic length, is very much dependent upon a Rall tree's branching structure. In addition to being unphysiological, the continuous tapering extensions to Rall's result suffer most of the limitations of the original equivalent cylinder. Interestingly, of all the previous models, the empirical cables could be regarded as the least equivalent, yet they have proven the most practical in application. There is no electrical mapping, just a relationship between somatic voltage responses for the tree and cable model that is generally approximate.

In principle, fully equivalent cables can replace previous models in all capacities in which they are used. In practice, computational considerations mean this is not always worthwhile. The new cables have many applications beyond this, however, and this is their strength. Previously unknown features of passive dendritic trees have been revealed, with significant insights gained concerning local and global processing capabilities of passive

trees. More detailed discussion of equivalent cable fine structure, and general implications of the equivalent cable result, is included in Chapter 8.

In the rest of this thesis, the terms "cable" and "equivalent cable" are generally employed as shorthand meanings for "fully equivalent cable".

Chapter 4

Matrix Methods for Constructing Fully Equivalent Cables

4.1 Introduction

If the physical and electrical structure of a passive dendritic tree model is expressed in a suitable matrix form, its equivalent cable can be constructed using matrix transformation procedures. In this chapter *discretised cable equations* are derived from the dimensionless linear cable equation. They can be collected together to form a *matrix equation*. The number of discrete cable equations required to represent a tree depends on its geometry, terminal boundary conditions, and the degree of accuracy required in the model. The accuracy is embodied in the basic electrotonic length, of which all cylinder lengths are an integral multiple, as discussed in section 2.5.2. The primary component of the matrix representation is the *tree matrix*, denoted A_T , which exhibits significant and exploitable structural features.

The equivalent cable construction process involves three stages: the tree matrix must first be symmetrised, the symmetric matrix then tri-diagonalised, and finally the tri-diagonal matrix must be de-symmetrised. Each step must be carried out, using similarity transformations, in a way that preserves essential matrix structure. In practice, this determines the specific tri-diagonalisation algorithms that may be employed in the second stage. The symmetrisation and de-symmetrisation transformations are independent of the tri-diagonalisation algorithm and critically dependent on the nature of discrete cable equations. In fact, the matrix structure conveniently lends itself to the efficient application of each transformation.

Two methods of tri-diagonalisation, namely *Lanczos tri-diagonalisation* and *Householder tri-diagonalisation* have been found suitable, but there may be others. The two

algorithms both work effectively, although their numerical nature limits any insight they may give into the biophysics underlying the cable construction process. The analytical rules of Chapters 5, 6 and 7 are much more revealing.

Both Lanczos and Householder procedures are presented in this chapter. The Lanczos method was introduced by Whitehead and Rosenberg (1993), and full details, extended to incorporate exogenous applied currents, have subsequently been given by Ogden, Rosenberg and Whitehead (1999). The Householder method was originally illustrated by Ogden, Lindsay and Rosenberg (1997), with full details given in Lindsay *et al.* (in press).

Although the algorithms central to the matrix methods are commonly employed in numerical computation applications (see Golub and Van Loan, 1990, for an overview of the Householder and Lanczos methods), it should be noted that the matrix formalism and the reduction procedures implement the appropriate algebraic operations with no discretisation error; performed algebraically, they will yield the same results as the analytical algorithm presented in Chapter 6 — the linear mapping between tree and cable is essentially identical in each case. For the purposes of equivalent cable construction (though not numerical simulation), the tree matrix is an exact representation of the physical structure of the passive tree model. Standard results that follow from the analytical method allow one to predict the number of cable sections, their length, and whether or not a disconnected section is associated with any particular sub-tree. Matrix procedures¹ will generate the same connected and disconnected sections, but without any guidance as to what to expect.

Technicalities of implementing the algorithms in a computer program are also discussed. Aspects such as storage, speed, and numerical stability are briefly covered. Practical computer algorithms are given, and the mechanics of the matrix methods are illustrated using simple algebraic examples.

4.2 The Matrix Representation of a Dendritic Tree

We now develop a set of discretised cable equations that describe branching dendritic structure in terms of electrical activity at a set of spatially distributed points over the tree. The objective is to form a matrix equation of the form

$$\frac{dv}{dt} = \mathbf{Av} + \mathbf{g}, \quad (4.1)$$

where v and \mathbf{g} are vectors describing potentials and applied currents at points over the tree, and \mathbf{A} is a matrix determined by the spatial structure of the tree.

¹When implemented computationally (essential for any dendritic tree other than the simplest singly branched structures or those with high levels of electrotonic symmetry), the Lanczos and Householder procedures exhibit markedly different numerical properties.

4.2.1 Discretisation Nodes and Terminology

Recall that, for the purpose of equivalent cable construction, all cylinder electrotonic lengths must be integral multiples of some basic, or quantum, electrotonic length, here denoted H . Suppose a tree is represented, to arbitrary accuracy, by n cylinders. In terms of H , the length of cylinder j is $k_j H$, where the integers k_1, k_2, \dots, k_n have no common factor. A tree can be represented by a number of *nodes* by subdividing the quantum length into z intervals of length h , so that

$$H = zh. \quad (4.2)$$

Nodes are automatically placed at each end of a cylinder to emphasize points of discontinuity, and internally so that the internodal electrotonic length is always h and the distance spanned by $z + 1$ nodes is H .

A node is *connected* to its nearest neighbouring node(s) and two connected nodes are always located on the same cylinder (though are not necessarily unique to that cylinder). A node common to multiple cylinders is referred to as a *shared node*, for example a branch point or diameter step; a node connected to two other nodes in the same cylinder is called (and must be) an *internal node*; a *terminal node* is connected to exactly one other node. There is one node that deserves special treatment, namely the *soma node* which marks the soma-to-tree connection point. It is useful (and essential in light of the tree matrix structure) to regard this node as a terminal node, yet it may also be shared between the trunk cylinders of several dendrites (consider multiple dendritic trees connected to a single soma treated as a point-like structure). The possibility of a shared soma node is discussed briefly, and the appropriate discrete cable equation is given².

A multi-cylinder tree model will be discretised by a minimal number of nodes when $H = h$ ($z = 1$, i.e. two nodes spanning each quantum length). However, when this level of discretisation is used, ambiguities can arise concerning the correct interpretation of an equivalent cable from the matrix representation that is eventually generated. Situations can arise where there are not enough nodes to adequately describe cable structure in terms of finite difference equations. An internal node is really required to properly convey the existence of a cable. Without one, any equation, not just the cable equation, could be operating in the cylinder.

In anticipation of this, a finer discretisation will be required, with each length H represented by at least three nodes so that $z \geq 2$. This guarantees the existence of an internal node for even the shortest possible cylinder. We rely on the fact that if the

²While it is useful to know that such a configuration is valid, such structures don't provide any additional insight when deriving and illustrating the construction procedures, which can naturally accommodate any terminal node provided boundary conditions are suitable.

dendritic cylinders have a common basic unit of length $H = zh$, then the same must be true of the equivalent cable cylinders. This fact is clearer from the analytical construction procedure in Chapter 6. When moving, for example, from $H = h$ to $H = 2h$ in the same multi-cylinder dendritic tree, no new structure is represented by the extra nodes, and consequently no new structure will appear in the equivalent cable — each cable cylinder is also guaranteed at least one internal node. Figure 4.1 illustrates the discretisation scheme for $z = 1$ and $z = 2$ on the same tree model.

Since the discretisation is merely a tool for describing an algebraic transformation of the tree model, different discretisation levels (different z) on the same tree will only influence round-off error in a computational implementation. If intended solely for cable construction purposes, there is no error associated with the discretisation itself. A discretisation level of $z = 2$ is therefore optimal. The matrix construction procedures only generate a discontinuous electrical mapping, from dendritic tree nodes to equivalent cable nodes. However, provided $z \geq 2$, it is possible to infer a continuous mapping³ from the discrete one, though this requires some knowledge of the analytical methodology given in Chapter 6.

Node Numbering

The discretisation nodes must now be numbered. Any well-ordered numbering system may be used, however the scheme outlined next will be used in examples. This scheme simplifies the matrix representation of the tree and the equivalent cable construction process (as well as the description of it), and thus is implemented both for reasons of efficiency and of clarity. (The computational advantages of careful branch numbering are already well established in compartmental modelling, e.g. Hines, 1984.)

Node “0” will always mark the tree-to-soma connection point. Each cylinder has a node nearest the soma (its *proximal* or *near-end* node) and a node furthest from the soma (*distal* or *far-end* node). It is an inevitable consequence of branching structure that if a node, n say, is common to more than two cylinders (e.g. a binary branch point) then it is impossible to guarantee consecutive numbering of the nodes on each cylinder that shares node n . However it is certainly possible to number, consecutively and increasing away from the soma, all nodes on a cylinder *except* the one closest to the soma. So, node numbers increase from near-end node to far-end node, except where a node has already been numbered (this may occur at a branch point) or must not be numbered (a cut end terminal, since, as will be seen later, nodes where the potential is known need not be

³It is practical in many situations to use $z = 1$ and generate the correct cable structure, however the corresponding discrete electrical mapping does not provide enough information to infer the continuous mapping.

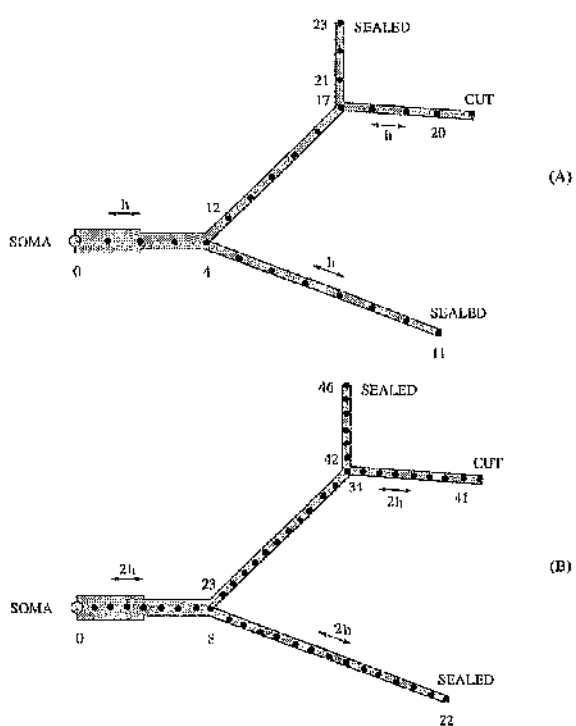


Figure 4.1: Discretisation of a dendritic tree. All nodes are equally spaced (electrotonically). Node numbering starts from 0 at the soma. The node at the cut terminal is not numbered. (A) discretisation level $z = 1$; (B) discretisation level $z = 2$.

represented).

Step through the individual cylinders in the following manner, starting with the cylinder (or one of the cylinders) that is (are) connected to the cell body. Once the nodes of a cylinder have been numbered, examine the tree structure at the far end. If any cylinders connect, choose one and continue the numbering. If none connect, step back through the cylinders that have already been numbered (in reverse order) until a cylinder is found that connects at its far end to an as yet unnumbered cylinder or group of cylinders — now choose one of these cylinder to continue the numbering. The numbering is complete when no cylinders with unnumbered nodes can be found.

Figure 4.1 illustrates a simple discretised tree, and some of the terminology introduced above. Note that a tree terminal which has been assigned a cut end boundary condition is represented by an unnumbered node since cut ends are not incorporated directly into the matrix representation. This is clarified later.

4.2.2 Discrete Cable Equations

Once a tree has been discretised, only the physical structure and electrical activity at nodes is of concern. A discrete cable equation can be associated with each numbered tree node, its complexity depending on tree structure at that node. Construction of equivalent cables is time-independent.

Start with the dimensionless cable equation for uniform passive cylinder j , as derived in Chapter 2,

$$\frac{\partial^2 v_j(x, t)}{\partial x^2} = \frac{\partial v_j(x, t)}{\partial t} + v_j(x, t) - \Omega \frac{i_j(x, t)}{c_j}, \quad 0 < x < l_j. \quad (4.3)$$

Axial current is given by

$$i_{a,j}(x, t) = -K c_j \frac{\partial v_j(x, t)}{\partial x}. \quad (4.4)$$

Finite Difference Formulae

Now consider how the continuous spatial derivatives are approximated in a discrete system. The forward and backward Taylor series for a sufficiently differentiable function f of x are

$$f(x + h) = f(x) + h f'(x) + \frac{h^2}{2} f''(x) + \frac{h^3}{6} f'''(x) + O(h^4) \quad (4.5)$$

and

$$f(x - h) = f(x) - h f'(x) + \frac{h^2}{2} f''(x) - \frac{h^3}{6} f'''(x) + O(h^4). \quad (4.6)$$

Here $O(h^a)$ represents terms involving the a^{th} , and higher, powers of of h . It can be defined properly by

$$0 < \left| \frac{O(h^a)}{h^a} \right| < B. \quad (4.7)$$

Basically, we can find a finite value B , independent of a , that can be used to define an upper bound for the additional terms.

Using these expansions, it is simple to obtain expressions for $f'(x)$ and $f''(x)$ which are correct to second order in h ,

$$f'(x) = \frac{f(x+h) - f(x-h)}{2h} + O(h^2), \quad (4.8)$$

$$f''(x) = \frac{f(x+h) - 2f(x) + f(x-h)}{h^2} + O(h^2). \quad (4.9)$$

These are the *central difference approximations* for first and second order derivatives.

Internal Nodes

Denote the transmembrane potential at node n by $v_n(t)$. Since the potential is continuous (as is its time derivative), this is well defined (as is dv_n/dt), whatever the tree structure at node n .

Consider first the internal node n connected to node p (nearer the soma) and node q (further from the soma). Using the given numbering scheme, $p < n < q$ and in fact $q = n+1$. The second order spatial derivative of the potential at node n can be approximated, using (4.9), as

$$\frac{\partial^2 v_n}{\partial x^2} = \frac{v_p - 2v_n + v_q}{h^2} + O(h^2). \quad (4.10)$$

Substituting this for the second order derivative in the cable equation for cylinder j (4.3) yields, after a slight rearrangement,

$$\frac{v_p - 2v_n + v_q}{h^2} - v_n = \frac{dv_n}{dt} - \Omega \frac{i_n}{c_j}, \quad (4.11)$$

correct to $O(h^2)$, where $i_n(t) = i_j(\text{node } n, t)$, the applied electrotonic current density at node n (it will soon be shown how the discrete current density relates to an actual applied current at the node). This is the *discrete cable equation* for internal node n . Note that the time-dependence of the potentials and applied currents has been suppressed.

Since each cable equation only describes electrical activity within a uniform dendritic segment, a direct substitution of the finite difference for the second order derivative can only be performed where n is an internal node. Greater care must be taken when treating shared nodes.

The Potential Gradient at Shared and Terminal Nodes

Changes in dendritic structure must be taken into account when constructing discrete cable equations for shared nodes that link two (diameter step), three (binary branch point) or

more (general branch point) cylinders, and also terminal nodes connected to only one other node. These changes are embodied in the terminal and joining boundary conditions.

In order to deal with the boundary conditions, we require an expression for the voltage gradient in terms of nodes that all lie on the same cylinder. There are several ways this may be done, yielding expressions correct to differing orders of h . The approach used here, which involves introducing "virtual" nodes, and subsequently removing them, gives an expression suitable for equivalent cable construction.

The first derivative of the potential at node n is, from the finite difference formula (4.8),

$$\frac{\partial v_n}{\partial x} = \frac{v_q - v_p}{2h} + O(h^2). \quad (4.12)$$

Unfortunately, n could be connected to any number of nodes, so nodes q and p don't have an immediate interpretation.

It is necessary to introduce some additional notation when dealing with voltage gradients because they may be discontinuous. If n is a shared node, for example, the gradient may take different values depending on the cylinder under consideration. The electrotonic space derivative of the potential at node n , in cylinder j , is therefore written as

$$\frac{\partial v_{n_j}(t)}{\partial x} = \left. \frac{\partial v_j(x, t)}{\partial x} \right|_{\text{node } n}. \quad (4.13)$$

Basically, node n is approached from a point on cylinder j .

There are two situations to be considered. Firstly, suppose node n is shared, and an expression is sought that involves only node n and those closer to the soma but also on the same cylinder. Equations (4.11) and (4.12) can be rearranged to give

$$v_q = h^2 \frac{dv_n}{dt} - v_p + (h^2 + 2) v_n + O(h^4), \quad v_q = v_p + 2h \frac{\partial v_n}{\partial x} + O(h^3). \quad (4.14)$$

The applied current at node n has been set to zero and will be dealt with explicitly later. Here, node q is fictitious, an imaginary extension of the cylinder, j , on which nodes p and n lie, such that the differential equations are still valid. It can now be eliminated simply by equating the two forms of v_q , yielding an expression for the potential gradient that is independent of structure beyond node n ,

$$\frac{2}{h} \frac{\partial v_{n_j}}{\partial x} = \frac{dv_n}{dt} + \left(1 + \frac{2}{h^2} \right) v_n - \frac{2}{h^2} v_p + O(h). \quad (4.15)$$

Similarly, if we want an expression for the potential gradient at node n , but this time in terms of nodes n and q on cylinder k , then node p can be eliminated to give

$$\frac{2}{h} \frac{\partial v_{n_k}}{\partial x} = - \frac{dv_n}{dt} - \left(1 + \frac{2}{h^2} \right) v_n + \frac{2}{h^2} v_q + O(h). \quad (4.16)$$

Note that equations (4.15) and (4.16) differ only in the direction electrotonic distance x is measured, towards or away from n (i.e. replace x with $-x$ in one equation to get the other). They are also correct only to $O(h)$, which is acceptable (in fact desirable, because these expressions have the exact form we want for the tree matrix representation) for equivalent cable construction, but may not be ideal for numerical simulation purposes.

Shared Node at a General Branch Point

Voltage continuity at a branch point node is already guaranteed by the discrete model. By imposing conservation of axial and applied currents we may link cylinders in a single discrete cable equation.

It is useful to denote the c-value of the uniform cylinder section between two connected nodes m and n by c_{mn} . If m and n lie on cylinder j then $c_{mn} = c_j$. Clearly $c_{mn} = c_{nm}$; however, where possible, we use the convention that the node closest to the soma is subscripted first.

Another important geometric quantity, the *c-sum* at node n , is defined by

$$C_n = \sum_k c_{kn}, \quad (4.17)$$

where the sum is taken over all nodes connected to node n . When node n is a binary branch point (parent cylinder P connected to left, L , and right, R , child cylinders) this yields $C_n = c_P + c_L + c_R$. If node n marks a step in diameter (parent P meets single child C) then $C_n = c_P + c_C$. If n is an internal node of cylinder j then $C_n = 2c_j$. If cylinder j terminates at node n with a current injection boundary condition then $C_n = c_j$. The c-sum is not required for unnumbered cut terminal nodes.

Consider shared node n , connected to node p on the parent cylinder and nodes j on the child cylinders. Conventions for the direction of current flow imply that the axial current flowing *into* the branch point from the parent cylinder plus any current injected *into* the core at the branch point, equals the total axial current flowing *out of* the branch point into the child cylinders.

Equation (2.96), in conjunction with equation (4.4), gives a form of the current conservation law in terms of potential gradients and injected current at node n ,

$$-\frac{i_{A_n}}{K} + c_{pn} \frac{\partial v_{n,p}}{\partial x} = \sum_j c_{nj} \frac{\partial v_{n,j}}{\partial x}, \quad (4.18)$$

where $i_{A_n}(t)$ is current applied at node n .

Using the finite difference formulae for the voltage gradients, equation (4.15) for the parent cylinder and equation (4.16) for each of the child cylinders, discretise the first order

derivatives in (4.18) to give

$$-\frac{2}{h} \frac{i_{A_n}}{K} + c_{pn} \left[\left(1 + \frac{2}{h^2}\right) v_n - \frac{2}{h^2} v_p + \frac{dv_n}{dt} \right] = \sum_j c_{nj} \left[2v_j - (2 + h^2) v_n - h^2 \frac{dv_n}{dt} \right] + O(h). \quad (4.19)$$

Rearranging gives the discrete cable equation for a general branch point node,

$$\frac{2c_{pn}}{h^2 C_n} v_p - \left(\frac{2}{h^2} + 1 \right) v_n + \frac{2}{h^2 C_n} \sum_j c_{jn} v_j = \frac{dv_n}{dt} - 2\Omega \frac{i_n}{C_n}, \quad (4.20)$$

correct to $O(h)$, and where, taking into account equation (2.99),

$$i_n := \frac{i_{A_n} \tau}{h}. \quad (4.21)$$

As can now be seen, in the discrete formalism the current density basically averages the point current source over the internodal length. This is useful because the electrical mapping that relates electrotonic current densities between a tree and its fully equivalent cable is an equally valid mapping for the actual applied currents. The τ appears simply because the rate of charge flow is measured in electrotonic rather than physical time.

There are several other important properties of the general discrete cable equation to note: the sum of the node potential coefficients is -1 ; the sum of node potential coefficients apart from node n is $2/h^2$; the coefficient of v_n is $-(1 + 2/h^2)$; all these quantities are independent of any specific c -values. This equation links all nodes connected to n .

The following particular cases, several illustrated in Figure 4.2, are of more practical use when representing realistic dendritic geometry. Any discrete cable equation can easily be derived as a special case of the general discrete cable equation (4.20).

Binary Branch Point

Simply set to three the number of cylinders meeting at node n in equation (4.20). The shared node is connected to node p on the parent cylinder (P) and nodes l and r on the left (L) and right (R) child cylinders, so

$$\frac{2c_P}{h^2 C_n} v_p - \left(\frac{2}{h^2} + 1 \right) v_n + \frac{2c_R}{h^2 C_n} v_r + \frac{2c_L}{h^2 C_n} v_l = \frac{dv_n}{dt} - 2\Omega \frac{i_n}{C_n}. \quad (4.22)$$

Abrupt Change in Diameter

A node that marks an abrupt step in diameter is shared by only two cylinders. Node n is connected to node p on the parent cylinder (P) and node q on the child cylinder (C). From equation (4.20), the discrete cable equation in this case is

$$\frac{2c_P}{h^2 C_n} v_p - \left(\frac{2}{h^2} + 1 \right) v_n + \frac{2c_C}{h^2 C_n} v_q = \frac{dv_n}{dt} - 2\Omega \frac{i_n}{C_n}. \quad (4.23)$$

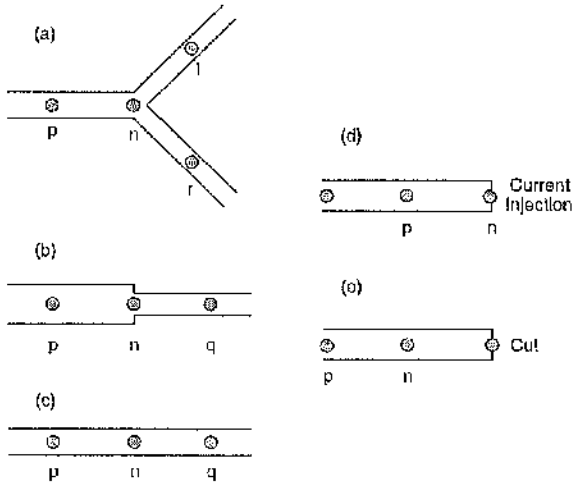


Figure 4.2: Some simple structures illustrating node connectivity in discrete cable equations. In each case, node n relates to the discrete cable equation that accounts for the specific structure illustrated. (a) Binary branch point. (b) Diameter step. (c) Internal node. (d) Current injection terminal. (e) Cut terminal.

Only this equation, and certain simplified cases of it, are required to describe unbranching structure, and thus it is vital in a discrete equivalent cable representation. Note that the ratio of coefficients of v_q and v_p equals the ratio of c -values for the cylinders C and P . The sum of these coefficients must of course still be $2/h^2$.

Internal Node Revisited

Not surprisingly, if $c_C = c_P$ then the two adjoining cylinders may be collected together and replaced with one cylinder, j say, that has their combined length — node n then becomes an internal node of this cylinder. For consistency, rewrite equation (4.11) as

$$\frac{v_p}{h^2} - \left(\frac{2}{h^2} + 1 \right) v_n + \frac{v_q}{h^2} = \frac{dv_n}{dt} - 2\Omega \frac{i_n}{C_n}. \quad (4.24)$$

Since $C_n = 2c_j$, the earlier choice of i_n (4.21) for the general shared node is now seen to be consistent with that for the internal node (4.11).

Terminal Nodes — Current Injection Boundary Condition

Suppose node n , on cylinder j , marks the terminal of a dendritic tree (in which case it is always at the far end of the cylinder). It is connected to a single node, p . If the terminal is subject to a current injection boundary condition, and current i_{A_n} is injected, then

equation (2.91) becomes⁴.

$$-Kc_j \frac{\partial v_{n_j}}{\partial x} = -i_{A_n}. \quad (4.25)$$

Using the appropriate finite difference approximation for the derivative, where n is at the far end of the cylinder (4.15), produces

$$\frac{2v_p}{h^2} - \left(\frac{2}{h^2} + 1 \right) v_n = \frac{dv_n}{dt} - 2\Omega \frac{i_n}{C_n}, \quad (4.26)$$

where i_n takes the usual form (4.21). Set $i_{A_n}(t) = 0$ to yield the sealed end condition. Recall that $C_n = c_j$ in this situation. The i_n now represents the boundary condition, rather than arbitrary applied currents.

Recall that node n may be treated as a point where the diameter falls abruptly to zero (since there is no current leak). Equation (4.26) could also have been derived simply by setting $c_C = 0$ in the discrete cable equation for a diameter step (4.23).

Terminal Nodes --- Soma-to-Tree Connection Node

The soma node, if chosen as origin, may be assigned any boundary condition, since this node does not interfere with critical elements of the cable construction process. It is convenient then to just assign a current injection boundary condition (this need only be temporary, just for the reduction process). Denote the soma node by s (it is number "0" using the numbering scheme outlined previously). The equation can be derived in a similar manner to the current injection boundary condition at a dendritic terminal (4.26), except that c_P rather than c_C is set to zero in the equation for a diameter step (4.23), giving

$$-\left(\frac{2}{h^2} + 1 \right) v_s + \frac{2}{h^2} v_q = \frac{dv_s}{dt} - 2\Omega \frac{i_s}{C_s}. \quad (4.27)$$

It has been assumed here that only one node, q , is connected to the soma node, i.e. we are dealing with a single dendritic tree. If multiple dendritic trees connect to a point-like soma representation subject to a current injection condition, then the appropriate equation can be found from the general discrete cable equation (4.20) by setting $c_P = 0$, as above,

$$-\left(\frac{2}{h^2} + 1 \right) v_s + \frac{2}{h^2 C_s} \sum_j c_{sj} v_j = \frac{dv_s}{dt} - 2\Omega \frac{i_s}{C_s}. \quad (4.28)$$

Terminal Nodes — Local Origin

The matrix methods must be applied Y-junction by Y-junction if full information about disconnected sections is required. This involves isolating the Y-junction, transforming it,

⁴Recall that charge is constrained to flow in the direction of decreasing x , so positive injected current implies a negative axial current, and vice versa.

then attaching the cable connected section at the local origin, keeping aside the disconnected section if one has been generated.

The local origin, node 0, is connected to nodes l and r on the left and right branches, and can be assigned a temporary sealed end. From (4.28)

$$-\left(\frac{2}{h^2} + 1\right)v_0 + \frac{2c_L}{h^2C_0}v_l + \frac{2c_R}{h^2C_0}v_r = \frac{dv_0}{dt} - 2\Omega \frac{i_0}{C_0}. \quad (4.29)$$

Terminal Nodes — Cut End Boundary condition

The potential at terminal node q on cylinder j is fixed at zero (membrane potential is fixed at rest), so

$$v_q = 0. \quad (4.30)$$

The cut condition must be incorporated into the discrete cable equation describing the single node, n , to which it is connected. Assuming $z \geq 2$, then n must be internal to cylinder j , so equation (4.24), in conjunction with (4.30), becomes

$$\frac{v_p}{h^2} - \left(\frac{2}{h^2} + 1\right)v_n = \frac{dv_n}{dt} - 2\Omega \frac{i_n}{C_n}. \quad (4.31)$$

If node n is internal but connected to two cut terminals, then extending this argument yields,

$$-\left(\frac{2}{h^2} + 1\right)v_n = \frac{dv_n}{dt} - 2\Omega \frac{i_n}{C_n}. \quad (4.32)$$

Thus, terminal nodes with cut boundary conditions⁵ are skipped during node numbering.

It was noted previously that equivalent cable structure (though not the full electrical mapping) could usually be determined even when $z = 1$. This may be desirable for reasons of efficiency when the cable structure, but not the electrical mapping, is required.

As a warning, however, it is useful at this point to illustrate some of the ambiguities and limitations of discrete cable equations associated with certain dendritic structures when $H = h$. The main problem involves short structures, i.e. of length H or $2H$. Dendritic trees models are highly unlikely to be represented so simply, but these are typical lengths for disconnected sections.

The most striking example is the cylinder represented by two nodes, each assigned a cut end condition, as illustrated in Figure 4.3a. No discrete cable equations describe

⁵For trees exhibiting certain geometrical properties, it is acceptable to use more general time-varying voltage boundary conditions. A constant non-zero boundary voltage condition is generally valid, provided all voltage terminals on the tree satisfy exactly the same constant condition. It was originally thought that a general voltage condition was acceptable in all situations, (Ogden *et al.*, 1999), but analytical results in Chapter 6 show this is not actually the case.

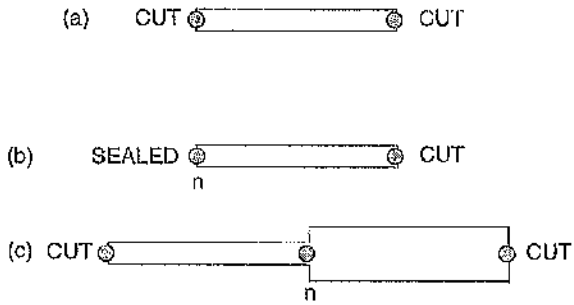


Figure 4.3: Problems encountered with discrete cable equations if describing short cable structure when $z = 1$. (a) A quantum length cable with two cut ends contains no numbered nodes. (b) A quantum length cable with one cut and one current injection terminal is represented by one numbered node. (c) A cable of two quantum lengths, but subject at each end to a cut terminal, is also represented by just one numbered node.

this structure! However, it is always possible to infer its existence by checking whether electrotonic length has been preserved by the cable sections that are actually produced.

Consider also the following two situations: (1) a node that has been assigned a cut condition connected to a node, n , that has been assigned a current injection condition; (2) a node, n , marking a diameter step connected to two nodes that have been assigned cut conditions. By making the appropriate simplifications to equations (4.23) and (4.26), it turns out that the same discrete cable equation describes both structures, i.e. equation (4.32). The two cables, illustrated in Figures 4.3b and 4.3c, have different lengths but cannot be distinguished by their discrete cable equations, hence the ambiguity.

4.2.3 The Matrix Representation of a Dendritic Tree

Once a dendritic tree is represented by k nodes, numbered from zero to $k - 1$ (by the given procedure) a matrix representation for the entire tree may be formulated.

We first introduce some additional notation. The k -length vector of node potentials is denoted v_T ; similarly, the k -length vector i_T represents applied currents at each node. So,

$$v_T = \begin{bmatrix} v_0 \\ v_1 \\ \vdots \\ \vdots \\ v_{k-2} \\ v_{k-1} \end{bmatrix}, \quad i_T = \begin{bmatrix} i_0 \\ i_1 \\ \vdots \\ \vdots \\ i_{k-2} \\ i_{k-1} \end{bmatrix}. \quad (4.33)$$

The diagonal matrix of the tree node c-sums is

$$\mathbf{D}_T = \text{diag} \{C_0, C_1, \dots, C_{k-2}, C_{k-1}\}. \quad (4.34)$$

Each discrete cable equation may be written in the form

$$A_j v_T = I_j \frac{dv_T}{dt} - 2\Omega D_j^{-1} i_T. \quad (4.35)$$

Here, A_j is the j^{th} row of a connectivity matrix, \mathbf{A}_T . The entries in this row are all zero except the j^{th} and those corresponding to nodes connected to j . Similarly, I_j is the j^{th} row of the $k \times k$ identity matrix, with only one non-zero element, i.e. a "1" in location j . Likewise, D_j^{-1} is the j^{th} row of \mathbf{D}_T^{-1} , with a single non-zero element, C_j^{-1} , in the j^{th} slot.

For example, an internal node n connected to nodes p and q has non-zero entries in the p^{th} , n^{th} , and q^{th} slots of A_n . A binary branch node, n connected to nodes p , l and r has non-zero entries in the p^{th} , n^{th} , l^{th} and r^{th} slots of A_n . A current injection terminal node n , connected to node p , has non-zero entries in only the p^{th} and n^{th} slots. An internal node n connected to node p and an unnumbered cut terminal node has non-zero elements in just the p^{th} and n^{th} slots of A_n . Specific examples are illustrated in the next section.

The discrete cable equations are collected together to form the matrix equation,

$$A_T v_T = \frac{dv_T}{dt} - 2\Omega D_T^{-1} i_T. \quad (4.36)$$

Properties of the Tree Matrix

The $k \times k$ square connectivity matrix \mathbf{A}_T is referred to as the *tree matrix*, and represents the geometry and boundary condition types (cut or current injection) of the tree model. Denote the element in row i and column j of \mathbf{A}_T by a_{ij} . Since the coefficient of v_n in discrete cable equation n is always non-zero, the diagonal elements are all non-zero, and in fact identical⁶,

$$a_{ii} = -\left(1 + \frac{2}{h^2}\right), \quad 0 \leq i \leq k-1. \quad (4.37)$$

The row and column numbers of each non-zero off-diagonal element define two nodes that are directly connected, so the tree matrix structure mimics the connectivity of the tree. The tree matrix is not symmetric since $a_{ij} \neq a_{ji}$, however it is structurally symmetric in the sense that

$$a_{ij} \neq 0 \iff a_{ji} \neq 0. \quad (4.38)$$

⁶This is not actually a requirement for the origin node (usually the soma node) but, for cable construction, the origin type is irrelevant and may as well be assumed scaled so that the constant diagonal is maintained.

This follows trivially from the reflexive property of node connectivity, i.e. if node i is connected to j , then node j must also be connected to i . From the discrete cable equations, it can be seen that all off-diagonal elements are non-negative.

The node numbering scheme used, in conjunction with the structure of the second order difference equations, ensures that the tree matrix is almost tri-diagonal, i.e. elements are concentrated on the diagonal, sub-diagonal and super-diagonal. Off-tri-diagonal elements only arise because the presence of branch points prevents consecutive numbering of all the nodes on each cylinder. Branching also gives rise to consecutively numbered nodes that are not connected, since numbering must proceed directly from a terminal node to another cylinder.

A counting argument will show how for each pair of non-zero off-tri-diagonal elements there exists a pair of zero element on the sub- and super-diagonals. Also, the tree matrix for a dendritic tree represented by k nodes contains $3k - 2$ non-zero elements, enough, in fact, to fill just the central-, sub- and super-diagonals.

It should first be noted however that an unbranched structure is represented by a purely tri-diagonal tree matrix, as illustrated schematically in Figure 4.4a. In fact, it is possible to place several unbranching structures together in the same matrix⁷, as illustrated for two cables in Figure 4.4c. A pair of zero elements on the sub- and super-diagonals indicate that they are separate. Singly branched structure (Y-junctions) have very similar structure, with two tri-diagonal portions of the matrix divided by a pair of zero elements but linked by a pair of off-tri-diagonal elements, Figure 4.4b.

Any tree with N terminals can be divided into a set of N paths, each consisting of consecutively numbered nodes. There is one path, the *soma path*, where numbering starts from "0" and ends on a dendritic terminal, plus $N - 1$ additional paths each starting with a node connected to a branch point and ending on a dendritic terminal (or a node connected to a terminal in the case of a voltage boundary condition). Observe that these paths are uniquely determined by the numbering scheme and have the property that every tree node lies on exactly one path. Each path must contribute a tri-diagonal portion to the tree matrix, plus additional off-tri-diagonal elements arising from the connection of that path to the rest of the tree.

Now consider any path starting with node p and connected to another path at the branch point described by node j . The numbering scheme ensures that $p > j + 1$. Tree connectivity ensures that elements a_{jp} and a_{pj} of the matrix A_T are non-zero and off-tri-diagonal, while elements $a_{p(p-1)} = a_{(p-1)p} = 0$ since node $p = 1$, which must be a

⁷These structures hint at the procedure for generating an equivalent cable — tri-diagonalisation of a tree matrix to generate a cable matrix. Furthermore, it is clear how a tree matrix can represent multiple disjoint sections (connected and disconnected sections).

dendritic terminal, and therefore cannot be connected to node p . Since the soma path does not connect to another path, each non-soma path contributes a pair of non-zero off-tri-diagonal entries and a pair of zero elements on the sub- and super-diagonals of A_T , in total $N - 1$ pairs of non-zero off-tri-diagonal elements and $N - 1$ pairs of zero elements on the sub- and super-diagonals of A_T .

If the tree is represented by k nodes then there are $k - 2N$ nodes that lie within paths. Each such element, j say, must connect to nodes $j - 1$ and $j + 1$ and so contributes two off-diagonal elements to the j^{th} row of A , giving a total of $2(k - 2N)$ off-diagonal elements. The off-tri-diagonal elements due to connections between paths have already been determined as $2(N - 1)$. Since the starting node, p say, of each path (including the soma path) must also be connected to node $p + 1$, there are a further N off-diagonal elements, one each in row p . Finally, each of the N terminal nodes must connect to just one other node, yielding a further N off-diagonal elements. In total, then, there are $2(k - 2N) + 2(N - 1) + N + N = 2(k - 1)$ off-diagonal elements. Add the k diagonal elements, and the argument is complete.

Tree Matrix Examples

Tree matrix examples one, two and three below represent the dendritic trees in Figure 4.5. To simplify the matrices $D = (2 + h^2)$ is used.

Example One

The tree matrix for the tree in Figure 4.5a is

$$A_T = \frac{1}{h^2} \begin{bmatrix} D & 2 & 0 & 0 & 0 & 0 & 0 & 0 & 0 \\ 1 & D & 1 & 0 & 0 & 0 & 0 & 0 & 0 \\ 0 & \frac{2c_P}{C_2} & D & \frac{2c_R}{C_2} & 0 & 0 & 0 & \frac{2c_L}{C_2} & 0 \\ 0 & 0 & 1 & D & 1 & 0 & 0 & 0 & 0 \\ 0 & 0 & 0 & 1 & D & 1 & 0 & 0 & 0 \\ 0 & 0 & 0 & 0 & 1 & D & 1 & 0 & 0 \\ 0 & 0 & 0 & 0 & 0 & 2 & D & 0 & 0 \\ 0 & 0 & 1 & 0 & 0 & 0 & 0 & D & 1 \\ 0 & 0 & 0 & 0 & 0 & 0 & 0 & 2 & D \end{bmatrix}. \quad (4.39)$$

The soma node “0” is sealed and described by equation (4.27). The two dendritic tips are sealed, so nodes “6” and “8” are described by equation (4.26) Internal nodes “1”, “3”, “4”, “5” and “7” are described by equation (4.24). Node 2 is a binary branch point described by equation (4.22).

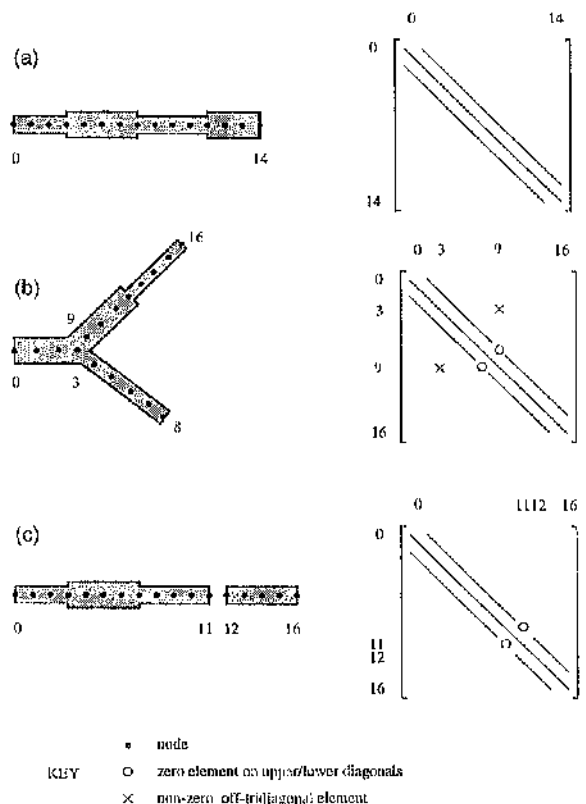


Figure 4.4: Branched trees, unbranched cables and their tree matrix representation. (a) Any single unbranched structure has a perfectly tri-diagonal tree matrix. (b) A singly branched tree has nearly tri-diagonal structure. (c) Placing two unbranched cables in the same matrix representation gives a tri-diagonal matrix, however the sub-matrices representing each cable are separated by two zero elements along the diagonal.

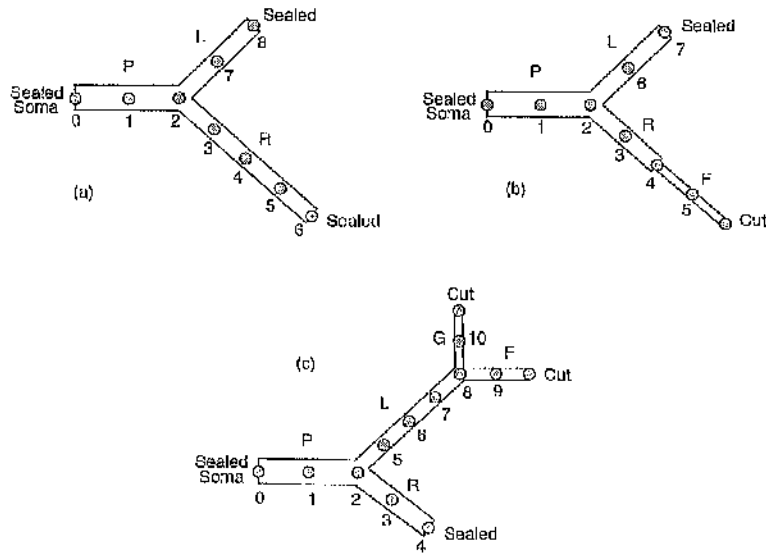


Figure 4.5: Simple examples of discretised dendritic trees. (a) Dendritic tree for Example One, consisting of cylinders P , R , and L . (b) Dendritic tree for Example Two, consisting of cylinders P , R , L , F . (c) Dendritic tree for Example Three, consisting of cylinders P , R , L , F , and G .

Example Two

The tree matrix for the tree in Figure 4.5b is

$$A_T = \frac{1}{h^2} \begin{bmatrix} D & 2 & 0 & 0 & 0 & 0 & 0 & 0 \\ 1 & D & 1 & 0 & 0 & 0 & 0 & 0 \\ 0 & \frac{2c_P}{C_2} & D & \frac{2c_R}{C_2} & 0 & 0 & \frac{2c_L}{C_2} & 0 \\ 0 & 0 & 1 & D & 1 & 0 & 0 & 0 \\ 0 & 0 & 0 & \frac{2c_R}{C_4} & D & \frac{2c_F}{C_4} & 0 & 0 \\ 0 & 0 & 0 & 0 & 1 & D & 0 & 0 \\ 0 & 0 & 1 & 0 & 0 & 0 & D & 1 \\ 0 & 0 & 0 & 0 & 0 & 0 & 2 & D \end{bmatrix}. \quad (4.40)$$

Again the soma node is assigned a sealed condition. Node "5" is an internal node connected to a cut terminal, so is described by equation (4.31). Node "4" is a point of abrupt diameter change described by equation (4.23).

Example Three

The tree matrix for the tree in Figure 4.5c is

$$A_T = \frac{1}{h^2} \begin{bmatrix} D & 2 & 0 & 0 & 0 & 0 & 0 & 0 & 0 & 0 & 0 & 0 \\ 1 & D & 1 & 0 & 0 & 0 & 0 & 0 & 0 & 0 & 0 & 0 \\ 0 & \frac{2c_P}{C_2} & D & \frac{2c_R}{C_2} & 0 & \frac{2c_L}{C_2} & 0 & 0 & 0 & 0 & 0 & 0 \\ 0 & 0 & 1 & D & 1 & 0 & 0 & 0 & 0 & 0 & 0 & 0 \\ 0 & 0 & 0 & 2 & D & 0 & 0 & 0 & 0 & 0 & 0 & 0 \\ 0 & 0 & 1 & 0 & 0 & D & 1 & 0 & 0 & 0 & 0 & 0 \\ 0 & 0 & 0 & 0 & 0 & 1 & D & 1 & 0 & 0 & 0 & 0 \\ 0 & 0 & 0 & 0 & 0 & 0 & 1 & D & 1 & 0 & 0 & 0 \\ 0 & 0 & 0 & 0 & 0 & 0 & 0 & \frac{2c_L}{C_8} & D & \frac{2c_E}{C_8} & \frac{2c_G}{C_8} \\ 0 & 0 & 0 & 0 & 0 & 0 & 0 & 0 & 1 & D & 0 & 0 \\ 0 & 0 & 0 & 0 & 0 & 0 & 0 & 0 & 0 & 1 & 0 & D \end{bmatrix} \quad (4.41)$$

Algebraic structure of the Y-junction Tree Matrix

Consider the general Y-junction illustrated in Figure 4.6. The left branch is formed from m cylinders each of length H , while the right branch is formed from n cylinders also of length H . Cylinders, and nodes, are labelled from 1 to m on the left branch, then from $m+1$ to $m+n$ on the right branch. Both terminals are sealed, as is the junction node. A discretisation level of $z = 1$ is used simply to avoid including the internal nodes (two connected cylinders can easily be given the same c-value to produce the appropriate matrix for $z = 2$).

The algebraic structure of the corresponding tree matrix is very simple, with a single pair of off-tri-diagonal elements due to the single binary branch point; there is a corre-

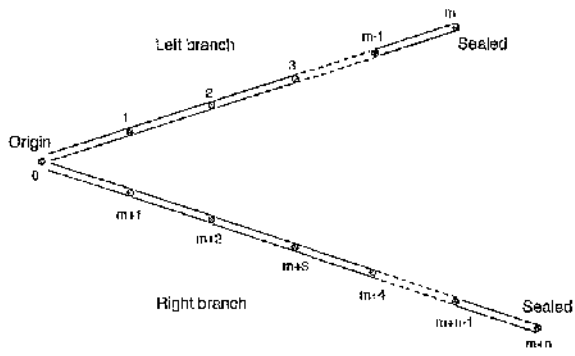


Figure 4.6: Schematic of a general Y-junction.

sponding pair of zero elements, one on the super- and one on the sub-diagonal.

$$\frac{1}{h^2} \begin{bmatrix} D & \frac{2c_1}{C_0} & 0 & 0 & 0 & \cdots & \frac{2c_{m+1}}{C_0} & 0 & 0 & \cdots & 0 \\ \frac{2c_1}{C_1} & D & \frac{2c_2}{C_1} & 0 & 0 & \cdots & 0 & 0 & 0 & \cdots & 0 \\ 0 & \frac{2c_2}{C_2} & D & \frac{2c_3}{C_2} & 0 & \cdots & 0 & 0 & 0 & \cdots & 0 \\ 0 & 0 & \frac{2c_3}{C_3} & D & \ddots & \cdots & 0 & 0 & 0 & \cdots & 0 \\ \vdots & \vdots & \vdots & \ddots & \ddots & \ddots & \frac{2c_m}{C_{m-1}} & \vdots & \vdots & \ddots & \vdots \\ 0 & 0 & 0 & \cdots & 2 & D & 0 & 0 & 0 & \cdots & 0 \\ \frac{2c_{m+1}}{C_{m+1}} & 0 & 0 & \cdots & 0 & 0 & D & \frac{2c_{m+2}}{C_{m+1}} & 0 & \cdots & 0 \\ 0 & 0 & 0 & \cdots & 0 & 0 & \frac{2c_{m+2}}{C_{m+2}} & D & \frac{2c_{m+3}}{C_{m+2}} & \cdots & 0 \\ 0 & 0 & 0 & \cdots & 0 & 0 & 0 & \frac{2c_{m+3}}{C_{m+3}} & D & \ddots & 0 \\ \vdots & \vdots & \vdots & \ddots & \vdots & \vdots & \vdots & \vdots & \ddots & \ddots & \frac{2c_{m+n}}{C_{m+n-1}} \\ 0 & 0 & 0 & \cdots & 0 & 0 & 0 & 0 & 0 & 2 & D \end{bmatrix} \quad (4.42)$$

Eigenvalues and Eigenvectors

A non-zero vector ν is an *eigenvector* of a $k \times k$ square matrix A provided there exists a scalar μ , called an *eigenvalue*, such that

$$A\nu = \mu\nu. \quad (4.43)$$

Suppose B is a nonsingular matrix of the same order as A , then

$$BAB^{-1}(B\nu) = \mu(B\nu). \quad (4.44)$$

Matrix BAB^{-1} therefore has the same eigenvalues as A , but different eigenvectors, namely $B\nu$. Matrix B is a *similarity transform*, and matrix BAB^{-1} is *similar* to A .

If $A\nu = \mu\nu$, then for $0 \leq i \leq k-1$, it follows that

$$\sum_{j=0}^{k-1} a_{ij}\nu_j = \mu\nu_i, \quad (4.45)$$

where ν_i is the i^{th} element of ν . This may be rewritten

$$(a_{ii} - \mu)\nu_i = - \sum_{j=0, j \neq i}^{k-1} a_{ij}\nu_j. \quad (4.46)$$

If ν_i is the largest component of ν then

$$|a_{ii} - \mu| \leq \sum_{j=0, j \neq i}^{k-1} |a_{ij}| \frac{|\nu_j|}{|\nu_i|} \leq \sum_{j=0, j \neq i}^{k-1} |a_{ij}|. \quad (4.47)$$

This result, known as *Gershgorin's circle theorem*, simply says that the magnitude of the difference between an eigenvalue and the central diagonal element in row i is less than the sum of the magnitudes of the off-diagonal elements in row i .

For the particular case of the tree matrix, the central diagonal element is always $-(1 + 2/h^2)$, whatever node we are dealing with. For internal nodes, diameter steps, branch points, and current injection terminals, the sum of the off-diagonal elements is $2/h^2$. For internal nodes connected to cut terminals, the sum is $1/h^2$. It follows from equation (4.47) that

$$\left| 1 + \frac{2}{h^2} + \mu \right| \leq \frac{2}{h^2}, \quad (4.48)$$

Consider the complex plane. Any circle centred on $-(1 + 2/h^2)$ with radius $|\mu|$ must lie in the left half-plane (negative real part). No circle may contain the origin, thus $\mu = 0$ is not an eigenvalue.

It will be shown shortly that a tree matrix may be symmetrised by a similarity transform. The eigenvalues of any symmetric matrix are real, and consequently the tree matrix has real eigenvalues. It follows from (4.48) that

$$-\left(1 + \frac{4}{h^2}\right) \leq \mu \leq -1, \quad (4.49)$$

so bounds for the matrix eigenvalues can be determined. The significance of this result is discussed further in the next section.

4.3 Transforming a Tree Matrix to a Cable Matrix — Equivalent Cable Construction

4.3.1 Introduction and Outline Theory

In overview, three matrix transformations (similarity transformations), denoted S , T and X , are applied to the tree matrix equation as follows: first the tree matrix is symmetrised (S), the result is tri-diagonalised (T), followed by de-symmetrisation (X). This sequence of transformations generates a matrix equation that describes an equivalent cable. The

new equation carries a form similar to the tree matrix equation, i.e. the matrix elements are coefficients of node potentials in discrete cable equations. Matrices S , T and X are all nonsingular square matrices of the same size as A_T .

A tree matrix, though not symmetric, has just the right form that it can be easily symmetrised using a simple scale transformation. Equation (4.36) then becomes

$$(S A_T S^{-1})(S v_T) = \frac{d(S v_T)}{dt} - 2\Omega(S D_T^{-1} i_T), \quad (4.50)$$

where $A_{TS} = S A_T S^{-1}$ is called the *Symmetric Tree Matrix*.

The tri-diagonalisation collapses the branching dendritic structure into an unbranching cable structure (from one symmetric matrix form to another), so that (4.50) becomes

$$(T S A_T S^{-1} T^{-1})(T S v_T) = \frac{d(T S v_T)}{dt} - 2\Omega(T S D_T^{-1} i_T), \quad (4.51)$$

where $A_{CS} = T S A_T S^{-1} T^{-1}$ is the tri-diagonal *Symmetric Cable Matrix*.

The de-symmetrisation of A_{CS} has much in common with the symmetrisation process. Using another scale transformation, a matrix equation is generated that is a collection of discrete cable equations representing an equivalent cable. Equation (4.51) becomes

$$(X T S A_T S^{-1} T^{-1} X^{-1})(X T S v_T) = \frac{d(X T S v_T)}{dt} - 2\Omega(X T S D_T^{-1} i_T), \quad (4.52)$$

or

$$A_C v_C = \frac{dv_C}{dt} - 2\Omega D_C^{-1} i_C, \quad (4.53)$$

where $A_C = X T S A_T S^{-1} T^{-1} X^{-1}$, $v_C = X T S v_T$, and $i_C = D_C X T S D_T^{-1} i_T$. These three quantities are, respectively, the *Cable Matrix*, a vector of cable node potentials, and a vector of injected currents over the cable nodes. As with D_T , we have defined a diagonal matrix of equivalent cable c-sums,

$$D_C = \text{diag } \{\bar{C}_0, \bar{C}_1, \dots, \bar{C}_{k-2}, \bar{C}_{k-1}\}, \quad (4.54)$$

where \bar{C}_j is the c-sum at cable node j .

The cable matrix is determined entirely by the tree matrix and the node chosen as origin (usually “0”) and, like the tree matrix, defines cable shape and boundary condition types. When mapped from tree to cable, tree vectors v_T and i_T together determine electrical activity on the equivalent cable – they do not influence its shape.

The Lanczos and Householder procedures may be applied to any tree matrix, however complicated the tree might be. However, since disconnected sections are associated with a specific sub-tree, it is usually only practical to generate them using a Y-junction by Y-junction approach, whereby a Y-junction is isolated, discretised, numbered, transformed

to its equivalent cable, with the branch point chosen as a local origin and assigned a temporary sealed boundary condition. Its connected section is reattached to the local origin while, if the Y-junction is degenerate, the disconnected section is kept aside and marked as associated with the sub-tree. On completion of the cycle, the final connected section and any disconnected sections may be collected together in one matrix, provided one makes sure the electrical mapping and equivalent cable nodes have been made consistent.

4.3.2 Some Properties of Tree and Cable Matrices

The Electrical Mapping

It is convenient to define the electrical mapping from dendritic tree nodes to equivalent cable nodes by

$$M = XTS. \quad (4.55)$$

The inverse, which defines the electrical mapping from cable to tree, is easily obtained from its component matrices. Both S and X are diagonal, while T is orthogonal ($T^{-1} = T^T$), therefore

$$M^{-1} = S^{-1}T^TX^{-1}. \quad (4.56)$$

In practice M directly maps potentials between the equivalent cable nodes and the tree nodes, that is,

$$v_C = Mv_T, \quad \text{and} \quad v_T = M^{-1}v_C. \quad (4.57)$$

To map applied currents (including non-zero current boundary conditions) between tree and cable, simply use the modified mappings

$$M_I = D_C M D_T^{-1} \quad \text{and} \quad M_I^{-1} = D_T M^{-1} D_C^{-1}. \quad (4.58)$$

so that

$$i_C = M_I i_T, \quad \text{and} \quad i_T = M_I^{-1} i_C. \quad (4.59)$$

Disconnected Sections

The structure of A_T has been thoroughly described in section 4.2.3. It is useful at this point to describe some general properties of A_{CS} and A_C , before actually showing how to generate them.

The whole point of generating A_{CS} is that it is tri-diagonal, and represents an unbranched dendrite. However, it is possible that the symmetric cable matrix actually consists of a set of distinct tri-diagonal square submatrices located along the block diagonal; adjacent matrices are separated by a pair of zeros, one on the sub-diagonal and one on the super-diagonal. This possible matrix structure has already been illustrated in Figure

4.4. and may be interpreted as multiple disjoint cable sections, provided the discrete cable equations are acceptable, i.e. they describe properly terminated unbranched structure.

Exact conditions under which this can occur (essentially electrical symmetries implicit in the tree geometry) are discussed in more detail in section 4.3.4 (in mathematical terms) and in Chapter 6 (in terms of the physical structure of the tree).

Consider the important case of the general Y-junction. Denote the $k_c \times k_c$ connected section sub-matrix by A_{con} , and, if it exists, the $k_d \times k_d$ disconnected section sub-matrix by A_{dis} . For degenerate Y-junctions, $k = k_c + k_d$ and, in block form,

$$A_{CS} = \begin{bmatrix} A_{\text{con}} & \mathbf{0} \\ \mathbf{0} & A_{\text{dis}} \end{bmatrix}, \quad (4.60)$$

in which case the tri-diagonalisation operation for the Y-junction matrix may be written in block form as

$$\mathbf{T} = \begin{bmatrix} \mathbf{T}_{\text{con}} \\ \mathbf{T}_{\text{dis}} \end{bmatrix} \quad (4.61)$$

where \mathbf{T}_{con} is a $k_c \times k$ matrix and \mathbf{T}_{dis} is a $k_d \times k$ matrix.

For non-degenerate Y-junctions, $k = k_c$ and

$$A_{CS} = A_{\text{con}}, \quad \mathbf{T} = \mathbf{T}_{\text{con}}. \quad (4.62)$$

Once a complete tree has been reduced, the full equivalent cable sub-matrix may be built up. The leading sub-matrix, now denoted $A_{\text{con}}^{(0)}$ describes the connected section, while additional square $k_i \times k_i$ sub-matrices are denoted $A_{\text{dis}}^{(i)}$ where $1 \leq i \leq r$, form the set of r disconnected sections. So, in block notation,

$$A_{CS} = \begin{bmatrix} A_{\text{con}}^{(0)} & \mathbf{0} & \mathbf{0} & \mathbf{0} & \mathbf{0} & \mathbf{0} \\ \mathbf{0} & A_{\text{dis}}^{(1)} & \mathbf{0} & \mathbf{0} & \mathbf{0} & \mathbf{0} \\ \mathbf{0} & \mathbf{0} & A_{\text{dis}}^{(2)} & \mathbf{0} & \mathbf{0} & \mathbf{0} \\ \mathbf{0} & \mathbf{0} & \mathbf{0} & \ddots & \mathbf{0} & \mathbf{0} \\ \mathbf{0} & \mathbf{0} & \mathbf{0} & \mathbf{0} & A_{\text{dis}}^{(r-1)} & \mathbf{0} \\ \mathbf{0} & \mathbf{0} & \mathbf{0} & \mathbf{0} & \mathbf{0} & A_{\text{dis}}^{(r)} \end{bmatrix} \quad (4.63)$$

where

$$k = k_c + \sum_{i=1}^r k_i. \quad (4.64)$$

The tri-diagonalisation operation may be written

$$T = \begin{bmatrix} T_{\text{con}}^{(0)} \\ T_{\text{dis}}^{(1)} \\ \vdots \\ \vdots \\ T_{\text{dis}}^{(r-1)} \\ T_{\text{dis}}^{(r)} \end{bmatrix} \quad (4.65)$$

where $T_{\text{con}}^{(0)}$ is a $k_c \times k$ matrix that relates tree node potentials to cable connected section node potentials; similarly, $T_{\text{dis}}^{(i)}$ is a $k_i \times k$ matrix that relates tree node potentials to cable disconnected section i 's node potentials. Thus,

$$A_{\text{dis/con}}^{(i)} = T_{\text{dis/con}}^{(i)} A_{TS} \left(T_{\text{dis/con}}^{(i)} \right)^{-1}. \quad (4.66)$$

The rows of T are essentially a set of basis vectors spanning n -dimensional space. Any distribution of electrical activity (scaled appropriately by S and X) over a tree can be written as a linear combination of these vectors. In general, some activity is mapped to the connected section, while the rest maps to the disconnected sections.

Associated with each sub-matrix $A_{\text{con/dis}}^{(i)}$ is a subspace σ_i (closed under multiplication by A_{TS}), with

$$\sigma_i = \text{span} \left\{ x : \text{where } x \text{ is a row of } T_{\text{dis/con}}^{(i)} \right\}. \quad (4.67)$$

Subspace σ_0 describes activity that the origin can detect, and remaining subspaces describe activity that the origin cannot detect.

Note that, when applied Y-junction by Y-junction, the Householder tri-diagonalisation will automatically generate the invariant subspaces and their corresponding sub-matrices, i.e. it generates the disconnected section if a Y-junction is degenerate; the Lanczos procedure will only do so after some effort to restart the process after early termination.

Spectral Properties of the Tree and Cable Matrices

For most of this thesis, we will not be concerned directly with the temporal properties of the cable equation, however it is useful to consider some important properties of the tree matrix eigenvalues. It has already been shown (4.49) that the eigenvalues of a tree matrix are negative, and lie in the range -1 to $-(1 + 4/h^2)$. Clearly, the smaller the internodal interval the greater the range of eigenvalues. The tree matrix eigenvalues have an important physical interpretation, and are related to the decay time constants of characteristic voltage distributions over the tree model nodes.

Suppose that i_T is zero. If ν_i is an eigenvector of A_T and μ_i is the corresponding real eigenvalue then,

$$A_T \nu_i = \mu_i \nu_i. \quad (4.68)$$

From equation (4.36), regarding the eigenvectors as distributions of potentials of the tree nodes, we may then write

$$\mu_i \nu_i = \frac{d\nu_i}{dt}. \quad (4.69)$$

This equation has solutions of the form

$$\nu_i = k_i e^{\mu_i t}. \quad (4.70)$$

Eigenvector ν_i is essentially a characteristic distribution of node potentials (whose initial distribution is given by k_i) which decays exponentially over the whole tree with time constant $\tau_i = -1/\mu_i$ (given in units of the membrane time constant, τ) of the tree matrix A_T . Importantly, time constants can never be greater than τ .

Since M is a similarity transform (a product of three similarity transforms) the eigenvalues of A_C are the same as those of A_T . The corresponding eigenvectors, or characteristic voltage distributions, are given by $M\nu_i$. Thus, a tree eigenvector potential is mapped by M to the equivalent cable eigenvector potential that will decay at the same characteristic rate. This is an important feature for the equivalence of a dendritic tree and its equivalent cable.

It is vital that one distinguishes between time constants determined by matrix eigenvalues (of which there are finitely many⁸) and the time constants that are characteristic of the original spatially continuous model (denoted τ_i^r , and of which there are infinitely many, see Rall, 1969a). For example, the voltage response at the soma due to a configuration of inputs at $t = 0$ somewhere on the tree can often be expressed as an infinite sum of decay time constants, that is

$$v_S(t) = \sum_{i=0}^{\infty} B_i e^{-\mu_i t} \quad (4.71)$$

where the B_i are coefficients determined by initial conditions.

Typically only a very small proportion of the largest matrix eigenvalues will give reasonable approximations to actual time constants. This is an unavoidable consequence of approximating a continuous model by a discrete model. A finer discretisation (smaller h , more nodes) can improve the accuracy of the larger matrix time constants, but still only a small proportion usually are acceptable. For the purposes of simulations, the larger

⁸For a $k \times k$ tree matrix, there are at most k eigenvalues. There are less than k if the tree matrix has repeated eigenvalues. The existence of disconnected sections, i.e. electrical degeneracy in the tree, is associated with the existence of repeated (degenerate) eigenvalues in the tree matrix.

time constants dominate the structure of voltage transients since the effects of the smaller (faster) constants can only be significant at initiation of the transient.

Sealed Trees in Particular

If all terminals on a tree are sealed, then the sum of non-zero elements in any row of the tree matrix must be -1 . Therefore, the potential distribution

$$\nu = [1, 1, \dots, 1, 1]^T \quad (4.72)$$

is an eigenvector of A_T , with corresponding eigenvalue -1 , i.e.

$$A_T \nu = -\nu. \quad (4.73)$$

This uniform distribution therefore decays with characteristic time constant τ , the membrane time constant.

Mapping this uniform potential to the equivalent cable always give a uniform distribution over the connected cable section. This is explained in more detail in Chapter 6 (conservation of coefficients), however, it follows because, for sealed trees, the sum of each row of M associated with a cable connected section node is unity. Alternatively, a physical argument demands that the cable origin must also observe the same uniform decay of voltage. The connected section of the equivalent cable must also be sealed, otherwise this is not possible, and so

$$A_{\text{con}}^{(0)} \nu = -\bar{\nu}, \quad (4.74)$$

where

$$\bar{\nu} = M_0 \nu = [1, 1, \dots, 1, 1]^T \quad (4.75)$$

is a k_c -length vector.

Partial Generation of the Cable

Under some circumstances, the complete equivalent cable may not be required, or it may not be practical to generate the full cable because of numerical considerations. For example, the connected section may be all that is of interest. In such situations the tri-diagonalisation and de-symmetrisation need only be partially completed.

Let T_m be the $m \times n$ matrix that generates the $m \times m$ leading sub-matrix of the full symmetric cable matrix. Only this sub-matrix need be de-symmetrised so let X_m denote the leading $m \times m$ sub-matrix of X . This partial cable matrix equation can be written

$$A_C^{(m)} v_C^{(m)} = \frac{dv_C^{(m)}}{dt} + i_C^{(m)}, \quad (4.76)$$

where superscripted matrices and vectors describe m nodes of the equivalent cable, and the partial cable matrix is

$$\mathbf{A}_C^{(m)} = \mathbf{X}_m \mathbf{T}_m \mathbf{S} \mathbf{A}_T \mathbf{S}^{-1} \mathbf{T}_m^T \mathbf{X}_m^{-1}. \quad (4.77)$$

The mappings from tree to partial cable and from partial cable to tree are then

$$\mathbf{M}_m = \mathbf{X} \mathbf{T}_m \mathbf{S}_m, \quad \mathbf{M}_m^{-1} = \mathbf{S}^{-1} \mathbf{T}_m^T \mathbf{X}_m^{-1} \quad (4.78)$$

though there is information missing, and the full space of electrical activity over the tree will not be accounted for in the mapping.

4.3.3 The Symmetric Tree Matrix

There is a non-singular $k \times k$ diagonal matrix \mathbf{S} such that the $k \times k$ tree matrix, \mathbf{A}_T , can be symmetrised,

$$\mathbf{S} \mathbf{A}_T \mathbf{S}^{-1} = \mathbf{A}_{TS}. \quad (4.79)$$

Transformation \mathbf{S} consists of non-zero scaling factors,

$$\mathbf{S} = \text{diag } \{s_0, s_1, \dots, s_{k-2}, s_{k-1}\}, \quad (4.80)$$

where

$$s_i = \begin{cases} 1 & i = 0 \\ s_j \sqrt{\frac{c_{ji}}{a_{ij}}} & 1 \leq i \leq k-1 \end{cases}. \quad (4.81)$$

Each scaling factor fixes two off-tri-diagonal elements. After initialising one scaling factor (s_0), there are just the right number of off-diagonal elements, i.e. $2(k - 1)$ to be symmetrised by a further $k - 1$ scaling factors.

Denoting the elements of \mathbf{A}_{TS} by \bar{a}_{ij} , it is easy to check that, for $i \neq j$,

$$\bar{a}_{ij} = a_{ji} - a_{ij} \frac{s_i}{s_j} = a_{ji} \frac{s_j}{s_i} = \sqrt{a_{ij} a_{ji}}. \quad (4.82)$$

and the central diagonal is unaltered. In fact, there is a clear structure to the s_i . Suppose $j > i$. Since $a_{ij} = 2c_{ij}/h^2 C_i$, then from (4.81),

$$s_i = s_j \sqrt{\frac{C_i}{C_j}}. \quad (4.83)$$

By recursive substitution for s_j so that s_i is expressed in terms of lower and lower numbered scaling factors, there is repeated cancellation of the denominator, and we obtain

$$s_i = \sqrt{\frac{C_i}{C_0}}. \quad (4.84)$$

since $s_0 = 1$.

Also, non-zero off-diagonal elements of A_{TS} may be written

$$\bar{a}_{ij} = \bar{a}_{ji} = \frac{2c_{ij}}{h^2 \sqrt{C_i^s C_j^s}}, \quad (4.85)$$

where c_{ij} is the c-value of the cylinder section linking connected nodes i and j .

Matrix S is trivially nonsingular, and its inverse is easily obtained,

$$S^{-1} = \text{diag} \{ s_0^{-1}, s_1^{-1}, \dots, s_{k-2}^{-1}, s_{k-1}^{-1} \}. \quad (4.86)$$

As an example, the symmetric form of the tree matrix in example two (4.40), is

$$A_{TS} = \frac{1}{h^2} \begin{bmatrix} D & \sqrt{2} & 0 & 0 & 0 & 0 & 0 & 0 \\ \sqrt{2} & D & \sqrt{\frac{2c_P}{C_2}} & 0 & 0 & 0 & 0 & 0 \\ 0 & \sqrt{\frac{2c_P}{C_2}} & D & \sqrt{\frac{2c_{R1}}{C_2}} & 0 & 0 & \sqrt{\frac{2c_L}{C_2}} & 0 \\ 0 & 0 & \sqrt{\frac{2c_{R1}}{C_2}} & D & \sqrt{\frac{2c_{R1}}{C_4}} & 0 & 0 & 0 \\ 0 & 0 & 0 & \sqrt{\frac{2c_{R1}}{C_4}} & D & \sqrt{\frac{2c_{R2}}{C_4}} & 0 & 0 \\ 0 & 0 & 0 & 0 & \sqrt{\frac{2c_{R2}}{C_4}} & D & 0 & 0 \\ 0 & 0 & \sqrt{\frac{2c_L}{C_2}} & 0 & 0 & 0 & D & \sqrt{2} \\ 0 & 0 & 0 & 0 & 0 & 0 & \sqrt{2} & D \end{bmatrix}, \quad (4.87)$$

with

$$S = \text{diag} \left\{ 1, \sqrt{2}, \sqrt{\frac{C_2}{c_P}}, \sqrt{\frac{2c_{R1}}{c_P}}, \sqrt{\frac{C_4}{c_P}}, \sqrt{\frac{2c_{R2}}{c_P}}, \sqrt{\frac{2c_L}{c_P}}, \sqrt{\frac{c_L}{c_P}} \right\}. \quad (4.88)$$

Algebraic Structure of A_{TS} and S .

If we write

$$W_i = \sqrt{C_i C_{i+1}}, \quad \text{and} \quad W_{ij} = \sqrt{C_i C_j}, \quad (4.89)$$

then the symmetric form of the general Y-junction tree matrix given in equation (4.42) is

$$\frac{1}{h^2} \begin{bmatrix} D & \frac{c_1}{W_0} & 0 & 0 & 0 & \cdots & \frac{2c_{m+1}}{W_{0(m+1)}} & 0 & 0 & \cdots & 0 \\ \frac{c_1}{W_0} & D & \frac{c_2}{W_1} & 0 & 0 & \cdots & 0 & 0 & 0 & \cdots & 0 \\ 0 & \frac{c_2}{W_1} & D & \frac{c_3}{W_2} & 0 & \cdots & 0 & 0 & 0 & \cdots & 0 \\ 0 & 0 & \frac{c_3}{W_2} & D & \ddots & \cdots & 0 & 0 & 0 & \cdots & 0 \\ \vdots & \vdots & \vdots & \ddots & \ddots & \ddots & \vdots & \vdots & \vdots & \ddots & 0 \\ 0 & 0 & 0 & \cdots & \frac{c_m}{W_{m-1}} & D & 0 & 0 & 0 & \cdots & 0 \\ \frac{c_{m+1}}{W_{0(m+1)}} & 0 & 0 & \cdots & 0 & 0 & D & \frac{c_{m+2}}{W_{m+1}} & 0 & \cdots & 0 \\ 0 & 0 & 0 & \cdots & 0 & 0 & \frac{c_{m+2}}{W_{m+1}} & D & \frac{c_{m+3}}{W_{m+2}} & \cdots & 0 \\ 0 & 0 & 0 & \cdots & 0 & 0 & 0 & \frac{c_{m+3}}{W_{m+2}} & D & \ddots & 0 \\ \vdots & \vdots & \vdots & \ddots & \vdots & \vdots & \vdots & \vdots & \ddots & \ddots & \frac{c_{m+n}}{W_{m+n-1}} \\ 0 & 0 & 0 & \cdots & 0 & 0 & 0 & 0 & 0 & \frac{c_{m+n}}{W_{m+n-1}} & D \end{bmatrix} \quad (4.90)$$

with

$$S = \text{diag} \left\{ 1, \sqrt{\frac{C_1}{C_0}}, \sqrt{\frac{C_2}{C_0}}, \sqrt{\frac{C_3}{C_0}}, \dots, \dots, \sqrt{\frac{C_{m+n}}{C_0}} \right\} \quad (4.91)$$

4.3.4 Lanczos Tri-diagonalisation

This method of tri-diagonalisation was introduced by Lanczos (1950). General discussion of Lanczos tri-diagonalisation and its startling convergence properties can be found in Golub and Van Loan (1990) and Paige (1976, 1980). It has been used extensively in nuclear physics (Whitehead *et al.*, 1977), and it is via this field that the method found its way to neuronal modelling. Previously, an outline of the general ideas underlying the process, with specific application to equivalent cables, and in particular the connected section, has been given in Whitehead and Rosenberg (1993). Further details are presented in Ogden *et al.* (1999), and expanded upon even further here.

Lanczos tri-diagonalisation does not naturally generate disconnected sections since the algorithm terminates after generating the connected section, however, with a little effort, it is often possible to restart the algorithm if necessary.

When using the Lanczos procedure, we set $\mathbf{T} = \mathbf{L}$.

General Theory

The Lanczos method is normally associated with solving the eigenproblem,

$$\mathbf{A}\mathbf{x} = \mu\mathbf{x}, \quad (4.92)$$

where A is generally large, symmetric, and sparsely filled⁹.

First, choose an initial, normalised Lanczos vector, u_0 . The choice is very significant for the progress of the algorithm, but may depend on the reasons for using the process in the first place (in the case of equivalent cable construction the initial vector has an important physical meaning). After pre-multiplying u_0 by A , the result may be expressed as a linear combination of the first Lanczos vector (u_0) and a new normalised Lanczos vector (u_1), orthogonal to the first. This action is then repeated with the newly generated Lanczos vector, again pre-multiplying by A , and choosing yet another normalised Lanczos vector, which will be orthogonal to all previous Lanczos vectors. In this manner, the following tri-diagonal structure is built up.

$$\begin{aligned} Au_0 &= \alpha_0 u_0 + \beta_0 u_1 \\ Au_1 &= \beta_0 u_0 + \alpha_1 u_1 + \beta_1 u_2 \\ Au_2 &= \beta_1 u_1 + \alpha_2 u_2 + \beta_2 u_3 \\ Au_3 &= \beta_2 u_2 + \alpha_3 u_3 + \beta_3 u_4 \\ \vdots &= \ddots \quad \ddots \quad \ddots \end{aligned}$$

The coefficients of the u_i are the elements of the new tri-diagonal matrix. Observe that orthogonality of the u_i implies

$$\alpha_i = u_i^T A u_i, \quad (4.93)$$

and

$$\beta_i = u_{i+1}^T A_{TS} u_i. \quad (4.94)$$

After one iteration, enough elements have been generated to construct a 1×1 matrix,

$$A^{(1)} = \left[\begin{array}{c} \alpha_0 \end{array} \right]. \quad (4.95)$$

After a second iteration, a 2×2 matrix,

$$A^{(2)} = \left[\begin{array}{cc} \alpha_0 & \beta_0 \\ \beta_0 & \alpha_1 \end{array} \right], \quad (4.96)$$

may be constructed, and so on. Thus, the j th iteration of the algorithm produces enough elements to construct a $j \times j$ matrix, denoted $A^{(j)}$, whose diagonal is given by α_0 to α_{j-1} and super- and sub-diagonals given by β_0 to β_{j-2} .

⁹While the method may be extended to unsymmetric matrices, this is at the cost of introducing bi-orthogonal sets of Lanczos vectors. For tree matrices, it is much more convenient to take advantage of structure and symmetrisation — a very quick process. In fact, it is more efficient to generate A_{TS} directly from tree data, bypassing A_T altogether.

Extraordinary convergence properties of the method mean that information about A 's extremal eigenvalues emerge long before tri-diagonalisation is complete. Essentially, as j increases, the extremal eigenvalues (largest and smallest) of $A^{(j)}$ are better and better approximations to the extremal eigenvalues of A .

This is not, however, the reason we use Lanczos tri-diagonalisation. For our purpose, the most important property of the Lanczos tri-diagonalisation is that it preserves essential matrix structure, allowing eventual interpretation as an equivalent cable.

Provided the convergence properties and extremal eigenvalues are the points of interest, the Lanczos' advantages over a more stable Householder method are storage and speed. These have been vital consideration for the massive sparse matrices commonly found in nuclear shell model calculations (Whitehead *et al.*, 1977). Highly complicated dendritic trees are also likely to require huge sparse matrices for a reasonable representation. The major pitfall when using the Lanczos procedure is that roundoff errors, and a loss of orthogonality among the Lanczos vectors, can be troublesome.

It can happen that after some iteration, $j < k$, element β_{j-1} is zero, at which point the algorithm terminates prematurely, with the construction of a subspace. This happens when the initial vector, u_0 , is deficient in some of the eigenvectors of A , i.e. u_0 can be expressed as a linear combination of $j < k$ eigenvectors. In this situation, A has repeated, or degenerate, eigenvalues. The $j \times j$ tri-diagonal matrix that has been produced is non-degenerate, i.e. contains exactly one copy of each of the eigenvalues of A .

Application to the Tree Matrix

For the specific case of a $k \times k$ symmetric tree matrix, there are several factors in our favour that simplify Lanczos tri-diagonalisation: the central diagonal is a known constant and the choice of initial Lanczos vector is fixed by the node chosen as origin.

The standard unit vectors, e_i , are useful, where

$$e_0 = \begin{bmatrix} 1 \\ 0 \\ 0 \\ \vdots \\ 0 \\ 0 \end{bmatrix}, \quad e_1 = \begin{bmatrix} 0 \\ 1 \\ 0 \\ \vdots \\ 0 \\ 0 \end{bmatrix}, \quad \dots \quad e_i = \begin{bmatrix} 0 \\ 0 \\ \vdots \\ 1 \\ \vdots \\ 0 \end{bmatrix}, \quad \dots \quad (4.97)$$

It is useful to think of e_i as representing node i on the dendritic tree. The set of orthonormal Lanczos vectors play a similar role for equivalent cable, with u_i representing node i on the cable.

The initial, normalised Lanczos vector, u_0 , must represent the node chosen as origin. For example, if the soma node is taken as origin, as would normally be the case, then

$$u_0 = e_0. \quad (4.98)$$

Lanczos Vector Structure

When tri-diagonalising the symmetric tree matrix, the resulting tridiagonal matrix must be of an acceptable form. The central diagonal elements of A_{CS} must be constant and equal to that in A_{TS} if it is to be eventually interpreted as a set of discrete cable equations. The general Lanczos procedure does not produce this constant diagonal, so we now prove the following result which shows how tree matrix connectivity can impose interesting structure on the Lanczos vectors, and thereby ensure the cable matrix structure we require.

Let A be a symmetric tree connectivity matrix with constant diagonal element D . If A is tri-diagonalised by the Lanczos method, taking initial vector u_0 to be a standard unit vector, then the diagonal elements of the resulting tri-diagonal matrix are also all the same and equal to D .

Proof: First, observe that $\alpha_i = u_i^T A u_i$ may be written

$$\alpha_i = \sum_{p=0}^{k-1} \sum_{q=0}^{k-1} a_{pq} u_p^{(i)} u_q^{(i)}, \quad (4.99)$$

where $u_p^{(i)}$ denotes the p^{th} element of u_i . The central diagonal of A_{TS} is constant, u_i is normalised, and $a_{pq} = 0$ unless node p is connected to node q , so equation (4.99) may be simplified to

$$\alpha_i = D + \sum_{p=0}^{k-1} \sum_{q \rightarrow p} a_{pq} u_p^{(i)} u_q^{(i)}, \quad (4.100)$$

where $q \rightarrow p$ means that the sum is over all nodes connected to p . It remains to show that if nodes p and q are connected then one of $u_p^{(i)}$ and $u_q^{(i)}$ must be zero, in other words two connected nodes do not both contribute to the same Lanczos vector¹⁰. Once this has been shown, it follows immediately that $\alpha_i = D$, for all i . Clearly, this is the case for the initial unit Lanczos vector ($i = 0$), so $\alpha_0 = D$.

Suppose now that Lanczos vector u_{i-1} only has non-zero elements contributed by nodes that are either (1) all an even number (or zero) of h from the origin, called *even-distant* nodes, or (2) all an odd number of h from the origin, called *odd-distant* nodes. In either case, no two nodes that contribute to this Lanczos vector are connected.

¹⁰We say a tree node, i , contributes to vector u_j if the i^{th} element of u_j is non-zero.

From the general Lanczos vector/tri-diagonal matrix structure above we can write

$$\beta_{i-1}u_i + \beta_{i-2}u_{i-2} = Au_{i-1} - \alpha_{i-1}u_{i-1}, \quad 1 \leq i \leq k-1, \quad (4.101)$$

provided we set $\beta_{-1} = 0$ and $u_{-1} = 0$. Now observe that the p^{th} element of the right hand side of this expression can be rewritten

$$[(A - \alpha_{i-1}I) u_{i-1}]_p = \sum_{j=0, j \neq p}^{k-1} a_{pj} u_j^{(i-1)} \quad (4.102)$$

Restricting the sum to the non-zero elements, i.e. where j is connected to p , gives

$$[(A - \alpha_{i-1}I) u_{i-1}]_p = \sum_{j \rightarrow p} a_{pj} u_j^{(i-1)} \quad (4.103)$$

Consider first situation (1), where non-zero elements of u_{i-1} are contributed by even-distant nodes. If p is odd-distant then those nodes connected to p must be even-distant, so when p is odd-distant (4.103) may be non-zero. If p is even-distant then those nodes connected to node p are odd-distant, and (4.103) must be zero. Consequently, if only even-distant nodes contribute to u_{i-1} then it must be true that only odd-distant nodes contribute to $\beta_{i-1}u_i + \beta_{i-2}u_{i-2}$ (the left hand side of 4.101).

A similar argument for situation (2) shows that if only odd-distant nodes contribute to u_{i-1} then it must be true that only even-distant nodes contribute to $\beta_{i-1}u_i + \beta_{i-2}u_{i-2}$.

Now, we can establish initially that since u_0 has one contribution from the origin node (counted as even-distant), then u_1 has contributions from odd-distant nodes. It then follows that u_2 has contributions from even-distant nodes.

Now, suppose u_{i-2} has contributions from odd-distant (even-distant) nodes and u_{i-1} has contributions from even-distant (odd-distant). The latter ensures that $\beta_{i-1}u_i + \beta_{i-2}u_{i-2}$ has contributions from odd-distant (even-distant) nodes, while the former now ensures that u_i on its own must have contributions only from odd-distant (even-distant) nodes. This argument holds true for $i = 1$ and $i = 2$, and so by induction holds for all i . Thus, only unconnected nodes contribute to u_i , and the result follows.

This result gives some insight into how the Lanczos vectors develop, and consequently how the electrical mapping is built up.

Further consideration of equation (4.103), and a similar induction argument to that above show that only nodes connected to those nodes that contribute to u_{i-1} may actually contribute to u_{i-1} . This leads to an evolution of the Lanczos vectors which ensures that the equivalent cable structure that is j internodal lengths from the origin depends only on dendritic tree structure up to j internodal lengths from the origin. Furthermore, there

must be an even number of internodal electrotonic lengths (h) between any two nodes contributing to a particular Lanczos vector.

Since \mathbf{u}_0 is always a standard unit vector, orthogonality ensures that the origin never actually contributes to any other vector. This may be taken as an indication that equivalent cable structure is independent of the nature of the origin boundary condition (though of course it will depend on the location of the origin). The physical structure of a dendritic tree determines whether or not a node that *may* contribute actually *does* contribute to a Lanczos vector.

The Lanczos algorithm applied to the symmetric tree matrix therefore yields

$$\begin{aligned} \mathbf{A}_{TS}\mathbf{u}_0 &= D\mathbf{u}_0 + \beta_0\mathbf{u}_1 \\ \mathbf{A}_{TS}\mathbf{u}_1 &= \beta_0\mathbf{u}_0 + D\mathbf{u}_1 + \beta_1\mathbf{u}_2 \\ \mathbf{A}_{TS}\mathbf{u}_2 &= \beta_1\mathbf{u}_1 + D\mathbf{u}_2 + \beta_2\mathbf{u}_3 \\ \mathbf{A}_{TS}\mathbf{u}_3 &= \beta_2\mathbf{u}_2 + D\mathbf{u}_3 + \beta_3\mathbf{u}_4 \\ \vdots &= \ddots \quad \ddots \quad \ddots \end{aligned}$$

The coefficients of the \mathbf{u}_i are the elements of the tri-diagonal symmetric cable matrix. Without loss of generality, the β_i are chosen to be positive. The tri-diagonalisation is complete when k orthonormal Lanczos vectors (\mathbf{u}_0 to \mathbf{u}_{k-1}) have been generated, spanning the complete k -dimensional vector space.

Transformation \mathbf{L} is a row-partitioned matrix of transposed orthonormal Lanczos vectors (\mathbf{u}_i^T), so

$$\mathbf{L} = \begin{bmatrix} \mathbf{u}_0^T \\ \mathbf{u}_1^T \\ \mathbf{u}_2^T \\ \vdots \\ \vdots \\ \mathbf{u}_{k-1}^T \end{bmatrix}. \quad (4.104)$$

Orthonormality of the Lanczos vectors implies that \mathbf{L} is an orthogonal matrix, and so $\mathbf{L}^T = \mathbf{L}^{-1}$, allowing simple inversion of \mathbf{L} .

The algorithm will terminate when a vector \mathbf{u}_m has been generated such that no new vector \mathbf{u}_{m+1} is required to represent $\mathbf{A}_{TS}\mathbf{u}_m$, i.e. $\beta_m = 0$. At this point, the connected section ($\mathbf{A}_{\text{con}}^{(0)}$) has been generated. If, when applied to a $k \times k$ symmetric tree matrix, the algorithm terminates when $m = (k - 1)$, so that k Lanczos vectors have been produced, then we are finished; the entire space of electrical activity over the dendritic tree is represented on the equivalent cable connected section. If instead the algorithm terminates prematurely after producing $m < k$ Lanczos vectors, a subspace has been generated; this subspace describes electrical activity that can be observed and distinguished by the origin.

Any additional subspaces and sub-matrices that are associated with disconnected sections can be generated provided suitable new initial normalised Lanczos vectors, orthogonal to all previous Lanczos vectors, can be found. However, if a complex branched dendritic tree is treated as a single unit, it is not clear exactly how to choose a new vector (unlike u_0 for the connected section). For a tree with several orders of branching, there are usually many possible new choices of orthonormal vector, most of which will not allow a proper physical interpretation of the resulting sub-matrix as a disconnected section. As stated previously, since a disconnected section is associated with a specific sub-tree, it is usually only practical to generate the new vector if the Lanczos algorithm is applied in a Y-junction by Y-junction manner. For each Y-junction there is a maximum of one additional subspace to determine. A method, based on analytical results and observations presented in Chapter 6, is available for finding the new Lanczos vector, and is discussed in Section 4.3.4.

Once a new Lanczos vector has been found, the tri-diagonalisation process can be restarted and continued as before.

Partial Generation of the Cable

Denote the matrix of the first m transposed Lanczos vectors by L_m , so

$$L_m = \begin{bmatrix} u_0^T \\ u_1^T \\ \vdots \\ \vdots \\ u_{m-1}^T \end{bmatrix}. \quad (4.105)$$

This is obtained once the leading $m \times m$ symmetric cable sub-matrix is obtained, representing the connected section of the equivalent cable. So,

$$A_C^{(m)} = X_m L_m S A_T S^{-1} L_m^T X_m^{-1}. \quad (4.106)$$

Y-junctions and Disconnected Sections

For a Y-junction by Y-junction reduction of a tree, the complete Lanczos procedure must be applied to each Y-junction. Before transformation, the Y-junction's nodes must be renumbered from zero (using the standard scheme). When the connected section is reattached, the nodes that form the intermediate dendritic structure must be renumbered to ensure consecutive numbering. It is essential that we keep track of the correct electrical mapping from original tree to final equivalent cable. This is merely a record keeping task, ensuring that we can relate the nodes involved in each electrical mapping through all the

intermediate structures. Eventually the matrices \mathbf{X} , \mathbf{T} , \mathbf{A}_{CS} and \mathbf{A}_C for the complete equivalent cable and the mapping from the original tree can be constructed from the matrices generated for each Y-junction.

The Y-junction approach is acceptable because the branch point nature of the temporary origin (like any origin) does not influence construction of the Y-junction's equivalent cable. The local origin can be temporarily assigned at sealed boundary condition. The intermediate dendritic structures generated by the process are, as seen by the origin, electrically equivalent.

In fact, any terminating substructure may be isolated, transformed and re-attached in this way. However, the Y-junction is the basic unit of branching dendritic structure and is the key to choosing new Lanczos vectors to restart the tri-diagonalisation and generate disconnected sections.

If a Y-junction is degenerate, we need to re-initialise construction of its equivalent cable with a new orthonormal Lanczos vector. It was clear for the connected section which node the initial vector should represent (the origin). We need to choose a new Lanczos vector that will also represent a terminal node on the equivalent cable. An approach that has been effective, and is based on analytically derived results, is to restart where the connected section finished, at the only (non-origin) equivalent cable terminal node we have knowledge of at this stage. It is possible to construct a new Lanczos vector which, in a sense, also represents this node — it incorporates the same boundary condition, but represents structure on the far side of the node, i.e. beyond the connected section.

If a connected section terminated prematurely with cable node $(m - 1)$, represented by Lanczos vector \mathbf{u}_{m-1} , choose a new vector \mathbf{u}_m where the only possible non-zero elements are at the same locations as non-zero elements in \mathbf{u}_{m-1} but adjusted to ensure orthogonality with \mathbf{u}_{m-1} as well as \mathbf{u}_0 to \mathbf{u}_{m-2} . So, if

$$\mathbf{u}_{m-1} = \begin{bmatrix} p_0 \\ p_1 \\ \vdots \\ p_{k-2} \\ p_{k-1} \end{bmatrix} \quad \text{and} \quad \mathbf{u}_m = \begin{bmatrix} q_0 \\ q_1 \\ \vdots \\ q_{k-2} \\ q_{k-1} \end{bmatrix} \quad (4.107)$$

then $p_i = 0$ implies $q_i = 0$. Solving for the q_i using

$$\mathbf{L}_m \mathbf{u}_m = 0 \quad (4.108)$$

allows one to generate a new vector \mathbf{u}_m . The tri-diagonalisation of the Y-junction's symmetric tree matrix can now be restarted.

Computational Lanczos Tri-diagonalisation

Lanczos tri-diagonalisation is a powerful tool for finding extremal eigenvalues of large sparse symmetric matrices (Paige, 1980; Golub and Van Loan, 1990), although, due to inherent instability, it is not the preferred choice as a general method of tri-diagonalisation. Other techniques (see Golub and Van Loan, 1990) offer more favourable numerical properties.

Round-off errors and loss of orthogonality among the Lanczos vectors are the major concerns. The complexity of a dendritic tree, its boundary conditions, and the number of nodes by which it is represented, as well as the working significance of floating point arithmetic, will determine how much of an equivalent cable can be constructed before arithmetic errors begin to manifest themselves unacceptably. Double floating point arithmetic, at least, should be used when working with complicated structures.

When transforming a complicated tree there may be a loss of acceptable accuracy at distances far (greater than the maximum origin-to-terminal electrotonic distance) from the origin along the connected section. Similar problems can arise for the Y-junction approach after several orders of branching have been transformed. Disconnected sections associated with the simpler substructures can often be generated, but errors may make it impossible to complete a connected section and thus choose a new Lanczos vector if a Y-junction is highly irregular and represented by a large numbers of nodes. Note that it is possible to use analytical results from Chapter 6 at each stage of the Y-by-Y reduction to ensure that cable section lengths are correct. If correct degeneracy is ensured for each Y-junction transformed, the final equivalent cable sections must inevitably exhibit the right electrotonic lengths.

Four subtly different algorithms, along with an error analysis, are fully discussed by Paige (1972, 1976). In a limited test of complex trees, we have found no single algorithm to give significant advantage over the others when generating equivalent cables. A version of the algorithm Paige calls $A(1,7)$ is given below. It is modified, to our advantage, for equivalent cable generation since the central diagonal element is always known and need not be computed each iteration.

The initial Lanczos vector is \mathbf{u}_0 , and let $\mathbf{q}_0 = \mathbf{A}_{TS}\mathbf{u}_0$. The repeated central diagonal element is D . For $j = 0$ to termination, repeat steps (4.109) to (4.113) :

$$\alpha_j = D \quad (= \mathbf{u}_j^T \mathbf{A}_{TS} \mathbf{u}_j) \quad (4.109)$$

$$\mathbf{w}_j = \mathbf{q}_j - \alpha_j \mathbf{u}_j \quad (4.110)$$

$$\beta_{j+1} = +\sqrt{\mathbf{w}_j^T \mathbf{w}_j} \quad (4.111)$$

$$\mathbf{u}_{j+1} = \mathbf{w}_j / \beta_{j+1} \quad (4.112)$$

$$q_{j+1} = A_{TS}u_{j+1} - \beta_{j+1}u_j. \quad (4.113)$$

If a Y-junction is degenerate, the process is restarted.

Calculating the central diagonal using equation (4.109) and comparing to the known value, D , is a useful indicator of where the algorithm loses stability.

Rounding errors can become significant when w_j becomes small due to cancellation. Element β_{j+1} is then small, indicating a sudden narrowing of the cable. This could be considered an approximate termination point if errors are significant enough.

It may be possible to improve the process by re-orthogonalisation, i.e. to combat loss of orthogonality, after each iteration the new Lanczos vector, u_{j+1} , is forced to be orthogonal to all previous vectors u_0 to u_j (details in Golub and Van Loan, 1990).

4.3.5 Householder Tri-diagonalisation

Householder Reflections

A *Householder reflection* H takes the form

$$H = I - 2vv^T/v^Tv, \quad (4.114)$$

where I is the identity matrix and v is a *Householder vector*. Matrix H is square, orthogonal, and idempotent, i.e. it is its own inverse, so

$$H = H^T = H^{-1}. \quad (4.115)$$

When a vector x is pre-multiplied by H , then x is reflected in a k -dimensional hyperplane defined by the orthogonal complement¹¹ of $\text{span}(v)$. The idea extends simply to matrices: pre-multiplication of an $n \times m$ matrix by H reflects each column vector of the matrix in the hyperplane; post-multiplication of an $m \times n$ matrix reflects each row-vector of the matrix in the hyperplane.

Householder reflections are typically used to zero a selected portion of a matrix row or column. The conventional method of doing this involves constructing the Householder vector using the matrix elements one wishes to zero, moving progressively from the bottom-right to the top-left of the matrix (details can be found in Golub and van Loan, 1990). On application of this method to tree matrices, the resulting symmetric matrix does not have a direct interpretation as an equivalent cable, and thus seems to fail. It is therefore necessary to implement another Householder strategy.

¹¹The orthogonal complement of a vector space, S is the space spanned by vectors y where $y^T x = 0$ for all $x \in S$.

The Householder Operation

To summarise, Householder reflections will be used to zero a single element at a time. Repeated post- and pre-multiplication of the symmetric tree matrix by a series of suitable Householder reflections generates the symmetric cable matrix¹². A custom implementation of the new algorithm also makes it possible to take advantage of the high level of sparsity that is maintained in intermediate full matrices, and store them efficiently. This is not usually possible using “off the shelf” Householder implementations which typically store full intermediate matrices.

Consider a $k \times k$ symmetric matrix \mathbf{A} , and denote its elements by a_{ij}^* . The Householder reflection required to zero element a_{mn} is, in block matrix form,

$$\mathbf{H}_{mn} = \begin{bmatrix} \mathbf{I}_m & \mathbf{0} & \mathbf{0} & \mathbf{0} & \mathbf{0} \\ \mathbf{0} & \alpha & \mathbf{0} & \beta & \mathbf{0} \\ \mathbf{0} & \mathbf{0} & \mathbf{I}_{n-m-2} & \mathbf{0} & \mathbf{0} \\ \mathbf{0} & \beta & \mathbf{0} & -\alpha & \mathbf{0} \\ \mathbf{0} & \mathbf{0} & \mathbf{0} & \mathbf{0} & \mathbf{I}_{k-n} \end{bmatrix}, \quad (4.116)$$

where $n > m + 1$, \mathbf{I}_j is the $j \times j$ identity matrix, and

$$\alpha = \frac{a_{m(m+1)}^*}{\sqrt{(a_{m(m+1)}^*)^2 + (a_{mn}^*)^2}} \quad \text{and} \quad \beta = \frac{a_{mn}^*}{\sqrt{(a_{m(m+1)}^*)^2 + (a_{mn}^*)^2}} \quad (4.117)$$

so that

$$\alpha^2 + \beta^2 = 1. \quad (4.118)$$

The corresponding Householder vector is

$$v = \pm \begin{bmatrix} 0 & \cdots & 0 & \sqrt{1-\alpha} & 0 & \cdots & 0 & -\sqrt{1+\alpha} & 0 & \cdots & 0 \end{bmatrix}, \quad (4.119)$$

though it is not used explicitly.

It is easy to show that post-multiplication of \mathbf{A} by \mathbf{H}_{mn} will zero off-tri-diagonal element a_{mn}^* , while pre-multiplication of \mathbf{A} by \mathbf{H}_{mn} will zero off-tri-diagonal element a_{nm}^* . Individually, the reflections disrupt matrix symmetry and destroy the constant diagonal. Combined, however, pre- and post-multiplication by \mathbf{H}_{mn} , referred to as a *Householder operation*, e.g.

$$\mathbf{B} = \mathbf{H}_{mn} \mathbf{A} \mathbf{H}_{mn}, \quad (4.120)$$

will zero a pair of elements while maintaining matrix symmetry and the constant diagonal (a proof of the latter is given later).

¹²The process is similar to the application of Givens’ rotations (Golub and van Loan, 1990), except that this method destroys essential matrix structure. The Householder reflection employed does however share some structural similarities with Givens’ rotations.

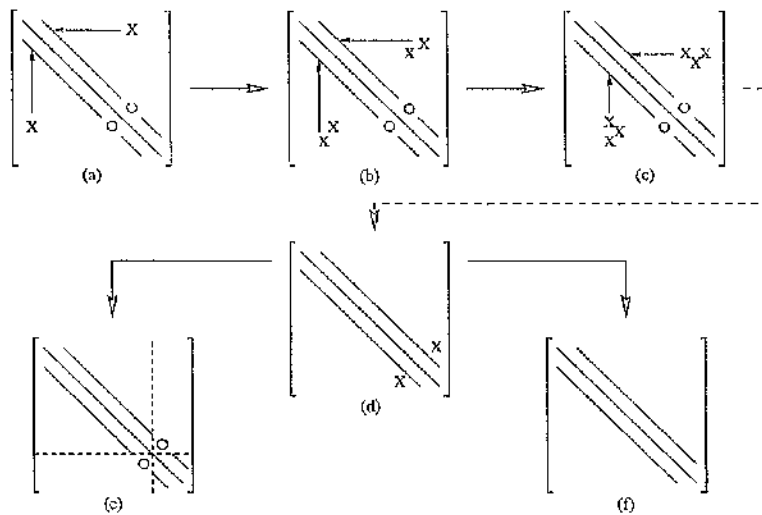


Figure 4.7: Schematic of the Householder tri-diagonalisation procedure applied to the tree matrix for a general Y-junction. (a) The symmetric tree has one pair of off-tri-diagonal elements. (b) zeroing this element produces new off-tri-diagonal element further towards the lower-right corner of the matrix. (c)–(d) repeat until tri-diagonality is achieved. The resulting cable matrix will represent either (e) two sections (one connected, one disconnected) or (f) one section (connected).

Denoting elements of \mathbf{B} by b_{ij} , this pair of reflections essentially map the unwanted off-tri-diagonal elements a_{mn}^* and a_{nm}^* into locations $b_{m(m+1)}$ and $b_{(m+1)m}$, while modifying or producing additional off-tri-diagonal elements. Note that operation \mathbf{H}_{mn} ensures that element $b_{m(m+1)} = b_{(m+1)m}$ is positive.

The Tri-diagonalisation Procedure

Element zeroing must be done in a controlled manner. Unstructured application of Householder reflections to zero off-tri-diagonal elements is not effective because the reflection can spawn many new off-tri-diagonal elements in the resulting matrix.

The structure of the Householder operation \mathbf{H}_{mn} guarantees that only rows and columns $m+1$ and n will be modified. Furthermore, provided the leading $(m-1) \times (m-1)$ sub-matrix is already tri-diagonal then new non-zero elements are introduced only in row $m+1$ or higher (and column $m+1$ or higher). All that happens in row m and column m is that a pair of elements are zeroed. These facts are easily verified. Starting with the lowest numbered row which contains a non-zero off-tri-diagonal element, it is possible to funnel off-tri-diagonal elements towards to bottom-right of the matrix until they must disappear entirely.

Denote the matrix produced after application of the r^{th} reflection by $\mathbf{A}^{(r)}$, with ele-

ments $a_{ij}^{(r)}$. Denote the r^{th} reflection by \mathbf{H}_r , so

$$\mathbf{A}^{(r)} = \mathbf{H}_r \mathbf{A}^{(r-1)} \mathbf{H}_r \quad (4.121)$$

The procedure starts of course with the symmetric tree matrix, so write

$$\mathbf{A}^{(0)} = \mathbf{A}_{TS} \quad (4.122)$$

A tri-diagonal matrix will be generated after p such operations, so

$$\mathbf{A}_{CS}^* = (\mathbf{H}_p \mathbf{H}_{p-1} \cdots \mathbf{H}_2 \mathbf{H}_1) \mathbf{A}_{TS} (\mathbf{H}_1^{-1} \mathbf{H}_2^{-1} \cdots \mathbf{H}_{p-1}^{-1} \mathbf{H}_p^{-1}). \quad (4.123)$$

The superscript * simply indicates that the matrix generated may not yet be the symmetric cable matrix. Very occasionally negative element on the sub- and super-diagonals will appear in \mathbf{A}_{CS}^* . This can happen where structure is automatically tri-diagonal without the need to apply a Householder operation which would ensure that the elements are non-negative. In practice, this seems to only happen in matrix structure representing disconnected sections.

Suppose that $a_{m(m+1)}^{(p)}$ and $a_{(m+1)m}^{(p)}$ are two such negative elements. By pre- and post-multiplying with the matrix

$$\mathbf{R}^{(m)} = \begin{bmatrix} \mathbf{I}_m & \mathbf{0} & \mathbf{0} \\ \mathbf{0} & -1 & \mathbf{0} \\ \mathbf{0} & \mathbf{0} & \mathbf{I}_{k-m} \end{bmatrix}, \quad (4.124)$$

the sign of each entry in row $m+1$ and column $m+1$ are inverted, except the $(m+1, m+1)$ diagonal entry (the sign of which is actually inverted twice). Negative elements may be introduced on sub- and super-diagonals further down the matrix, so a series of correction matrices will chase the negatives to the bottom-right of the matrix until they disappear. Thus, if q such operations are required,

$$\mathbf{A}_{CS} = (\mathbf{R}_q \mathbf{R}_{q-1} \cdots \mathbf{R}_2 \mathbf{R}_1) \mathbf{A}_{CS}^* (\mathbf{R}_1^{-1} \mathbf{R}_2^{-1} \cdots \mathbf{R}_{q-1}^{-1} \mathbf{R}_q^{-1}). \quad (4.125)$$

We write

$$\mathbf{T} = \mathbf{H} = \mathbf{R}_q \mathbf{R}_{q-1} \cdots \mathbf{R}_2 \mathbf{R}_1 \mathbf{H}_p \mathbf{H}_{p-1} \cdots \mathbf{H}_2 \mathbf{H}_1 \quad (4.126)$$

It may be more efficient to correct any negative elements during the tri-diagonalisation, rather than after. When moving from one row, a say, where off-tri-diagonal elements have been zeroed, to a new row, b , where off-tri-diagonal elements must still be zeroed, then if $b > a+1$ check intermediate rows for negative elements on the super-diagonal, and correct them if necessary.

The Householder process assumes that node 0 is origin. If a tree node other than the soma node is to be used as origin, then number it "0" instead and number the rest of the tree using the usual scheme, but with respect to the origin rather than the soma node.

A Constant Central Diagonal is Guaranteed

As with the Lanczos method, it is the structure of \mathbf{A}_{TS} , this time on conjunction with the structure of the Householder operation, that guarantees the central diagonal element is the required constant. Again, an induction argument is used.

Let $\mathbf{A}^{(c)}$ be a tree connectivity matrix or any full intermediate matrix generated during the Householder tri-diagonalisation as described above. Suppose that the matrix structure satisfies two conditions, namely (1) the diagonal elements are identical and equal to D , and (2) the row and column number of any off-tri-diagonal element correspond to tree nodes that are separated by an odd number of h .

We now show that application of a Householder operation to a matrix of this form guarantees that the resulting matrix has a similar structure, i.e. it also satisfies conditions (1) and (2).

The simple structure of Householder operation \mathbf{H}_{mn} , where $n > m + 1$, ensures that, when it is applied to a matrix $\mathbf{A}^{(c)}$, only rows $m + 1$ and n plus columns $m + 1$ and n are operated upon. The only diagonal elements that can possibly be modified are therefore $a_{(m+1)(m+1)}^{(c)}$ and $a_{nn}^{(c)}$. Simple algebraic expansion of $\mathbf{A}^{(c+1)} = \mathbf{H}_{mn}\mathbf{A}^{(c)}\mathbf{H}_{mn}$ show that

$$a_{(m+1)(m+1)}^{(c+1)} = D + 2\alpha\beta a_{(m+1)n} \quad (4.127)$$

and

$$a_{nn}^{(c+1)} = D - 2\alpha\beta a_{(m+1)n} \quad (4.128)$$

Clearly, the constant diagonal is maintained if $a_{(m+1)n}^{(c)} = 0$. Condition (2) guarantees this since nodes $m + 1$ and n must be separated by an even number of h , so it remains to show that condition (2) always holds.

Again, without going into full details, it may be shown that the Householder operation produces

$$a_{(m+1)i}^{(c+1)} = \alpha a_{(m+1)i}^{(c)} + \beta a_{ni}^{(c)}, \quad m + 2 \leq i \leq k - 1, \quad i \neq n \quad (4.129)$$

$$a_{in}^{(c+1)} = -\alpha a_{in}^{(c)} + \beta a_{i(m+1)}^{(c)}, \quad m + 2 \leq i \leq k - 1, \quad i \neq n \quad (4.130)$$

$$a_{(m+1)n}^{(c+1)} = (\beta^2 - \alpha^2) a_{(m+1)n}^{(c)} = 0. \quad (4.131)$$

Off-tri-diagonal elements in the lower tri-angle must maintain the symmetry so do not need to be considered.

Since rows $m + 1$ and n in $\mathbf{A}^{(c)}$ correspond to nodes separated by an even number of h , condition (2) ensures that the same element positions in each row may be occupied by non-zero elements. Essentially, equation (4.129) says that row m in $\mathbf{A}^{(c+1)}$ is a linear combination of these two rows and so maintains condition (2) type structure in this

row. Similarly equation (4.129) ensures that condition (2) type structure is maintained in column n of $\mathbf{A}^{(c+1)}$.

Since the initial symmetric tree matrix satisfies conditions (1) and (2), it follows that all intermediate matrices and the final symmetric cable matrix must also satisfy conditions (1) and (2). Therefore the central diagonal is maintained.

Computational Householder Algorithm

Symmetry allows us to concentrate on the upper triangular section of the matrix. The following discussion of rows applies equally to columns.

Initially, go to row zero of the symmetric tree matrix. Let r_c denote the current row and $\mathbf{A}^{(c)}$ indicate the current matrix of interest. Initially, $r_c = 0$ and $\mathbf{A}^{(c)} = \mathbf{A}_{TS} = \mathbf{A}^{(0)}$.

1. Move down the rows of matrix $\mathbf{A}^{(c)}$, starting with row r_c , checking the elements in each row j for non-zero elements other than $a_{j(j-1)}^{(c)}$, $a_{jj}^{(c)}$ and $a_{j(j+1)}^{(c)}$.

For each row j satisfying the tri-diagonality, also check if elements $a_{j(j+1)}^{(c)}$ and $a_{j(j+1)}^{(c)}$ are non-negative; if negative, they must be made positive using a correction operation.

As soon as we find a row j that does not satisfy tri-diagonal structure, stop, and set $r_c = j$. If no such row is found, we are finished.

2. Select an off-tri-diagonal elements in row j . To zero it, construct the appropriate Householder reflection, and pre- and post-multiply $\mathbf{A}^{(c)}$ by it. Now increment the current matrix (i.e. $c \rightarrow c + 1$). Repeat (2) until there are no more off-tridiagonal elements in row r_c . After each operation a full intermediate symmetric matrix is produced.
3. Repeat stages (1) and (2) until a tri-diagonal symmetric cable matrix has been generated.

Figure 4.7 illustrates the procedure schematically for a general Y-junction symmetric tree matrix.

The simple structure of Householder reflection \mathbf{H}_{mn} ensures that each zeroing operation will only modify rows $m+1$ and n and columns $m+1$ and n of the current intermediate matrix. Furthermore, since only elements in rows/columns m or greater are actually altered, and the structure of intermediate matrices (as highlighted in the prior subsection) suggests that approximately at least half of the elements in any one row are zero, then

Householder operation H_{mn} may be applied efficiently, involving a maximum of roughly $(k - m - 1)$ element modifications.

The Householder operations by which the symmetric tree matrix is manipulated into the symmetric cable matrix maintain a high level of sparsity in intermediate matrices. The temporary off-tri-diagonal elements are small in number and may be stored in triplet form.

The electrical mapping between tree and fully equivalent cable can be stored in terms of the sequence of individual Householder reflections, each of which may be stored as a triplet. For example, H_{mn} is the triplet (m, n, β) (α and the structure of H_{mn} , follow from equation (4.118)). Of course, to appreciate the connection between dendritic tree and fully equivalent cable, a full electrical mapping matrix M is required. Since H is not generally sparse, if it is built up during each step of the tri-diagonalisation then a large amount of storage space may be required.

4.3.6 Extracting the Equivalent Cable

De-symmetrising the Symmetric Cable Matrix

Matrix A_{CS} is assumed to be the symmetrised form of a tri-diagonal connectivity matrix, A_C , i.e.

$$A_{CS} = X^{-1} A_C X. \quad (4.132)$$

where

$$X = \text{diag } \{x_0, x_1, \dots, x_{k-2}, x_{k-1}\}. \quad (4.133)$$

This is similar to the symmetrisation of the tree matrix. The elements of A_{CS} , which are known, are denoted \bar{b}_{ij} , while the elements of A_C are denoted b_{ij} . Equation (4.82) implies that

$$\bar{b}_{i(i+1)} = \bar{b}_{(i+1)i} = b_{i(i+1)} \frac{x_i}{x_{i+1}} = b_{(i+1)i} \frac{x_{i+1}}{x_i} = \sqrt{b_{i(i+1)} b_{(i+1)i}}. \quad (4.134)$$

The task now is to determine the b_{ij} and x_i .

The de-symmetrisation procedure may be partitioned into three distinct stages. Stage (A) describes how to start the equivalent cable connected section, stage (B) describes a recursive procedure that simply produces the main body of the cable section, and stage (C) describes how cables terminate, and how to restart if additional sub-matrices need to be de-symmetrised.

Stage A. We require knowledge of the boundary condition at cable node 0. We have assumed a general current injection condition, so the cable origin is described by equation (4.27),

$$-\left(\frac{2}{h^2} + 1\right)v_0 + \frac{2}{h^2}v_1 = \frac{dv_0}{dt} - 2\Omega \frac{i_0}{C_0}. \quad (4.135)$$

Consequently the first row of the cable matrix must be

$$\begin{bmatrix} D & \frac{2}{h^2} & \dots \\ \vdots & \ddots & \dots \end{bmatrix} \quad (4.136)$$

so that $b_{00} = D$ and $b_{01} = 2/h^2$.

Stage B. Given the super-diagonal element $b_{i(i+1)}$, equation (4.134) allows us to determine the lower diagonal element $b_{(i+1)i}$ using

$$b_{(i+1)i} = \frac{\bar{b}_{i(i+1)}^2}{b_{i(i+1)}}. \quad (4.137)$$

The fact that the sum of the two off-diagonals in each row is always $2/h^2$ (except possibly when a terminal is reached) ensures that

$$b_{(i+1)(i+2)} = \frac{2}{h^2} - b_{(i+1)i}, \quad (4.138)$$

An iterative procedure that cycles through (4.137) and (4.138) can be initialised with $i = 0$ since b_{01} is known. Since $x_0 = 1$, the scaling factors can be determined, again drawing parallels with the symmetrisation,

$$x_{i+1} = x_i \sqrt{\frac{b_{i(i+1)}}{b_{(i+1)i}}}. \quad (4.139)$$

Note however, that if $\bar{b}_{(i+1)(i+2)} = 0$, then it must be the case that $b_{(i+1)(i+2)} = 0$, and the process terminates because the end of the cable connected section has been reached, whatever value equation (4.138) might yield. The terminal boundary condition of the connected section falls out naturally from the desymmetrisation procedure. In fact, if the terminal is sealed, then equation (4.26) demands that $b_{(i+1)i} = 2/h^2$ and equation (4.138) produces $b_{(i+1)(i+2)} = 0$ anyway. If the terminal is cut, however, then equation (4.31) demands that $b_{(i+1)i} = 1/h^2$ (this is strictly only true provided $z \geq 2$, so cable node $(i+1)$ is actually an internal node connected to an unnumbered cut terminal) so that equation (4.138) will not produce the expected zero element. In either case, it is necessary to move onto stage (C) and restart the de-symmetrisation, unless of course $i = k-2$, in which case the full matrix has been de-symmetrised and there are no disconnected sections.

Stage C. Suppose the de-symmetrisation has terminated at row p . Scaling factors x_1, x_2, \dots, x_p have been determined. It is necessary to restart the de-symmetrisation with row $p+1$. The scaling factors must also be reinitialised since there are two less non-zero off-diagonal elements with which to specify the x_i . We therefore choose $x_{p+1} = 1$.

It is at this stage that a discretisation level of $z \geq 2$ becomes very useful. This allows to look examine symmetric cable matrix structure in rows $p+1$ and $p+2$ and determine

the boundary condition with which the disconnected section starts. There are several situations that must be considered.

If the terminal is sealed and connected to an internal node then equation equations (4.24) and (4.26) ensure the unsymmetrised and unsymmetrised forms of the first two rows of the sub-matrix are, respectively

$$\begin{bmatrix} D & \frac{2}{h^2} & \dots & \dots \\ \frac{1}{h^2} & D & \frac{1}{h^2} & \dots \\ \vdots & \vdots & \vdots & \end{bmatrix}, \quad \begin{bmatrix} D & \frac{\sqrt{2}}{h^2} & \dots & \dots \\ \frac{\sqrt{2}}{h^2} & D & \dots & \dots \\ \vdots & \vdots & \vdots & \end{bmatrix} \quad (4.140)$$

If the terminal is cut, in which case node $(p+1)$ is internal then, from equation 4.31, and assuming node $p+1$ is connected to a diameter step node, then the unsymmetrised and symmetrised forms of the first two rows are, respectively,

$$\begin{bmatrix} D & \frac{1}{h^2} & \dots & \dots \\ \frac{2c_P}{(c_P+c_Q)h^2} & D & \frac{2c_Q}{(c_P+c_Q)h^2} & \dots \\ \vdots & \vdots & \vdots & \end{bmatrix}, \quad \begin{bmatrix} D & \frac{1}{h^2} \frac{\sqrt{2c_P}}{(c_P+c_Q)} & \dots & \dots \\ \frac{1}{h^2} \frac{\sqrt{2c_P}}{(c_P+c_Q)} & D & \dots & \dots \\ \vdots & \vdots & \vdots & \end{bmatrix} \quad (4.141)$$

where c_P is the c-value of the cylinder on which the cut terminal lies, and c_Q is the connecting cylinder.

So, if the disconnected section is represented by more than two *numbered* nodes, element $b_{(p+1)(p+2)}$ in equation (4.141) is less than that in equation (4.140), and the two terminal types can be distinguished in their symmetrised form. The first row is easily determined, and one can return to stage (B) to complete the disconnected section.

However, if the structure is represented by just two *numbered* nodes, then two slightly different configurations may be produced. Either the leading node $p+1$ is sealed, but connected to an internal node that then connects to a cut terminal, giving, respectively, unsymmetric and symmetric matrix structure

$$\begin{bmatrix} D & \frac{2}{h^2} \\ \frac{1}{h^2} & D \end{bmatrix}; \quad \begin{bmatrix} D & \frac{\sqrt{2}}{h^2} \\ \frac{\sqrt{2}}{h^2} & D \end{bmatrix} \quad (4.142)$$

Otherwise the leading node is the internal node, and, setting $c_Q = 0$ in (4.141), the unsymmetric and symmetric forms are

$$\begin{bmatrix} D & \frac{1}{h^2} \\ \frac{2}{h^2} & D \end{bmatrix}, \quad \begin{bmatrix} D & \frac{\sqrt{2}}{h^2} \\ \frac{\sqrt{2}}{h^2} & D \end{bmatrix} \quad (4.143)$$

Clearly, the symmetric forms are identical, while the unsymmetric forms differ. One might think that the choice of unsymmetric matrix then doesn't matter, however the order of boundary conditions must be chosen so that the electrical mapping is correct — only one form is actually correct.

The key is to look at the electrical mapping associated with node $p+1$, i.e. row $p+1$ of tri-diagonalising matrix \mathbf{T} . If the location of non-zero elements in this row correspond to internal nodes then node $p+1$ is internal, otherwise it is sealed.

Finally, it is possible that an internal node connects to two cut terminals. From equation (4.32), the matrix form is,

$$\begin{bmatrix} D \end{bmatrix}. \quad (4.144)$$

Note that, similarly to the s_i , the x_i may be expressed

$$x_i = \sqrt{\frac{\bar{C}_q}{\bar{C}_i}} \quad (4.145)$$

where \bar{C}_i is the c-sum for *cable* node i , and q is the cable c-sum of the initial cylinder of the cable section the boundary of which is represented by node q .

Equivalent Cable Structure

Discrete cable equation (4.23) for a diameter step implies that c-value ratios are given by ratios of super- and sub-diagonal elements in the same row, so

$$\frac{c_{i(i+1)}}{c_{(i-1)i}} = \frac{b_{i(i+1)}}{\frac{2}{h^2} - b_{i(i+1)}}. \quad (4.146)$$

Given the c-value of the cylinder on which node 0 lies, the remaining connected section c-values follow. For each disconnected section, choose an initial non-zero c-value for one section and the c-values of remaining sections follow.

It is possible to extract cable c-values direct from the symmetric cable matrix by following an algorithm similar to the de-symmetrisation, but discarding elements of \mathbf{A}_{CS} once used.

The Electrical Mapping

After symmetrisation, tri-diagonalisation, and de-symmetrisation, the matrix equation for the tree (4.36) becomes a matrix equation for the cable,

$$\mathbf{A}_C v_C = \frac{\partial v_C}{\partial t} - 2\Omega \mathbf{D}_C^{-1} g_C. \quad (4.147)$$

where

$$\mathbf{A}_C = M \mathbf{A}_T M^{-1}, \quad v_C = M v_T, \quad i_C = \mathbf{D}_C M \mathbf{D}_T^{-1} i_T. \quad (4.148)$$

The electrical mapping, M is given by

$$M = XTS. \quad (4.149)$$

To map electrical quantities from cable to tree, the inverse of M is required. It can be obtained quite simple from its component transformations. Matrices S and X are easily inverted, and, since T is a product of orthogonal transformations, $T^{-1} = T^T$. Thus,

$$M^{-1} = S^{-1}T^{-1}X^{-1}. \quad (4.150)$$

4.3.7 Further Computational Considerations

The tree and cable matrices can be efficiently stored since they are sparse and nearly tri-diagonal. It has already been explained that a tree matrix based on k numbered nodes contains $3k - 2$ non-zero entries. The elements of the main diagonal can be stored as one element, which suffices for all tree and cable matrices (and intermediate matrices generated during Householder tri-diagonalisation). The $2k - 2$ elements are respectively the row and column of the element while the last is the element value.

However, it is more practical to build the symmetric tree matrix directly from tree data. Diagonal matrix S (k elements) is straightforwardly constructed (equation 4.85), while the symmetric cable matrix is constructed using equation (4.85). The symmetrisation matrix S is stored in a k -length vector, while the off-diagonal elements of symmetric matrix ATS can be stored as $k - 1$ row-columns-value triplets.

Specific computational considerations for the Lanczos and Householder procedures are given in their respective sections earlier in this chapter.

After completing the tri-diagonalisation operation, the symmetric cable matrix may be stored as a single $(k - 1)$ -length vector; it can be built up element by element during the tri-diagonalisation. The cable matrix, super- and sub-diagonals, can be stored as two $(k - 1)$ -length vectors. The de-symmetrisation matrix, X is just another k -length vector.

It should be noted, however, that it is not actually necessary to store the cable matrix. The equivalent cable structure is easily extracted from the symmetric cable matrix using a modified de-symmetrisation algorithm, while matrix X is given by equation (4.145).

In conclusion, the passage from dendritic tree to fully equivalent cable can be achieved with high speed and efficient memory utilisation in view of the sparse nature of dendritic structure matrices. However, the electrical mapping, being an association between points on the dendritic tree and fully equivalent cable, requires calculations on full matrices for a complete specification and therefore is inevitably slow and memory intensive.

4.4 Algebraic Examples of the Matrix Methods

4.4.1 The Lanczos Method

We illustrate the Lanczos procedure with a simple algebraic example. Consider the Y-junction in Figure 4.5b. Set $h = 1$ for convenience. The branches have a total electrotonic length of 8, and so the equivalent cable must have electrotonic length 8.

The tree matrix is

$$A_T = \begin{bmatrix} D & 2 & 0 & 0 & 0 & 0 & 0 & 0 \\ 1 & D & 1 & 0 & 0 & 0 & 0 & 0 \\ 0 & \frac{2c_P}{C_2} & D & \frac{2c_R}{C_2} & 0 & 0 & \frac{2c_L}{C_2} & 0 \\ 0 & 0 & 1 & D & 1 & 0 & 0 & 0 \\ 0 & 0 & 0 & \frac{2c_R}{C_4} & D & \frac{2c_F}{C_4} & 0 & 0 \\ 0 & 0 & 0 & 0 & 1 & D & 0 & 0 \\ 0 & 0 & 1 & 0 & 0 & 0 & D & 1 \\ 0 & 0 & 0 & 0 & 0 & 0 & 2 & D \end{bmatrix}. \quad (4.151)$$

After symmetrisation, using equations (4.82) and (4.84), the tree matrix becomes

$$A_{TS} = \begin{bmatrix} D & \sqrt{2} & 0 & 0 & 0 & 0 & 0 & 0 \\ \sqrt{2} & D & \sqrt{\frac{2c_P}{C_2}} & 0 & 0 & 0 & 0 & 0 \\ 0 & \sqrt{\frac{2c_P}{C_2}} & D & \sqrt{\frac{2c_R}{C_2}} & 0 & 0 & \sqrt{\frac{2c_L}{C_2}} & 0 \\ 0 & 0 & \sqrt{\frac{2c_R}{C_2}} & D & \sqrt{\frac{2c_F}{C_4}} & 0 & 0 & 0 \\ 0 & 0 & 0 & \sqrt{\frac{2c_R}{C_4}} & D & \sqrt{\frac{2c_F}{C_4}} & 0 & 0 \\ 0 & 0 & 0 & 0 & \sqrt{\frac{2c_F}{C_4}} & D & 0 & 0 \\ 0 & 0 & \sqrt{\frac{2c_L}{C_2}} & 0 & 0 & 0 & D & \sqrt{2} \\ 0 & 0 & 0 & 0 & 0 & 0 & \sqrt{2} & D \end{bmatrix}, \quad (4.152)$$

with symmetrising scale transformation

$$S = \text{diag} \left\{ 1, \sqrt{2}, \sqrt{\frac{C_2}{c_P}}, \sqrt{\frac{2c_R}{c_P}}, \sqrt{\frac{C_4}{c_P}}, \sqrt{\frac{2c_F}{c_P}}, \sqrt{\frac{2c_L}{c_P}}, \sqrt{\frac{c_L}{c_P}} \right\}. \quad (4.153)$$

The Lanczos method can now be applied. Recall that $C_4 = c_R + c_F$. Take the soma, node 0, as the origin. The initial Lanczos vector is $u_0 = e_0$, and so, apply the first cycle of the procedure

$$A_{TS}u_0 = Du_0 + \sqrt{2}e_1 \quad (4.154)$$

Set $u_1 = e_1$ to satisfy the tri-diagonal structure and orthonormality of the u_i , so

$$A_{TS}u_1 = \sqrt{2}u_0 + Du_1 + \sqrt{\frac{2c_P}{C_2}}e_2. \quad (4.155)$$

In this case, set $u_2 = e_2$ since the tri-diagonal structure and orthonormality of the u_i is already ensured. Non-tri-diagonal structure is now encountered in the matrix, so

$$A_{TS}u_2 = \sqrt{\frac{2c_P}{C_2}}u_1 + Du_2 + \sqrt{\frac{2c_R}{C_2}}e_3 + \sqrt{\frac{2c_L}{C_2}}e_5. \quad (4.156)$$

Choosing

$$u_3 = \sqrt{\frac{c_R}{c_R + c_L}}e_3 + \sqrt{\frac{c_L}{c_R + c_L}}e_6, \quad (4.157)$$

ensures that

$$A_{TS}u_2 = \sqrt{\frac{2c_P}{C_2}}u_1 + Du_2 + \sqrt{\frac{2(c_R + c_L)}{C_2}}u_3. \quad (4.158)$$

Now, the next iteration yields

$$A_{TS}u_3 = \sqrt{\frac{2(c_R + c_L)}{C_2}}u_2 + Du_3 + \sqrt{\frac{2c_R^2}{C_4(c_R + c_L)}}e_4 + \sqrt{\frac{2c_L C_4}{C_4(c_R + c_L)}}e_7. \quad (4.159)$$

Choosing

$$u_4 = \sqrt{\frac{c_R^2}{c_R^2 + c_L C_4}}e_4 + \sqrt{\frac{c_L C_4}{c_R^2 + c_L C_4}}e_7 \quad (4.160)$$

allows this stage to be rewritten in tri-diagonal form,

$$A_{TS}u_3 = \sqrt{\frac{2(c_R + c_L)}{C_2}}u_2 + Du_3 + \sqrt{\frac{2(c_R^2 + c_L C_4)}{C_4(c_R + c_L)}}u_4. \quad (4.161)$$

After some algebraic effort to ensure symmetry, the next cycle produces,

$$\begin{aligned} A_{TS}u_4 &= \sqrt{\frac{2(c_R^2 + c_L C_4)}{C_4(c_R + c_L)}}u_3 + Du_4 \\ &\quad + [-c_L c_F \sqrt{c_R}e_3 + c_R c_F \sqrt{c_L}e_6 + c_R(c_R + c_L)\sqrt{c_F}e_5] \\ &\quad \times \frac{1}{c_R + c_L} \sqrt{\frac{2}{C_4(c_R^2 + c_L C_4)}}. \end{aligned} \quad (4.162)$$

This can be rewritten

$$A_{TS}u_4 = \sqrt{\frac{2(c_R^2 + c_L C_4)}{C_4(c_R + c_L)}}u_3 + Du_4 + \sqrt{\frac{2c_R c_F}{C_4(c_R + c_L)}}u_5, \quad (4.163)$$

where

$$\begin{aligned} u_5 &= \sqrt{\frac{1}{c_R c_F (c_R^2 + c_L C_4)(c_R + c_L)}} \times \\ &\quad [-c_L c_F \sqrt{c_R}e_3 + c_R c_F \sqrt{c_L}e_6 + c_R(c_R + c_L)\sqrt{c_F}e_5]. \end{aligned} \quad (4.164)$$

It is easy to check that $u_5 \cdot u_3 = 0$.

At the next iteration the algorithm terminates, since $A_{TS}u_5$ can be expressed in terms of u_4 and u_5 ,

$$A_{TS}u_5 = \sqrt{\frac{2c_R c_F}{C_4(c_R + c_L)}} u_4 + Du_5, \quad (4.165)$$

The connected section sub-matrix is complete, but two vectors have yet to be found. Another Lanczos vector, orthogonal to all the previous six, must be found so we may initialise construction of the disconnected section sub-matrix. Choose vector u_6 to be similar to u_5 , with coefficients of e_3 and e_6 having the same relative size (i.e. $-\sqrt{c_R/c_L}$) to ensure orthogonality with u_0 to u_4 . Just change the value of the coefficient of e_5 , so that u_6 can be made orthogonal to u_5 . If N is a normalisation factor and K is a constant then

$$u_6 = N \left(e_3 - \sqrt{\frac{c_R}{c_L}} e_6 + K e_5 \right). \quad (4.166)$$

The dot product of u_5 and u_6 must be zero so $K = \sqrt{c_F/c_R}$, and, after normalisation,

$$u_6 = -\sqrt{\frac{c_L c_R}{c_R^2 + c_L C_4}} e_3 + \sqrt{\frac{c_R^2}{c_R^2 + c_L C_4}} e_6 - \sqrt{\frac{c_L c_F}{c_R^2 + c_L C_4}} e_5. \quad (4.167)$$

Now, the Lanczos method may be continued as before

$$A_{TS}u_6 = Du_6 - \sqrt{\frac{2c_L c_4}{(c_R^2 + c_L C_4)}} e_4 + \sqrt{\frac{2c_R^2}{c_R^2 + c_L C_4}} e_7, \quad (4.168)$$

and so we must take

$$u_7 = -\sqrt{\frac{c_L c_4}{(c_R^2 + c_L C_4)}} e_4 + \sqrt{\frac{c_R^2}{c_R^2 + c_L C_4}} e_7, \quad (4.169)$$

so that

$$A_{TS}u_6 = Du_6 + \sqrt{2}u_7. \quad (4.170)$$

Finally, the Lanczos method can be completed,

$$A_{TS}u_7 = \sqrt{2}u_6 + Du_7. \quad (4.171)$$

The symmetric cable matrix is, from the expressions for $A_{TS}u_i$,

$$A_{CS} = \begin{bmatrix} D & \sqrt{2} & 0 & 0 & 0 & 0 & 0 & 0 & 0 \\ \sqrt{2} & D & \sqrt{\frac{2c_P}{C_2}} & 0 & 0 & 0 & 0 & 0 & 0 \\ 0 & \sqrt{\frac{2c_R}{C_2}} & D & \sqrt{\frac{2(c_R+c_L)}{C_2}} & 0 & 0 & 0 & 0 & 0 \\ 0 & 0 & \sqrt{\frac{2(c_R+c_L)}{C_2}} & D & \sqrt{\frac{2(c_R^2+c_L C_4)}{C_4(c_R+c_L)}} & 0 & 0 & 0 & 0 \\ 0 & 0 & 0 & \sqrt{\frac{2(c_R^2+c_L C_4)}{C_4(c_R+c_L)}} & D & \sqrt{\frac{2c_R c_F}{C_4(c_R+c_L)}} & 0 & 0 & 0 \\ 0 & 0 & 0 & 0 & \sqrt{\frac{2c_R c_F}{C_4(c_R+c_L)}} & D & 0 & 0 & 0 \\ 0 & 0 & 0 & 0 & 0 & 0 & D & \sqrt{2} & 0 \\ 0 & 0 & 0 & 0 & 0 & 0 & \sqrt{2} & D & 0 \end{bmatrix}. \quad (4.172)$$

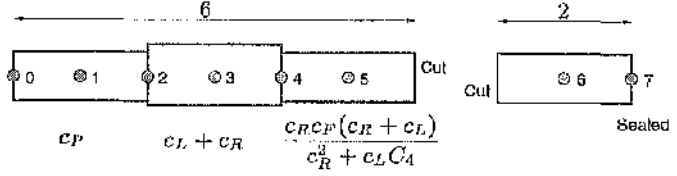


Figure 4.8: The equivalent cable for the Lanczos example in section 4.4. All lengths are electrotonic. The first cylinder, connected to the origin, is the same in both structures and has electrotonic length 2 and c-value c_P . The diameter of the disconnected section doesn't matter — set it to 1. See text for more details.

Note that the disconnected section submatrix begins with an internal node connected to a cut terminal, since elements of u_6 are contributed by internal nodes of the tree. It is easy to check that all the Lanczos vectors are orthonormal, as is expected.

The cable matrix can be extracted using the procedure given in section 4.3.6. The first super-diagonal element is 2, from equation (4.26) for the sealed end at node 0. The first three nodes on the connected section form the same cylinder as those on the original dendritic tree. Cable nodes 2-4 are described by discrete cable equation (4.23). The connected section terminates at node 5, with a cut terminal, equation (4.31). Recall that this equation represents an internal node connected to the cut terminal node. The disconnected section must have length 2 for the equivalent cable to have total length 8. The disconnected section symmetric submatrix is characteristic of a $2h$ length structure represented by 2 nodes, one at a sealed terminal and the other at an internal node connected to both terminals.

The cable matrix is

$$A_C = \begin{bmatrix} D & 2 & 0 & 0 & 0 & 0 & 0 & 0 \\ 1 & D & 1 & 0 & 0 & 0 & 0 & 0 \\ 0 & \frac{2c_P}{C_2} & D & \frac{2(c_R+c_L)}{C_2} & 0 & 0 & 0 & 0 \\ 0 & 0 & 1 & D & 1 & 0 & 0 & 0 \\ 0 & 0 & 0 & \frac{2(c_R^2+c_L C_4)}{C_4(c_R+c_L)} & D & \frac{2c_R c_F}{C_4(c_R+c_L)} & 0 & 0 \\ 0 & 0 & 0 & 0 & 1 & D & 0 & 0 \\ 0 & 0 & 0 & 0 & 0 & 0 & D & 1 \\ 0 & 0 & 0 & 0 & 0 & 0 & 2 & D \end{bmatrix}, \quad (4.173)$$

with de-symmetrising scale transformation

$$X = \text{diag} \left\{ 1, \frac{1}{\sqrt{2}}, \sqrt{\frac{c_P}{C_2}}, \sqrt{\frac{c_P}{2(c_R+c_L)}}, \sqrt{\frac{c_P(c_R^2+c_L C_4)}{C_4(c_R+c_L)^2}}, \sqrt{\frac{c_P(c_R^2+c_L C_4)}{2c_R c_F(c_R+c_L)}}, 1, \frac{1}{\sqrt{2}} \right\}. \quad (4.174)$$

The c-value ratio for cylinders either side of a non-terminal equivalent cable node, n , is given by the ratio of elements in row n of the cable matrix, either side of the diagonal. Not

surprisingly, the first cylinder (length 2) must have c-value c_P to initialise the c-values. The second (length 2) has c-value $c_R + c_L$. The third and final connected section cylinder has c-value $c_R c_F (c_R + c_L) / (c_R^2 + c_L C_4)$.

The electrical mapping is

$$M = XLS = \begin{bmatrix} 1 & 0 & 0 & 0 & 0 & 0 & 0 & 0 \\ 0 & 1 & 0 & 0 & 0 & 0 & 0 & 0 \\ 0 & 0 & 1 & 0 & 0 & 0 & 0 & 0 \\ 0 & 0 & 0 & \frac{c_R}{c_R + c_L} & 0 & 0 & \frac{c_L}{c_R + c_L} & 0 \\ 0 & 0 & 0 & 0 & \frac{c_R}{c_R + c_L} & 0 & 0 & \frac{c_L}{c_R + c_L} \\ 0 & 0 & 0 & -\frac{c_L}{c_R + c_L} & 0 & 1 & \frac{c_L}{c_R + c_L} & 0 \\ 0 & 0 & 0 & -pC_R & 0 & -pC_F & pc_R & 0 \\ 0 & 0 & 0 & 0 & -pC_4 & 0 & 0 & pc_R \end{bmatrix}. \quad (4.175)$$

The total surface area of the original tree is (scaled by a constant)

$$S_{tree} = c_P + c_R + c_L + c_F. \quad (4.176)$$

Note that, since the tree had a cut terminal, total surface area need not be preserved in the connected section, and in fact, in this particular case, it is less than the tree surface area,

$$S_{con} = c_P + (c_R + c_L) + \frac{c_R c_F (c_R + c_L)}{(c_R^2 + c_L C_4)} = c_P + (c_R + c_L) + c_F \left[\frac{c_R^2 + c_R c_L}{c_R^2 + c_R c_L + c_F c_L} \right] < S_{tree}. \quad (4.177)$$

When trees have cut terminals, it is more common for surface area to be greater in the connected section than in the tree.

Figure 4.8 shows the original dendritic tree and the equivalent cable that has just been generated.

4.4.2 The Householder Method

To illustrate the construction process, consider a very simple singly branched Rall tree, with a parent limb (P) and two child limbs (L and R), each of quantum length, H , with a discretisation level of $z = 2$ so there are three nodes per cylinder. Trees with higher levels of complexity generally exhibit a much more elaborate algebraic structure, and are less practical for demonstration purposes.

The Tree Matrix

$$A_T = \frac{1}{h^2} \begin{bmatrix} D & 2 & 0 & 0 & 0 & 0 & 0 \\ 1 & D & 1 & 0 & 0 & 0 & 0 \\ 0 & \frac{2c_P}{C_2} & D & \frac{2c_L}{C_2} & 0 & \frac{2c_R}{C_2} & 0 \\ 0 & 0 & 1 & D & 1 & 0 & 0 \\ 0 & 0 & 0 & 2 & D & 0 & 0 \\ 0 & 0 & 1 & 0 & 0 & D & 1 \\ 0 & 0 & 0 & 0 & 0 & 2 & D \end{bmatrix} \quad (4.178)$$

The Symmetric Tree Matrix

$$A^{(0)} = A_{TS} = \frac{1}{h^2} \begin{bmatrix} D & \sqrt{2} & 0 & 0 & 0 & 0 & 0 \\ \sqrt{2} & D & \sqrt{\frac{2c_P}{C_2}} & 0 & 0 & 0 & 0 \\ 0 & \sqrt{\frac{2c_P}{C_2}} & D & \sqrt{\frac{2c_L}{C_2}} & 0 & \sqrt{\frac{2c_R}{C_2}} & 0 \\ 0 & 0 & \sqrt{\frac{2c_L}{C_2}} & D & \sqrt{2} & 0 & 0 \\ 0 & 0 & 0 & \sqrt{2} & D & 0 & 0 \\ 0 & 0 & \sqrt{\frac{2c_R}{C_2}} & 0 & 0 & D & \sqrt{2} \\ 0 & 0 & 0 & 0 & 0 & \sqrt{2} & D \end{bmatrix} \quad (4.179)$$

with

$$S = \text{diag} \left\{ 1, \sqrt{2}, \sqrt{\frac{C_2}{c_P}}, \sqrt{\frac{2c_L}{c_P}}, \sqrt{\frac{c_L}{c_P}}, \sqrt{\frac{2c_R}{c_P}}, \sqrt{\frac{c_R}{c_P}} \right\} \quad (4.180)$$

Tri-diagonalisation

We want to zero elements $\bar{a}_{25}^{(0)}$ and $\bar{a}_{52}^{(0)}$. The first Householder reflection takes the form

$$H_1 = H_{14} = \begin{bmatrix} 1 & 0 & 0 & 0 & 0 & 0 & 0 \\ 0 & 1 & 0 & 0 & 0 & 0 & 0 \\ 0 & 0 & 1 & 0 & 0 & 0 & 0 \\ 0 & 0 & 0 & \alpha & 0 & \beta & 0 \\ 0 & 0 & 0 & 0 & 1 & 0 & 0 \\ 0 & 0 & 0 & \beta & 0 & -\alpha & 0 \\ 0 & 0 & 0 & 0 & 0 & 0 & 1 \end{bmatrix} \quad (4.181)$$

where

$$\alpha = \sqrt{\frac{c_L}{c_R + c_L}} \quad \text{and} \quad \beta = \sqrt{\frac{c_R}{c_R + c_L}}, \quad (4.182)$$

yielding

$$A^{(1)} = \frac{1}{h^2} \begin{bmatrix} D & \sqrt{2} & 0 & 0 & 0 & 0 & 0 \\ \sqrt{2} & D & \sqrt{\frac{2c_P}{C_2}} & 0 & 0 & 0 & 0 \\ 0 & \sqrt{\frac{2c_P}{C_2}} & D & \sqrt{\frac{2(c_L+c_R)}{C_2}} & 0 & 0 & 0 \\ 0 & 0 & \sqrt{\frac{2(c_L+c_R)}{C_2}} & D & \sqrt{\frac{2c_L}{c_L+c_R}} & 0 & \sqrt{\frac{2c_R}{c_L+c_R}} \\ 0 & 0 & 0 & \sqrt{\frac{2c_L}{c_L+c_R}} & D & \sqrt{\frac{2c_R}{c_L+c_R}} & 0 \\ 0 & 0 & 0 & 0 & \sqrt{\frac{2c_R}{c_L+c_R}} & D & -\sqrt{\frac{2c_L}{c_L+c_R}} \\ 0 & 0 & 0 & \sqrt{\frac{2c_R}{c_L+c_R}} & 0 & -\sqrt{\frac{2c_L}{c_L+c_R}} & D \end{bmatrix}. \quad (4.183)$$

Now elements $a_{36}^{(1)}$ and $a_{63}^{(1)}$, must be zeroed with Householder reflection

$$H_2 = H_{36} = \begin{bmatrix} 1 & 0 & 0 & 0 & 0 & 0 & 0 \\ 0 & 1 & 0 & 0 & 0 & 0 & 0 \\ 0 & 0 & 1 & 0 & 0 & 0 & 0 \\ 0 & 0 & 0 & 1 & 0 & 0 & 0 \\ 0 & 0 & 0 & 0 & \alpha & 0 & \beta \\ 0 & 0 & 0 & 0 & 0 & 1 & 0 \\ 0 & 0 & 0 & 0 & \beta & 0 & -\alpha \end{bmatrix}, \quad (4.184)$$

where again α and β take the same form as in equation (4.182). Note that this is only because of the simplicity and symmetry of the example. In general, much more algebraic complexity is observed in the intermediate matrices, and expressions for α and β .

After application of this reflection, the symmetric cable matrix is generated.

$$A_{CS} = A^{(2)} = \begin{bmatrix} D & \sqrt{2} & 0 & 0 & 0 & 0 & 0 \\ \sqrt{2} & D & \sqrt{\frac{2c_P}{C_2}} & 0 & 0 & 0 & 0 \\ 0 & \sqrt{\frac{2c_P}{C_2}} & D & \sqrt{\frac{2(c_L+c_R)}{C_2}} & 0 & 0 & 0 \\ 0 & 0 & \sqrt{\frac{2(c_L+c_R)}{C_2}} & D & \sqrt{2} & 0 & 0 \\ 0 & 0 & 0 & \sqrt{2} & D & 0 & 0 \\ 0 & 0 & 0 & 0 & 0 & D & \sqrt{2} \\ 0 & 0 & 0 & 0 & 0 & \sqrt{2} & D \end{bmatrix}. \quad (4.185)$$

De-symmetrisation

Simply apply the de-symmetrisation algorithm yields

$$A_C = \begin{bmatrix} D & \frac{2}{h^2} & 0 & 0 & 0 & 0 & 0 \\ 1 & D & 1 & 0 & 0 & 0 & 0 \\ 0 & \frac{2c_P}{C_2} & D & \frac{2(c_L+c_R)}{C_2} & 0 & 0 & 0 \\ 0 & 0 & 1 & D & 1 & 0 & 0 \\ 0 & 0 & 0 & 2 & D & 0 & 0 \\ 0 & 0 & 0 & 0 & 0 & D & 1 \\ 0 & 0 & 0 & 0 & 0 & 2 & D \end{bmatrix} \quad (4.186)$$

with

$$X = \text{diag} \left\{ 1, \frac{1}{\sqrt{2}}, \sqrt{\frac{c_P}{C_2}}, \sqrt{\frac{c_P}{2(c_L+c_R)}}, \sqrt{\frac{c_P}{(c_L+c_R)}}, 1, \frac{1}{\sqrt{2}} \right\} \quad (4.187)$$

Cable C-values

With the parent cylinder, length H , unaltered by the transformation, it has c-value c_P . By examining ratios of off-diagonal elements in row 2, the diameter changes at node 2 to $c_L + c_R$ (the simple Rall sum), and the cable terminates with a sealed end at node 4 after a further length H . The disconnected section is of length H , starts with a cut terminal (examining row 5 of the mapping below tells us node 5 is an internal node connected to a cut terminal), and ends with a sealed terminal.

Electrical Mapping

The electrical mapping is

$$M = X H_2 H_1 S = \begin{bmatrix} 1 & 0 & 0 & 0 & 0 & 0 & 0 \\ 0 & 1 & 0 & 0 & 0 & 0 & 0 \\ 0 & 0 & 1 & 0 & 0 & 0 & 0 \\ 0 & 0 & 0 & \frac{c_L}{c_L+c_R} & 0 & \frac{c_R}{c_L+c_R} & 0 \\ 0 & 0 & 0 & 0 & \frac{c_L}{c_L+c_R} & 0 & \frac{c_R}{c_L+c_R} \\ 0 & 0 & 0 & 1 & 0 & -1 & 0 \\ 0 & 0 & 0 & 0 & 1 & 0 & -1 \end{bmatrix} \quad (4.188)$$

4.5 Observations and Discussion of Matrix Methods

The Householder and Lanczos methods have both been found to work effectively, producing the same cable structure with the same boundary conditions when applied to the same matrix representation of a discretised dendritic tree model (numerical errors aside). These

methods do not constitute a proof that equivalent cables exist as concrete mathematical objects (they could feasibly, though it is unlikely, be a strange facet of the matrix method itself). We develop an analytical theory for cable construction in the remaining chapters of this thesis.

The tree matrix developed in this section is designed primarily for the purpose of equivalent cable construction. However, the discretisation may be extended to the time derivative and the system of equations may be solved by some appropriate numerical scheme. If not used for cable construction, boundary conditions other than cut or current injection may be incorporated into the discretisation scheme. Lindsay *et al.* (in press) outline the relevant extensions and why this is not the ideal approach to numerical simulation.

For either the Lanczos or Householder method, any disconnected sections are generated using a Y-junction by Y-junction approach. It is possible to apply the Householder method to any tree matrix and generate the connected section matrix plus a set of additional sub-matrices. However, although there seems to often be the right number of sub-matrices representing sections that are correctly terminated, these matrices do not always correspond to the expected disconnected sections. Essentially, the subspaces of electrical activity described by a group of disconnected sections are mixed up and the electrical mappings, though describing activity not seen by the soma, do not correspond to the expected mappings for a specific Y-junction. Recovering the desired mappings and disconnected sections from these matrices may not strictly be necessary, but a method for doing so has not yet been found for a general tree.

It has already been noted that the Householder method preserves a high level of sparsity. Exactly why has not yet been fully investigated, but it is undoubtably a consequence of the structure of the symmetric connectivity matrix and the Householder operation employed. This is, however, a more general linear algebra problem, and may be of benefit in areas other than neuronal modelling. For large matrices, and where possible, a sparse Householder algorithm is always preferable to the general Householder which stores a full intermediate matrix.

Chapter 5

Foundations of Equivalent Cable Construction

5.1 Introduction

Results generated by the matrix methods described in Chapter 4 suggest very strongly that fully equivalent cables exist as well defined, concrete mathematical objects (though the matrix methods do not constitute a proof of their existence). It seems that dendritic trees of arbitrary geometry (represented by the multi-cylinder passive model described in Chapter 2) may be transformed to their equivalent cables straightforwardly and efficiently using the Lanczos and Householder procedures. Questions now arise concerning why the reduction procedures work at all. What features does the general system of linear cable equations exhibit that permit this interesting and surprising result? What is the theoretical foundation for the construction of fully equivalent cables?

If the matrix methods of equivalent cable construction are applied algebraically, one can observe, even for some fairly simple tree structures, an incredible level of complexity in the resulting expressions for the equivalent cable potentials and c-values, in terms of the corresponding tree potentials and c-values. How does this process always guarantee that connected and disconnected cable sections terminate with appropriate boundary conditions? When and why should disconnected sections be expected? Is it possible to clarify why the equivalent cable for a general Y-junction contains at most one disconnected section? There are further results (described later) that are particular to certain trees and their cables and which are also not clearly explained. The natural progression at this stage is to try and determine the underlying rules of cable construction that are implemented by the matrix methods.

The Lanczos and Householder procedures on their own do not give enough insight to

determine these rules easily, if at all, but some general features of equivalent cable shape and electrical mapping structure observed in results generated by these methods hint at equivalent cable features that must be guaranteed during cable construction (for example, the first cable cylinder is always Rail-like, and the electrical mapping is always seen to exhibit structure consistent with a vitally important construction rule — the “isolation condition”, which will be formally developed later). These features have been key factors for the development and testing of the analytical theory.

The formulation of the analytical construction procedure eventually reveals a reasonably straightforward set of underlying principles and construction rules which can form the basis of an effective cable construction algorithm. The algorithm involves repeated application of a set of rules, producing one cable cylinder after each cycle through the rules. This repetition can lead to the expected rapid accumulation of algebraic complexity in expressions for the electrical mapping and cable c-values. Fortunately these expressions need not be dealt with directly.

The analytical theory of equivalent cable construction is developed in Chapters 5, 6 and 7. The analytical rules are derived for, and applied to, the multi-cylinder representation of a passive dendritic tree, with the only trees explicitly considered being Y-junctions (singly branched trees). Any tree may then be transformed by successive reductions (the validity of this Y-junction by Y-junction approach is also confirmed by the analytical rules). All cylinder electrotonic lengths are a multiple of some basic electrotonic length. A cable equation is associated with each uniform cylinder, acceptable boundary conditions are imposed at terminals, and joining conditions apply where cylinders meet.

To introduce some of the most important ideas that are employed in cable construction, in this chapter we will concentrate of the fundamental principles from which the rules will eventually follow. This is most easily done by considering specific examples. A fairly loosely defined first-principles scheme for cable construction is described and then used to construct fully equivalent cables for two specific Y-junctions. This will allow us to observe how the construction procedure naturally consists of two distinct sets of rules,

- *Electrical continuity rules:* These rules guarantee voltage continuity and current conservation between adjacent equivalent cable cylinders, but in a way that does not uniquely determine cable structure.
- *Isolation-termination rules:* These rules ensure that any dendritic sub-tree may be transformed in isolation from structure it is connected to. These rules simultaneously guarantee eventual termination of the equivalent cable. The cable structure is uniquely defined in the process.

This chapter will be concerned mainly with the electrical continuity construction rules.

The most important special cases will be listed, and it is shown that they do what is claimed. We then describe the isolation condition, the simplest and most fundamental of the isolation–termination rules. Chapter 6 contains full technical details, showing how general forms for each set of rules follow from the first-principles approach and other considerations.

As would be expected from the matrix results, the analytical rules depend entirely on the c -values and relative electrotonic lengths of dendritic cylinders. Specific electrical parameters (membrane conductance per unit area, internal resistivity, membrane capacitance per unit area) that describe the passive tree need not be known. The shape and electrical mapping of an equivalent cable is entirely dependent on geometry. The *application* of the analytical rules does not require one to actually solve the system of cable equations, although the *derivation* of some analytical rules does involve the use of Laplace transforms (however, the manner in which they are used may be regarded as unconventional).

5.2 The Multi-cylinder Tree Model in the Laplace Domain

Laplace transforms are commonly employed where they can simplify the task of obtaining solutions to differential equations — one solves the transformed equation, then determines the inverse, either analytically (there are many well known pairs of function and their inverse transform) or by numerical means (e.g. contour integration and residue calculus). The novelty of their use when generating equivalent cables lies in the fact that the information sought is not the solutions themselves but rather how they are combined to give the correct electrical mapping. The electrical continuity rules are derived in the Laplace domain, that is, the electrical mapping they produce relates Laplace transformed cable potentials to Laplace transformed tree potentials. Linearity guarantees that the electrical mapping is equally valid for the untransformed tree and cable potentials.

Throughout this chapter, as in Chapter 4, it is understood that lower case letters are used to denote quantities expressed in terms of electrotonic length and time. Also, “electrotonic length” will often be referred to simply as “length”.

5.2.1 The Laplace Transform

The Laplace transform of a function $f(t)$, where $t > 0$, is defined by

$$\bar{f}(s) = \mathcal{L}[f(t); s] = \int_0^\infty e^{-st} f(t) dt. \quad (5.1)$$

Given $\bar{f}(s)$, the inverse Laplace transform allows us to find $f(t)$ such that $\bar{f}(s) = \mathcal{L}[f(t); s]$. We write

$$f(t) = \mathcal{L}^{-1}[\bar{f}(s); t]. \quad (5.2)$$

Properties of the Laplace Transform and the Inverse Laplace Transform

If the Laplace transforms of two functions f and g exist then

$$\mathcal{L}[\alpha f(t) + \beta g(t); s] = \alpha \mathcal{L}[f(t); s] + \beta \mathcal{L}[g(t); s]. \quad (5.3)$$

where α and β are constants. Also,

$$\mathcal{L}^{-1}[\alpha \bar{f}(s) + \beta \bar{g}(s); t] = \alpha \mathcal{L}^{-1}[\bar{f}(s); t] + \beta \mathcal{L}^{-1}[\bar{g}(s); t] = \alpha f(t) + \beta g(t). \quad (5.4)$$

If f is a differentiable function of t then

$$\mathcal{L}\left[\frac{\partial f(t)}{\partial t}; s\right] = sf(s) - f(0). \quad (5.5)$$

5.2.2 The Cable Equation

From Chapter 2, the dimensionless cable equation for a uniform cylinder with electrotonic length t and c-value c is,

$$\frac{\partial^2 v}{\partial x^2} = \frac{\partial v}{\partial t} + v - \Omega \frac{i}{c}, \quad 0 < x < l, \quad (5.6)$$

where x and t are electrotonic length and time respectively, $v(x, t)$ is the cylinder potential, $i(x, t)$ represents applied currents, and Ω is a constant.

The Laplace transform of the cable equation, *with respect to electrotonic time t* , is

$$\frac{\partial^2 \bar{v}(x, s)}{\partial x^2} = (1 + s)\bar{v}(x, s) - v(x, 0) - \Omega \frac{\bar{i}(x, s)}{c}, \quad 0 < x < l, \quad s > 0, \quad (5.7)$$

or

$$\frac{\partial^2 \bar{v}(x, s)}{\partial x^2} = w^2 \bar{v}(x, s) + \bar{f}(x, s), \quad 0 < x < l, \quad s > 0, \quad (5.8)$$

where

$$w^2 = (1 + s) \quad \text{and} \quad \bar{f}(x, s) = -\Omega \frac{\bar{i}(x, s)}{c} - v(x, 0). \quad (5.9)$$

Axial Current

From equation (2.98), the Laplace transformed axial current is

$$\bar{i}_a(x, s) = -Kc \frac{\partial \bar{v}(x, s)}{\partial x}. \quad (5.10)$$

5.2.3 Boundary Conditions

The boundary conditions listed in Chapter 2 as being acceptable for equivalent cable construction are almost identical in the Laplace domain, since temporal, rather than spatial, dependence is being transformed. Conditions (2.91), (2.93), (2.94), (2.95) and (2.86) become:

Current Injection Condition

The time-varying axial current is specified at boundary $x = l$ on a cylinder,

$$\bar{i}_a(l, s) = -Kc \frac{\partial \bar{v}(l, s)}{\partial x} = \bar{\kappa}(s). \quad (5.11)$$

Recall that $x = l$ may be regarded as a point where the cylinder diameter falls abruptly to zero. The sealed end special case is

$$\frac{\partial \bar{v}(l, s)}{\partial x} = 0. \quad (5.12)$$

Cut End Condition

The potential at $x = l$ is set to zero, i.e. the transmembrane potential is fixed at the resting potential,

$$\bar{v}(l, s) = 0. \quad (5.13)$$

Recall that $x = l$ may be regarded as a point where the diameter jumps abruptly to infinity.

Joining Condition

Suppose a parent cylinder (p) meets n child cylinders (c_1, c_2, \dots, c_n) at a junction. Voltage continuity may be expressed

$$\bar{v}_p(l_p, s) = \bar{v}_{c_k}(0, s), \quad (5.14)$$

for all k where $1 \leq k \leq n$. The current conservation condition may be expressed

$$\bar{i}_{a,p}(l_p, s) + \bar{i}_A(s) = \sum_{k=1}^n \bar{i}_{a,c_k}(0, s), \quad (5.15)$$

where $\bar{i}_A(s)$ is the Laplace transform of an applied current source at the junction.

5.2.4 Solutions of the Laplace Transformed Cable Equation

From here onwards, the s -dependence in the Laplace domain will be suppressed, by writing

$$\bar{v}(x) = \bar{v}(x, s) \quad \text{and} \quad \bar{i}_a(x) = \bar{i}_a(x, s). \quad (5.16)$$

General Solution

The Laplace transformed cable equation (5.8) has general solution

$$\bar{v}(x) = \alpha \sinh \omega x + \beta \cosh \omega x + \frac{1}{\omega} \int_0^x \bar{f}(y) \sinh \omega(x-y) dy. \quad (5.17)$$

The integral term represents the contribution to the potential due to the initial state of the membrane and input currents along the cylinder, while the coefficients α and β are determined by boundary conditions.

Cylinder with a Sealed End

If a cylinder terminates at $x = l$ with a sealed end boundary condition, then

$$\left. \frac{\partial \bar{v}}{\partial x} \right|_{x=l} = 0. \quad (5.18)$$

Suppose there are also no external current sources (except at $t = 0$), and the membrane potential is initially zero, so that $\bar{f}(x) = 0$. If \bar{v}_0 is the potential at $x = 0$ then the coefficients in the general solution (5.17) become

$$\alpha = -\bar{v}_0 \frac{\sinh \omega l}{\cosh \omega l} \quad \text{and} \quad \beta = \bar{v}_0, \quad (5.19)$$

which yields, using standard identities for hyperbolic trigonometric functions,

$$\bar{v}(x) = \bar{v}_0 \frac{\cosh \omega(l-x)}{\cosh \omega l}. \quad (5.20)$$

Cylinder with a Cut End

Similarly, if the cylinder terminates at $x = l$ with a cut end boundary condition then

$$\bar{v}(l) = 0. \quad (5.21)$$

Again \bar{v}_0 is the potential at $x = 0$. The coefficients in the general solution (5.17) are

$$\alpha = -\bar{v}_0 \frac{\cosh \omega l}{\sinh \omega l} \quad \text{and} \quad \beta = \bar{v}_0, \quad (5.22)$$

which yields

$$\bar{v}(x) = \bar{v}_0 \frac{\sinh \omega(l-x)}{\sinh \omega l}. \quad (5.23)$$

5.3 The Strategy for Equivalent Cable Construction

Consider a cylinder with length l and c-value c . If the potential and axial current at end $x = 0$ are given by $\bar{v}(0) = v_J$ and $\bar{i}_a(0) = i_J$, then α and β in equation (5.17) can be replaced to give

$$\bar{v}(x) = \bar{v}_J \cosh \omega x - \frac{\bar{i}_J}{K \omega c} \sinh \omega x + \frac{1}{\omega} \int_0^x \bar{f}(y) \sinh \omega(x-y) dy. \quad (5.24)$$

For reasons that will become apparent this solution will be referred to as the *generator equation*.

Thus if the potential and axial current at one end of a cylinder are known, an expression for the potential throughout the cylinder is obtained, provided the distribution of applied currents in the cable cylinder can also be specified (this is easily done, following from the linearity of the system). Once the equivalent cable origin has been chosen, it is possible to

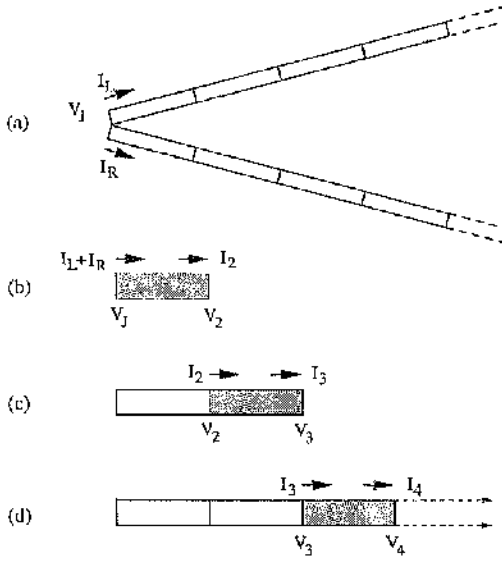


Figure 5.1: Fully equivalent cable construction from first principles for a general Y-junction. Cable construction is based on voltage continuity and current conservation. (a) A general Y-junction formed from cylinders (of arbitrary diameters, but represented here as identical segments). Initialise the procedure with the voltage at the junction (V_J) and current flowing into left (I_L) and right (I_R) child branches. (b) Construct the first cable cylinder using this information then determine the axial current (I_2) and potential (V_2) at the end of this first cylinder. (c) Use these two new quantities to generate the second cable cylinder. (d) Repeat this procedure until the equivalent cable is constructed. The cylinder determined at each stage is shaded. Note that cable cylinder diameters are also different, in general.

take advantage of this in the following way. Given the potential at the origin, and the axial current flowing from the origin into the tree structure that is the target of the procedure, we can write down an expression for the potential throughout the first equivalent cable cylinder, using the generator equation. Consequently, expressions for the potential and axial current at the end of the first cylinder can be obtained. Voltage continuity and current conservation in the cable ensure that the potential and axial current at $x = 0$ in the second equivalent cable cylinder (i.e. where the second cylinder connects to the first) are known; again using the generator equation, an expression for the potential in the second cable cylinder can now be obtained.

In principle, this process, illustrated in Figure 5.1, can be repeated to generate an expression for the potential in each cable cylinder. However, the algorithm above is rather loosely specified. Several questions must still be answered, such as how are the c-value and lengths of the cable segments determined, and how does the procedure terminate?

So far, we simply have the basis of a constructive mechanism for fully equivalent cable generation. The algorithm can be used as a first principles approach (the technique is illustrated in examples in the next section). For more practical purposes, the algorithm is used in Chapter 6 to generate the general construction rules. The electrical continuity rules follow directly, while the isolation-termination rules follow from the need to impose a certain structure on the electrical mapping.

It should be clear that the construction mechanism automatically ensures that the steady-state input conductance of the cable connected section will equal that of the tree since we initialise the cable potential and axial current with the tree origin potential and axial current.

5.4 Examples of Cable Construction from First Principles

5.4.1 Example One

Consider the simple Y-junction in Figure 5.2a. The left cylinder (L) has electrotonic length l , c-value c^L , and terminates with a sealed end. The right cylinder (R) has electrotonic length $3l$, c-value c^R , and also terminates with a sealed end. The two cylinders meet at $x = 0$. For simplicity suppose that there are no input current terms. The potential in equivalent cable cylinder k will be denoted ϕ_k , its axial current $i_{a,k}^c$, and its c-value is c_k^o .

The potentials in the left and right branches are, from equation (5.20),

$$\bar{v}_L(x) = \bar{v}_J \frac{\cosh \omega(l-x)}{\cosh \omega l}, \quad 0 \leq x \leq l. \quad (5.25)$$

$$\bar{v}_R(x) = \bar{v}_J \frac{\cosh \omega(3l-x)}{\cosh 3\omega l}, \quad 0 \leq x \leq 3l. \quad (5.26)$$

The potential at the junction is $\bar{v}_L(0) = \bar{v}_R(0) = \bar{v}_J$, and only at this point are the left and right potentials related. Choose the junction point as origin. The total axial current flowing into the two cylinders is \bar{i}_J . Using equation (5.10),

$$\begin{aligned}\bar{i}_J &= -Kc^L \frac{\partial \bar{v}_L(0)}{\partial x} - Kc^R \frac{\partial \bar{v}_R(0)}{\partial x} \\ &= \omega K \bar{v}_J \left[c^L \frac{\sinh \omega l}{\cosh \omega l} + c^R \frac{\sinh 3\omega l}{\cosh 3\omega l} \right].\end{aligned}\quad (5.27)$$

Cable Cylinder One

Apply the generator equation (5.24) using v_J and i_J to try and generate the first cable cylinder,

$$\bar{\phi}_1(x) = \bar{v}_J \cosh \omega x - \bar{v}_J \left[\frac{c^L}{c_1^G} \frac{\sinh \omega l \sinh \omega x}{\cosh \omega l} + \frac{c^R}{c_1^G} \frac{\sinh 3\omega l \sinh \omega x}{\cosh 3\omega l} \right]. \quad (5.28)$$

Using standard identities for the hyperbolic functions,

$$\begin{aligned}\bar{\phi}_1(x) &= \bar{v}_J \cosh \omega x \left(1 - \frac{c^L}{c_1^G} - \frac{c^R}{c_1^G} \right) + \frac{c^L}{c_1^G} \bar{v}_J \frac{\cosh \omega(l-x)}{\cosh \omega l} + \frac{c^R}{c_1^G} \bar{v}_J \frac{\cosh \omega(3l-x)}{\cosh 3\omega l} \\ &= \bar{v}_J \cosh \omega x \left(1 - \frac{(c^L + c^R)}{c_1^G} \right) + \frac{c^L}{c_1^G} \bar{v}_L(x) + \frac{c^R}{c_1^G} \bar{v}_R(x).\end{aligned}\quad (5.29)$$

Note that c_1^G has not been specified at this stage (we regard ϕ_1 , in the form above, as a framework potential function). Nevertheless, voltage continuity and current conservation are guaranteed at the origin, whatever structure the Y-junction is connected to, and whatever value c_1^G may eventually take.

Of course, it is well established from the Rall equivalent cylinder result given in Chapter 3 that

$$c_1^G = c^L + c^R. \quad (5.30)$$

This value removes the spurious term $\bar{v}_J \cosh \omega x$ (which cannot be interpreted as a cable solution), leaving a linear combination of Y-junction potentials.

The c-value of the first cable cylinder has now been found, as has its potential function. What, then, is its electrotonic length? Note that $v_L(x)$ is only valid for length l since the left branch has length l . Choose the length of cylinder one to be l , otherwise the right-branch contribution to the potential function is partially invalid. Thus,

$$\bar{\phi}_1(x) = \frac{c^L}{c_1^G} \bar{v}_L(x) + \frac{c^R}{c_1^G} \bar{v}_R(x), \quad 0 \leq x \leq l. \quad (5.31)$$

Now that cable cylinder c-value c_1^G has been specified, we regard ϕ_1 as a fully specified potential function, i.e. no longer a framework potential. More generally, ϕ_k is regarded as a framework potential until c_k^G has been determined, at which point it can be substituted for and the unique potential function has been determined.

The construction procedure has succeeded for the first cable cylinder. Perhaps this is not too surprising though, since the first cylinder is almost identical to Rall's equivalent cylinder, the difference being that, at $x = l$, $\bar{\phi}_1$ cannot terminate since $\bar{v}_R(l)$ and $\partial\bar{v}_R(l)/\partial x$ are both unconstrained. We must proceed with the construction.

Cable Cylinder Two

From continuity of voltage and conservation of current,

$$\bar{\phi}_2(0) = \bar{\phi}_1(l) = \frac{c^L}{c_1^G} \bar{v}_J \frac{1}{\cosh \omega l} + \frac{c^R}{c_1^G} \bar{v}_J \frac{\cosh 2\omega l}{\cosh 3\omega l}, \quad (5.32)$$

$$\bar{i}_{a,2}^c(0) = \bar{i}_{a,1}^c(l) = -K c_1^c \frac{\partial \bar{\phi}_1(l)}{\partial x} = K \omega c^R \bar{v}_J \frac{\sinh 2\omega l}{\cosh 3\omega l}. \quad (5.33)$$

The generator equation (5.24) gives an expression for the potential in the second cable cylinder,

$$\bar{\phi}_2(x) = \frac{c^L}{c_1^G} \bar{v}_J \frac{\cosh \omega x}{\cosh \omega l} + \frac{c^R}{c_1^G} \bar{v}_J \frac{\cosh 2\omega l \cosh \omega x}{\cosh 3\omega l} - \bar{v}_J \frac{c^R}{c_2^G} \frac{\sinh 2\omega l \sinh \omega x}{\cosh 3\omega l}. \quad (5.34)$$

Rearranging gives

$$\begin{aligned} \bar{\phi}_2(x) &= \frac{c^L}{c_1^G} \bar{v}_J \frac{\cosh \omega x}{\cosh \omega l} + \frac{c^R}{c_1^G} \bar{v}_J \frac{1}{2} \left[\frac{\cosh \omega(2l+x)}{\cosh 3\omega l} + \frac{\cosh \omega(2l-x)}{\cosh 3\omega l} \right] \\ &\quad - \frac{c^R}{c_2^G} \bar{v}_J \frac{1}{2} \left[\frac{\cosh \omega(2l+x)}{\cosh 3\omega l} - \frac{\cosh \omega(2l-x)}{\cosh 3\omega l} \right] \\ &= \frac{c^R}{c_1^G} \frac{1}{2} \left(1 - \frac{c_1^G}{c_2^G} \right) \bar{v}_J \frac{\cosh \omega(2l+x)}{\cosh 3\omega l} + \frac{c^R}{c_1^G} \frac{1}{2} \left(1 + \frac{c_1^G}{c_2^G} \right) \bar{v}_J \frac{\cosh \omega(2l-x)}{\cosh \omega 3l} \\ &\quad + \frac{c^L}{c_1^G} \bar{v}_J \frac{\cosh \omega x}{\cosh \omega l} \\ &= \frac{c^R}{c_1^G} \frac{1}{2} \left(1 - \frac{c_1^G}{c_2^G} \right) \bar{v}_R(l-x) + \frac{c^R}{c_1^G} \frac{1}{2} \left(1 + \frac{c_1^G}{c_2^G} \right) \bar{v}_R(l+x) + \frac{c^L}{c_1^G} \bar{v}_L(l-x). \end{aligned} \quad (5.35)$$

The second cable cylinder, like the first, must have length l since this is the maximum range for which the three components of the expression are valid. At this point, there is no clear choice for c_2^G , but it is insightful to check for the possibility of termination at $x = l$. Clearly, $\bar{v}_R(2l)$ and $\partial\bar{v}_R(2l)/\partial x$ are unrestricted, however, observe that if the sum of the coefficients of $\bar{v}_R(l-x)$ and $\bar{v}_L(l-x)$ is zero (i.e. coefficients have the same magnitude but opposite sign), then

$$\frac{c^R}{c_1^G} \frac{1}{2} \left(1 - \frac{c_1^G}{c_2^G} \right) + \frac{c^L}{c_1^G} = 0, \quad (5.36)$$

and at $x = l$ in cable cylinder two, voltage continuity at the tree junction ensures these two terms will cancel giving

$$\bar{\phi}_2(l) = \frac{c^R}{c_1^G} \frac{1}{2} \left(1 + \frac{c_1^G}{c_2^G} \right) \bar{v}_R(2l). \quad (5.37)$$

If the right hand cylinder were actually length $2l$, and satisfied a cut end condition at the terminal, then $\bar{\phi}_2(l) = 0$, and the cable terminates. Bear this in mind, as we proceed now to the next cable cylinder, without specifying c_2^G in potential $\bar{\phi}_2$.

Cable Cylinder Three

Once more, voltage continuity and current conservation give the required information for the proximal end of the next cylinder,

$$\bar{\phi}_3(0) = \bar{\phi}_2(l) = \bar{v}_J \left[\frac{c^R}{c_1^G} \frac{1}{2} \left(1 - \frac{c_1^G}{c_2^G} \right) + \frac{c^L}{c_1^G} \right] + \frac{c^R}{c_1^G} \frac{1}{2} \left(1 + \frac{c_1^G}{c_2^G} \right) \frac{\cosh \omega l}{\cosh 3\omega l} \quad (5.38)$$

$$\begin{aligned} \bar{i}_{a,3}^c(0) &= \bar{i}_{a,2}^c(l) = -K c_2^G \frac{\partial \bar{\phi}_2(l)}{\partial x} \\ &= -K \omega c_2^G \bar{v}_J \left[\frac{c^R}{c_1^G} \frac{1}{2} \left(1 - \frac{c_1^G}{c_2^G} \right) \frac{\sinh 3\omega l}{\cosh 3\omega l} - \frac{c^R}{c_1^G} \frac{1}{2} \left(1 + \frac{c_1^G}{c_2^G} \right) \frac{\sinh \omega l}{\cosh 3\omega l} + \frac{c^L}{c_2^G} \frac{\sinh \omega l}{\cosh \omega l} \right]. \end{aligned} \quad (5.39)$$

The generator equation (5.24) gives

$$\begin{aligned} \bar{\phi}_3(x) &= \bar{v}_J \left[\frac{c^R}{c_1^G} \frac{1}{2} \left(1 - \frac{c_1^G}{c_2^G} \right) + \frac{c^L}{c_1^G} \right] \cosh \omega x + \frac{c^R}{c_1^G} \frac{1}{2} \left(1 + \frac{c_1^G}{c_2^G} \right) \frac{\cosh \omega l \cosh \omega x}{\cosh 3\omega l} \\ &\quad + \frac{c_2^G}{c_3^G} \frac{c^R}{c_1^G} \frac{1}{2} \left(1 - \frac{c_1^G}{c_2^G} \right) \bar{v}_J \frac{\sinh 3\omega l \sinh \omega x}{\cosh 3\omega l} - \frac{c_2^G}{c_3^G} \frac{c^R}{c_1^G} \frac{1}{2} \left(1 + \frac{c_1^G}{c_2^G} \right) \bar{v}_J \frac{\sinh \omega l \sinh \omega x}{\cosh 3\omega l} \\ &\quad + \frac{c_2^G}{c_3^G} \frac{c^L}{c_1^G} \bar{v}_J \frac{\sinh \omega l \sinh \omega x}{\cosh \omega l} \\ &= \bar{v}_J \cosh \omega x \left[\left(1 + \frac{c_2^G}{c_3^G} \right) \left(\frac{c^R}{c_1^G} \frac{1}{2} \left(1 - \frac{c_1^G}{c_2^G} \right) + \frac{c^L}{c_1^G} \right) \right] \\ &\quad - \frac{c_2^G}{c_3^G} \frac{c^R}{c_1^G} \frac{1}{2} \left(1 - \frac{c_1^G}{c_2^G} \right) \bar{v}_J \frac{\sinh \omega (3l-x)}{\cosh 3\omega l} - \frac{c_2^G}{c_3^G} \frac{c^L}{c_1^G} \bar{v}_J \frac{\sinh \omega (l-x)}{\cosh \omega l} \\ &\quad + \frac{1}{2} \left(1 - \frac{c_2^G}{c_3^G} \right) \frac{c^R}{c_1^G} \frac{1}{2} \left(1 + \frac{c_1^G}{c_2^G} \right) \bar{v}_J \frac{\cosh \omega (l+x)}{\cosh 3\omega l} \\ &\quad + \frac{1}{2} \left(1 + \frac{c_2^G}{c_3^G} \right) \frac{c^R}{c_1^G} \frac{1}{2} \left(1 + \frac{c_1^G}{c_2^G} \right) \bar{v}_J \frac{\cosh \omega (l-x)}{\cosh 3\omega l} \\ &= \bar{v}_J \cosh \omega x \left[\left(1 + \frac{c_2^G}{c_3^G} \right) \left(\frac{c^R}{c_1^G} \frac{1}{2} \left(1 - \frac{c_1^G}{c_2^G} \right) + \frac{c^L}{c_1^G} \right) \right] \\ &\quad - \frac{c_2^G}{c_3^G} \frac{c^R}{c_1^G} \frac{1}{2} \left(1 - \frac{c_1^G}{c_2^G} \right) \bar{v}_R(x) - \frac{c_2^G}{c_3^G} \frac{c^L}{c_2^G} \bar{v}_L(x) \\ &\quad + \frac{1}{2} \left(1 - \frac{c_2^G}{c_3^G} \right) \frac{c^R}{c_1^G} \frac{1}{2} \left(1 + \frac{c_1^G}{c_2^G} \right) \bar{v}_R(2l-x) \\ &\quad + \frac{1}{2} \left(1 + \frac{c_2^G}{c_3^G} \right) \frac{c^R}{c_1^G} \frac{1}{2} \left(1 + \frac{c_1^G}{c_2^G} \right) \bar{v}_R(2l+x). \end{aligned} \quad (5.40)$$

It is easy to check that voltage continuity and current conservation have been guaranteed at the point where the second and third cable cylinders meet, even though c_2^G and

c_3^G are both still unspecified. Potential $\bar{\phi}_3$ is valid for length l . Again, an unwanted term proportional to $\bar{v}_J \cosh \omega x$ has been produced. This time, it can be set to zero by ensuring that c_2^G satisfies the condition (5.36) for the cancellation of $\bar{v}_R(l-x)$ and $\bar{v}_L(l+x)$ at $x=l$ in potential $\bar{\phi}_2(x)$. The second cylinder potential (5.35) then simplifies to

$$\bar{\phi}_2(x) = \frac{c_2^L}{c_1^G} (\bar{v}_L(l-x) - \bar{v}_R(l+x)) + \bar{v}_R(l+x), \quad 0 \leq x \leq l. \quad (5.41)$$

and equation (5.36) itself gives up the c-value,

$$c_2^G = \frac{c_1^G c^R}{2c^L + c^R}. \quad (5.42)$$

The third cylinder potential (5.40) can be rewritten

$$\bar{\phi}_3(x) = -\frac{c_2^G c^L}{c_3^G c_1^G} (\bar{v}_L(x) - \bar{v}_R(x)) + \frac{1}{2} \left(1 - \frac{c_2^G}{c_3^G}\right) \bar{v}_R(2l-x) + \frac{1}{2} \left(1 + \frac{c_2^G}{c_3^G}\right) \bar{v}_R(2l+x). \quad (5.43)$$

Now investigate termination of the third cable cylinder. Since $\bar{v}_L(l)$ does not satisfy a cut condition, it is impossible for cable cylinder three to satisfy a cut condition. However, $\partial \bar{v}_L(l)/\partial x = 0$ and $\partial \bar{v}_R(3l)/\partial x = 0$ because of the left and right sealed terminals. Is it possible to choose c_3^G such that the cable can terminate with a sealed end at this stage?

The axial current at $x=l$ on cable cylinder three is

$$\begin{aligned} \bar{i}_{a,3}^e(l) &= -K c_3^G \frac{\partial \bar{\phi}_3(l)}{\partial x} \\ &= c_2^G \frac{c_L}{c_1^G} \frac{\bar{i}_{a,R}(l)}{c^R} - \frac{1}{2} (c_3^G - c_2^G) \frac{\bar{i}_{a,R}(l)}{c^R}. \end{aligned} \quad (5.44)$$

Therefore, $\bar{i}_{a,3}^e(l)$ is zero provided

$$c_2^G \frac{c^L}{c_1^G} = \frac{1}{2} (c_3^G - c_2^G). \quad (5.45)$$

Consequently, the third cable cylinder potential (5.43) can now be written in its fully determined form,

$$\begin{aligned} \bar{\phi}_3(x) &= -\frac{c^L}{c^R + 3c^L} (\bar{v}_L(x) - \bar{v}_R(x)) \\ &\quad \frac{c^L}{c^R + 3c^L} \bar{v}_R(2l-x) + \frac{c^R + 2c^L}{c^R + 3c^L} \bar{v}_R(2l+x), \quad 0 \leq x \leq l, \end{aligned} \quad (5.46)$$

with (5.45) giving

$$c_3^G = \frac{c^R(c^R + 3c^L)}{c^R + 2c^L}. \quad (5.47)$$

Thus, after length $3l$, it is possible to force termination of the cable by carefully choosing c_3^G such that $\bar{\phi}_3(x)$ satisfies a sealed condition at $x=l$.

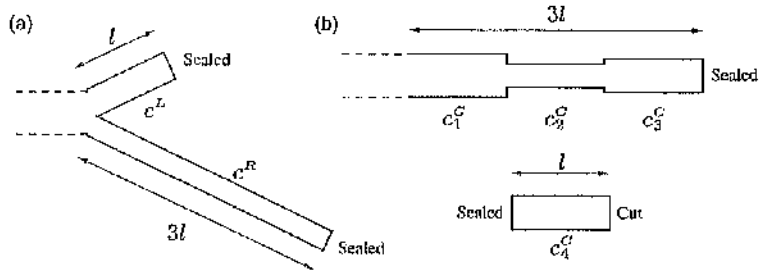


Figure 5.2: A simple Y-junction and its equivalent cable, determined from first principles. (a) The Y-junction has one limb with electrotonic length l , c-value c^L , another with electrotonic length $3l$, c-value c^R ; both terminals are sealed. (b) The equivalent cable has a connected section, length $3l$, with a sealed terminal, and a disconnected section of length l . The connected section is formed from three cylinders each with length l , and c-values c_1^G to c_3^G . The disconnected section consists of one cylinder with cut and sealed terminals. See text for full details.

Cable Cylinder Four — The Disconnected Section

The total electrotonic length of left and right Y-junction limbs was $4l$, so the fully equivalent cable is incomplete. There must be a disconnected section of length l . Without going into great detail (disconnected sections are discussed in Chapter 6), we can only write one function which satisfies a sealed end condition at $x = 0$ and a cut condition at $x = l$, namely

$$\bar{\phi}_4(x) = A [v_L(l-x) - \bar{v}_R(l-x) - \bar{v}_R(l+x) + \bar{v}_R(3l-x)]. \quad (5.48)$$

where A is a non-zero real constant. There is no other acceptable form. Also choose $c_4^G = 1$ (though it may take any value — the equivalent cable and electrical mapping will be correct whatever).

Summary of Cable Potential Functions and C-values

It is a trivial step now to take the inverse Laplace transform of the cable cylinder potential functions, simply by replacing barred potentials with unbarred potentials. So, in the physical domain, the Y-junction potentials are mapped to the fully equivalent cable by

$$\begin{aligned} \phi_1(x) &= \frac{c^L}{c_1^G} v_L(x) + \frac{c^R}{c_1^G} v_R(x). \\ \phi_2(x) &= \frac{c^L}{c_1^G} (v_L(l-x) - v_R(l-x)) + v_R(l+x). \\ \phi_3(x) &= -\frac{c^L}{c^R + 3c^L} (v_L(x) - v_R(x)) + \frac{c^L}{c^R + 3c^L} v_R(2l-x) + \frac{c^R + 2c^L}{c^R + 3c^L} v_R(2l+x). \\ \phi_4(x) &= v_L(l-x) - v_R(l-x) - v_R(l+x) + v_R(3l-x). \end{aligned} \quad (5.49)$$

The potential functions ϕ_1, \dots, ϕ_4 form a set of four linear independent homogeneous equations. It is simple to invert the mapping and write the tree potentials in terms of cable potentials,

$$\begin{aligned} v_L(x) &= \phi_1(x) + \frac{c^R}{c^R + 2c^L} [\phi_2(l-x) - \phi_3(x)] + \frac{c^R}{c^R + 3c^L} \phi_4(l-x) \\ v_R(x) &= \phi_1(x) - \frac{c^L}{c^R + 2c^L} [\phi_2(l-x) - \phi_3(x)] - \frac{c^L}{c^R + 3c^L} \phi_4(l-x) \\ v_R(2l-x) &= \frac{c^R + c^L}{c^R + 2c^L} \phi_2(l-x) + \frac{c^L}{c^R + 2c^L} \phi_3(x) - \frac{c^L}{c^R + 3c^L} \phi_4(l-x) \\ v_R(2l+x) &= \phi_3(x) - \frac{c^L}{c^R + 3c^L} \phi_4(l-x). \end{aligned} \quad (5.50)$$

The c-values of the cable cylinders are

$$c_1^C = c^L + c^R, \quad c_2^C = \frac{c_1^C c^R}{c^R + 2c^L}, \quad c_3^C = \frac{c^R(c^R + 3c^L)}{c^R + 2c^L}, \quad c_4^C = 1. \quad (5.51)$$

Figure 5.2 illustrates the original simple Y-junction and its equivalent cable.

Discussion of Example One

This very simple example provides no clear set of rules to follow when evaluating cable cylinder potential functions and c-values, though it does hint at a distinct division of labour between constructing a cylinder's potential function (a framework potential function) and subsequently determining its c-value. There are some indications of rules which must be applied to one potential to generate the next framework potential --- note the terms

$$\frac{1}{2} \left(1 + \frac{c_k^C}{c_{k+1}^C} \right) \quad \text{and} \quad \frac{1}{2} \left(1 - \frac{c_k^C}{c_{k+1}^C} \right), \quad (5.52)$$

in $\bar{\phi}_2$ (5.35) where $k = 1$, and in $\bar{\phi}_3$ (5.43) where $k = 2$. Furthermore, the choice of c-values appear geared towards arranging termination of part (a local termination) or all of the potential function.

The first principles construction algorithm seems to preserve voltage continuity and current conservation independently of the cable c-values that are eventually chosen. Therefore, it is not directly responsible for determining c-values.

5.4.2 Example Two

Now consider the Y-junction in Figure 5.3a. The right branch consists of one cylinder which has length l and terminates with a cut end. The left branch has electrotonic length $2l$, but consists of two cylinders, each of length l . One cylinder, denoted L , meets the right branch at the junction. The other, denoted Q , meets L at one end and terminates with a sealed terminal at the other. Again, we suppose that there are no input current terms.

The potential at the junction is denoted \bar{v}_J . The potential where cylinders L and Q meet is denoted \bar{v}_X . The axial current flowing into cylinder L is denoted \bar{i}_L . From equation (5.20) (for cylinder Q), (5.23) (for cylinder R), and (5.24) (for cylinder L), the potentials in the left and right branches can be expressed

$$\bar{v}_L(x) = \bar{v}_J \cosh \omega x - \frac{\bar{i}_L}{K \omega c^L} \sinh \omega x, \quad 0 \leq x \leq l. \quad (5.53)$$

$$\bar{v}_Q(x) = \bar{v}_X \frac{\cosh \omega(l-x)}{\cosh \omega l}, \quad 0 \leq x \leq l. \quad (5.54)$$

$$\bar{v}_R(x) = \bar{v}_J \frac{\sinh \omega(l-x)}{\sinh \omega l}, \quad 0 \leq x \leq l. \quad (5.55)$$

Since voltage continuity requires that $\bar{v}_L(l) = \bar{v}_Q(0)$, we may solve for \bar{i}_L to obtain

$$\bar{v}_L(x) = \bar{v}_J \cosh \omega x + (\bar{v}_X - \bar{v}_J \cosh \omega l) \frac{\sinh \omega x}{\sinh \omega l}. \quad (5.56)$$

Choose the junction point as origin. The total axial current flowing into the two cylinders is \bar{i}_J . Using equation (5.10),

$$\begin{aligned} \bar{i}_J &= -K c^L \frac{\partial \bar{v}_L(0)}{\partial x} - K c^R \frac{\partial \bar{v}_R(0)}{\partial x} \\ &= \omega K \left[\bar{v}_J c^R \frac{\cosh \omega l}{\sinh \omega l} + c^L (\bar{v}_X - \bar{v}_J \cosh \omega l) \frac{1}{\sinh \omega l} \right]. \end{aligned} \quad (5.57)$$

Cable Cylinder One

Apply the generator equation (5.24) using v_J and i_J to try and generate the first cable cylinder,

$$\bar{\phi}_1(x) = \bar{v}_J \cosh \omega x - \left[\bar{v}_J \frac{c^R}{c_1^G} \frac{\cosh \omega l \sinh \omega x}{\sinh \omega l} + \frac{c^L}{c_1^G} (\bar{v}_X - \bar{v}_J \cosh \omega l) \frac{\sinh \omega x}{\sinh \omega l} \right]. \quad (5.58)$$

Using standard identities for the hyperbolic functions,

$$\begin{aligned} \bar{\phi}_1(x) &= \bar{v}_J \cosh \omega x \left(1 - \frac{c^L}{c_1^G} - \frac{c^R}{c_1^G} \right) + \frac{c^L}{c_1^G} \left[\bar{v}_J \cosh \omega x + (\bar{v}_X - \bar{v}_J \cosh \omega l) \frac{\sinh \omega x}{\sinh \omega l} \right] \\ &\quad + \frac{c^R}{c_1^G} \bar{v}_J \frac{\sinh \omega(l-x)}{\sinh \omega l} \\ &= \bar{v}_J \cosh \omega x \left(1 - \frac{(c^L + c^R)}{c_1^G} \right) + \frac{c^L}{c_1^G} \bar{v}_L(x) + \frac{c^R}{c_1^G} \bar{v}_R(x). \end{aligned} \quad (5.59)$$

This is exactly the same framework form for the first potential obtained in the previous example. For the same reasons, we must choose $c_1^G = c^L + c^R$, the "Rall-like" sum of diameters. Thus, as before,

$$\bar{\phi}_1(x) = \frac{c^L}{c_1^G} \bar{v}_L(x) + \frac{c^R}{c_1^G} \bar{v}_R(x), \quad 0 \leq x \leq l. \quad (5.60)$$

Cable Cylinder Two

From continuity of voltage and conservation of current,

$$\bar{\phi}_2(0) = \bar{\phi}_1(l) = \frac{c^L}{c_1^G} [\bar{v}_J \cosh \omega l + (\bar{v}_X - \bar{v}_J \cosh \omega l)] \quad (5.61)$$

$$\begin{aligned} \bar{i}_{a,2}^c(0) &= \bar{i}_{a,1}^c(l) = -K c_1^c \frac{\partial \bar{\phi}_1(l)}{\partial x} \\ &= -K \omega c^L \left[\bar{v}_J \sinh \omega l + (\bar{v}_X - \bar{v}_J \cosh \omega l) \frac{\cosh \omega l}{\sinh \omega l} \right] \\ &\quad + K \omega c^R \bar{v}_J \frac{1}{\sinh \omega l}. \end{aligned} \quad (5.62)$$

The generator equation (5.24) gives an expression for the potential in the second cable cylinder.

$$\begin{aligned} \bar{\phi}_2(x) &= \frac{c^L}{c_1^G} [\bar{v}_J \cosh \omega l + (\bar{v}_X - \bar{v}_J \cosh \omega l)] \cosh \omega x \\ &\quad + \frac{c^L}{c_2^G} \left[\bar{v}_J \sinh \omega l + (\bar{v}_X - \bar{v}_J \cosh \omega l) \frac{\cosh \omega l}{\sinh \omega l} \right] \sinh \omega x \\ &\quad - \frac{c^R}{c_2^G} \bar{v}_J \frac{\sinh \omega x}{\sinh \omega l}. \end{aligned} \quad (5.63)$$

After some algebraic effort, this can be rewritten as

$$\begin{aligned} \bar{\phi}_2(x) &= -\frac{c_1^G c^R}{c_2^G c_1^Q} \bar{v}_J \frac{\sinh \omega x}{\sinh \omega l} \\ &\quad + \frac{c^L}{c^L + c^Q} \left(1 - \frac{c_1^G c^Q}{c_2^G c^L} \right) \frac{c^L}{c_1^G} \left[\bar{v}_J \cosh \omega(l-x) + (\bar{v}_X - \bar{v}_J \cosh \omega l) \frac{\sinh \omega(l-x)}{\sinh \omega l} \right] \\ &\quad + \frac{c^Q}{c^L + c^Q} \left(1 + \frac{c_1^G}{c_2^G} \right) \frac{c^L}{c_1^G} \bar{v}_X \frac{\cosh \omega(l-x)}{\cosh \omega x} \end{aligned} \quad (5.64)$$

$$\begin{aligned} &= -\frac{c_1^G c^R}{c_2^G c_1^Q} \bar{v}_R(l-x) + \frac{c^L}{c^L + c^Q} \left(1 - \frac{c_1^G c^Q}{c_2^G c^L} \right) \frac{c^L}{c_1^G} \bar{v}_L(l-x) \\ &\quad + \frac{c^Q}{c^L + c^Q} \left(1 + \frac{c_1^G}{c_2^G} \right) \frac{c^L}{c_1^G} \bar{v}_Q(x). \end{aligned} \quad (5.65)$$

The individual contributions from the tree cylinder potentials are each valid only for length l , and so restrict the second cable cylinder to length l . At this point, as in the previous example, there is no clear choice for c_2^G . Observe again, however, that if the sum of the coefficients of $v_R(l-x)$ and $\bar{v}_L(l-x)$ is zero, then

$$-\frac{c_1^G c^R}{c_2^G c_1^Q} + \frac{c^L}{c^L + c^Q} \left(1 - \frac{c_1^G c^Q}{c_2^G c^L} \right) \frac{c^L}{c_1^G} = 0, \quad (5.66)$$

This yields

$$c_2^G = \frac{c_1^G (c^Q c_1^Q + c^R c^L)}{(c^L)^2}. \quad (5.67)$$

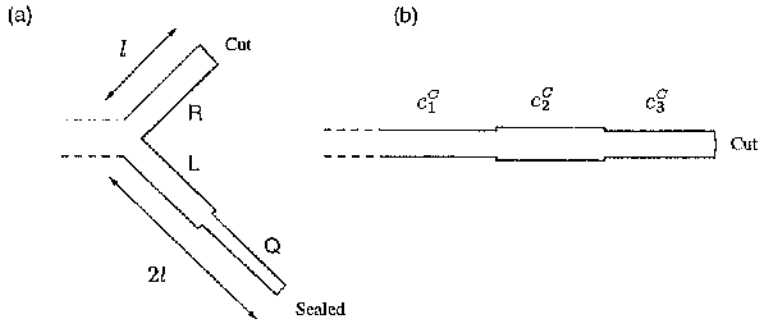


Figure 5.3: The Y-junction and its fully equivalent cable for first-principles example two. See text for full details.

and

$$\bar{\phi}_2(x) = \frac{(c^L)^2 c^R}{c_1^G (c_1^G c^Q + c^L c^R)} (\bar{v}_L(l-x) - \bar{v}_R(l-x)) + \frac{c^Q c^L}{(c_1^G c^Q + c^L c^R)} \bar{v}_Q(x), \quad 0 \leq x \leq l. \quad (5.68)$$

This potential would immediately satisfy a cut terminal at $x = l$ if the longer branch satisfied a cut terminal. It does not however, so the process continues.

Cable Cylinder Three

Once more, voltage continuity and current conservation give the required information for the proximal end of the next cylinder,

$$\bar{\phi}_3(0) = \bar{\phi}_2(l) = \frac{c^Q c^L}{(c_1^G c^Q + c^L c^R)} \bar{v}_X \frac{1}{\cosh \omega l} \quad (5.69)$$

$$\begin{aligned} \bar{i}_{a,3}^c(0) &= \bar{i}_{a,2}^c(l) = -K c_2^G \frac{\partial \bar{\phi}_2(l)}{\partial x} \\ &= K \omega c_2^G \frac{(c^L)^2 c^R}{c_1^G (c_1^G c^Q + c^L c^R)} \bar{v}_X \frac{1}{\sinh \omega l}. \end{aligned} \quad (5.70)$$

After even more algebraic effort, the generator equation (5.24) gives

$$\begin{aligned} \bar{\phi}_3(x) &= -\frac{c^Q c^L}{(c_1^G c^Q + c^L c^R)} \bar{v}_X \frac{\cosh \omega x}{\cosh \omega l} + \frac{c_2^G}{c_3^G c_1^G (c_1^G c^Q + c^L c^R)} \bar{v}_X \frac{(c^L)^2 c^R}{\sinh \omega l} \frac{\sinh \omega x}{\sinh \omega l} \\ &= -\frac{c_2^G}{c_3^G c_1^G (c_1^G c^Q + c^L c^R)} (\bar{v}_L(x) - \bar{v}_R(x)) + \frac{c^Q c^L}{(c_1^G c^Q + c^L c^R)} \bar{v}_Q(l-x). \end{aligned} \quad (5.71)$$

As usual, it is easy to check that voltage continuity and current conservation have been guaranteed at the point where the second and third cable cylinders meet, even though c_3^G is still unspecified. Potential $\bar{\phi}_3$ is valid for length l .

We now look once more to see if we can terminate the equivalent cable at this stage (in fact if the cable is going to terminate, it has to terminate here since we have reached the maximum cable length).

At $x = l$, $v_R(l)$ satisfies a cut terminal condition. Can we choose c_3^C so that the other two contributions to the potential satisfy a cut terminal where they meet at $x = l$? This requires

$$-\frac{c_2^C}{c_3^C} \frac{(c^L)^2 c^R}{c_1^C (c_1^C c^Q + c^L c^R)} + \frac{c^Q c^L}{(c_1^C c^Q + c^L c^R)} = 0, \quad (5.72)$$

which yields

$$c_3^C = \frac{c_2^C c^L c^R}{c_1^C c^Q} = \frac{c^R (c_1^C c^Q + c^L c^R)}{c^L c^Q}. \quad (5.73)$$

The third cable cylinder potential can therefore be rewritten

$$\bar{\phi}_3(x) = \frac{c^Q c^L}{(c_1^C c^Q + c^L c^R)} [\bar{v}_R(x) - \bar{v}_L(x) + \bar{v}_Q(l-x)]. \quad (5.74)$$

Summary of Cable Potential Functions and C-values

As in the first example, take inverse Laplace transforms of the potential functions to obtain

$$\begin{aligned} \phi_1(x) &= \frac{c^L}{c_1^C} v_L(x) + \frac{c^R}{c_1^C} v_R(x). \\ \phi_2(x) &= \frac{(c^L)^2 c^R}{c_1^C (c_1^C c^Q + c^L c^R)} (v_L(l-x) - v_R(l-x)) + \frac{c^Q c^L}{(c_1^C c^Q + c^L c^R)} v_Q(x). \\ \phi_3(x) &= \frac{c^Q c^L}{(c_1^C c^Q + c^L c^R)} [v_R(x) - v_L(x) + v_Q(l-x)]. \end{aligned}$$

The inverse mapping can be obtained quite easily by analysing these three linearly independent equations,

$$\begin{aligned} v_R(x) &= \phi_1(x) - \phi_2(l-x) + \phi_3(x) \\ v_L(x) &= \phi_1(x) + \frac{c^R}{c^L} [\phi_2(l-x) - \phi_3(x)] \\ v_Q(x) &= \frac{c^Q c_1^C}{c^Q c_1^C + c^R c^L} \phi_2(x) + \frac{c^R c^L}{c^Q c_1^C + c^R c^L} \phi_3(l-x). \end{aligned}$$

The equivalent cable c-values are

$$c_1^C = c^L + c^R, \quad c_2^C = \frac{c_1^C (c^Q c_1^C + c^R c^L)}{(c^L)^2}, \quad c_3^C = \frac{c^R (c_1^C c^Q + c^L c^R)}{c^L c^Q}. \quad (5.75)$$

Discussion of Example Two

The second example has progressed much as the first, with framework potential functions determined from the first-principles construction algorithm, and then additional assumptions being made to determine c-values in a way that ensures termination is possible. Note the coefficients

$$\frac{c^L}{c^L + c^Q} \left(1 - \frac{c_k^C}{c_{k+1}^C} \frac{c^Q}{c^L} \right), \quad \text{and} \quad \frac{c^Q}{c^L + c^Q} \left(1 + \frac{c_k^C}{c_{k+1}^C} \right), \quad (5.76)$$

from equation (5.65), where $k = 1$. For the specific situation where $c^L = c^Q$, these simplify to the coefficients highlighted from the previous example, equation (5.52).

A general mechanism for choosing c -values is still not clear, but again seems to be associated with ensuring termination of the cable. In particular, the two contributions to potential ϕ_2 (5.68) are again arranged so that they satisfy a local cut condition. Even in this simple example, algebraic complexity rapidly accumulates.

5.5 An Introduction to the Construction Rules

5.5.1 Potential Function Components and Component Diagrams

A potential function, ϕ_k , for a cable cylinder with length l , is a linear combination of contributions from tree cylinder potentials. Each contribution is referred to as a “component”. A component is a directed segment of a tree cylinder potential. A component has a *coefficient* which determines its strength compared to other components; a *source* point, which is the point on the tree it describes when $x = 0$; a *destination* point, which is the point on the tree it describes when $x = l$; a direction that is either inward, towards the origin (if the destination is closer than the source to the origin) or outwards, away from the origin (if the destination is further than the source from the origin).

For example, consider example one. Potential ϕ_1 (5.49) contains two outward components; one lies on the left branch, one on the right, both with the origin as source. The left component has the sealed end at $x = l$ as destination while the right component has an internal point $x = l$ as destination. The left coefficient is c^L/c_1^C and the right coefficient is c^R/c_1^C . Potential ϕ_4 (5.49) has four components. Three lie on the right cylinder, and one lies on the left. There are three inward components, and one outward component.

Component diagrams are useful for illustrating the contributions a Y-junction’s left and right limb potentials make to each cable potential. Figure 5.4 shows component diagrams for the four cable cylinder potentials determined in example one, and summarised in (5.49).

5.5.2 The Electrical Continuity Rules

The electrical continuity rules are applied to potential function ϕ_k to generate ϕ_{k+1} in a framework potential form, i.e. without specifying cable cylinder c -value c_{k+1}^C .

Consider now two connected tree cylinders, denoted P and Q , each with length l . Voltage continuity ensures that $v_P(l) = v_P(0)$. Suppose potential ϕ_k contains a component $v_P(x)$. The electrical continuity rules determine contributions to ϕ_{k+1} that arise entirely because of the existence of $v_P(x)$ in ϕ_k . In fact, two components are introduced by $v_P(x)$,

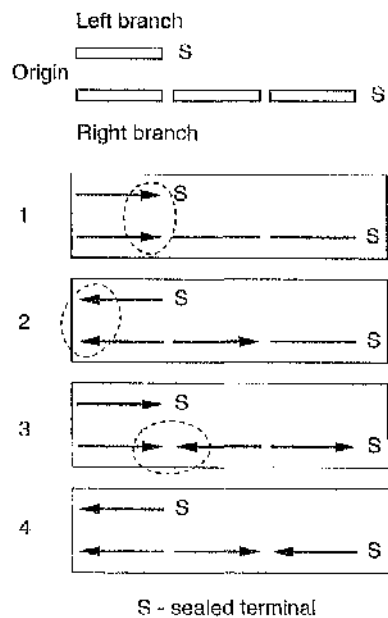


Figure 5.4: Component diagrams for the cable potential functions generated for a simple Y-junction with both terminals sealed. Top — a schematic of a simple Y-junction. The left branch is one basic length; the right branch is three quantum lengths. Boxes 1–4 — component diagrams showing the direction and location of the components of the four potential functions. Each arrow represents one component, showing its length, direction, source and destination. Branch segments that do not contribute components to the potential function are represented as lines. In 1–3, the circled components are those whose coefficients are matched up to determine c-values and/or arrange partial or full termination of the function.

and we use the notation " \rightarrow " to indicate this, like so

$$v_P(x) \rightarrow \frac{c^P}{c^P + c^Q} \left(1 - \frac{c_k^C}{c_{k+1}^C} \frac{c^Q}{c^P} \right) v_P(l-x) + \frac{c^Q}{c^P + c^Q} \left(1 + \frac{c_k^C}{c_{k+1}^C} \right) v_Q(x). \quad (5.77)$$

This is the electrical continuity rule for reflection-transmission of a tree potential at a diameter step. Potential v_P in ϕ_k has introduced two new component in ϕ_{k+1} . One is transmitted along cylinder Q , i.e. in the same direction as the original component. The other new component is reflected in the opposite direction, back along cylinder P . At $x = 0$, the two new components meet at the diameter step, while at $x = l$ they describe structure that is length $2l$ apart.

It is easy to confirm that voltage continuity between the original component and those it generates has been guaranteed, irrespective of the actual equivalent cable c-values, since

$$\begin{aligned} & \frac{c^P}{c^P + c^Q} \left(1 - \frac{c_k^C}{c_{k+1}^C} \frac{c^Q}{c^P} \right) v_P(l) + \frac{c^Q}{c^P + c^Q} \left(1 + \frac{c_k^C}{c_{k+1}^C} \right) v_Q(0) \\ &= \left[\frac{c^P}{c^P + c^Q} \left(1 - \frac{c_k^C}{c_{k+1}^C} \frac{c^Q}{c^P} \right) + \frac{c^Q}{c^P + c^Q} \left(1 + \frac{c_k^C}{c_{k+1}^C} \right) \right] v_P(l) \\ &= v_P(l). \end{aligned} \quad (5.78)$$

Noting that current conservation in the tree ensures

$$c^P \frac{\partial v_P(l)}{\partial x} = c^Q \frac{\partial v_Q(0)}{\partial x}, \quad (5.79)$$

then it can be shown that current conservation is guaranteed between component $v_P(x)$ (in ϕ_k) and the components it generates in ϕ_{k+1} , i.e.

$$\begin{aligned} c_k^C \frac{\partial v_P(l)}{\partial x} &= -c_{k+1}^C \left[\frac{c^P}{c^P + c^Q} \left(1 - \frac{c_k^C}{c_{k+1}^C} \frac{c^Q}{c^P} \right) \right] \frac{\partial v_P(l)}{\partial x} \\ &\quad + c_{k+1}^C \left[\frac{c^Q}{c^P + c^Q} \left(1 + \frac{c_k^C}{c_{k+1}^C} \right) \right] \frac{\partial v_Q(0)}{\partial x}. \end{aligned} \quad (5.80)$$

Internal Point

Important special cases include reflection-transmission at an internal point of a cylinder. Set $c^P = c^Q$ in (5.77) to obtain.

$$v_P(x) \rightarrow \frac{1}{2} \left(1 - \frac{c_k^C}{c_{k+1}^C} \right) v_P(l-x) + \frac{1}{2} \left(1 + \frac{c_k^C}{c_{k+1}^C} \right) v_Q(x) \quad (5.81)$$

Sealed Terminal

A single component is reflected from a sealed (or current injection) terminal. Set $c^Q = 0$ in (5.77) to obtain

$$v_P(x) \rightarrow v_P(l-x) \quad (5.82)$$

Cut Terminal

A single component is also reflected from a cut terminal. Letting $c^Q \rightarrow \infty$ in (5.77) gives

$$v_P(x) \rightarrow -\frac{c_k^G}{c_{k+1}^G} v_P(l-x) \quad (5.83)$$

Reflection from the Origin — The Isolation Condition

Reflection from the origin is only acceptable (i.e. independent of structure connected to the Y-junction) when the two coefficients of the components that meet at the origin sum to zero — this is the “isolation condition”. Consider two cylinders, denoted L and R , each with length l , and suppose a potential function contains the pair of components $v_L(l-x) - v_R(l-x)$. Because of voltage continuity, $v_L(0) = v_R(0)$ and so this combination satisfies a cut condition at $x = l$. The component pair is therefore reflected from the origin just like a single component reflected from a cut terminal,

$$v_L(x) - v_R(x) \rightarrow -\frac{c_k^G}{c_{k+1}^G} [v_L(l-x) - v_R(l-x)] \quad (5.84)$$

Since a potential function is simply a sum of components, then voltage continuity and current conservation are guaranteed between a potential function ϕ_k and framework potential function ϕ_{k+1} . Additional properties of the electrical continuity rules are described in detail in Chapter 6.

5.6 Example One Using the Analytical Construction Rules

We can repeat example one, though much more rapidly, using the analytical construction rules directly. Recall Figure 5.2a. Example two could be repeated in a similar manner.

Cable Cylinder One

Cable construction is always initialised with the “Rall-like” potential function,

$$\phi_1(x) = \frac{c^L}{c_1^G} v_L(x) + \frac{c^R}{c_1^G} v_R(x), \quad 0 \leq x \leq l. \quad (5.85)$$

and c-value

$$c_1^G = c^L + c^R. \quad (5.86)$$

Cable Cylinder Two

The left cylinder component in ϕ_1 reaches a sealed terminal at $x = l$, and so, using (5.82), it produces a single reflected component, with the same coefficient, in ϕ_2 . The other component of ϕ_1 reaches an internal point of the right cylinder, and so, using (5.81) contributes two new components to ϕ_2 , a reflected component where the coefficient is multiplied by $0.5(1 - c_1^G/c_2^G)$, and a transmitted component where the coefficient is multiplied by $0.5(1 + c_1^G/c_2^G)$. Thus,

$$\phi_2(x) = \frac{c^R}{c_1^G} \frac{1}{2} \left(1 - \frac{c_1^G}{c_2^G} \right) \bar{v}_R(l-x) + \frac{c^R}{c_1^G} \frac{1}{2} \left(1 + \frac{c_1^G}{c_2^G} \right) \bar{v}_R(l+x) + \frac{c^L}{c_1^G} \bar{v}_L(l-x). \quad (5.87)$$

We must apply the isolation condition to ensure that any additional structure connected to the Y-junction does not interfere with the procedure, so

$$\frac{c^R}{c_1^G} \frac{1}{2} \left(1 - \frac{c_1^G}{c_2^G} \right) + \frac{c^L}{c_1^G} = 0, \quad (5.88)$$

yielding

$$c_2^G = \frac{c_1^G c^R}{2c^L + c^R}, \quad (5.89)$$

and

$$\bar{\phi}_2(x) = \frac{c^L}{c_1^G} (\bar{v}_L(l-x) - \bar{v}_R(l-x)) + \bar{v}_R(l+x). \quad (5.90)$$

Cable Cylinders Three and Four

The isolation condition has linked the two contributions that meet at the junction. When $x = l$ in ϕ_2 , they are reflected together using (5.84), as if from a cut terminal, contributing two linked components to ϕ_3 . The remaining component of ϕ_2 , on the right branch, again reaches an internal point at $x = l$, and again using (5.81) contributes two new components to ϕ_3 , one reflected and one transmitted. And so,

$$\begin{aligned} \phi_3(x) &= -\frac{c_2^G}{c_3^G} [\bar{v}_L(x) - \bar{v}_R(x)] \\ &\quad + \frac{1}{2} \left(1 - \frac{c_2^G}{c_3^G} \right) \bar{v}_R(2l-x) + \frac{1}{2} \left(1 + \frac{c_2^G}{c_3^G} \right) \bar{v}_R(2l+x). \end{aligned} \quad (5.91)$$

The more complicated isolation-termination rules developed in Chapter 6 could be brought into play here (they will produce an identical result), but we have to choose

$$c_3^G = \frac{c^R(c^R + 3c^L)}{c^R + 2c^L}, \quad (5.92)$$

anyway, if termination of the cable connected section (with a cut end) is to be forced at this stage, as was done when using the first-principles algorithm. Again, discussion of disconnected sections will be left until Chapter 6.

5.7 Discussion

The first-principles algorithm for cable construction in the Laplace domain generates equivalent cables effectively for simple structures of the type considered in the two examples. Tedious algebra makes the process generally impractical. Fortunately, the first-principles approach yields a much more efficient method for generating potential functions, i.e. the electrical continuity rules. These rules remove a whole layer of complexity in the construction process since they embody the algebraic manipulation used in the Laplace domain, and therefore allow us to bypass it altogether. However, the first-principles method does not directly indicate a general method, i.e. a set of rules, for determining cable cylinder c-values. It only suggests that they are evaluated by arranging some or all contributions to a potential function in a way that allows them to satisfy local cut or sealed boundary conditions. A key feature of these additional rules is that when two components meet at the origin, they must have coefficients of the same magnitude but opposite sign — this is the “isolation condition”, discussed in full in Chapter 6. The isolation condition is just one of the isolation–termination rules, whose dual function is to ensure that the isolation condition is always satisfied, and that termination is eventually guaranteed.

Chapter 6

The General Analytical Construction Rules

6.1 Introduction

In this chapter we derive a complete set of equivalent cable construction rules for the general Y-junction. The analytical method is an iterative two-stage process, and two distinct sets of construction rules are developed,

- *Electrical Continuity Rules:* These first stage rules generate a *framework potential function* for each cable cylinder. The framework potential function is a linear combination of tree cylinder potentials, with coefficients expressed in terms of tree and cable c-values. It guarantees voltage continuity and current conservation between equivalent cable cylinders, but in a manner that leaves their c-values undetermined. Cable cylinder lengths are found straightforwardly at this stage. These rules will at times also be called *reflection and transmission rules* — a reference to the way in which one cable cylinder potential is used to generate the next.
- *Isolation-Termination Rules:* These second stage rules ensure that, when transforming a Y-junction (or any sub-tree), the structure of its equivalent cable depends only on the local tree structure being transformed, i.e. any structure connected to the Y-junction (or sub-tree) does not influence the cable construction process. To achieve this, these rules *uniquely* determine equivalent cable c-values in terms of tree c-values; consequently the framework potential function becomes a uniquely defined *potential function*. The choice of c-value simultaneously guarantees that cable sections will eventually terminate with an appropriate boundary condition.

The rules are applied repeatedly, “ensuring continuity” then “preparing for termination”, one after the other, generating an equivalent cable cylinder and its associated

portion of the electrical mapping (its potential function) at each step, starting with the cylinder connected to the origin. The full electrical mapping between tree and cable is the complete set of cable cylinder potential functions (i.e. those that describe all connected and disconnected sections).

The electrical continuity rules follow directly from a generalised application of the first-principles approach introduced in Chapter 5. Consequently, this involves a consideration of tree cylinder potentials in the Laplace domain, so recall, from section 5.2, the form of the boundary conditions, the dimensionless cable equation, and its general solution in the Laplace domain. The resulting electrical continuity rules (which generate framework potential functions) are straightforwardly also valid in the physical (electrotonic) domain. Rules are given for relating potentials, current densities, and injected currents between a tree and its fully equivalent cable.

To derive the isolation–termination rules, we consider the conditions that must be satisfied if we insist that it must be possible to transform dendritic sub-trees in isolation from structure they are connected to. This consideration leads directly to the isolation condition, from which the full set of self-reinforcing isolation–termination rules will eventually follow.

As the isolation–termination rules are developed, there are hints that there may be an even deeper mathematical structure which is not revealed directly by the approach used.

6.2 Notation and Terminology for the General Y-junction

This section gives notation and terminology for describing the general Y-junctions and equivalent cables used to determine the general rules of cable construction.

6.2.1 Electrical and Physical Properties of Tree and Cable Cylinders Geometry

A general Y-junction is illustrated in Figure 6.1. It consists of a left branch (L), formed from m_L cylinders, and a right branch (R), formed from m_R cylinders. Each of the $(m_L + m_R)$ cylinders has electrotonic length l , so the total electrotonic length of the two branches is $(m_L + m_R)l$. As discussed in Chapter 3, l is an arbitrarily small quantum electrotonic length which allows for the required resolution of the model. Without loss of generality, we set $m_L \leq m_R$ — the left branch is always the shorter of the two, though of course the choice is immaterial when $m_L = m_R$.

The n^{th} cylinder (counting from origin to tip) of branch j has c-value c_n^j . The c-value sum, or *c-sum*, of cylinders n and $n+1$ (the two cylinders that meet at length nl from

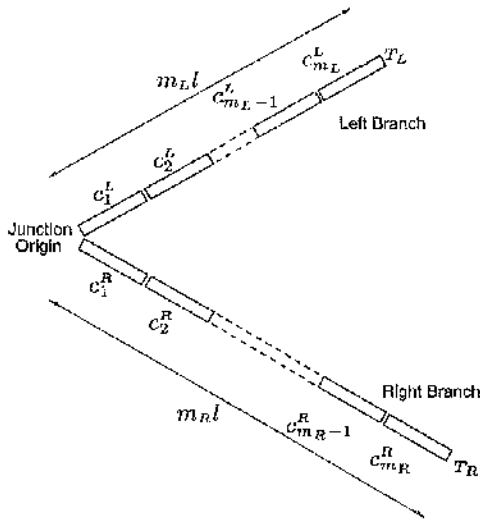


Figure 6.1: The general Y-junction. See text for details of notation.

the origin) on branch j is

$$c_{sn}^j = c_n^j + c_{n+1}^j. \quad (6.1)$$

Terminal Conditions

The left and right branch terminal boundary conditions are denoted T_L and T_R . Branch j (L or R) may terminate with either a current injection condition (generalised (S)ealed) or a (C)ut condition, represented, respectively

$$T_j=S \quad \text{and} \quad T_j=C. \quad (6.2)$$

Membrane Potentials and Voltage Continuity

The potential in the n^{th} cylinder of branch j is denoted

$$v_n^j(x, t), \quad 0 \leq x \leq l. \quad (6.3)$$

Since the potential is continuous, then

$$v_n^j(l, t) = v_{n+1}^j(0, t), \quad (6.4)$$

and at the junction,

$$v_1^R(0, t) = v_1^L(0, t). \quad (6.5)$$

It is sometimes useful to represent the potential in each branch by one function valid for the length of the branch. The potential in the left branch is

$$v_L(x, t), \quad 0 \leq x \leq m_L l, \quad (6.6)$$

and in the right branch,

$$v_R(x, t), \quad 0 \leq x \leq m_R l, \quad (6.7)$$

so that, at the origin, $x = 0$,

$$v_L(0, t) = v_R(0, t). \quad (6.8)$$

The whole-branch potential and individual cylinder potentials are related by

$$v_n^j(x, t) = v_j((n-1)l + x, t). \quad (6.9)$$

Axial Current and Current Conservation

The axial current in the n^{th} cylinder of branch j is denoted

$$i_{a,n}^j(x, t) = -K c_n^j \frac{\partial v_n^j(x, t)}{\partial x}. \quad (6.10)$$

Since current is conserved,

$$i_{a,n}^j(l, t) + i_{A,n}^j(t) = i_{a,n+1}^j(0, t), \quad (6.11)$$

where $i_{A,n}^j(t)$ is an external source injecting current at $x = nl$ along cylinder j . This may also be written as

$$c_n^j \frac{\partial v_n^j}{\partial x} \Big|_{x=l} - \frac{i_{A,n}^j(t)}{K} = c_{n+1}^j \frac{\partial v_{n+1}^j}{\partial x} \Big|_{x=0}, \quad (6.12)$$

or equivalently

$$c_n^j \frac{\partial v_j}{\partial x} \Big|_{x=(nl)^-} - \frac{i_{A,n}^j(t)}{K} = c_{n+1}^j \frac{\partial v_j}{\partial x} \Big|_{x=(nl)^+}, \quad (6.13)$$

where $(nl)^-$ denotes point nl approached from a point closer to the origin, and $(nl)^+$ denotes point nl approached from a point further from the junction.

Fully Equivalent Cables

As will become clear, the equivalent cable for the general Y-junction will also consist of $(m_L + m_R)$ cylinders, each of length l . The potential in the k^{th} cable cylinder is

$$\phi_k(x), \quad 0 \leq x \leq l, \quad (6.14)$$

while its c-value is denoted c_k^c . Axial current is denoted $i_{a,k}^c$.

All the time-dependent expressions above, for the electrotonic domain, have their Laplace transformed equivalents with s replacing t (though suppressed for most of this chapter); potentials and currents are replaced with their transformed (barred) quantities.

6.2.2 Framework Potentials and Uniquely Defined Potentials

The two stages of fully equivalent cable construction have the result that after the electrical continuity rules are applied, an intermediate expression for a cable cylinder's potential is obtained – it is expressed in terms of the corresponding cylinder's c-value, which has not actually been determined. The isolation–termination rules then determine the c-value and the potential is uniquely defined. Although both forms of the potential are written using the ϕ_k notation, the difference is always very clear.

6.2.3 Potential Function Components and Component Diagrams

Potential function components and component diagrams were introduced in Chapter 5. The potential function for a cable cylinder, k (with length l) is a linear combinations of tree potentials. A *component* of a cable potential function is a weighted tree potential, valid over a specific range of a tree cylinder. The following properties can be associated with a component:

1. A *coefficient*, or *weight*, indicating the significance of the contribution this component makes to the potential function. The relative significance of components can be measured by comparing their coefficients.
2. A *source point*, which is the position on the tree associated with the component when $x = 0$ on the cable cylinder.
3. A *destination point*, or *end point*, which is the position on the tree associated with the component when $x = l$ on the cable cylinder.
4. A *direction*, which is determined by relative positions of source and destination points. A component is an *inward component* when the destination is closer to the junction than the source; a component is an *outward component* when the destination is further from the junction than the source.
5. A *length*, which is the range of validity of the component, i.e. the distance from source to destination. All components of the same potential function necessarily have the same length.

There is in fact a great deal of structure (determined primarily by the electrical continuity rules) to the components of a potential function. Components never overlap, and often many source or destination points are common to pairs of components.

For the specific case where all cylinders are of the same length, l , (as in the representation used for the general Y-junction), components exhibit a simple structure and will

have either the form

$$wv_n^j(x), \quad (6.15)$$

or

$$wv_n^j(l - x), \quad (6.16)$$

where w is the weight. The first form is the outward component since as x increases along the cable cylinder, $v_n^j(x)$ represents the potential moving outwards away from the junction. The second form is the inward component since as x increases, $v_n^j(l - x)$ represents the potential moving inwards towards the junction.

Component diagrams will be used extensively to illustrate the nature of the general analytical construction procedure.

6.3 The Electrical Continuity Rules

Although we shall eventually specialise to the binary Y-junction, we consider initially a general junction point, where an arbitrary number of cylinders meet, as illustrated in Figure 6.2.

The rules, which will relate transmembrane potential, electrotonic current density, and applied currents between a tree and its fully equivalent cable are derived by considering the effect the generator equation,

$$\bar{v}(x) = \bar{v}_J \cosh \omega x - \frac{i_J}{K\omega c} \sinh \omega x + \frac{1}{\omega} \int_0^x f(y) \sinh \omega(x - y) dy, \quad (6.17)$$

(which we restate here for convenience) has on a single component that ends on the branch point.

6.3.1 Derivation of General Reflection–Transmission Rules

At a branch point, suppose there are $n + 1$ cylinders of interest, that is, one *primary* cylinder (numbered “0”) that connects to n *secondary* cylinders (numbered “1” to “n”), each of length l . For convenience, the direction of x in the cylinders is specified as follows: in each of the secondary cylinders, x increases away from the junction, and point $x = 0$ marks the junction; for the primary cylinder, x increases towards the junction and $x = l$ marks the location of the junction. (Note that the primary cylinder need not be a parent cylinder, though conventions for current flow differ from those specified in Chapter 2, and used until now, when this is not the case. This does not matter, as long as voltage continuity holds and the current conservation condition is correctly specified.)

Denote the potential in cylinder j by $\bar{v}_j(x)$, and the potential at the junction by \bar{v}_J , so that

$$\bar{v}_J = \bar{v}_0(l) = \bar{v}_j(0), \quad (6.18)$$

for any secondary cylinder $1 \leq j \leq n$. Denote the axial current in cylinder j by $\bar{i}_{a,j}(x)$. Taking account of the above conventions for the direction of current flow, current conservation demands that,

$$\bar{i}_{a,0}(l) + \bar{i}_T = \sum_{j=1}^n \bar{i}_{a,j}(0), \quad (6.19)$$

where \bar{i}_T represents a point current source at the junction.

From equation (6.17), the potential in the primary cylinder, valid for $0 \leq x \leq l$, is

$$\bar{v}_0(x) = \bar{v}_J \cosh \omega(l-x) + \frac{\bar{i}_{a,0}(l)}{Kw c_0} \sinh \omega(l-x) + \frac{1}{\omega} \int_l^x \bar{f}_0(y) \sinh \omega(l-x-y) dy. \quad (6.20)$$

The potential in secondary cylinder j , also valid for $0 \leq x \leq l$, is

$$v_j(x) = \bar{v}_J \cosh \omega x - \frac{\bar{i}_{a,j}(0)}{Kw c_j} \sinh \omega x + \frac{1}{\omega} \int_0^x \bar{f}_j(y) \sinh \omega(x-y) dy. \quad (6.21)$$

Now, suppose the k^{th} equivalent cable cylinder has been constructed. It has length l and c-value c_k^C . Suppose also that cylinder k 's potential function, a linear combination of tree cylinder potentials, is known, and assume that a component is contributed by the primary cylinder, so the potential function can be written

$$\bar{\phi}_k(x) = \Gamma \bar{v}_0(x) + \dots, \quad (6.22)$$

where Γ is the component coefficient and the dots simply indicate the remaining components of the potential function. The axial current in cable cylinder k is

$$\bar{i}_{a,k}^C(x) = -Kc_k^C \frac{\partial \bar{\phi}_k(x)}{\partial x} = -K\Gamma c_k^C \frac{\partial \bar{v}_0(x)}{\partial x} + \dots, \quad (6.23)$$

where, again, the dots indicate the contribution from all other components of cable potential function k . Current conservation between cable cylinders k and $k+1$ requires that

$$\bar{i}_{a,k}^C(l) + \bar{i}_C = \bar{i}_{a,k+1}^C(0), \quad (6.24)$$

where \bar{i}_C is a current source injecting into the point where the two cylinders meet.

At the distal end of cable cylinder k ,

$$\bar{\phi}_k(l) = \Gamma \bar{v}_J + \dots, \quad (6.25)$$

and

$$\bar{i}_{a,k}^C(l) = -\Gamma K c_k^C \frac{\partial \bar{v}_0(l)}{\partial x} + \dots = \Gamma \frac{c_k^C}{c_0^C} \left[-K c_0^C \frac{\partial \bar{v}_0(l)}{\partial x} \right] + \dots = \Gamma \frac{c_k^C}{c_0^C} \bar{i}_{a,0}(l) + \dots. \quad (6.26)$$

Expressions for the potential and axial current at $x = l$ on cable cylinder k have been obtained. Now take advantage of voltage continuity and current conservation where cable

cylinders k and $k+1$ meet. It is possible to use the generator equation (6.17) to write down an expression for the potential function in cable cylinder $k+1$,

$$\phi_{k+1}(x) = \phi_k(l) \cosh \omega x - \frac{\bar{i}_{a,k}^*(l) + \bar{i}_C}{Kw c_{k+1}^G} \sinh \omega x + \frac{1}{\omega} \int_0^x \bar{f}_{k+1}(y) \sinh \omega(x-y) dy, \quad (6.27)$$

which can be expanded using equations (6.25) and (6.26),

$$\begin{aligned} \bar{\phi}_{k+1}(x) &= \Gamma \left[\bar{v}_J \cosh \omega x - \frac{c_k^G}{c_{k+1}^G} \frac{\bar{i}_{a,0}(l)}{Kw c_0} \sinh \omega x - \frac{\bar{i}_C^*}{Kw c_{k+1}^G} \sinh \omega x \right. \\ &\quad \left. + \frac{1}{\omega} \int_0^x \bar{f}_{k+1}^*(y) \sinh \omega(x-y) dy \right] + \dots, \end{aligned} \quad (6.28)$$

where \bar{f}_{k+1}^* is the portion of the input current density term contributed to the cable cylinder $k+1$ on application of the generator equation to component $v_0(x)$. Also, \bar{i}_C^* is the portion of i_C injected into the cable diameter step due to the current injected at the general junction point. The dots in this expression represent the contributions due to other components in $\bar{\phi}_k$.

For the moment we are only interested in how the generator equation affects the component contributed by the primary cylinder, so, without loss of generality (because of linearity) ignore the coefficient Γ , and just consider the term

$$\begin{aligned} \bar{\phi}_{k+1}^*(x) &= \bar{v}_J \cosh \omega x - \frac{c_k^G}{c_{k+1}^G} \frac{\bar{i}_{a,0}(l)}{Kw c_0} \sinh \omega x - \frac{\bar{i}_C^*}{Kw c_{k+1}^G} \sinh \omega x \\ &\quad + \frac{1}{\omega} \int_0^x \bar{f}_{k+1}^*(y) \sinh \omega(x-y) dy, \end{aligned} \quad (6.29)$$

which is obtained by just applying the generator equation to initial component

$$\bar{\phi}_k^* = \bar{v}_0(x). \quad (6.30)$$

With a little algebraic effort, equation (6.29) can be rewritten as a linear combination of the potentials in the primary and secondary cylinders. Introduce into the right hand side of equation (6.29) several new terms whose sum is zero, like so

$$\begin{aligned} \bar{\phi}_{k+1}^*(x) &= \frac{\sum_{j=0}^n c_j}{\sum_{j=0}^n c_j} \bar{v}_J \cosh \omega x - \frac{c_k^G}{c_{k+1}^G} \frac{\bar{i}_{a,0}(l)}{Kw c_0} \sinh \omega x - \frac{\bar{i}_C^*}{Kw c_{k+1}^G} \sinh \omega x \\ &\quad + \left[\frac{c_k^G}{c_{k+1}^G} \frac{\sum_{j=1}^n c_j \bar{i}_{a,0}(l) \sinh \omega x}{\sum_{j=0}^n c_j Kw c_0} - \frac{c_k^G}{c_{k+1}^G} \frac{\sum_{j=1}^n c_j \bar{i}_{a,0}(l) \sinh \omega x}{\sum_{j=0}^n c_j Kw c_0} \right] \\ &\quad + \frac{\sinh \omega x}{Kw \sum_{j=0}^n c_j} \left(\bar{i}_{a,0}(l) + \bar{i}_T - \sum_{r=1}^n \bar{i}_{a,r}(0) \right) \\ &\quad + \left[\frac{c_k^G}{c_{k+1}^G} \sum_{r=1}^n \left(\frac{c_r}{\sum_{j=0}^n c_j} \bar{v}_J \cosh \omega x \right) - \frac{c_k^G}{c_{k+1}^G} \sum_{r=1}^n \left(\frac{c_r}{\sum_{j=0}^n c_j} \bar{v}_J \cosh \omega x \right) \right] \\ &\quad + \frac{1}{\omega} \int_0^x \bar{f}_{k+1}^*(y) \sinh \omega(x-y) dy. \end{aligned} \quad (6.31)$$

The hyperbolic sine and cosine terms can be collected together into the following form,

$$\begin{aligned}
\bar{\phi}_{k+1}^*(x) = & \frac{c_0}{\sum_{j=0}^n c_j} \left(1 - \frac{c_k^G \sum_{j=1}^n c_j}{c_{k+1}^G c_0} \right) \bar{v}_J \cosh \omega x + \sum_{r=1}^n \frac{c_r}{\sum_{j=0}^n c_j} \left(1 + \frac{c_k^G}{c_{k+1}^G} \right) \bar{v}_J \cosh \omega x \\
& + \frac{c_0}{\sum_{j=0}^n c_j} \left(1 - \frac{c_k^G \sum_{j=1}^n c_j}{c_{k+1}^G c_0} \right) \frac{\bar{i}_{a,0}(l) \sinh \omega x}{K \omega c_0} \\
& - \frac{c_k^G \bar{i}_{a,0}(l) \sinh \omega x}{c_{k+1}^G K \omega c_0} \left(1 - \frac{\sum_{j=1}^n c_j}{\sum_{j=0}^n c_j} \right) - \sum_{r=1}^n \frac{\bar{i}_{a,r}(0) \sinh \omega x}{K \omega \sum_{j=0}^n c_j} \\
& + \left[\frac{\bar{i}_T}{\sum_{j=0}^n c_j} - \frac{\bar{i}_C^*}{c_{k+1}^G} \right] \frac{\sinh \omega x}{K \omega} \\
& + \frac{1}{\omega} \int_0^x \bar{f}_{k+1}^*(y) \sinh \omega(x-y) dy. \tag{6.32}
\end{aligned}$$

The final form is starting to emerge. Once more using current conservation at the tree junction, as well as

$$1 - \frac{\sum_{j=1}^n c_j}{\sum_{j=0}^n c_j} = \frac{c_0}{\sum_{j=0}^n c_j}, \tag{6.33}$$

equation (6.32) can be rearranged to give

$$\begin{aligned}
\bar{\phi}_{k+1}^*(x) = & \frac{c_0}{\sum_{j=0}^n c_j} \left(1 - \frac{c_k^G \sum_{j=1}^n c_j}{c_{k+1}^G c_0} \right) \left[\bar{v}_J \cosh \omega x + \frac{\bar{i}_{a,0}(l) \sinh \omega x}{K \omega c_0} \right] \\
& + \sum_{r=1}^n \frac{c_r}{\sum_{j=0}^n c_j} \left(1 + \frac{c_k^G}{c_{k+1}^G} \right) \left[\bar{v}_J \cosh \omega x - \frac{\bar{i}_{a,r}(0) \sinh \omega x}{K \omega c_r} \right] \\
& + \left[\frac{\bar{i}_T}{\sum_{j=0}^n c_j} + \frac{c_k^G \bar{i}_T}{c_{k+1}^G \sum_{j=0}^n c_j} - \frac{\bar{i}_C^*}{c_{k+1}^G} \right] \frac{\sinh \omega x}{K \omega} \\
& + \frac{1}{\omega} \int_0^x \bar{f}_{k+1}^*(y) \sinh \omega(x-y) dy. \tag{6.34}
\end{aligned}$$

Now, carefully organise the electrotonic current densities by choosing

$$\bar{f}_{k+1}^*(x) = \frac{c_0}{\sum_{j=0}^n c_j} \left(1 - \frac{c_k^G \sum_{j=1}^n c_j}{c_{k+1}^G c_0} \right) \bar{f}_0(l-x) + \sum_{r=1}^n \frac{c_r}{\sum_{j=0}^n c_j} \left(1 + \frac{c_k^G}{c_{k+1}^G} \right) \bar{f}_r(x). \tag{6.35}$$

Then, zero the contribution due to applied current terms by setting

$$\left[\frac{\bar{i}_T}{\sum_{j=0}^n c_j} + \frac{c_k^G \bar{i}_T}{c_{k+1}^G \sum_{j=0}^n c_j} - \frac{\bar{i}_C^*}{c_{k+1}^G} \right] = 0. \tag{6.36}$$

This may be rewritten

$$\bar{i}_C^* = \bar{i}_T \left[\frac{c_k^G + c_{k+1}^G}{\sum_{j=0}^n c_j} \right]. \tag{6.37}$$

These choices allow the potential in cable cylinder $k + 1$ to be written as a linear combination of the potentials in the cylinders that meet at the junction,

$$\bar{\phi}_{k+1}^*(x) = \frac{c_0}{\sum_{j=0}^n c_j} \left(1 - \frac{c_k^C}{c_{k+1}^C} \frac{\sum_{j=1}^n c_j}{c_0} \right) \bar{v}_0(l-x) + \sum_{r=1}^n \frac{c_r}{\sum_{j=0}^n c_j} \left(1 + \frac{c_k^C}{c_{k+1}^C} \right) \bar{v}_r(x). \quad (6.38)$$

The relationships (6.35), (6.37), and (6.38), must also be valid for the original untransformed potentials and applied currents, so we can now summarise the general electrical continuity rules.

The Electrical Continuity Rules — A. The Membrane Potential

Simply taking the inverse Laplace transform of equation (6.38) gives

$$\phi_{k+1}^*(x, t) = \frac{c_0}{\sum_{j=0}^n c_j} \left(1 - \frac{c_k^C}{c_{k+1}^C} \frac{\sum_{j=1}^n c_j}{c_0} \right) v_0(l-x, t) + \sum_{r=1}^n \frac{c_r}{\sum_{j=0}^n c_j} \left(1 + \frac{c_k^C}{c_{k+1}^C} \right) v_r(x, t). \quad (6.39)$$

Expression (6.39) encapsulates the electrical continuity rules entirely. It basically says that, if a tree cylinder, j say, contributes a component $v_j(x)$ to cable cylinder k 's potential function, then, on application of the generator equation, this component introduces a number of components in cable cylinder $(k+1)$'s potential function. The number of new components will depend on the tree structure at point $x = l$ on cylinder j . It should be clear now why these rules may also be referred to as reflection and transmission rules: if there are $n + 1$ paths away from component v_j 's destination, then equation (6.39) generates $n + 1$ terms in the new potential function. A single component may be *reflected* from the junction back down the primary cylinder (its direction is opposite to that of the original component), while all other components are *transmitted* along all the connecting cylinders (their directions are the same as that of the original component). Of all the new components, only the single reflected one can possibly be zero, in which case there is a total of n new components, all transmitted.

Figure 6.2 shows a component diagram illustrating the original component in ϕ_k and those it generates in ϕ_{k+1} , for both the general and the zero-reflection situation. Note that if multiple components of cable potential ϕ_k have the same destination, they must each generate contributions to the same components in potential ϕ_{k+1} . It is also possible that multiple contributions to the same new component may cancel.

The Electrical Continuity Rules — B. Electrotonic Current Density

Consider equation (6.35), in conjunction with the expression for \bar{f} (5.9). Since the initial potential distribution in the cable is related to that in the tree by the potential mapping,

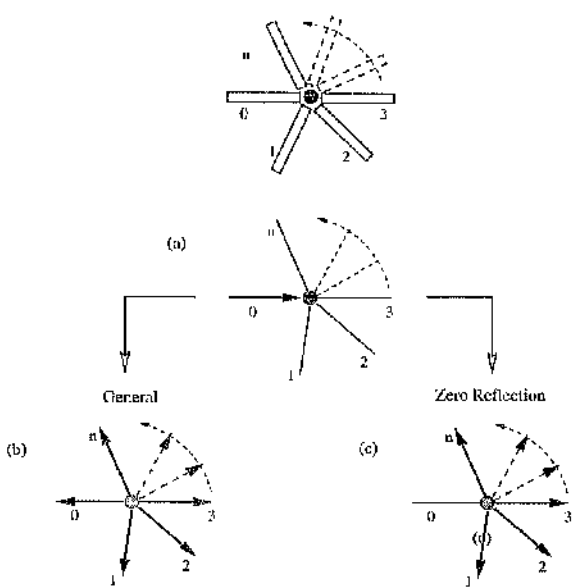


Figure 6.2: Component diagrams illustrating the electrical continuity rules at the general branch point, where $n + 1$ cylinders meet. (a) A single component of potential function k is directed towards the branch point. (b) In general, this single component generates $n + 1$ components in potential function $k + 1$. Each component emanates from the branch point. There are n transmitted components, on cylinders 1 to n , plus one reflected component on cylinder 0. (c) Under certain conditions, there is no reflected component, so just n transmitted components are generated.

we can use the electrical continuity rules for potentials (6.39) to give (after taking the inverse Laplace transform)

$$\frac{i_{k+1}^*(x, t)}{c_{k+1}^C} = \frac{c_0}{\sum_{j=0}^n c_j} \left(1 - \frac{c_k^C \sum_{j=1}^n c_j}{c_{k+1}^C c_0} \right) \frac{i_0(l-x, t)}{c_0} + \sum_{r=1}^n \frac{c_r}{\sum_{j=0}^n c_j} \left(1 + \frac{c_k^C}{c_{k+1}^C} \right) \frac{i_r(x, t)}{c_r}. \quad (6.40)$$

and so

$$i_{k+1}^*(x, t) = \frac{1}{\sum_{j=0}^n c_j} \left[\left(c_{k+1}^C - \frac{c_k^C \sum_{j=1}^n c_j}{c_0} \right) i_0(l-x, t) + (c_{k+1}^C + c_k^C) \sum_{r=1}^n i_r(x, t) \right], \quad (6.41)$$

which defines the relationship between current densities on tree and cable.

The Electrical Continuity Rules — C. Applied Current Sources

Taking the inverse Laplace transform of equation (6.37) gives the relationship between applied current sources on the tree and those on the equivalent cable,

$$i_C^*(t) = i_T(t) \left[\frac{c_k^C + c_{k+1}^C}{\sum_{j=0}^n c_j} \right] \quad (6.42)$$

The contribution to applied current at the cable discontinuity is thus equal to the current injected at the branch point multiplied by the ratio of cable c-sum to tree branch point c-sum.

The Use of Laplace Transforms

We have seen how powerful the Laplace approach has been. By considering general solutions of the Laplace transformed cable equation, we have formed a set of reflection-transmission rules that are valid for solutions of the untransformed cable equation. Now that these rules have been developed, we can return to, and remain in, the physical (electrotonic) domain.

6.3.2 General Observations Concerning the Electrical Continuity Rules

For convenience, from now on the time-dependence in expressions for potentials and currents will be suppressed. We write

$$v(x) = v(x, t), \quad i_a(x) = i_a(x, t), \quad \text{and} \quad i(x) = i(x, t). \quad (6.43)$$

Voltage Continuity and Current Conservation

Voltage continuity and current conservation have been guaranteed between a component of cable cylinder k and those it generates in cylinder $k+1$, without the need to specify

c_{k+1}^C , thus

$$v_0(l) = \phi_{k+1}^*(0), \quad (6.44)$$

and

$$c_k^C \frac{\partial v_0(l)}{\partial x} - \frac{i_C^*}{K} = c_{k+1}^C \frac{\partial \phi_{k+1}^*(0)}{\partial x}. \quad (6.45)$$

Since this will be true for all components that contribute to potential function ϕ_k , it must hold that

$$\phi_k(l) = \phi_{k+1}(0), \quad (6.46)$$

and also,

$$c_k^C \frac{\partial \phi_k(l)}{\partial x} - \frac{i_C}{K} = c_{k+1}^C \frac{\partial \phi_{k+1}(0)}{\partial x}. \quad (6.47)$$

Coefficient Conservation in a Potential Function

Significantly, the sum of the coefficients of the components in ϕ_{k+1}^* (6.39) is equal to the coefficient of the single component in ϕ_k^* , i.e. one,

$$\frac{c_0}{\sum_{j=0}^n c_j} \left(1 - \frac{c_k^C}{c_{k+1}^C} \frac{\sum_{j=1}^n c_j}{c_0} \right) + \sum_{r=1}^n \frac{c_r}{\sum_{j=0}^n c_j} \left(1 + \frac{c_k^C}{c_{k+1}^C} \right) = 1. \quad (6.48)$$

Again, this result is independent of cable c -values. We refer to this condition as *conservation of coefficients*. It is always valid, except for reflection from a cut end, as will be seen. (This result is particularly significant for trees with all terminals sealed¹.)

Zero Reflected Component

Note that the reflected component in equation (6.39) has zero magnitude when

$$\frac{c_k^C}{c_{k+1}^C} = \frac{c_0}{\sum_{j=1}^n c_j}. \quad (6.49)$$

Figure 6.2c illustrates the component diagram in this case.

The Relationship Between Applied Currents and Electrotonic Current Density

Consider the situation in equation (6.42) when applied current is injected at an internal point of a cylinder, and mapped to an internal point of a cable cylinder so that $c_k^C = c_{k+1}^C$, $n = 1$ and $c_0 = c_1$. The relationship (6.42) between i_C and i_T may then be expressed

$$\frac{i_C^*}{c_k^C} = \frac{i_T^*}{c_0}. \quad (6.50)$$

¹As noted in Chapter 4 regarding cable matrix eigenvectors.

From the relationship between electrotonic current densities (6.41), under the same conditions we obtain

$$\frac{i_k^*(x)}{c_k^C} = \frac{i_0(x)}{c_0}. \quad (6.51)$$

Clearly, the mapping between internal points of tree cylinder and cable cylinder is identical for applied currents and electrotonic current density. However, they will not be identical when mapping from a point of discontinuity. The current densities are not strictly valid at these points (the boundary conditions describe electrical activity at the boundaries), however they can be given a useful interpretation.

Suppose that a current injected at a branch point can be regarded as divided among the connecting cylinders. A portion of the current is injected into each, though the injecting point is still the branch point. This is simply a useful abstraction. We introduce the quantity i_{ST} , where

$$i_{ST} = i_0(l) + \sum_{r=1}^n i_r(0). \quad (6.52)$$

The individual current densities are then expressed

$$i_0(l) = \frac{c_0 i_{ST}}{\sum_{j=0}^n c_j} \quad \text{and} \quad i_r(0) = \frac{c_r i_{ST}}{\sum_{j=0}^n c_j}, \quad (6.53)$$

so the portion of current associated with a cylinder is determined by its c-value.

Now, from equation (6.41), observe that, if $x = 0$ marks a diameter step on cable cylinder $k+1$,

$$\begin{aligned} i_{k+1}^*(0) &= \frac{c_0}{\sum_{j=0}^n c_j} \left(c_{k+1}^C - \frac{c_k^C \sum_{j=1}^n c_j}{c_0} \right) \frac{i_0(l)}{c_0} + \sum_{r=1}^n \frac{c_r}{\sum_{j=0}^n c_j} (c_{k+1}^C + c_k^C) \frac{i_r(0)}{c_r} \\ &= \frac{c_0}{\sum_{j=0}^n c_j} \left(c_{k+1}^C - \frac{c_k^C \sum_{j=1}^n c_j}{c_0} \right) \frac{i_{ST}}{\sum_{j=0}^n c_j} + \frac{\sum_{j=1}^n c_j}{\sum_{j=0}^n c_j} (c_{k+1}^C + c_k^C) \frac{i_{ST}}{\sum_{j=0}^n c_j} \\ &= i_{ST} \frac{c_{k+1}^C}{\sum_{j=0}^n c_j}. \end{aligned} \quad (6.54)$$

We introduce the quantity i_{SC} , where

$$i_{SC} = i_k^*(l) + i_{k+1}^*(0). \quad (6.55)$$

Now, summing the two cable contributions given by equations (6.51) and (6.54) gives

$$i_{SC} = i_{ST} \left[\frac{c_k^C + c_{k+1}^C}{\sum_{j=0}^n c_j} \right] \quad (6.56)$$

In conclusion, the sum of the contributions to the current density at a point are mapped between cable and tree in the same way as the actual applied currents at the point.

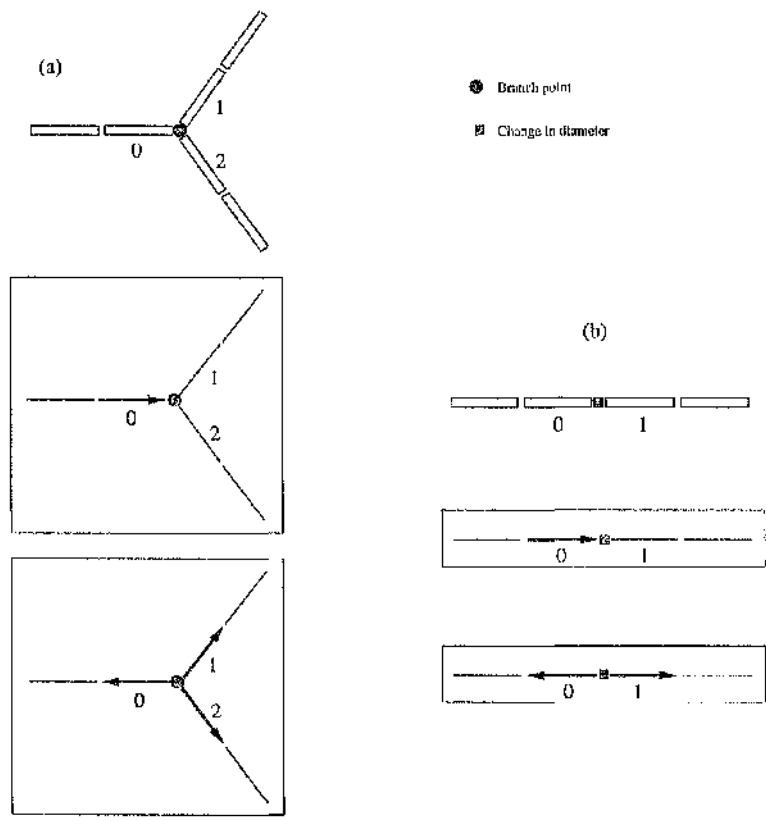


Figure 6.3: Reflection and Transmission at (a) binary branch point and (b) diameter step. The electrical continuity rules generate components directed along all paths away from the point of discontinuity. It is possible that the reflected component (that directed away from the discontinuity along cylinder 0) in each case has zero coefficient.

6.3.3 Reflection and Transmission at Specific Geometrical Structure

Reflection and Transmission at a Binary Branch Point

If, as in Figure 6.3a, $x = l$ marks a binary branch point where the primary cylinder ("0") meets two secondary cylinders ("1" and "2"), then

$$\begin{aligned}\phi_{k+1}^*(x) &= \frac{c_0}{(c_0 + c_1 + c_2)} \left(1 - \frac{c_k^C}{c_{k+1}^C} \frac{(c_1 + c_2)}{c_0} \right) v_0(l - x) \\ &\quad + \frac{c_1}{(c_0 + c_1 + c_2)} \left(1 + \frac{c_k^C}{c_{k+1}^C} \right) v_1(x) \\ &\quad + \frac{c_2}{(c_0 + c_1 + c_2)} \left(1 + \frac{c_k^C}{c_{k+1}^C} \right) v_2(x).\end{aligned}\quad (6.57)$$

Reflection and Transmission at a Diameter Step

In Figure 6.3b, $x = l$ marks a point where the primary cylinder ("0") meets a single secondary cylinder ("1"), so

$$\phi_{k+1}^*(x) = \frac{c_0}{(c_0 + c_1)} \left(1 - \frac{c_k^C}{c_{k+1}^C} \frac{c_1}{c_0} \right) v_0(l - x) + \frac{c_1}{(c_0 + c_1)} \left(1 + \frac{c_k^C}{c_{k+1}^C} \right) v_1(x). \quad (6.58)$$

Reflection and Transmission at an Interior Point of a Cylinder

If $x = l$ marks an interior point of the primary cylinder ("0") then $c_0 = c_1$ in equation (6.58) and

$$\phi_{k+1}^*(x) = \frac{1}{2} \left(1 - \frac{c_k^C}{c_{k+1}^C} \right) v_0(l - x) + \frac{1}{2} \left(1 + \frac{c_k^C}{c_{k+1}^C} \right) v_0(l + x). \quad (6.59)$$

Another interesting result occurs when $c_0 = \sum_{j=1}^n c_j$ in the general equation (6.39), so that

$$\phi_{k+1}^*(x) = \frac{1}{2} \left(1 - \frac{c_k^C}{c_{k+1}^C} \right) v_0(l - x) + \sum_{j=1}^n \frac{c_j}{2c_0} \left(1 + \frac{c_k^C}{c_{k+1}^C} \right) v_j(x). \quad (6.60)$$

The reflected component behaves as if the primary branch is uniformly extended at the branch point. This condition is essentially Rall's 3/2 power law for impedance matching.

Reflection at Terminals

At terminals subject to current injection or cut conditions, there are no secondary cylinders, and so no transmitted components.

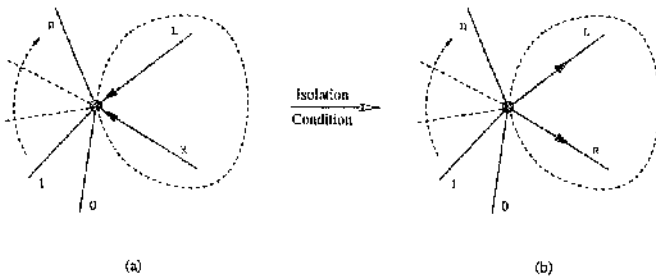


Figure 6.4: Component diagram illustrating reflection of origin bound components in a Y-junction, provided the isolation condition holds. No components are transmitted into structure connected to the Y-junction.

Consider the diameter step, equation (6.58), and let $c_1 = 0$ to obtain the reflection rule for a current condition.

$$\phi_{k+1}^*(x) = v_0(l - x). \quad (6.61)$$

Thus the reflected component retains the same coefficient.

Let $c_1 \rightarrow \infty$ in (6.58) to obtain the reflection rule for a cut end condition,

$$\phi_{k+1}^*(x) = -\frac{c_k^C}{c_{k+1}^C} v_0(l - x). \quad (6.62)$$

(These rules are easily checked by applying the generator equation directly to a component that reaches a cut terminal at $x = l$.) Clearly coefficient conservation is violated in this situation.

Here, it becomes clear why non-zero voltage conditions are generally invalid for equivalent cable construction — the assumption of voltage continuity between cable cylinders would be broken, i.e.,

$$\phi_{k+1}^*(0) \neq -\frac{c_k^C}{c_{k+1}^C} v_0(l) \quad \text{unless} \quad \phi_{k+1}^*(0) = v_0(l) = 0. \quad (6.63)$$

Reflection at a Local Origin — The Isolation Condition

Consider the situation in which a single Y-junction is being transformed. The junction point has been chosen as a local origin. Denote the two branches L (left) and R (right).

Suppose the potential function for cable cylinder k , of length l , contains two components, one from each tree branch, directed towards the origin, and both with the origin as destination, so

$$\phi_k = p v_L(l - x) + q v_R(l - x) + \dots, \quad 0 \leq x \leq l, \quad (6.64)$$

where p and q are constant coefficients. A number of other cylinders, numbered "0" to "n" may be connected to the origin, but are not part of the Y-junction that we wish to

transform. Only the left and right branches contribute additional components, represented in this equation by the dots. (for convenience, just assume x increases away from the junction for all cylinders, and $x = 0$ marks the junction) Applying the reflection/transmission rules (6.39) to each component yields

$$\begin{aligned}\phi_{k+1}(x) = & p \left[\frac{c_L}{(c_R + c_L + \sum_{j=0}^n c_j)} \left(1 - \frac{c_k^C}{c_{k+1}^C} \frac{(c_R + \sum_{j=0}^n c_j)}{c_L} \right) v_L(x) \right. \\ & + \frac{c_R}{(c_R + c_L + \sum_{j=0}^n c_j)} \left(1 + \frac{c_k^C}{c_{k+1}^C} \right) v_R(x) \\ & + \sum_0^n \frac{c_i}{(c_R + c_L + \sum_{j=0}^n c_j)} \left(1 + \frac{c_k^C}{c_{k+1}^C} \right) v_i(x) \Big] \\ & + q \left[\frac{c_R}{(c_R + c_L + \sum_{j=0}^n c_j)} \left(1 - \frac{c_k^C}{c_{k+1}^C} \frac{(c_L + \sum_{j=0}^n c_j)}{c_R} \right) v_R(x) \right. \\ & + \frac{c_L}{(c_R + c_L + \sum_{j=0}^n c_j)} \left(1 + \frac{c_k^C}{c_{k+1}^C} \right) v_L(x) \\ & \left. \left. + \sum_0^n \frac{c_i}{(c_R + c_L + \sum_{j=0}^n c_j)} \left(1 + \frac{c_k^C}{c_{k+1}^C} \right) v_i(x) \right] + \dots \quad (6.65)\right.\end{aligned}$$

This can be rearranged into a more illuminating form,

$$\begin{aligned}\phi_{k+1}(x) = & (p+q) \left[\sum_0^n \frac{c_i}{(c_R + c_L + \sum_{j=0}^n c_j)} \left(1 + \frac{c_k^C}{c_{k+1}^C} \right) v_i(x) + \frac{c_L v_L(x) + c_R v_R(x)}{(c_R + c_L + \sum_{j=0}^n c_j)} \right] \\ & - \frac{c_k^C}{c_{k+1}^C} \left[\frac{p(c_R + \sum_{j=0}^n c_j) - qc_L}{(c_R + c_L + \sum_{j=0}^n c_j)} v_L(x) + \frac{q(c_L + \sum_{j=0}^n c_j) - pc_R}{(c_R + c_L + \sum_{j=0}^n c_j)} v_R(x) \right] + \dots \quad (6.66)\end{aligned}$$

If no restrictions are imposed on the values of p and q , then the equivalent cable potentials depend, in general, on structure connected to the Y-junction. If, however, we can guarantee that

$$p + q = 0, \quad (6.67)$$

then equation (6.64) becomes

$$\phi_k = p(v_L(x) - v_R(x)) + \dots \quad (6.68)$$

and equation (6.66) simplifies substantially to

$$\phi_{k+1}(x) = -\frac{c_k^C}{c_{k+1}^C} p(v_L(x) - v_R(x)) + \dots \quad (6.69)$$

To understand the appearance of the reflection coefficient in equation (6.69), note that voltage continuity at the junction (origin) ensures that components of the form

$$\xi(x) = v_L(l-x) - v_R(l-x) \quad (6.70)$$

behave as if $x = l$ is a cut end, since

$$\xi(l) = 0. \quad (6.71)$$

It is significant that coefficient conservation still holds, unlike when a single component reflects from a real cut terminal.

To guarantee that Y-junctions or any sub-tree may be transformed in isolation from the rest of the tree, we must ensure that components contributed by tree cylinders that meet at the origin are always equal in magnitude and opposite in sign, i.e. their sum is zero. This requirement will subsequently be referred to as the *isolation condition*, and is a critical link between the electrical continuity rules and the isolation-termination rules, which follow from the need to maintain this condition in all cable potential functions. Figure 6.4 illustrates reflection of components from the local origin when the isolation condition holds.

6.3.4 Electrical Continuity Rules in the General Y-junction

Initialisation of the Construction Procedure

Enough information is now available to generate the framework potential function for a cable cylinder, given the potential function for the prior cylinder. The process must be initialised with the potential function for the cylinder connected to the origin. The initial cable potential function, $\phi_1(x)$, is essentially the same for any Y-junction --- the simple Rall combination of the left and right cylinders connected at the origin junction,

$$\phi_1(x) = \frac{c_1^L}{c_1^L + c_1^R} v_L(x) + \frac{c_1^R}{c_1^L + c_1^R} v_R(x). \quad (6.72)$$

The Rall-like c-value is

$$c_1^G = c_1^L + c_1^R. \quad (6.73)$$

Components

Only a limited subset of the full range of possible electrical continuity rules need be considered: reflection and transmission at a diameter step, reflection at cut terminals, reflection at current terminals, and reflection at the origin (junction) when the isolation condition holds.

Since all tree cylinders have length l , all components, and consequently all cable cylinders, will have length l . This is an inevitable consequence of the electrical continuity rules, which need only be applied where cylinders connect (and not internally).

The notation “ \rightarrow ” is used to indicate the contribution a component (with unit coefficient) of equivalent cable cylinder k makes, when the electrical continuity rules are applied at $x = l$, to generate the framework potential for cable cylinder $k + 1$.

For the general Y-junction, components can be directed away from the origin (branch point), in which case,

$$v_n^j(x) \rightarrow \frac{c_n^j}{c_{sn}^j} \left(1 - \frac{c_k^C}{c_{k+1}^C} \frac{c_{n+1}^j}{c_n^j} \right) v_n^j(l-x) + \frac{c_{n+1}^j}{c_{sn}^j} \left(1 + \frac{c_k^C}{c_{k+1}^C} \right) v_{n+1}^j(x). \quad (6.74)$$

They may also be directed towards the origin,

$$v_{n+1}^j(l-x) \rightarrow \frac{c_n^j}{c_{sn}^j} \left(1 + \frac{c_k^C}{c_{k+1}^C} \right) v_n^j(l-x) + \frac{c_{n+1}^j}{c_{sn}^j} \left(1 - \frac{c_k^C}{c_{k+1}^C} \frac{c_n^j}{c_{n+1}^j} \right) v_{n+1}^j(x). \quad (6.75)$$

Components with a terminal as destination will either be reflected from a sealed end,

$$v_n^j(x) \rightarrow v_n^j(l-x), \quad (6.76)$$

or reflected from a cut end,

$$v_n^j(x) \rightarrow -\frac{c_k^C}{c_{k+1}^C} v_n^j(l-x). \quad (6.77)$$

Pairs of components satisfying the isolation may be reflected from the local origin,

$$v_1^L(l-x) - v_1^R(l-x) \rightarrow -\frac{c_k^C}{c_{k+1}^C} (v_1^L(x) - v_1^R(x)). \quad (6.78)$$

It is common for two components, $v_n^j(x)$ and $v_{n+1}^j(l-x)$ to appear in the same potential function, $\phi_k(x)$ say. Since they have the same destination, at $x = l$, both contribute to the same two new components (see Figure 6.5),

$$\begin{aligned} \alpha v_n^j(x) + \beta v_{n+1}^j(l-x) &\rightarrow \frac{c_n^j}{c_{sn}^j} \left[\alpha \left(1 - \frac{c_k^C}{c_{k+1}^C} \frac{c_{n+1}^j}{c_n^j} \right) + \beta \left(1 + \frac{c_k^C}{c_{k+1}^C} \right) \right] v_n^j(l-x) \\ &\quad + \frac{c_{n+1}^j}{c_{sn}^j} \left[\alpha \left(1 + \frac{c_k^C}{c_{k+1}^C} \right) + \beta \left(1 - \frac{c_k^C}{c_{k+1}^C} \frac{c_n^j}{c_{n+1}^j} \right) \right] v_{n+1}^j(x) \\ &= p v_n^j(l-x) + q v_{n+1}^j(x). \end{aligned} \quad (6.79)$$

Conservation of coefficients means that

$$\alpha + \beta = p + q. \quad (6.80)$$

6.4 The Isolation-Termination Rules

The isolation-termination rules follow primarily from the requirement that the isolation condition is always satisfied, whatever the structure of tree or cable. First, to illustrate the strategy for deriving these rules, consider the initial three cylinders of the equivalent

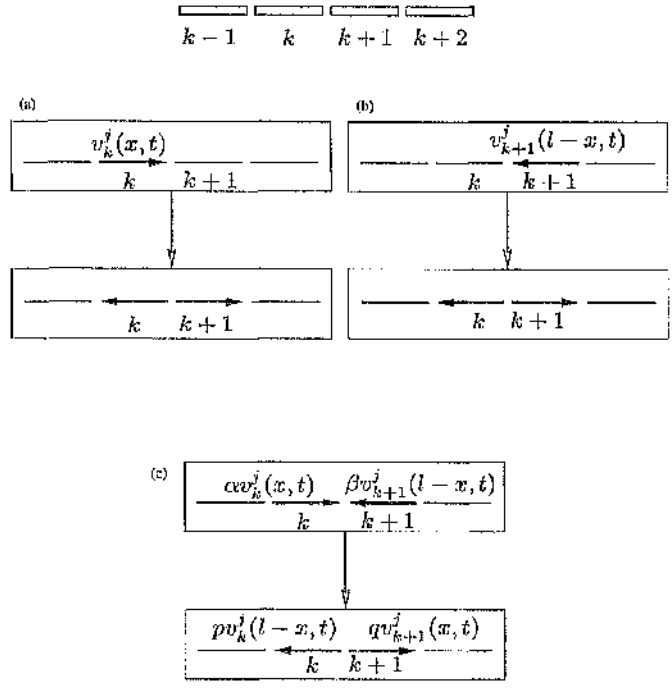


Figure 6.5: Component diagrams for component structure relevant to the general Y-junction. (a) Reflection of component $v_n^j(x)$ at $x = l$ generates a origin-directed reflected component and a terminal-directed transmitted component. (b) Reflection of component $v_{n+1}^j(l - x)$ at $x = l$ generates a terminal-directed reflected component and a origin-directed transmitted component. (c) Components $\alpha v_n^j(x)$ and $\beta v_{n+1}^j(l - x)$ contribute to the same two components on application of the electrical continuity rules.

cable for a general Y-junction. The ideas introduced can then be generalised to give the rule for the k^{th} cable cylinder — first assuming no terminals have been encountered in the process, then taking into account termination of both left and right branches. Only cylinder potentials are considered. The mapping of applied currents follows straightforwardly (replace the potential at a point with the current divided by c-sum at that point).

6.4.1 Cable Cylinders “1” to “3”

Cable Cylinder “1”

The initial cable cylinder must have the Rall-like potential function

$$\phi_1(x) = \frac{c_1^L}{c_1^G} v_L(x) + \frac{c_1^R}{c_1^G} v_R(x), \quad 0 \leq x \leq l, \quad (6.81)$$

where

$$c_1^G = c_1^L + c_1^R. \quad (6.82)$$

The sum of the two component coefficients is one,

$$\frac{c_1^L}{c_1^G} + \frac{c_1^R}{c_1^G} = 1. \quad (6.83)$$

This condition will be referred to as *rule one*, or the *Rall-like* condition. The immediate implication of this rule, combined with coefficient conservation, is that the sum of component coefficients in any subsequent cable potential function is always one unless at some point a component is reflected from a cut terminal. A component diagram for this potential is illustrated in Figure 6.6

Cable Cylinder “2”

Application of electrical continuity rules (6.74) to each of the two components of ϕ_1 gives a framework potential function,

$$\begin{aligned} \phi_2(x) = & \frac{c_1^L}{c_{s1}^L} \left(1 - \frac{c_1^G}{c_2^G} \frac{c_2^L}{c_1^L} \right) \frac{c_1^L}{c_1^G} v_L(l-x) + \frac{c_1^R}{c_{s1}^R} \left(1 - \frac{c_1^G}{c_2^G} \frac{c_2^R}{c_1^R} \right) \frac{c_1^R}{c_1^G} v_R(l-x) \\ & + \frac{c_2^L}{c_{s1}^L} \left(1 + \frac{c_1^G}{c_2^G} \right) \frac{c_1^L}{c_1^G} v_L(l+x) + \frac{c_2^R}{c_{s1}^R} \left(1 + \frac{c_1^G}{c_2^G} \right) \frac{c_1^R}{c_1^G} v_R(l+x), \quad 0 \leq x \leq l, \end{aligned} \quad (6.84)$$

where c_2^G must be chosen so that the coefficients of $v_L(l-x)$ and $v_R(l-x)$ satisfy the isolation condition, i.e. their sum is zero,

$$\frac{c_1^L}{c_{s1}^L} \left(1 - \frac{c_1^G}{c_2^G} \frac{c_2^L}{c_1^L} \right) \frac{c_1^L}{c_1^G} + \frac{c_1^R}{c_{s1}^R} \left(1 - \frac{c_1^G}{c_2^G} \frac{c_2^R}{c_1^R} \right) \frac{c_1^R}{c_1^G} = 0. \quad (6.85)$$

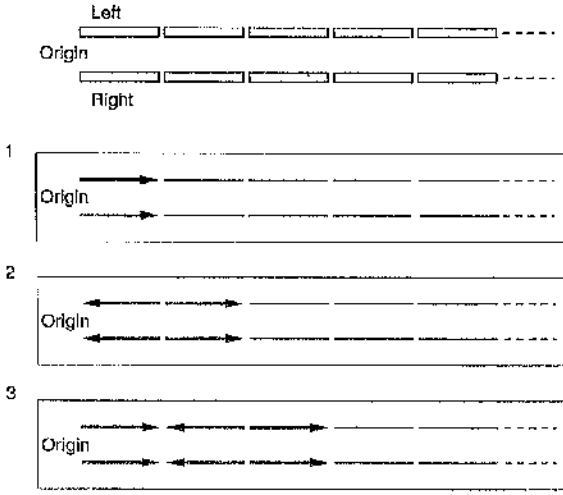


Figure 6.6: Component diagrams for the first three equivalent cable cylinders (1–3) for the general Y-junction.

Simply rearranging gives

$$c_2^G = \frac{c_1^G(c_1^L c_2^L c_{s1}^R + c_1^R c_2^R c_{s1}^L)}{((c_1^L)^2 c_{s1}^R + (c_1^R)^2 c_{s1}^L)}, \quad (6.86)$$

and so

$$\begin{aligned} \phi_2(x) = & \frac{c_1^L c_2^R (c_1^L c_2^R - c_2^L c_1^R)}{c_1^G (c_1^L c_2^L c_{s1}^R + c_1^R c_2^R c_{s1}^L)} (v_L(l-x) - v_R(l-x)) \\ & + \frac{c_1^L c_2^L c_{s1}^R}{(c_1^L c_2^L c_{s1}^R + c_1^R c_2^R c_{s1}^L)} v_L(l+x) + \frac{c_1^R c_2^R c_{s1}^L}{(c_1^L c_2^L c_{s1}^R + c_1^R c_2^R c_{s1}^L)} v_R(l+x), \quad 0 \leq x \leq l. \end{aligned} \quad (6.87)$$

Note the left-right symmetry in equations (6.84) through (6.87) — swap around the L and R , and the expressions are unaltered. This is expected, given the generality of the structure being transformed. The isolation condition will also be referred to as *rule two*.

Cable Cylinder “3”

The second potential function may be regarded as consisting of essentially three components — two directed away from the origin, the other towards. Applying the electrical continuity rules (6.74) to the outward components and (6.78) to the inward components of ϕ_2 gives a framework potential function,

$$\begin{aligned} \phi_3(x) = & \frac{c_2^G}{c_3^G} \frac{c_1^L c_2^R (c_1^L c_2^R - c_2^L c_1^R)}{(c_1^L c_2^L c_{s1}^R + c_1^R c_2^R c_{s1}^L)} (v_L(x) - v_R(x)) \\ & + \frac{c_2^L}{c_{s2}^L} \left(1 - \frac{c_2^G c_3^L}{c_3^G c_2^L}\right) \frac{c_1^L c_2^L c_{s1}^R}{(c_1^L c_2^L c_{s1}^R + c_1^R c_2^R c_{s1}^L)} v_L(2l-x) \\ & + \frac{c_2^R}{c_{s2}^R} \left(1 - \frac{c_2^G c_3^R}{c_3^G c_2^R}\right) \frac{c_1^R c_2^R c_{s1}^L}{(c_1^L c_2^L c_{s1}^R + c_1^R c_2^R c_{s1}^L)} v_R(2l-x) \end{aligned}$$

$$\begin{aligned}
& + \frac{c_3^L}{c_{s2}^L} \left(1 + \frac{c_3^C}{c_3^G} \right) \frac{c_1^L c_2^L c_{s1}^R}{(c_1^L c_2^L c_{s1}^R + c_1^R c_2^R c_{s1}^L)} v_L(2l+x) \\
& + \frac{c_3^R}{c_{s2}^R} \left(1 + \frac{c_3^C}{c_3^G} \right) \frac{c_1^R c_2^R c_{s1}^L}{(c_1^R c_2^R c_{s1}^L + c_1^L c_2^L c_{s1}^R)} v_R(2l+x), \quad 0 \leq x \leq l. \quad (6.88)
\end{aligned}$$

At this point, where two components have the origin as source, the requirement for isolation is not of immediate relevance. We still need to determine c_3 somehow. The trick is to choose c_3 so that, whatever the tree structure beyond the third cylinder of each branch (i.e. structure that is not represented in potential functions so far), components of $\phi_4(x)$ will satisfy the isolation condition (a similar idea leads to the k^{th} rule).

Writing equation (6.88) as

$$\begin{aligned}
\phi_3(x) = & A(v_L(x) - v_R(x)) + Bv_L(2l-x) + Cv_R(2l-x) \\
& + Dv_L(2l+x) + Ev_R(2l+x), \quad 0 \leq x \leq l, \quad (6.89)
\end{aligned}$$

the electrical continuity rules can be applied to give

$$\begin{aligned}
\phi_4(x) = & \left[A \frac{c_1^L}{c_{s1}^L} \left(1 - \frac{c_3^C c_2^L}{c_4^G c_1^L} \right) + B \frac{c_1^L}{c_{s1}^L} \left(1 + \frac{c_3^G}{c_4^G} \right) \right] v_L(l-x) \\
& + \left[-A \frac{c_1^R}{c_{s1}^R} \left(1 - \frac{c_3^C c_2^R}{c_4^G c_1^R} \right) + C \frac{c_1^R}{c_{s1}^R} \left(1 + \frac{c_3^G}{c_4^G} \right) \right] v_R(l-x) \\
& + \left[A \frac{c_2^L}{c_{s1}^L} \left(1 + \frac{c_3^G}{c_4^G} \right) + B \frac{c_2^L}{c_{s1}^L} \left(1 - \frac{c_3^G c_1^L}{c_4^G c_2^L} \right) \right] v_L(l+x) \\
& + \left[-A \frac{c_2^R}{c_{s1}^R} \left(1 + \frac{c_3^G}{c_4^G} \right) + C \frac{c_2^R}{c_{s1}^R} \left(1 - \frac{c_3^G c_1^R}{c_4^G c_2^R} \right) \right] v_R(l+x) \\
& + D \frac{c_3^L}{c_{s3}^L} \left(1 - \frac{c_3^G c_4^L}{c_4^G c_3^L} \right) v_L(3l-x) + E \frac{c_3^R}{c_{s3}^R} \left(1 - \frac{c_3^G c_4^R}{c_4^G c_3^R} \right) v_R(3l-x) \\
& + D \frac{c_4^L}{c_{s3}^L} \left(1 + \frac{c_3^G}{c_4^G} \right) v_L(3l+x) + E \frac{c_4^R}{c_{s3}^R} \left(1 + \frac{c_3^G}{c_4^G} \right) v_R(3l+x), \quad 0 \leq x \leq l. \quad (6.90)
\end{aligned}$$

The isolation condition will only be satisfied if

$$\frac{c_1^L}{c_{s1}^L} \left(1 - \frac{c_3^G c_2^L}{c_4^G c_1^L} \right) A + \frac{c_1^L}{c_{s1}^L} \left(1 + \frac{c_3^G}{c_4^G} \right) B + \frac{c_1^R}{c_{s1}^R} \left(1 - \frac{c_3^G c_2^R}{c_4^G c_1^R} \right) (-A) + \frac{c_1^R}{c_{s1}^R} \left(1 + \frac{c_3^G}{c_4^G} \right) C = 0. \quad (6.91)$$

Rewriting this in the form $M + (c_3^G/c_4^G)N$ gives

$$\frac{c_1^L}{c_{s1}^L} (A + B) + \frac{c_1^R}{c_{s1}^R} (-A + C) + \frac{c_3^G}{c_4^G} \left[-\frac{c_2^L}{c_{s1}^L} A + \frac{c_1^L}{c_{s1}^L} B + -\frac{c_2^R}{c_{s1}^R} (-A) + \frac{c_1^R}{c_{s1}^R} C \right] = 0. \quad (6.92)$$

It can easily be shown that $M = N$ by the following argument.

$$\begin{aligned}
N &= -\frac{c_2^L}{c_{s1}^L} A + \frac{c_1^L}{c_{s1}^L} B + -\frac{c_2^R}{c_{s1}^R} (-A) + \frac{c_1^R}{c_{s1}^R} C \\
&= \frac{c_1^L}{c_{s1}^L} A - A + \frac{c_1^L}{c_{s1}^L} B + \frac{c_1^R}{c_{s1}^R} (-A) + A + \frac{c_1^R}{c_{s1}^R} C,
\end{aligned}$$

$$\begin{aligned}
&= \frac{c_1^L}{c_{s1}^L} A + \frac{c_1^L}{c_{s1}^L} B + \frac{c_1^R}{c_{s1}^R} (-A) + \frac{c_1^R}{c_{s1}^R} C \\
&= M,
\end{aligned} \tag{6.93}$$

so that equation (6.92) can be rewritten

$$\left[\frac{c_1^L}{c_{s1}^L} (A + B) + \frac{c_1^R}{c_{s1}^R} (-A + C) \right] \left(1 + \frac{c_3}{c_4} \right) = 0, \tag{6.94}$$

or

$$\left[-\frac{c_2^L}{c_{s1}^L} A + \frac{c_1^L}{c_{s1}^L} B + -\frac{c_2^R}{c_{s1}^R} (-A) + \frac{c_1^R}{c_{s1}^R} C \right] \left(1 + \frac{c_3}{c_4} \right) = 0. \tag{6.95}$$

Cable c -values must be non-negative (and anyway, this condition must be independent of structure beyond the third cylinder of each Y-junction limb tree), so

$$\frac{c_1^L}{c_{s1}^L} (A + B) + \frac{c_1^R}{c_{s1}^R} (-A + C) = 0, \tag{6.96}$$

which is referred to as the *voltage-like form of rule three*, or equivalently

$$-\frac{c_2^L}{c_{s1}^L} A + \frac{c_1^L}{c_{s1}^L} B - \frac{c_2^R}{c_{s1}^R} (-A) + \frac{c_1^R}{c_{s1}^R} C = 0, \tag{6.97}$$

which is referred to as the *current-like form of rule three*. Note that M contributes the voltage-like rule, while N contributes the current-like rule.

To understand the nomenclature, consider the component diagram in Figure 6.6. For the voltage-like rule, note in equation (6.89) that if $A = -B$, then (6.96) requires that $A = C$, and the four associated components cancel at $x = l$, leaving

$$\phi_3(l) = Dv_L(3l) + Ev_R(3l). \tag{6.98}$$

For the current-like rule, now consider the spatial derivative of ϕ_3 ,

$$\frac{\partial \phi_3}{\partial x} \Big|_{l^-} = A \frac{\partial v_L}{\partial x} \Big|_{l^-} + B \frac{\partial v_L}{\partial x} \Big|_{l^+} - A \frac{\partial v_R}{\partial x} \Big|_{l^-} + C \frac{\partial v_R}{\partial x} \Big|_{l^+} + D \frac{\partial v_L}{\partial x} \Big|_{3l^-} + E \frac{\partial v_R}{\partial x} \Big|_{3l^-}. \tag{6.99}$$

If $c_2^L A = c_1^L B$, then (6.97) requires that $c_2^R (-A) = c_1^R C$, and, from equation (6.13), the two pairs of associated components satisfy a current injection condition at $x = l$, with the derivatives cancelling, leaving

$$\frac{\partial \phi_3}{\partial x} \Big|_{l^-} = D \frac{\partial v_L}{\partial x} \Big|_{3l^-} + E \frac{\partial v_R}{\partial x} \Big|_{3l^-} + \frac{B}{c_2^L} \frac{i_{A,1}^L}{K} + \frac{C}{c_2^R} \frac{i_{A,1}^R}{K}. \tag{6.100}$$

When generalising to rule k , both voltage- and current-like rule forms exist, which is significant for termination of the cable.

In either version of the rule, put in expressions for A , B , and C given by the electrical continuity rules in equation (6.88), and a unique expression for c_3^G is obtained. Using the

voltage form of rule three (6.96),

$$\begin{aligned} & \frac{c_1^L}{c_{s1}^L} \left(-\frac{c_2}{c_3} \frac{c_1^L c_1^R}{c_1^L c_2^L c_{s1}^R + c_1^R c_2^R c_{s1}^L} (c_1^L c_2^R - c_2^L c_1^R) \right. \\ & \left. + \frac{c_2^L}{c_{s2}^L} \left(1 - \frac{c_2}{c_3} \frac{c_3^L}{c_2^L} \right) \frac{c_1^L c_2^L c_{s1}^R}{(c_1^L c_2^L c_{s1}^R + c_1^R c_2^R c_{s1}^L)} \right) \\ & + \frac{c_1^R}{c_{s1}^R} \left(\frac{c_2}{c_3} \frac{c_1^L c_1^R}{c_1^L c_2^L c_{s1}^R + c_1^R c_2^R c_{s1}^L} (c_1^L c_2^R - c_2^L c_1^R) \right. \\ & \left. + \frac{c_2^R}{c_{s2}^R} \left(1 - \frac{c_2}{c_3} \frac{c_3^R}{c_2^R} \right) \frac{c_1^R c_2^R c_{s1}^L}{(c_1^L c_2^L c_{s1}^R + c_1^R c_2^R c_{s1}^L)} \right) = 0, \end{aligned} \quad (6.101)$$

which gives,

$$c_3^G = \frac{c_2^G}{c_1^G} \left(\frac{c_1^L c_1^R c_{s2}^L c_{s2}^R (c_1^L c_2^R - c_2^L c_1^R)^2 + ((c_1^L)^2 c_2^L c_3^L (c_{s1}^R)^2 c_{s2}^R + (c_1^R)^2 c_2^R c_3^R (c_{s1}^L)^2 c_{s2}^L) c_1^G}{((c_1^L)^2 (c_2^L)^2 (c_{s1}^R)^2 c_{s2}^R + (c_1^R)^2 (c_2^R)^2 (c_{s1}^L)^2 c_{s2}^L)} \right), \quad (6.102)$$

and the third potential function, valid for $0 \leq x \leq l$,

$$\begin{aligned} & \Omega_1 \Omega_2 \phi_3(x) = \\ & c_1^L c_1^R (c_1^L c_2^R - c_2^L c_1^R) [(c_1^L)^2 (c_2^L)^2 (c_{s1}^R)^2 c_{s2}^R + (c_1^R)^2 (c_2^R)^2 (c_{s1}^L)^2 c_{s2}^L] (v_R(x) - v_L(x)) \\ & + c_1^G c_1^L c_2^L c_{s1}^R \left[(c_1^R)^2 c_2^R (c_{s1}^L)^2 (c_2^L c_3^R - c_3^L c_2^R) + c_1^L c_1^R c_2^L (c_1^L c_2^R - c_2^L c_1^R)^2 \right] v_L(2l - x) \\ & + c_1^G c_1^R c_2^R c_{s1}^L \left[(c_1^L)^2 c_2^L (c_{s1}^R)^2 (c_2^R c_3^L - c_3^R c_2^L) + c_1^L c_1^R c_2^R (c_1^L c_2^R - c_2^L c_1^R)^2 \right] v_R(2l - x) \\ & + c_1^L c_2^L c_3^L c_{s1}^R c_{s2}^R \left[((c_1^L)^2 c_2^L (c_{s1}^R)^2 + (c_1^R)^2 c_2^R (c_{s1}^L)^2) c_1 + c_1^L c_1^R (c_1^L c_2^R - c_2^L c_1^R)^2 \right] v_L(2l + x) \\ & + c_1^R c_2^R c_3^R c_{s1}^L c_{s2}^L \left[((c_1^L)^2 c_2^L (c_{s1}^R)^2 + (c_1^R)^2 c_2^R (c_{s1}^L)^2) c_1 + c_1^L c_1^R (c_1^L c_2^R - c_2^L c_1^R)^2 \right] v_R(2l + x), \end{aligned} \quad (6.103)$$

where

$$\begin{aligned} \Omega_1 &= c_1^L c_2^L c_{s1}^R + c_1^R c_2^R c_{s1}^L \\ \Omega_2 &= c_1^L c_1^R c_{s2}^L c_{s2}^R (c_1^L c_2^R - c_2^L c_1^R)^2 + ((c_1^L)^2 c_2^L c_3^L (c_{s1}^R)^2 c_{s2}^R + (c_1^R)^2 c_2^R c_3^R (c_{s1}^L)^2 c_{s2}^L) c_1^G. \end{aligned} \quad (6.104)$$

The left-right symmetry is still maintained, as expected.

Clearly, at this point the level of complexity involved in the expressions for the cable potential functions and c-values is increasing rapidly. In fact, the expressions for c_3^G and $\phi_1(x)$ exhibit a similar increase in complexity over c_3^G and $\phi_2(x)$ as they themselves over c_2^G and $\phi_1(x)$. Fortunately, we can derive general rules for the k -th cable section by extending slightly the ideas used above.

Special cases of the first three cable cylinders

Consider potential ϕ_2 again (equation 6.87), and suppose the reflected components are zero, so

$$c_1^L c_2^R - c_2^L c_1^R = 0, \quad (6.105)$$

On rearranging, clearly this condition simply says that the ratio of first to second tree cylinder c-values is the same in each branch,

$$\frac{c_1^L}{c_2^L} = \frac{c_1^R}{c_2^R}. \quad (6.106)$$

Equivalently, the ratio of left to right c-values is the same for the first two tree cylinder in each branch. Write

$$r = \frac{c_1^L}{c_1^R} = \frac{c_2^L}{c_2^R}. \quad (6.107)$$

It is also clear from the framework potential (6.84) that both reflected components are zero only if

$$\frac{c_2^L}{c_1^L} = \frac{c_1^L}{c_2^L} = \frac{c_1^R}{c_2^R}, \quad (6.108)$$

so the same c-value ratio is exhibited by the first two cable cylinders. The cable potentials generated so far may be rewritten

$$\phi_1(x) = \frac{r}{1+r}v_L(x) + \frac{1}{1+r}v_R(x), \quad (6.109)$$

and

$$\phi_2(x) = \frac{r}{1+r}v_L(l+x) + \frac{1}{1+r}v_R(l+x). \quad (6.110)$$

Similarly, consider cable potential ϕ_3 (equation 6.103). If the above zero reflection condition (6.106) still holds true then the coefficients of $v_L(2l-x)$ and $v_R(2l-x)$ (which are the closest components to the origin that are also directed towards the origin) sum to zero (similarly to the original isolation condition). This follows directly from rule three (6.96).

In addition, the coefficients of reflected components $v_L(2l-x)$ and $v_R(2l-x)$ in ϕ_3 can only be zero if the condition

$$\frac{c_2}{c_3} = \frac{c_2^L}{c_3^L} = \frac{c_2^R}{c_3^R}, \quad (6.111)$$

also holds. Thus,

$$r = \frac{c_1^L}{c_1^R} = \frac{c_2^L}{c_2^R} = \frac{c_3^L}{c_3^R}, \quad (6.112)$$

and

$$\phi_3(x) = \frac{r}{1+r}v_L(2l+x) + \frac{1}{1+r}v_R(2l+x). \quad (6.113)$$

It can now be shown that the conditions for zero reflection are easily extended to the k^{th} tree cylinder in each branch.

6.4.2 The Piecewise Generalisation of Rall's Equivalent Cylinder

Consider a Y-junction where the left and right branches have the same electrotonic length, and terminate with the same boundary condition (we are not actually restricted to just cut and current injection conditions for the special case under consideration). A slight generalisation of Rall's equivalent cylinder is obtained if the 3/2 power law for diameters is relaxed so that

$$r = c_k^L/c_k^R, \quad 1 \leq k \leq m_L = m_R. \quad (6.114)$$

Suppose the k^{th} cable cylinder potential is of the form

$$\phi_k(x) = Av_L((k-1)l+x) + Bv_R((k-1)l+x), \quad 0 \leq x \leq l. \quad (6.115)$$

Now apply the electrical continuity rules at $x = l$ to generate the $(k+1)^{th}$ framework potential,

$$\begin{aligned} \phi_{k+1}(x) &= \frac{c_{k+1}^L}{c_{sk}^L} \left(1 + \frac{c_k^C}{c_{k+1}^C} \right) Av_L(kl+x) + \frac{c_{k+1}^R}{c_{sk}^R} \left(1 + \frac{c_k^C}{c_{k+1}^C} \right) Bv_R(kl+x) \\ &\quad + \frac{c_k^L}{c_{sk}^L} \left(1 - \frac{c_k^C}{c_{k+1}^C} \frac{c_{k+1}^L}{c_k^L} \right) Av_L(kl-x) + \frac{c_k^R}{c_{sk}^R} \left(1 - \frac{c_k^C}{c_{k+1}^C} \frac{c_{k+1}^R}{c_k^R} \right) Bv_R(kl-x). \end{aligned} \quad (6.116)$$

Note that the two reflected components are only both zero provided

$$\frac{c_k^C}{c_{k+1}^C} = \frac{c_k^L}{c_{k+1}^L} = \frac{c_k^R}{c_{k+1}^R}; \quad (6.117)$$

which follows automatically from the relaxed Rall condition so

$$\phi_{k+1}(x) = Av_L(kl+x) + Bv_R(kl+x). \quad (6.118)$$

Note that this is independent of the actual values taken by A and B .

Since $\phi_1(x)$ takes the form of equation (6.115), with $A = r/(1+r)$ and $B = 1/(1+r)$, and since the relaxed Rall condition holds for all k , then through mathematical induction it follows that

$$\phi_k = \frac{r}{1+r} v_L((k-1)l+x) + \frac{1}{1+r} v_R((k-1)l+x), \quad 0 \leq x \leq l, \quad (6.119)$$

for all k .

Equivalently, describing the left and right c -values by functions $c_L(x)$ and $c_R(x)$, which are stepwise uniform, then

$$\frac{c_L(x)}{c_R(x)} = r, \quad 0 \leq x \leq m_L l. \quad (6.120)$$

The potential in the cable is now represented by one function, ϕ_C , so we can write

$$\phi_C(x) = \frac{r}{1+r}v_L(x) + \frac{1}{1+r}v_R(x), \quad 0 \leq x \leq m_L l. \quad (6.121)$$

At $x = m_L l$ the cable (connected section) will terminate with the same type of condition as the Y-junction limbs.

It now remains to construct the disconnected section. Consider a cylinder with c-value c_k^D , described by the potential

$$\xi_k = v_L((k-1)l+x) - v_R((k-1)l+x), \quad 0 \leq x \leq l. \quad (6.122)$$

Again, note that this takes the form of equation (6.115), this time with $A = -B = 1$. Since the left and right branches satisfy condition (6.120), there must also be zero reflection on application of the electrical continuity rules to ξ_k , yielding

$$\xi_{k+1} = v_L(kl+x) - v_R(kl+x), \quad (6.123)$$

It is trivial to repeat the argument used for the connected section, starting this time with

$$\xi_1 = v_L(x) - v_R(x), \quad (6.124)$$

which satisfies a cut condition at $x = 0$. Therefore, the disconnected section c-values (superscripted by D) satisfy

$$\frac{c_k^D}{c_{k+1}^D} = \frac{c_k^L}{c_{k+1}^L} = \frac{c_k^R}{c_{k+1}^R}. \quad (6.125)$$

It is necessary to choose a c-value for one disconnected section cylinder so that the rest may be extracted from the ratios. It is convenient to choose $c_1^D = 1$.

The potential in the disconnected section can be written as

$$\phi_D(x) = v_L(x) - v_R(x), \quad 0 \leq x \leq m_L l. \quad (6.126)$$

which must satisfy the same type of boundary condition at $x = m_L l$ as the connected section. The disconnected and connected sections therefore have identical shape.

Figure 6.7 illustrates a few examples of piecewise cables. This is a very important special case. When tree structure deviates from the relaxed Rall conditions, there must at some point be reflected components, and the general analytical rules that follow must be used.

Note that the connected sections of such cables are identical to the lambda cables (Burke, 1997) obtained simply by moving from junction to Y-junction tips summing c-values (see Chapter 3). Rall's equivalent cylinder is the special case where $c_k^i/c_{k+1}^i = 1$ for all k .

This result is the discontinuous version of the continuous non-uniform cables mentioned in Chapter 3. A combination of both arguments allows for c-value profiles that are a mixture of continuously varying and discontinuous segments.

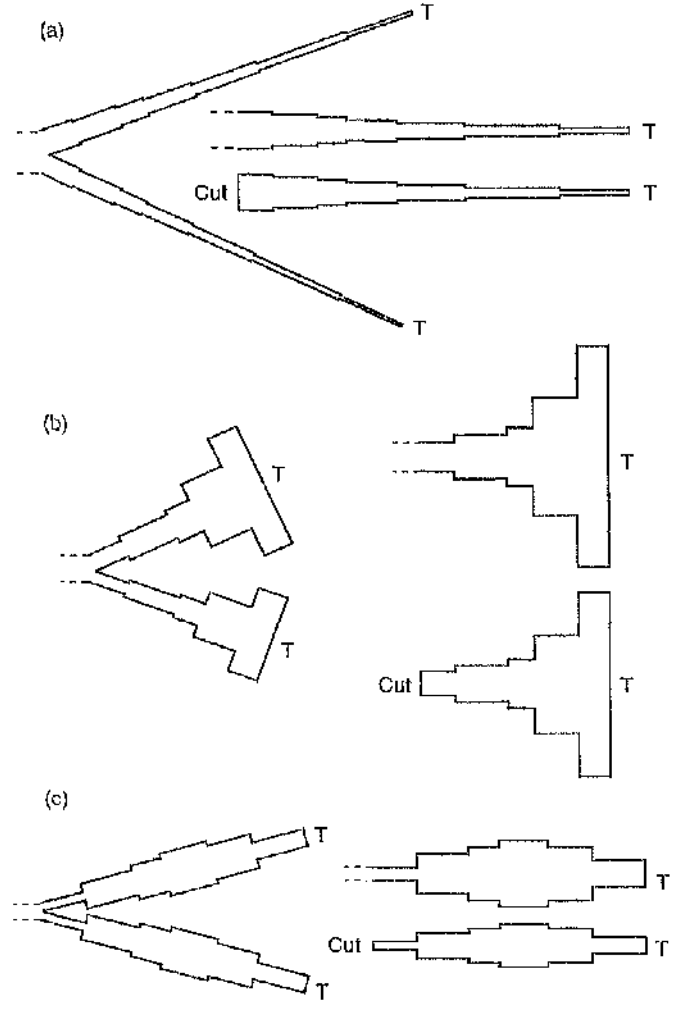


Figure 6.7: Examples of non-uniform generalised Rall trees. (a)–(c) Three examples of the piecewise generalisation of Rall's equivalent cylinder. Tree terminals satisfy the same boundary condition T . The ratio of the branch c -values is a constant. In each case the connected and disconnected sections have the same electrotonic length and diameter profile.

6.4.3 Cable Cylinder k — Prior to Left and Right Branch Termination

Consider equivalent cable cylinder k where $k \leq m_L, m_R$, i.e. for the moment we avoid the additional complexities introduced when terminals must be taken into account. General expressions for the current-like and voltage-like forms of rule k (for determining c-value c_k^G , and consequently potential ϕ_k) will be stated. A proof by mathematical induction will be given showing that these rules are correct if we require that the isolation condition must always be satisfied by any (even numbered) potential function. First, however, consider the general structure of cable potential function ϕ_k .

Part One: Potential Function k and Framework Potential $k+1$

The electrical continuity rules ensure that the potential function for the k^{th} equivalent cable cylinder for the general Y-junction can be expressed as a linear combination of components each with length l and lying along an entire Y-junction cylinder. The k -odd and k -even cases must be considered separately.

If k is odd and $k \geq 1$, then $\phi_k(x)$ can be expressed in a compact form,

$$\phi_k(x) = \sum_{i=L,R} \sum_{n=1}^{\frac{k+1}{2}} {}^k\alpha_n^i v_i(2(n-1)l + x) + {}^k\beta_n^i v_i(2nl - x), \quad (6.127)$$

where

$${}^k\beta_{\frac{k+1}{2}}^i = 0. \quad (6.128)$$

Figure 6.8a illustrates component diagrams for the potentials ϕ_k and ϕ_{k+1} when k is odd.

Constants ${}^k\alpha_n^i$ and ${}^k\beta_n^i$ are, respectively, the coefficients of the n^{th} outward and n^{th} inward components contributed by branch i to the k^{th} cable potential function. It is convenient to pair components that have the same destination. On each branch, numbering starts at $n = 1$ for the pair of components nearest the origin, increasing towards (but not yet reaching) the terminals.

Note that component ${}^k\alpha_n^i v_i(2(n-1)l + x)$ lies on odd numbered cylinder $(2n-1)$ while component ${}^k\beta_n^i v_i(2nl - x)$ lies on even numbered cylinder $2n$ (on branch i).

On each branch, there is one outward component that cannot be paired, i.e. that furthest from the origin, lying on the k^{th} cylinder. For notational convenience, each is paired with a *zero component*, i.e. a component with zero coefficient, hence condition (6.128).

If k is even and $k \geq 2$ then,

$$\phi_k(x) = \sum_{i=L,R} \sum_{n=0}^{\frac{k}{2}} {}^k p_n^i v_i((2n-1)l+x) + {}^k q_n^i v_i((2n+1)l-x), \quad (6.129)$$

where

$${}^k p_0^i = 0 \quad \text{and} \quad {}^k q_{\frac{k}{2}}^i = 0. \quad (6.130)$$

Figure 6.8b illustrates component diagrams for the potentials ϕ_k and ϕ_{k+1} when k is even..

Constants ${}^k p_n^i$ and ${}^k q_n^i$ are, respectively, coefficients of the n^{th} outward and n^{th} inward components contributed by branch i to the k^{th} cable potential function. Components with the same destination are paired. Numbering in this case starts at $n = 0$ for the two components that meet at the origin. These are paired with zero components for notational convenience, as, again, are those two terminal-directed components furthest from the origin (contributed by the k^{th} left and right branch cylinder), hence conditions (6.130).

Note that component ${}^k p_n^i v_i(2(n-1)l+x)$ lies on even numbered cylinder $2n$ while component ${}^k q_n^i v_i(2nl-x)$ lies on odd numbered cylinder $2n+1$.

The electrical continuity rules are now applied to both forms of ϕ_k . The isolation condition (rule two) is assumed to hold.

If k is odd, then applying the electrical continuity rules to equation (6.127) generates

$$\begin{aligned} \phi_{k+1}(x) &= \sum_{i=L,R} \sum_{n=1}^{\frac{k+1}{2}} \left[\left(\frac{c_{2n-1}^i}{c_{s(2n-1)}^i} \left(1 - \frac{c_k^C}{c_{k+1}^C} \frac{c_{2n}^i}{c_{2n-1}^i} \right) {}^k \alpha_n^i \right. \right. \\ &\quad + \frac{c_{2n-1}^i}{c_{s(2n-1)}^i} \left(1 + \frac{c_k^C}{c_{k+1}^C} \right) {}^k \beta_n^i \Big) v_i((2n-1)l-x) \\ &\quad + \left(\frac{c_{2n}^i}{c_{s(2n-1)}^i} \left(1 + \frac{c_k^C}{c_{k+1}^C} \right) {}^k \alpha_n^i \right. \\ &\quad \left. \left. + \frac{c_{2n}^i}{c_{s(2n-1)}^i} \left(1 - \frac{c_k^C}{c_{k+1}^C} \frac{c_{2n-1}^i}{c_{2n}^i} \right) {}^k \beta_n^i \right) v_i((2n-1)l+x) \right]. \quad (6.131) \end{aligned}$$

Since $k+1$ is even, this must take the form of equation (6.129) with $k+1$ replacing k , and so may be expressed as

$$\phi_{k+1}(x) = \sum_{i=L,R} \sum_{n=0}^{\frac{k+1}{2}} {}^{k+1} p_n^i v_i((2n-1)l+x) + {}^{k+1} q_n^i v_i((2n+1)l-x), \quad (6.132)$$

where

$${}^{k+1}p_n^i = \begin{cases} 0 & n=0 \\ \frac{c_{2n}^i}{c_{s(2n-1)}^i} \left[\left(1 + \frac{c_k^G}{c_{k+1}^G}\right) {}^k\alpha_n^i + \left(1 - \frac{c_k^G}{c_{k+1}^G} \frac{c_{2n-1}^i}{c_{2n}^i}\right) {}^k\beta_n^i \right] & 1 \leq n \leq \frac{k+1}{2} \end{cases} \quad (6.133)$$

and

$${}^{k+1}q_{n-1}^i = \begin{cases} \frac{c_{2n-1}^i}{c_{s(2n-1)}^i} \left[\left(1 - \frac{c_k^G}{c_{k+1}^G} \frac{c_{2n-1}^i}{c_{2n}^i}\right) {}^k\alpha_n^i + \left(1 + \frac{c_k^G}{c_{k+1}^G}\right) {}^k\beta_n^i \right] & 1 \leq n \leq \frac{k+1}{2} \\ 0 & n = \frac{k+3}{2} \end{cases} \quad (6.134)$$

Be sure to remember that ${}^k\beta_{\frac{k+1}{2}}^i = 0$, so ${}^{k+1}q_{\frac{k-1}{2}}^i$ and ${}^{k+1}p_{\frac{k+1}{2}}^i$ take a slightly simplified form.

If k is even, then applying the electrical continuity rules to equation (6.129) generates

$$\begin{aligned} \phi_{k+1}(x) = & \sum_{i=L,R} \left[\sum_{n=1}^{\frac{k}{2}} \left(\left(\frac{c_{2n}^i}{c_{s(2n)}^i} \left(1 - \frac{c_k^G}{c_{k+1}^G} \frac{c_{2n+1}^i}{c_{2n}^i}\right) {}^k p_n^i + \frac{c_{2n}^i}{c_{s(2n)}^i} \left(1 + \frac{c_k^G}{c_{k+1}^G}\right) {}^k q_n^i \right) v_i(2nl - x) \right. \right. \\ & + \left(\frac{c_{2n+1}^i}{c_{s(2n)}^i} \left(1 + \frac{c_k^G}{c_{k+1}^G}\right) {}^k p_n^i + \frac{c_{2n+1}^i}{c_{s(2n)}^i} \left(1 - \frac{c_k^G}{c_{k+1}^G} \frac{c_{2n}^i}{c_{2n+1}^i}\right) {}^k q_n^i \right) v_i(2nl + x) \Big) \\ & \left. - \frac{c_k^G}{c_{k+1}^G} {}^k q_0^i v_i(x) \right]. \end{aligned} \quad (6.135)$$

Since $k+1$ is odd, this may be expressed in the form of equation (6.127), with $k+1$ replacing k ,

$$\phi_{k+1}(x) = \sum_{i=L,R} \sum_{n=1}^{\frac{k+2}{2}} {}^{k+1}\alpha_n^i v_i(2(n-1)l + x) + {}^{k+1}\beta_n^i v_i(2nl - x), \quad (6.136)$$

where

$${}^{k+1}\alpha_n^i = \begin{cases} -\frac{c_k^G}{c_{k+1}^G} {}^k q_n^i & n=1 \\ \frac{c_{2n-1}^i}{c_{s(2n-1)}^i} \left[\left(1 + \frac{c_k^G}{c_{k+1}^G}\right) {}^k p_{n-1}^i + \left(1 - \frac{c_k^G}{c_{k+1}^G} \frac{c_{2(n-1)}^i}{c_{2n-1}^i}\right) {}^k q_{n-1}^i \right] & 2 \leq n \leq \frac{k+2}{2} \end{cases} \quad (6.137)$$

and

$${}^{k+1}\beta_n^i = \begin{cases} \frac{c_{2n}^i}{c_{s(2n)}^i} \left[\left(1 - \frac{c_k^G}{c_{k+1}^G} \frac{c_{2n+1}^i}{c_{2n}^i}\right) {}^k p_n^i + \left(1 + \frac{c_k^G}{c_{k+1}^G}\right) {}^k q_n^i \right] & 1 \leq n \leq \frac{k}{2} \\ 0 & n = \frac{k+2}{2} \end{cases} \quad (6.138)$$

In this case, remember that ${}^k q_{\frac{k}{2}}^i = 0$, so that ${}^{k+1}\beta_{\frac{k}{2}}^i$ and ${}^{k+1}\alpha_{\frac{k+2}{2}}^i$ take slightly simplified forms.

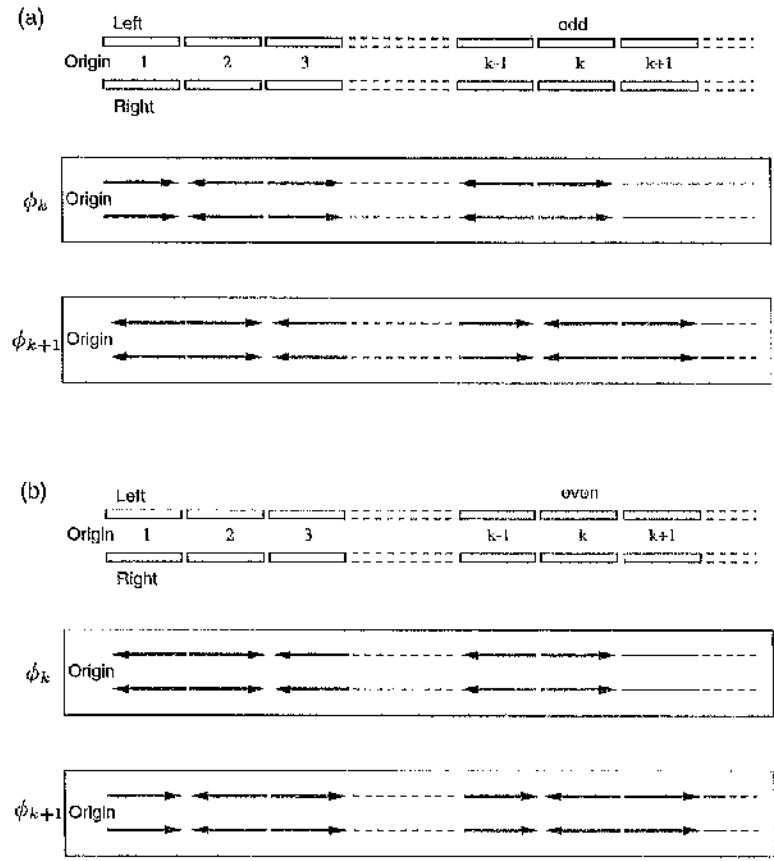


Figure 6.8: Component diagrams for the k^{th} and $(k+1)^{th}$ cable cylinder potential functions, prior to termination of either left or right branch. Dotted lines represent extended portions of each branch, with components following the given pattern. (a) k is odd. (b) k is even.

Part Two: Voltage and Current Forms of Rule k

Now, suppose that the k^{th} rule takes the following voltage-like and current-like forms.

If k is odd and $k \geq 3$, then assume the voltage-like form of rule k is

$$\sum_{i=L,R} \sum_{n=1}^{\frac{k+1}{2}} \left({}^k \alpha_n^i + {}^k \beta_n^i \right) {}^k E_n^i = 0, \quad (6.139)$$

while the current-like form of rule k is

$$\sum_{i=L,R} \sum_{n=1}^{\frac{k+1}{2}} \left(-\frac{c_{2n}^i}{c_{s(2n-1)}^i} {}^k \alpha_n^i + \frac{c_{2n-1}^i}{c_{s(2n-1)}^i} {}^k \beta_n^i \right) {}^k F_n^i = 0, \quad (6.140)$$

where

$${}^k E_{\frac{k+1}{2}}^i = 0 \quad \text{and} \quad {}^k F_{\frac{k+1}{2}}^i = 0, \quad (6.141)$$

so that the final term in each sum over n is always zero. The ${}^k E_n^i$ and ${}^k F_n^i$ are constants, referred to as the *voltage-rule coefficients* and *current-rule coefficients* respectively. Although the sum is over $(k+1)/2$ pairs of component coefficients for each branch, only $(k-1)/2$ have a non-zero current-rule or voltage-rule coefficient. The rules are written this way for notational convenience.

If k is even and $k \geq 4$, then the voltage-like form of rule k is

$$\sum_{i=L,R} \sum_{n=1}^{\frac{k}{2}} \left({}^k p_n^i + {}^k q_n^i \right) {}^k E_n^i = 0, \quad (6.142)$$

while the current-like form of rule k is

$$\sum_{i=L,R} \left[\sum_{n=1}^{\frac{k}{2}} \left(-\frac{c_{2n-1}^i}{c_{s(2n)}^i} {}^k p_n^i + \frac{c_{2n}^i}{c_{s(2n)}^i} {}^k q_n^i \right) {}^k F_n^i + {}^k q_0^i {}^k F_0^i \right] = 0. \quad (6.143)$$

where

$${}^k E_{\frac{k}{2}}^i = 0 \quad \text{and} \quad {}^k F_{\frac{k}{2}}^i = 0. \quad (6.144)$$

Again, although zero, the final term in each sum is included for notational convenience. Observe the additional term involving the coefficients of the two components with the destination as origin.

Note also that the isolation condition (rule two) may be written

$$\sum_{i=L,R} {}^2 q_0^i = 0, \quad (6.145)$$

so that

$${}^2F_0^i = 1. \quad (6.146)$$

Though similar to the k -even current-like form, this condition is regarded as voltage-like since the isolation condition arranges these inward components so that they can satisfy a cut condition when they meet at the junction. One of the main points of the remaining rules is to ensure that this is always the case, i.e. that

$$\sum_{i=L,R} {}^k q_0^i = 0. \quad (6.147)$$

From equations (6.96) and (6.97), the voltage and current rules (k -odd) are known to take these forms for rule three ($k = 3$), with

$${}^3E_1^i = \frac{c_1^i}{c_{s1}^i} \quad \text{and} \quad {}^3F_1^i = 1. \quad (6.148)$$

The “voltage-like” and “current-like” nomenclature can be explained quite simply, just as for rule three.

Consider first the voltage-like rules for rule k . If ${}^k\alpha_n^i + {}^k\beta_n^i = 0$ for $1 \leq n \leq (k-1)/2$, then, from potential function (6.127),

$$\phi_k(l) = {}^k\alpha_{\frac{k+1}{2}}^L v_L(kl) + {}^k\alpha_{\frac{k+1}{2}}^R v_R(kl), \quad (6.149)$$

for k odd. All the paired components have cancelled at this point since voltage continuity allows them to satisfy a cut condition.

Similarly, if ${}^k p_n^i + {}^k q_n^i = 0$ for $1 \leq n \leq (k-2)/2$, then from potential function (6.129),

$$\phi_k(l) = {}^k p_{\frac{k}{2}}^L v_L(kl) + {}^k p_{\frac{k}{2}}^R v_R(kl), \quad (6.150)$$

for k even, since at $x = l$ all other components cancel due to voltage continuity.

For the current-like rules, differentiate potential function (6.127) to give

$$\frac{\partial \phi_k(l)}{\partial x} = \sum_{i=L,R} \sum_{n=1}^{\frac{k+1}{2}} \left[{}^k \alpha_n^i \frac{\partial v_i}{\partial x} \Big|_{(2n-1)l^-} - {}^k \beta_n^i \frac{\partial v_i}{\partial x} \Big|_{(2n-1)l^+} \right] \quad (6.151)$$

Observe that, if $c_{2n}^i {}^k \alpha_n^i = c_{2n-1}^i {}^k \beta_n^i$ for $1 \leq n \leq (k-1)/2$, the current conservation law (6.13) can be used for each pair of components to give

$$\frac{\partial \phi_k}{\partial x} \Big|_{l^-} = {}^k \alpha_{\frac{k+1}{2}}^L \frac{\partial v_L}{\partial x} \Big|_{kl^-} + {}^k \alpha_{\frac{k+1}{2}}^R \frac{\partial v_R}{\partial x} \Big|_{kl^-} + \sum_{i=L,R} \sum_{n=1}^{\frac{k+1}{2}} \frac{{}^k \beta_n^i i_{A,2n-1}^i}{c_{2n}^i K}, \quad (6.152)$$

for k odd. Again, at $x = l$, all other terms involving derivatives have cancelled, contributing simply an applied current term since they satisfy a current injection condition.

The final case is slightly different. If $c_{2n+1}^i {}^k p_n^i = c_{2n}^i {}^k q_n^i$ for $1 \leq n \leq (k-2)/2$, then differentiating potential function (6.129) gives

$$\frac{\partial \phi_k}{\partial x} \Big|_{l^-} = {}^k q_0^L \frac{\partial v_L}{\partial x} \Big|_{0^+} + {}^k q_0^R \frac{\partial v_R}{\partial x} \Big|_{0^+} + {}^k p_{\frac{k}{2}}^L \frac{\partial v_L}{\partial x} \Big|_{kl^-} + {}^k p_{\frac{k}{2}}^R \frac{\partial v_R}{\partial x} \Big|_{kl^-} + \sum_{i=L,R} \sum_{n=1}^{\frac{k}{2}} \frac{{}^k q_n^i}{c_{2n+1}^i} \frac{i_{A,2n}^i}{K}, \quad (6.153)$$

for k even. In this case, as well as the two most distal components, two terms are contributed by the two components whose destination is the origin.

It is clear, from expressions (6.149), (6.150), (6.152), and (6.153), that cable cylinder k cannot terminate with either a cut or a current injection condition until $k \geq m_L, m_R$. Otherwise, there are components that don't end on a terminal, and are not paired with another component (zero components don't count since they are just a notational device). Components must have at least reached both terminals, though, except in special cases, termination doesn't actually occur until after this. Furthermore, when k is even, it will not be possible for a cable cylinder to satisfy a current injection condition unless the ${}^k q_0^i$ are zero.

Part Three: Ensuring ϕ_{k+1} Satisfies Rule $k - 1$

Now that the rules have been given, it is necessary to show that, under specific conditions, all rules must actually take these forms.

Recall that rule $k = 3$ was found by ensuring that component coefficients from $\phi_4(x)$ would satisfy rule two (the isolation condition), whatever Y-junction structure might be encountered beyond the third cylinder of each branch.

Assume that rule $(k-1)$ (k odd or k even) takes the voltage-like (6.139 and 6.142) and current-like (6.140 and 6.143) forms. We can now prove that rule k must also take these forms if we want to guarantee that rule $(k-1)$ holds for the component coefficients of the $(k+1)^{th}$ potential function, whatever structure is encountered beyond the k^{th} left and right branch cylinders.

If k is odd and $k \geq 3$, then $(k-1) \geq 2$ is even. We want rule $(k-1)$ to hold true for the ${}^{k+1} p_n^i$ and ${}^{k+1} q_n^i$ in ϕ_{k+1} (6.132), so, from equations (6.142) and (6.143), we require that

$$\sum_{i=L,R} \sum_{n=1}^{\frac{(k-1)}{2}} \left({}^{k+1} p_n^i + {}^{k+1} q_n^i \right) {}^{k-1} E_n^i = 0, \quad (6.154)$$

or

$$\sum_{i=L,R} \left[\sum_{n=1}^{\frac{(k-1)}{2}} \left(-\frac{c_{2n+1}^i}{c_{s(2n)}^i} {}^{k+1}p_n^i + \frac{c_{2n-k+1}^i}{c_{s(2n)}^i} {}^{k+1}q_n^i \right) {}^{k-1}F_n^i + {}^{k+1}q_0^i {}^{k-1}F_0^i \right] = 0. \quad (6.155)$$

If k is even and $k \geq 4$, then $(k-1)$ is odd and $(k-1) \geq 3$. We want rule $(k-1)$ to hold true for the ${}^{k-1}\alpha_n^i$ and ${}^{k+1}\beta_n^i$ in ϕ_{k+1} (equation 6.136). From equations (6.139) and (6.140), we require that the voltage-like rule

$$\sum_{i=L,R} \sum_{n=1}^{\frac{k}{2}} \left({}^{k+1}\alpha_n^i + {}^{k+1}\beta_n^i \right) {}^{k-1}E_n^i = 0, \quad (6.156)$$

and the current-like rule,

$$\sum_{i=L,R} \sum_{n=1}^{\frac{k}{2}} \left(-\frac{c_{2n}^i}{c_{s(2n-1)}^i} {}^{k+1}\alpha_n^i + \frac{c_{2n-1}^i}{c_{s(2n-1)}^i} {}^{k+1}\beta_n^i \right) {}^{k-1}F_n^i = 0. \quad (6.157)$$

are satisfied.

At this point, just the voltage-like forms of rule $(k-1)$ will be used, with the appropriate component coefficients substituted from framework potential ϕ_{k+1} . The current-like forms of rule $(k-1)$ could be used instead, however in the next section it is shown that the two expressions are in fact equivalent.

If k is odd, then use the voltage-like form of rule $(k-1)$ (6.154) and substitute for ${}^{k+1}p_n^i$ and ${}^{k+1}q_n^i$ using equations (6.133) and (6.134), (the coefficients of framework potential ϕ_{k+1} , 6.132) gives

$$\begin{aligned} & \sum_{i=L,R} \sum_{n=1}^{\frac{(k-1)}{2}} \left[\frac{c_{2n}^i}{c_{s(2n-1)}^i} \left(1 + \frac{c_k^C}{c_{k+1}^C} \right)^k \alpha_n^i + \frac{c_{2n}^i}{c_{s(2n-1)}^i} \left(1 - \frac{c_k^C}{c_{k+1}^C} \frac{c_{2n-1}^i}{c_{2n}^i} \right)^k \beta_n^i \right. \\ & \left. + \frac{c_{2n+1}^i}{c_{s(2n+1)}^i} \left(1 - \frac{c_k^C}{c_{k+1}^C} \frac{c_{2(n+1)}^i}{c_{2n+1}^i} \right)^k \alpha_{n+1}^i + \frac{c_{2n+1}^i}{c_{s(2n+1)}^i} \left(1 + \frac{c_k^C}{c_{k+1}^C} \right)^k \beta_{n+1}^i \right] {}^{k-1}E_n^i = 0, \end{aligned} \quad (6.158)$$

which may be rewritten as

$$\sum_{i=L,R} \sum_{n=1}^{\frac{(k-1)}{2}} \left[\frac{c_{2n}^i}{c_{s(2n-1)}^i} ({}^k\alpha_n^i + {}^k\beta_n^i) + \frac{c_{2n+1}^i}{c_{s(2n+1)}^i} ({}^k\alpha_{n+1}^i + {}^k\beta_{n+1}^i) \right] {}^{k-1}E_n^i$$

$$\begin{aligned}
& + \frac{c_k^C}{c_{k+1}^C} \sum_{i=L,R} \sum_{n=1}^{\frac{(k-1)}{2}} \left[\left(\frac{c_{2n-1}^i}{c_{s(2n-1)}} {}_k \alpha_n^i - \frac{c_{2n-1}^i}{c_{s(2n-1)}} {}_k \beta_n^i \right) \right. \\
& \left. + \left(-\frac{c_{2(n+1)}^i}{c_{s(2n+1)}} {}_k \alpha_{n+1}^i + \frac{c_{2n+1}^i}{c_{s(2n+1)}} {}_k \beta_{n+1}^i \right) \right] {}_{k-1} E_n^i = 0.
\end{aligned} \tag{6.159}$$

Of course, ${}^{k-1} E_{\frac{k-1}{2}}^i = 0$, so the final term in each sum over n does not contribute.

Note that this equation has the form

$$M + \left(\frac{c_k^C}{c_{k+1}^C} \right) N = 0. \tag{6.160}$$

If k is even, then using the voltage-like form of rule $k-1$ (6.156), and substituting for ${}^{k+1} \alpha_n^i$ and ${}^{k+1} \beta_n^i$ using equations (6.137) and (6.138), gives

$$\begin{aligned}
& \sum_{i=L,R} \left[\sum_{n=2}^{\frac{k}{2}} \left[\frac{c_{2n-1}^i}{c_{s(2(n-1))}^i} \left(1 + \frac{c_k^C}{c_{k+1}^C} \right) {}_k p_{n-1}^i + \frac{c_{2n-1}^i}{c_{s(2(n-1))}^i} \left(1 - \frac{c_k^C}{c_{k+1}^C} \frac{c_{2(n-1)}^i}{c_{2n-1}^i} \right) {}_k q_{n-1}^i \right. \right. \\
& \quad \left. + \frac{c_{2n}^i}{c_{s(2n)}^i} \left(1 - \frac{c_k^C}{c_{k+1}^C} \frac{c_{2n+1}^i}{c_{2n}^i} \right) {}_k p_n^i + \frac{c_{2n}^i}{c_{s(2n)}^i} \left(1 + \frac{c_k^C}{c_{k+1}^C} \right) {}_k q_n^i \right] {}_{k-1} E_n^i \\
& \quad \left. + \left(-\frac{c_k^C}{c_{k+1}^C} {}_k q_0^i + \frac{c_2^i}{c_{s2}^i} \left(1 - \frac{c_k^C}{c_{k+1}^C} \frac{c_3^i}{c_2^i} \right) {}_k p_1^i + \frac{c_2^i}{c_{s2}^i} \left(1 + \frac{c_k^C}{c_{k+1}^C} \right) {}_k q_1^i \right) {}_{k-1} E_1^i \right] = 0,
\end{aligned} \tag{6.161}$$

which may be rewritten as

$$\begin{aligned}
& \sum_{i=L,R} \left[\sum_{n=2}^{\frac{k}{2}} \left(\frac{c_{2n}^i}{c_{s(2n)}^i} ({}^k p_n^i + {}^k q_n^i) + \frac{c_{2n-1}^i}{c_{s(2(n-1))}^i} ({}^k p_{n-1}^i + {}^k q_{n-1}^i) \right) {}_{k-1} E_n^i + \frac{c_2^i}{c_{s2}^i} ({}^k p_1^i + {}^k q_1^i) {}_{k-1} E_1^i \right] \\
& + \frac{c_k^C}{c_{k+1}^C} \sum_{i=L,R} \left[\sum_{n=2}^{\frac{k}{2}} \left[\left(-\frac{c_{2n+1}^i}{c_{s(2n)}^i} {}_k p_n^i + \frac{c_{2n}^i}{c_{s(2n)}^i} {}_k q_n^i \right) + \left(\frac{c_{2n-1}^i}{c_{s2(n-1)}^i} {}_k p_{n-1}^i - \frac{c_{2(n-1)}^i}{c_{s2(n-1)}^i} {}_k q_{n-1}^i \right) \right] {}_{k-1} E_n^i \right. \\
& \quad \left. + \left(-\frac{c_3^i}{c_{s2}^i} {}_k p_1^i + \frac{c_2^i}{c_{s2}^i} {}_k q_1^i - {}_k q_0^i \right) {}_{k-1} E_1^i \right] = 0.
\end{aligned} \tag{6.162}$$

Note that ${}^{k-1} E_{\frac{k}{2}}^i = 0$, and again this equation has the form $M + (c_k^C/c_{k+1}^C)N = 0$.

Part Four: Equivalence of Voltage and Current Forms of Rule k

It may now be shown that $M = N$ for both the k -odd and k -even cases.

When k is odd and $k \geq 3$, begin with the expression for N from equation (6.159),

$$\begin{aligned}
N &= \sum_{i=L,R} \sum_{n=1}^{\frac{(k-1)}{2}} \left[\left(\frac{c_{2n}^i}{c_{s(2n-1)}^i} {}^k \alpha_n^i - \frac{c_{2n-1}^i}{c_{s(2n-1)}^i} {}^k \beta_n^i \right) \right. \\
&\quad \left. + \left(-\frac{c_{2(n+1)}^i}{c_{s(2n+1)}^i} {}^k \alpha_{n+1}^i + \frac{c_{2n+1}^i}{c_{s(2n+1)}^i} {}^k \beta_{n+1}^i \right) \right] {}^{k-1} E_n^i \\
&= \sum_{i=L,R} \sum_{n=1}^{\frac{(k-1)}{2}} \left[\left(\frac{c_{2n}^i}{c_{s(2n-1)}^i} ({}^k \alpha_n^i + {}^k \beta_n^i) - {}^k \beta_n^i \right) \right. \\
&\quad \left. + \left(\frac{c_{2n+1}^i}{c_{s(2n+1)}^i} ({}^k \alpha_{n+1}^i + {}^k \beta_{n+1}^i) - {}^k \alpha_{n+1}^i \right) \right] {}^{k-1} E_n^i \\
&= \sum_{i=L,R} \sum_{n=1}^{\frac{(k-1)}{2}} \left[\frac{c_{2n}^i}{c_{s(2n-1)}^i} ({}^k \alpha_n^i + {}^k \beta_n^i) + \frac{c_{2n+1}^i}{c_{s(2n+1)}^i} ({}^k \alpha_{n+1}^i + {}^k \beta_{n+1}^i) \right] {}^{k-1} E_n^i \\
&\quad - \sum_{i=L,R} \sum_{n=1}^{\frac{(k-1)}{2}} ({}^k \alpha_{n+1}^i + {}^k \beta_n^i) {}^{k-1} E_n^i. \tag{6.163}
\end{aligned}$$

Since coefficient conservation ensures that

$${}^k \alpha_{n+1}^i + {}^k \beta_n^i = {}^{k-1} p_n^i + {}^{k-1} q_n^i, \tag{6.164}$$

the last term may be written

$$\sum_{i=L,R} \sum_{n=1}^{\frac{(k-1)}{2}} ({}^{k-1} p_n^i + {}^{k-1} q_n^i) {}^{k-1} E_n^i, \tag{6.165}$$

which is the voltage-like form of the $(k-1)^{th}$ rule applied to potential function $k-1$ (equation 6.142), which must hold according to assumptions we have made, and so this term is zero. The remaining term is simply M , hence $M = N$ and the voltage- and current-like forms of the rule are seen to impose the same conditions on the component coefficients of ϕ_k .

If k is even and $k \geq 4$, then starting with N in equation (6.162),

$$\begin{aligned}
N &= \sum_{i=L,R} \left[\sum_{n=2}^{\frac{k}{2}} \left[\left(-\frac{c_{2n+1}^i}{c_{s(2n)}^i} {}^k p_n^i + \frac{c_{2n}^i}{c_{s(2n)}^i} {}^k q_n^i \right) + \left(\frac{c_{2n-1}^i}{c_{s(2n-1)}^i} {}^k p_{n-1}^i - \frac{c_{2(n-1)}^i}{c_{s(2(n-1))}^i} {}^k q_{n-1}^i \right) \right] {}^{k-1} E_n^i \right. \\
&\quad \left. + \left(-\frac{c_3^i}{c_{s2}^i} {}^k p_1^i + \frac{c_2^i}{c_{s2}^i} {}^k q_1^i - {}^k q_0^i \right) {}^{k-1} E_1^i \right] \\
&= \sum_{i=L,R} \left[\sum_{n=2}^{\frac{k}{2}} \left[\frac{c_{2n}^i}{c_{s(2n)}^i} ({}^k p_n^i + {}^k q_n^i) + \frac{c_{2(n-1)}^i}{c_{s(2(n-1))}^i} ({}^k p_{n-1}^i + {}^k q_{n-1}^i) - ({}^k p_n^i + {}^k q_{n-1}^i) \right] {}^{k-1} E_n^i \right]
\end{aligned}$$

$$\begin{aligned}
& + \left[\frac{c_2^i}{c_{s2}^i} \left({}^k p_1^i + {}^k q_1^i \right) - \left({}^k q_0^i + {}^k p_1^i \right) \right] {}^{k-1} E_n^i \\
= & \sum_{i=L,R} \left[\sum_{n=2}^{\frac{k}{2}} \left(\frac{c_{2n}^i}{c_{s(2n)}^i} \left({}^k p_n^i + {}^k q_n^i \right) + \frac{c_{2n-1}^i}{c_{s(2(n-1))}^i} \left({}^k p_{n-1}^i + {}^k q_{n-1}^i \right) \right) {}^{k-1} E_n^i \right. \\
& \quad \left. + \frac{c_2^i}{c_{s2}^i} \left({}^k p_1^i + {}^k q_1^i \right) {}^{k-1} E_1^i \right] - \sum_{i=L,R} \sum_{n=1}^{\frac{k}{2}} \left({}^k p_n^i + {}^k q_{n-1}^i \right) {}^{k-1} E_n^i. \quad (6.166)
\end{aligned}$$

In this case, coefficient conservation ensures that

$${}^k p_n^i + {}^k q_{n-1}^i = {}^{k-1} \alpha_n^i + {}^{k-1} \beta_n^i; \quad (6.167)$$

so that the second sum may be rewritten as

$$\sum_{i=L,R} \sum_{n=1}^{\frac{k}{2}} \left({}^{k-1} \alpha_n^i + {}^{k-1} \beta_n^i \right) {}^{k-1} E_n^i, \quad (6.168)$$

which is the voltage-like form of the $(k-1)^{th}$ rule applied to potential function $k-1$. This rule already holds true according to assumptions we have made, and so this term is zero. The remaining term is simply the voltage-like form of rule k -even, thus $N = M$. Again, the two rule forms are essentially the same condition.

Equations (6.159) and (6.162) can be rewritten as $M(1 + (c_k^G/c_{k+1}^G)) = 0$ or $N(1 + (c_k^G/c_{k+1}^G)) = 0$. It is therefore necessary that $M = N = 0$, since cable c-values should be non-negative (and anyway the rule should be independent of more distal cable structure).

By re-ordering the sums, one can extract from (6.159) and (6.162) the voltage-like and current-like forms of rule k . The expressions for M give the voltage-like rules, while the expressions for N give the current-like rules. They take the forms given in part two, and are now summarised below with the voltage-rule and current-rule coefficients for rule k expressed in terms of the voltage-rule coefficients for rule $k-1$, so that they may be determined iteratively.

Part Five: Summary of Pre-terminal Voltage-like and Current-like Rules

k odd and $k \geq 3$

The voltage-like rule is

$$\sum_{i=L,R} \sum_{n=1}^{\frac{k-1}{2}} \left({}^k \alpha_n^i + {}^k \beta_n^i \right) {}^k E_n^i = 0. \quad (6.169)$$

If $k = 3$ then

$${}^3E_1^i = \frac{c_1^i}{c_{s1}^i} \quad \text{and} \quad {}^3E_2^i = 0. \quad (6.170)$$

Otherwise $k \geq 5$ and

$${}^kE_n^i = \begin{cases} [{}^{k-1}E_1^i] \frac{c_2^i}{c_{s1}^i} & n = 1 \\ [{}^{k-1}E_n^i] \frac{c_{2n}^i}{c_{s(2n-1)}^i} + [{}^{k-1}E_{n-1}^i] \frac{c_{2n-1}^i}{c_{s(2n-1)}^i} & 2 \leq n \leq \frac{k-1}{2} \\ 0 & n = \frac{k+1}{2} \end{cases}. \quad (6.171)$$

The current-like rule is

$$\sum_{i=L,R} \sum_{n=1}^{\frac{k+1}{2}} \left(-\frac{c_{2n}^i}{c_{s(2n-1)}^i} {}^k\alpha_n^i + \frac{c_{2n-1}^i}{c_{s(2n-1)}^i} {}^k\beta_n^i \right) {}^kF_n^i = 0, \quad (6.172)$$

If $k = 3$ then

$${}^3F_1^i = 1 \quad \text{and} \quad {}^3F_2^i = 0. \quad (6.173)$$

Otherwise $k \geq 5$ and

$${}^kF_n^i = \begin{cases} -[{}^{k-1}E_1^i] & n = 1 \\ -[{}^{k-1}E_n^i] + [{}^{k-1}E_{n-1}^i] & 2 \leq n \leq \frac{k-1}{2} \\ 0 & n = \frac{k+1}{2} \end{cases}. \quad (6.174)$$

Remember that $[{}^{k-1}E_{\frac{k-1}{2}}^i] = 0$.

k even and $k \geq 4$

The voltage-like rule is

$$\sum_{i=L,R} \sum_{n=1}^{\frac{k}{2}} \left({}^k p_n^i + {}^k q_n^i \right) {}^k E_n^i = 0, \quad (6.175)$$

where

$${}^k F_n^i = \begin{cases} [{}^{k-1}E_{n+1}^i] \frac{c_{2n+1}^i}{c_{s(2n)}^i} + [{}^{k-1}E_n^i] \frac{c_{2n}^i}{c_{s(2n)}^i} & 1 \leq n \leq \frac{k-2}{2} \\ 0 & n = \frac{k}{2} \end{cases}. \quad (6.176)$$

Note that the coefficients of the two components that meet at the origin are not involved in this expression. The isolation condition has already ensured that ${}^k q_0^L = -{}^k q_0^R$ so these two components will automatically satisfy a cut terminal at $x = l$.

The current-like rule is

$$\sum_{i=L,R} \left[\sum_{n=1}^{\frac{k}{2}} \left(-\frac{c_{2n-1}^i}{c_{s(2n)}^i} {}^k p_n^i + \frac{c_{2n}^i}{c_{s(2n)}^i} {}^k q_n^i \right) {}^k F_n^i + {}^k q_0^i {}^k F_0^i \right] = 0, \quad (6.177)$$

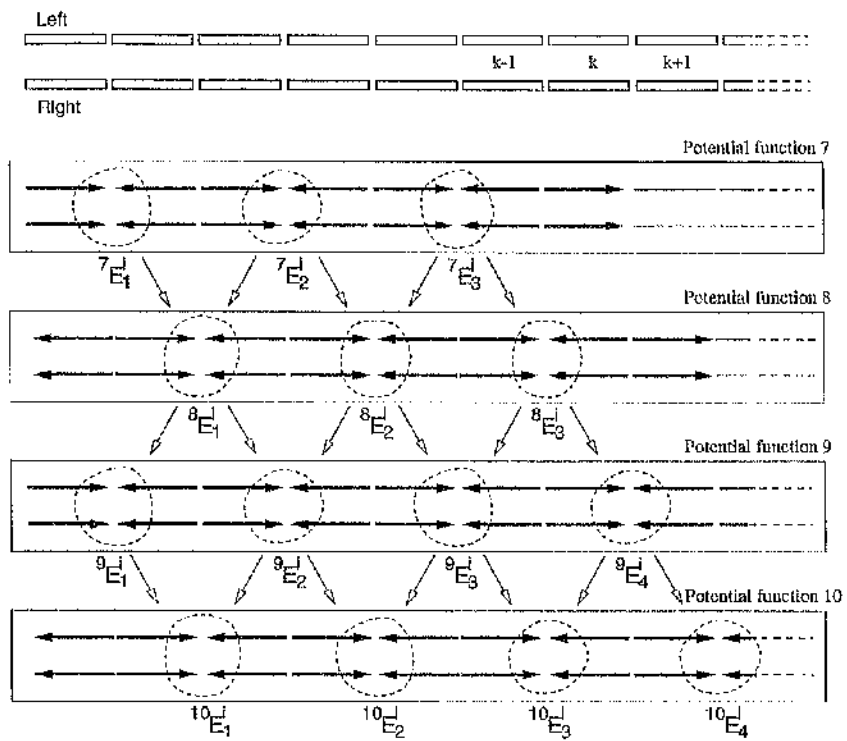


Figure 6.9: Interaction between voltage rule coefficients. See text for discussion.

where

$${}^k F_n^i = \begin{cases} -[{}^{k-1} E_1^i] & n = 0 \\ [{}^{k-1} E_n^i] - [{}^{k-1} E_{n+1}^i] & 1 \leq n \leq \frac{k-2}{2} \\ 0 & n = \frac{k}{2} \end{cases} . \quad (6.178)$$

Note that the coefficients of the two components that meet at the origin do contribute to this expression. Since these two components can only satisfy a cut terminal at $x = l$, the only way in which a current injection condition could be satisfied when k is even is if ${}^k q_0^L = {}^k q_0^R = 0$. Remember that ${}^{k-1} E_{\frac{k}{2}}^i = 0$.

The iterative procedure by which the voltage rule coefficients ${}^k E_n^i$ are determined can be visualised in Figure 6.9. Each new coefficient is some combination of two previous coefficients, except near the origin and furthest from the origin. At the origin, odd numbered voltage rule coefficients and even numbered current rule coefficients are determined by just one previous coefficient. The coefficients associated with the group of components furthest from the origin are determined by the furthest coefficient in the previous potential function.

Part Six: Rule Reinforcement

The rules of this form guarantee that the isolation condition will always be satisfied.

It was proven in parts three to five that if potential ϕ_k satisfies rule k , then potential ϕ_{k+1} must satisfy rule $k - 1$. Suppose now that z is a non-negative integer with $z < (k - 2)/2$. Using an identical argument to that in part three, but this time to ensure that potential ϕ_{k+2z+1} satisfies rule $k - 1$, reveals that the required condition is for rule k to be satisfied by component coefficients of potential ϕ_{k+2z} . Simply replace the coefficients ${}^k p_n^i$, ${}^k q_n^i$, ${}^k \alpha_n^i$, and ${}^k \beta_n^i$ with coefficients ${}^{k+2z} p_n^i$, ${}^{k+2z} q_n^i$, ${}^{k+2z} \alpha_n^i$, and ${}^{k+2z} \beta_n^i$, and the result follows straightforwardly because the relevant structure of potential function ϕ_{k+2z} , i.e. those components lying on the first $k - 1$ cylinders of each Y-junction branch, is like that of ϕ_k , whatever value is taken for z . This can be seen by considering the component diagrams in Figure 6.8. If k is odd, then $k + 2z$ is odd. If k is even, then $k + 2z$ is even.

As the cable is constructed, and more rules are applied, this leads to a cascading effect, with each new rule reinforcing previous rules. Consider step k , for example. Rule k will guarantee that ϕ_{k+1} satisfies rule $k - 1$. Inevitably, then, the coefficients of ϕ_{k+2} must satisfy rule $k - 2$. Potential ϕ_{k+3} must then satisfy rule $k - 3$, and so on, with ϕ_{k+r} satisfying rule $k - r$ for all $r < k - 1$. Eventually even-numbered potential function ϕ_{2k-2} must satisfy the isolation condition.

Of course, when one then moves to step $k + 1$, rule $k + 1$ ensures that potential ϕ_{k+2} satisfies rule k , which in turn ensures that ϕ_{k+3} satisfies rule $k - 1$, and so on with potential ϕ_{k+2+r} satisfying rule $k - r$.

There is continual reinforcement to ensure that the latest potential function satisfies all previous relevant rules. Component coefficients in odd numbered cable potential function ϕ_k will satisfy all odd numbered rules from 3 to k . For even numbered potential functions, the coefficients will satisfy all rules from 2 to k .

Basically, whatever the tree structure that might be encountered as one progresses with the cable construction, rule k ensures that the isolation condition is satisfied in a later potential. Figure 6.10 illustrates the reinforcement process. Further analysis of the rules will be given once terminals have been considered.

Part Seven: Conclusion and Application of Rule k

Given the results of parts one to six, the proof can now be completed.

First, assume rule $(k - 1)$ is valid. Potential ϕ_k must satisfy rule k if potential ϕ_{k+1} is to satisfy rule $k - 1$. As discussed in part six, this is sufficient to ensure that all previous rules are satisfied in later potential functions and that the isolation condition is always satisfied by even numbered potential functions.

It was explicitly shown that the third voltage- and current-like rules were of the form given above. Now consider $k = 4$. Rule four must take the given form if the component coefficients of ϕ_5 are to satisfy rule three. The validity of the remaining rules follow by

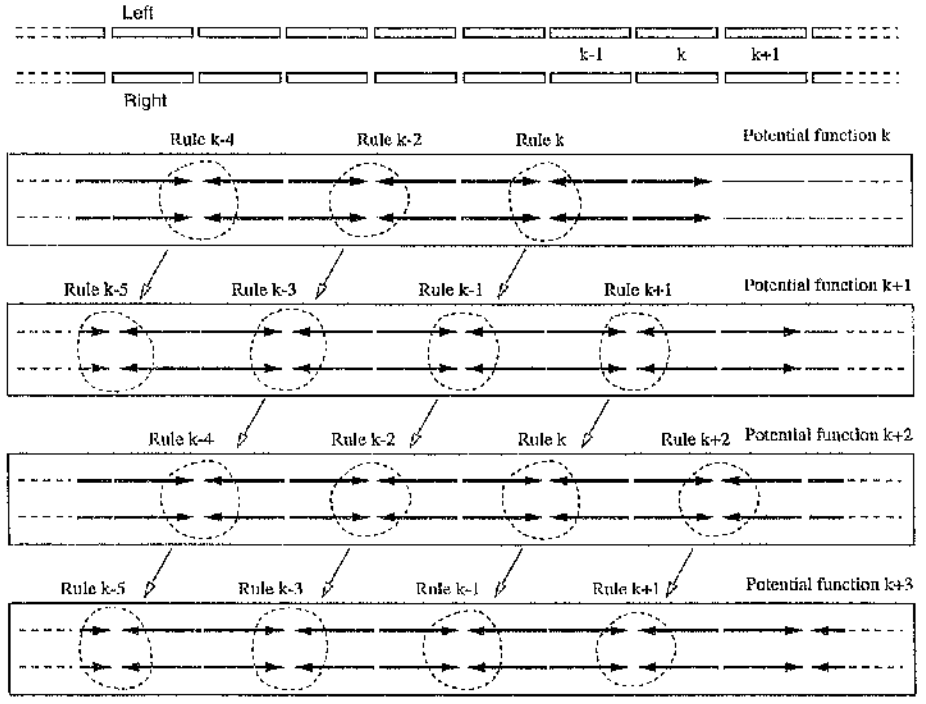


Figure 6.10: Rule reinforcement in potential functions. The circle surrounding a group of four components corresponds to the rule for which these components are the furthest from the origin, e.g. in potential function k , rule k involves the group of four components (two on each branch) that meet at a point $(k - 2)l$ from the junction, plus all components nearer to the origin. Arrows indicate the backward moving nature of rule reinforcement so that the isolation condition is always guaranteed.

induction.

To actually apply rule k and generate cable cylinder c-value c_k^G , it is necessary to replace the component coefficients in rule k (${}^k\alpha_n^i$ and ${}^k\beta_n^i$ if k is odd; ${}^kp_n^i$ and ${}^kq_n^i$ if k is even) with the coefficients from the k^{th} framework potential function, obtained by applying the electrical continuity rules to the $(k-1)^{th}$ potential function, which must have already been fully determined. The current-rule or voltage-rule coefficients are determined iteratively, initialised with those for $k = 3$.

Once c_k^G has been obtained, potential function ϕ_k can then be fully determined by substituting c_k^G into the framework potential function.

Left-right symmetry is maintained in all rules and expressions for c-values and potential functions.

Simplified Notation

Once boundary conditions are incorporated, the left-right symmetry in all previous rules and potential functions will disappear. In anticipation of this, write potential function k as a pair of separate left and right contributions.

$$\phi_k(x) = \Phi_k^L(x) + \Phi_k^R(x), \quad (6.179)$$

The isolation-termination rules can also be divided into left and right portions. Write the voltage-like form of rule k as

$${}^kV^L + {}^kV^R = 0, \quad (6.180)$$

and the current-like form of rule k as

$${}^kI^L + {}^kI^R = 0. \quad (6.181)$$

6.4.4 Cable cylinder k —

Approaching the Left Branch Termination: $k = m_L$ and $k = m_L + 1$

When $k = m_L$ or $k = m_L + 1$, the pre-terminal rules can still be applied.

When $k = m_L$, at last a component on the left branch reaches a terminal. Examination of the pre-terminal rules (6.169, 6.172, 6.175 or 6.177) at this stage reveals that they are completely independent of the boundary condition (remember that conditions (6.141) and (6.144) ensure the final term in each sum over n is zero anyway). No left branch c-values from non-existent structure beyond the terminal appear in either the rules, or the current-rule and voltage-rule coefficients. Also, of the component coefficients that would be used to generate the c-value, none have been influenced by the boundary condition. There has

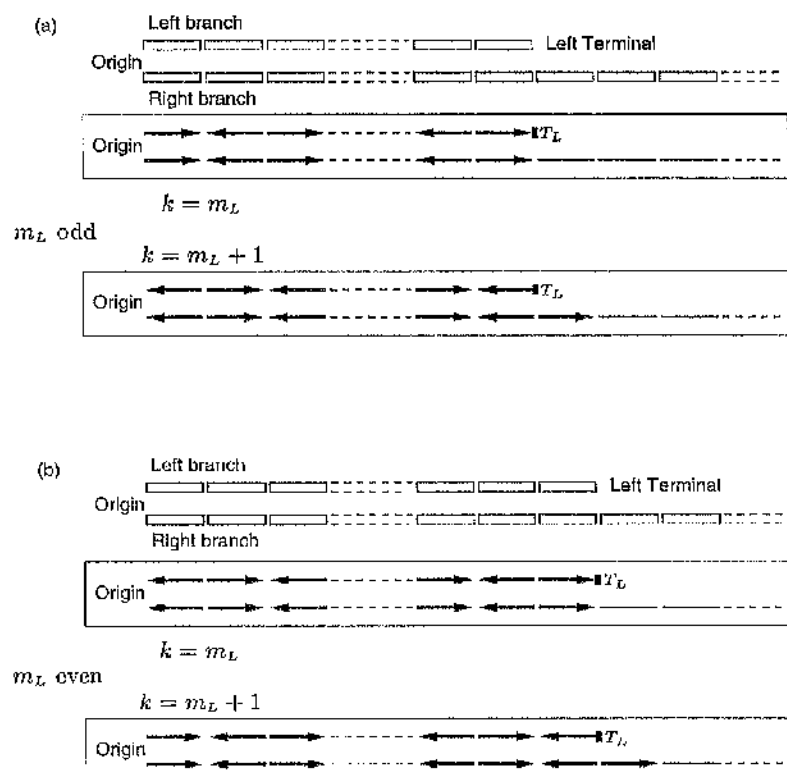


Figure 6.11: Component diagrams for the cable cylinder potential function $k = m_L$ and $k = m_L + 1$. (a) m_L is odd. (b) m_L is even.

been no opportunity for the electrical continuity rules to reflect a component from the terminal.

The situation changes slightly when $k = m_L + 1$. Again, no c-values beyond the terminal are explicitly involved in the rules. However, a component is now reflected from the left terminal, and its coefficient will indicate this fact. Thus, the form of the rule to be applied is identical to that where no terminals have been encountered, with only a single coefficient containing information about the terminal.

Moving to $k = m_L + 2$ and beyond, the rules themselves must now be adapted to account for the terminal.

6.4.5 Cable cylinder k —

Including the Left Branch Termination

It is possible to derive the rules that account for termination by adapting the proof for the pre-terminal rules and applying it to slightly altered forms of the potential functions and rules (which will be given below) with components restricted to the first m_L cylinders on the left branch and m_R cylinders on the right branch. General forms for the potential functions and rules are given in parts one and two, but parts three to seven follow those of the pre-terminal rules and it is unnecessary to repeat most of the detail.

Consider the situation where $k \geq m_L$ and $k \leq m_R$. We only consider one terminal at the moment. The treatment of the second terminal, i.e. $k > m_R$, will follow almost immediately. For convenience, we write $m = m_L$.

Note that rule one (The Rall-like condition) and rule two (isolation condition) are always the same no matter what value m_L takes.

It is essential that the boundary conditions are treated properly. The m^{th} left cylinder can be regarded as connected to cylinder $(m+1)$ (beyond the terminal) which has zero c-value if the terminal is sealed, and infinite c-value if the terminal is cut. It is then possible to write

$$\frac{c_m^L}{c_{sm}^L} = \begin{cases} 1 & T_L=S \\ 0 & T_L=C \end{cases} \quad \text{and} \quad \frac{c_{m+1}^L}{c_{sm}^L} = \begin{cases} 0 & T_L=S \\ 1 & T_L=C \end{cases}. \quad (6.182)$$

Part One: Potential Function k and Framework Potential Function $k+1$

It is necessary to take into account whether m is odd or even, as well as if k is odd or even. The potential functions now take four distinct forms, which can be extracted from the pre-terminal potential functions (6.127) and (6.129) with the sum over the left branch cut short because of the terminal. The right branch contribution to each potential is identical to that in pre-terminal potentials.

Figures 6.12a,b illustrate component diagrams for each of the four cases.

If $m \geq 1$ is odd and $k \geq m$ is odd, then $\phi_k(x)$ has the following general structure,

$$\phi_k(x) = \Phi_k^R(x) + \sum_{n=1}^{\frac{m+1}{2}} {}^k\alpha_n^L v_L(2(n-1)l+x) + {}^k\beta_n^L v_L(2nl-x). \quad (6.183)$$

where

$${}^k\beta_{\frac{m+1}{2}}^L = 0. \quad (6.184)$$

In this case, there is one component with the terminal as destination, and, as usual, it has been paired with a zero component for convenience.

If $m \geq 1$ is odd and $k \geq m+1$ is even, then $\phi_k(x)$ has the following general structure,

$$\phi_k(x) = \Phi_k^R(x) + \sum_{n=0}^{\frac{m-1}{2}} {}^k p_n^L v_L((2n-1)l+x) + {}^k q_n^L v_L((2n+1)l-x). \quad (6.185)$$

where

$${}^k p_0^L = 0. \quad (6.186)$$

Here, no components end on the terminal, but two components meet as the origin and are paired with zero components.

If $m \geq 2$ is even and $k \geq m+1$ is odd, then $\phi_k(x)$ has the following general structure,

$$\phi_k(x) = \Phi_k^R(x) + \sum_{n=1}^{\frac{m}{2}} {}^k\alpha_n^L v_L(2(n-1)l+x) + {}^k\beta_n^L v_L(2nl-x). \quad (6.187)$$

In this case, there are no components with the junction or terminal as destination.

If $m \geq 2$ is even and $k \geq m$ is even, then $\phi_k(x)$ has the following general structure,

$$\phi_k(x) = \Phi_k^R(x) + \sum_{n=0}^{\frac{m}{2}} {}^k p_n^L v_L((2n-1)l+x) + {}^k q_n^L v_L((2n+1)l-x). \quad (6.188)$$

where

$${}^k p_0^L = 0 \quad \text{and} \quad {}^k q_{\frac{m}{2}}^L = 0. \quad (6.189)$$

In this final case, two components meet at the origin, and a component also reaches the terminal, so there are three zero components.

Now apply the electrical continuity rules to generate ϕ_{k+1} and observe the situations in which there is reflection from the terminal. The isolation condition is always assumed

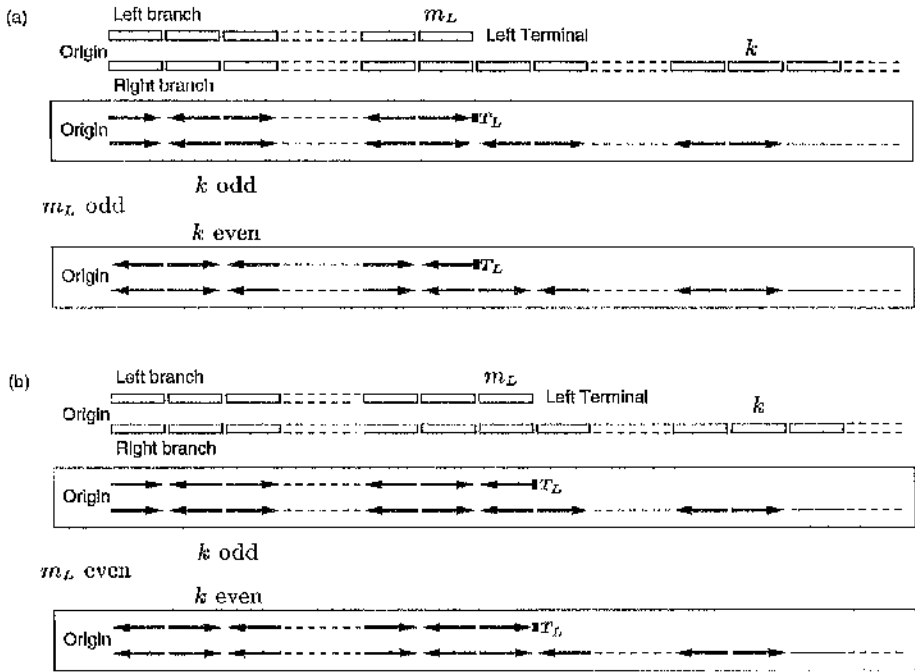


Figure 6.12: Component diagrams for the cable cylinder potential functions with $k > m_L$.
(a) m_L odd; (b) m_L even.

to hold.

If m is odd and k is odd, then $k+1$ is even and ϕ_{k+1} takes the form of equation (6.185) with $k+1$ replacing k ,

$$\phi_{k+1}(x) = \Phi_{k+1}^L(x) + \sum_{n=0}^{\frac{m-1}{2}} {}^{k+1}p_n^L v_L((2n-1)l+x) + {}^{k+1}q_n^L v_L((2n+1)l-x), \quad (6.190)$$

where

$${}^{k+1}p_n^L = \begin{cases} 0 & n=0 \\ \frac{c_{2n}^L}{c_{s(2n-1)}^L} \left[\left(1 + \frac{c_k^C}{c_{k+1}^L}\right) {}^k\alpha_n^L + \left(1 - \frac{c_k^C}{c_{k+1}^L} \frac{c_{2n-1}^L}{c_{2n}^L}\right) {}^k\beta_n^L \right] & 1 \leq n \leq \frac{(m-1)}{2} \end{cases} \quad (6.191)$$

and

$${}^{k+1}q_{n-1}^L = \begin{cases} \frac{c_{2n-1}^L}{c_{s(2n-1)}^L} \left[\left(1 - \frac{c_k^C}{c_{k+1}^L} \frac{c_{2n}^L}{c_{2n-1}^L}\right) {}^k\alpha_n^L + \left(1 + \frac{c_k^C}{c_{k+1}^L}\right) {}^k\beta_n^L \right] & 1 \leq n \leq \frac{m-1}{2} \\ \frac{{}^k\alpha_{\frac{m+1}{2}}^L}{c_{k+1}^L} & n = \frac{m+1}{2}, \quad T_L=S \\ -\frac{c_k^C}{c_{k+1}^L} {}^k\alpha_{\frac{m+1}{2}}^L & n = \frac{m+1}{2}, \quad T_L=C \end{cases} \quad (6.192)$$

If m is odd and k is even, then $k+1$ is odd and ϕ_{k+1} takes the form of equation (6.183) with $k+1$ replacing k ,

$$\phi_{k+1}(x) = \Phi_{k+1}^R(x) + \sum_{n=1}^{\frac{m+1}{2}} {}^{k+1}\alpha_n^L v_L(2(n-1)l+x) + {}^{k+1}\beta_n^L v_L(2nl-x), \quad (6.193)$$

where

$${}^{k+1}\alpha_n^L = \begin{cases} -\frac{c_k^C}{c_{k+1}^C} {}^k q_0^L & n = 1 \\ \frac{c_{2n-1}^L}{c_{s(2n-1)}^L} \left[\left(1 + \frac{c_k^C}{c_{k+1}^C} \right) {}^k p_{n-1}^L + \left(1 - \frac{c_k^C}{c_{k+1}^C} \frac{c_{2(n-1)}^L}{c_{2n-1}^L} \right) {}^k q_{n-1}^L \right] & 2 \leq n \leq \frac{m+1}{2} \end{cases} \quad (6.194)$$

and

$${}^{k+1}\beta_n^L = \begin{cases} \frac{c_{2n}^L}{c_{s(2n)}^L} \left[\left(1 - \frac{c_k^C}{c_{k+1}^C} \frac{c_{2n-1}^L}{c_{2n}^L} \right) {}^k p_n^L + \left(1 + \frac{c_k^C}{c_{k+1}^C} \right) {}^k q_n^L \right] & 1 \leq n \leq \frac{m-1}{2} \\ 0 & n = \frac{m+1}{2} \end{cases} \quad (6.195)$$

If m is even and k is odd, then $k+1$ is even and ϕ_{k+1} takes the form of equation (6.188) with $k+1$ replacing k ,

$$\phi_{k+1}(x) = \Phi_{k+1}^R(x) + \sum_{n=0}^{\frac{m}{2}} {}^{k+1}p_n^L v_L((2n-1)l+x) + {}^{k+1}q_n^L v_L((2n+1)l-x), \quad (6.196)$$

where

$${}^{k+1}p_n^L = \begin{cases} 0 & n = 0 \\ \frac{c_{2n}^L}{c_{s(2n-1)}^L} \left[\left(1 + \frac{c_k^C}{c_{k+1}^C} \right) {}^k \alpha_n^L + \left(1 - \frac{c_k^C}{c_{k+1}^C} \frac{c_{2n-1}^L}{c_{2n}^L} \right) {}^k \beta_n^L \right] & 1 \leq n \leq \frac{m}{2} \end{cases} \quad (6.197)$$

and

$${}^{k+1}q_{n-1}^L = \begin{cases} \frac{c_{2n-1}^L}{c_{s(2n-1)}^L} \left[\left(1 - \frac{c_k^C}{c_{k+1}^C} \frac{c_{2n-1}^L}{c_{2n}^L} \right) {}^k \alpha_n^L + \left(1 + \frac{c_k^C}{c_{k+1}^C} \right) {}^k \beta_n^L \right] & 1 \leq n \leq \frac{m}{2} \\ 0 & n = \frac{m+2}{2} \end{cases} \quad (6.198)$$

If m is even and k is even, then $k+1$ is odd and ϕ_{k+1} takes the form of equation (6.183) with $k+1$ substituting k ,

$$\phi_{k+1}(x) = \Phi_{k+1}^R(x) + \sum_{n=1}^{\frac{m}{2}} {}^{k+1}\alpha_n^L v_L(2(n-1)l+x) + {}^{k+1}\beta_n^L v_L(2nl-x). \quad (6.199)$$

where

$${}^{k+1}\alpha_n^L = \begin{cases} -\frac{c_k^C}{c_{k+1}^C} {}^k q_0^L & n = 1 \\ \frac{c_{2n-1}^L}{c_{s(2n-1)}^L} \left[\left(1 + \frac{c_k^C}{c_{k+1}^C} \right) {}^k p_{n-1}^L + \left(1 - \frac{c_k^C}{c_{k+1}^C} \frac{c_{2(n-1)}^L}{c_{2n-1}^L} \right) {}^k q_{n-1}^L \right] & 2 \leq n \leq \frac{m}{2} \end{cases} \quad (6.200)$$

and

$${}^k\beta_n^L = \begin{cases} \frac{c_{2n}^L}{c_{s(2n)}^L} \left[\left(1 - \frac{c_k^C}{c_{k+1}^C} \frac{c_{2n+1}^L}{c_{2n}^L} \right) {}^k p_n^L + \left(1 + \frac{c_k^C}{c_{k+1}^C} \right) {}^k q_n^L \right] & 1 \leq n \leq \frac{(m-2)}{2} \\ \frac{{}^k p_{\frac{m}{2}}^L}{-\frac{c_k^C}{c_{k+1}^C} {}^k p_{\frac{m}{2}}^L} & n = \frac{m}{2}, \quad T_L=S \\ & n = \frac{m}{2}, \quad T_L=C \end{cases} \quad (6.201)$$

The terminal type only has a direct influence on framework potential ϕ_{k+1} when k and m are both odd or both even.

Part Two: Voltage and Current Forms of Rule k

We now suppose the voltage- and current-like versions of rule k take the forms given below. They can be obtained from the pre-terminal rules (6.169), (6.172), (6.175) and (6.177) with the left sum cut short due to the terminal. The right branch contribution is written below in simplified form. We shall only consider the case where $m_L \geq 2$. When $m_L = 1$, extra care must be made to fit the rules into the general framework. This situation is dealt with much more easily in Chapter 7 concerning the branch-shifting method of cable construction.

If m is odd and $m \geq 3$, k is odd and $k \geq m$, then the voltage-like form of rule k is

$${}^k V^L + \sum_{n=1}^{\frac{m+1}{2}} \left({}^k \alpha_n^L + {}^k \beta_n^L \right) {}^k E_n^L = 0. \quad (6.202)$$

The current-like rule is

$${}^k I^L + \sum_{n=1}^{\frac{m+1}{2}} \left(-\frac{c_{2n}^L}{c_{s(2n-1)}^L} {}^k \alpha_n^L + \frac{c_{2n-1}^L}{c_{s(2n-1)}^L} {}^k \beta_n^L \right) {}^k F_n^L = 0, \quad (6.203)$$

Remember that ${}^k \beta_{\frac{m+1}{2}}^L = 0$. For the case $k = m$, where the boundary condition is not yet relevant, ${}^k E_{\frac{m+1}{2}}^L = 0$ and ${}^k F_{\frac{m+1}{2}}^L = 0$, as with the pre-terminal rules. These conditions will not necessarily hold when $k \geq m+2$.

It is useful to take into account condition (6.182) and rewrite the current-like rule,

$${}^k I^L = \sum_{n=1}^{\frac{m-1}{2}} \left(-\frac{c_{2n}^L}{c_{s(2n-1)}^L} {}^k \alpha_n^L + \frac{c_{2n-1}^L}{c_{s(2n-1)}^L} {}^k \beta_n^L \right) {}^k F_n^L - \begin{cases} 0 & T_L=S \\ {}^k \alpha_{\frac{m+1}{2}}^L {}^k F_{\frac{m+1}{2}}^L & T_L=C \end{cases} \quad (6.204)$$

If m is odd and $m \geq 3$, k is even and $k \geq m+1$, then the voltage-like form of rule k is

$${}^k V^R + \sum_{n=1}^{\frac{m-1}{2}} \left({}^k p_n^L + {}^k q_n^L \right) {}^k E_n^L = 0. \quad (6.205)$$

The current-like rule is

$${}^k I^R + \sum_{n=1}^{\frac{m-1}{2}} \left(-\frac{c_{2n+1}^L}{c_{s2n}^L} {}^k p_n^L + \frac{c_{2n}^L}{c_{s2n}^L} {}^k q_n^L \right) {}^k F_n^L + {}^k q_0^L {}^k F_0^L = 0. \quad (6.206)$$

If m is even and $m \geq 2$, k is odd and $k \geq m+1$, then the voltage-like form of rule k is

$${}^k V^R + \sum_{n=1}^{\frac{m}{2}} \left({}^k \alpha_n^L + {}^k \beta_n^L \right) {}^k E_n^L = 0, \quad (6.207)$$

while the current-like form is

$${}^k I^R + \sum_{n=1}^{\frac{m}{2}} \left(-\frac{c_{2n}^L}{c_{s(2n-1)}^L} {}^k \alpha_n^L + \frac{c_{2n-1}^L}{c_{s(2n-1)}^L} {}^k \beta_n^L \right) {}^k F_n^L = 0. \quad (6.208)$$

If m is even and $m \geq 2$, k is even and $k \geq m$ then the voltage-like form of rule k is

$${}^k V^R + \sum_{n=1}^{\frac{m}{2}} \left({}^k p_n^L + {}^k q_n^L \right) {}^k E_n^L = 0, \quad (6.209)$$

while the current-like form is

$${}^k I^R + \sum_{n=1}^{\frac{m}{2}} \left(-\frac{c_{2n+1}^L}{c_{s2n}^L} {}^k p_n^L + \frac{c_{2n}^L}{c_{s2n}^L} {}^k q_n^L \right) {}^k F_n^L + {}^k q_0^L {}^k F_0^L = 0. \quad (6.210)$$

Remember that ${}^k q_{\frac{m}{2}}^L = 0$. For the case $k = m$, where the boundary condition is not yet relevant, ${}^k E_{\frac{m}{2}}^L = 0$ and ${}^k F_{\frac{m}{2}}^L = 0$. These conditions don't necessarily hold when $k \geq m+2$.

Once more, the current-like rule can be rewritten by taking into account the terminal conditions (6.182). If $m = 2$ then

$${}^k I^L = {}^k q_0^L {}^k F_0^L - \begin{cases} 0 & T_L=S \\ {}^k p_1^L {}^k F_1^L & T_L=C \end{cases}. \quad (6.211)$$

Otherwise $m \geq 4$ and

$${}^k I^L = \sum_{n=1}^{\frac{m-2}{2}} \left(-\frac{c_{2n+1}^L}{c_{s2n}^L} {}^k p_n^L + \frac{c_{2n}^L}{c_{s2n}^L} {}^k q_n^L \right) {}^k F_n^L + {}^k q_0^L {}^k F_0^L - \begin{cases} 0 & T_L=S \\ {}^k p_{\frac{m}{2}}^L {}^k F_{\frac{m}{2}}^L & T_L=C \end{cases}. \quad (6.212)$$

Observe how, in each of the rules above, coefficients of components that end on a cut terminal, or have the origin as destination, are not involved in the voltage-like rules. Similarly, coefficient of components that end on a sealed terminal are not involved in the current-like rules.

It remains now to show that the rules must always take the form set out above, and to find expressions that relate the current-rule and voltage-rule coefficients so they may be determined iteratively.

Part Three to Part Seven

The remaining derivation of the post-terminal rules follows the same pattern as the derivation of the pre-terminal rules.

As before, all forms of rule k are found by requiring that potential function ϕ_{k+1} satisfies rule $k - 1$. Again, only the voltage-like forms of rule $k - 1$ need be used. This will generate an expression for rule k in the form $M + (c_k^G/c_{k+1}^G)N$, where M is the voltage-like rule and N is the current-like rule.

Once more, it can be shown that $M = N$ by taking advantage of coefficient conservation and the fact that rule $k - 1$ has been satisfied by potential ϕ_{k-1} . The procedure works for both current injection and cut terminal boundary conditions.

Yet again, re-order the sums in the resulting expressions and extract the voltage-like (from M) and current-like (from N) rules. These rules can be found in the full isolation-termination rules summary of section 6.4.7.

Each new rule still reinforces previous rules in later potential functions so that potential function ϕ_k where k is odd satisfies all odd numbered rules from 3 to k , and where k is even satisfies all even numbered rules from 2 to k .

Note that the pre-terminal version of rule $m + 1$ is identical to the post-terminal version of rule $m + 1$ in every case. At this point, either can be used. The transition from pre-terminal to post-terminal is smooth, and the mathematical induction progresses straightforwardly, initialised for post-terminal rules by rule $m + 1$.

6.4.6 Cable Cylinder k —

Beyond Both Left and Right Terminals

The left and right Y-junction branches contribute independently to the voltage- and current-like rules, i.e. the form of the left branch contribution does not depend on structure in the right branch. If one derived the rules for $k > m_R$ using the same approach as

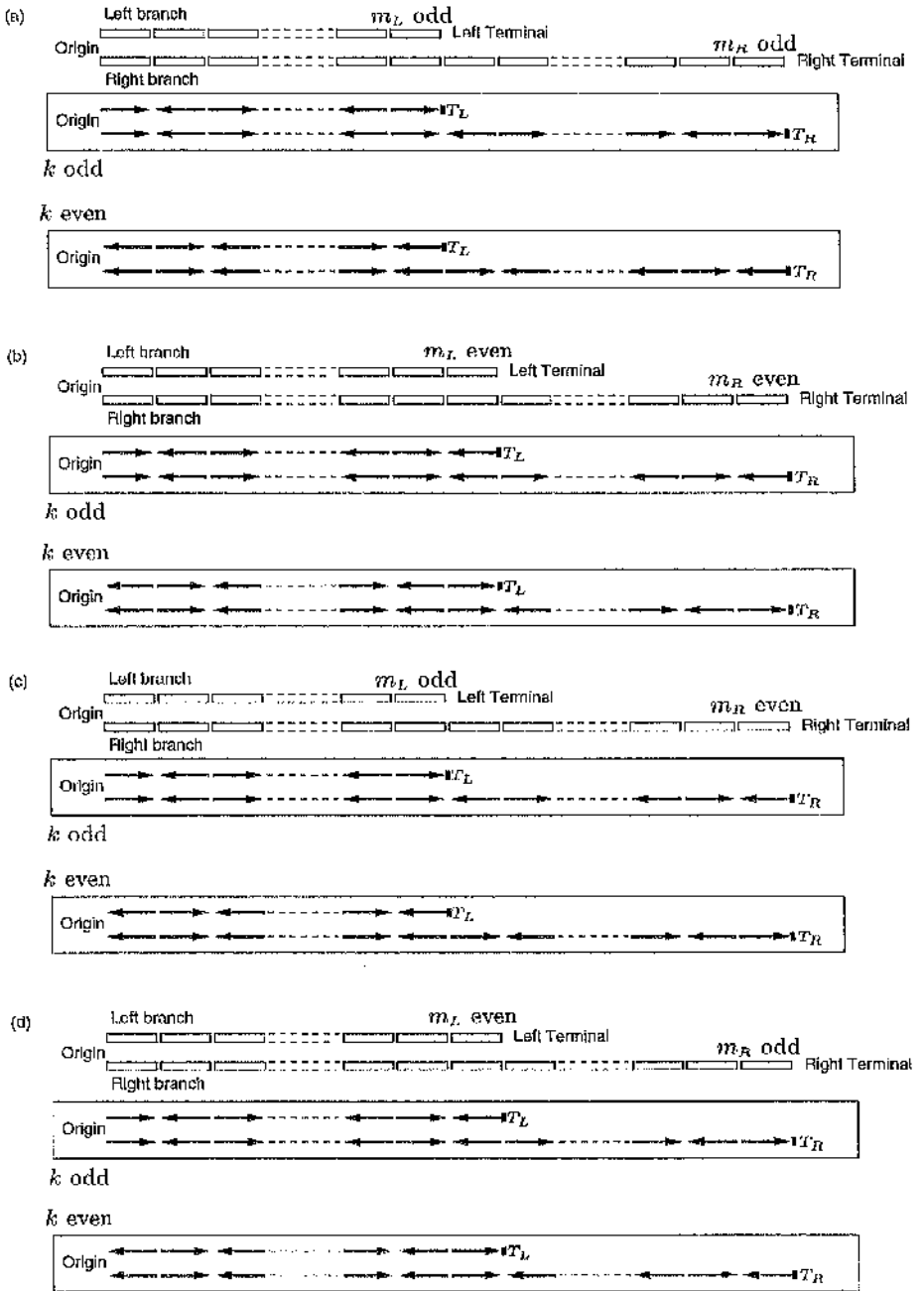


Figure 6.13: Component diagrams for the cable cylinder potential functions with $k > m_L, m_R$. (a) m_L odd, m_R odd; (b) m_L even, m_R even. (c) m_L odd, m_R even. (d) m_L even, m_R odd.

above, it would emerge that the right branch post-terminal contribution is similar to the left branch post-terminal contribution, of course with R replacing L , and so m_R replacing m_L .

The purpose of all rules, both pre- and post-terminal is to ensure rule reinforcement is maintained, even though when $k > m_k + 1$ enough rules are already satisfied to ensure that the isolation condition will always hold. Since rule k ensures that potential ϕ_{2k-2} satisfies the isolation condition, if $k > m_R + 1$ then $2k - 2 > 2m_R \geq m_L + m_R$. The reinforcement procedure is now ensuring isolation in cable cylinders that will never actually exist. If the isolation condition were the only condition we wished to maintain, then perhaps alternative rules could be employed now. However, it is the rule-reinforcement structure that is necessary to ensure eventual termination, and subsequent construction of disconnected sections, rather than just one specific rule. It is vital that all odd rules are satisfied in odd potentials and all even rules are satisfied in even potentials, otherwise there is no way to guarantee termination.

6.4.7 Full Isolation-Termination Rules Summary ($m_L, m_R \geq 2$)

In general, the voltage-like form of rule k can be expressed

$$\sum_{i=L,R} {}^k V^i = 0, \quad (6.213)$$

and the current-like form of rule k can be expressed

$$\sum_{i=L,R} {}^k I^i = 0. \quad (6.214)$$

Rule k is applied to the framework potential ϕ_k to generate the c-value c_k^c . To understand termination and construction of the disconnected sections, the rule structure is considered in greater detail in following subsections. For $m_L, m_R \geq 2$, the rules are divided into the following categories. (For $m_L = 1$ or $m_R = 1$, the branch shifting method described in Chapter 7 can be used.)

A. Universal Conditions: $k = 1, k = 2, k = 3$

The first three rules always take the same form, whatever the structure of the Y-junction. Trivially, rule one is the Rall-like condition, while rule two is the isolation condition,

$${}^2 V^i = {}^2 q_0^i. \quad (6.215)$$

Rule three is of the general form summarised below, and is used to initialise the voltage-rule and current-rule coefficients.

B. Pre-terminal Conditions: $k \leq m_i + 1$ and k is odd

The contribution from branch i to the voltage-like form of rule k is

$${}^k V^i = \sum_{n=1}^{\frac{k+1}{2}} \left({}^k \alpha_n^i + {}^k \beta_n^i \right) {}^k E_n^i. \quad (6.216)$$

If $k = 3$ then

$${}^3 E_1^i = \frac{c_1^i}{c_{s1}^i} \quad \text{and} \quad {}^3 E_2^i = 0. \quad (6.217)$$

Otherwise, $k \geq 5$ and

$${}^k E_n^i = \begin{cases} [{}^{k-1} E_1^i] \frac{c_2^i}{c_{s1}^i} & n = 1 \\ [{}^{k-1} E_n^i] \frac{c_{2n}^i}{c_{s(2n-1)}^i} + [{}^{k-1} E_{n-1}^i] \frac{c_{2n-1}^i}{c_{s(2n-1)}^i} & 2 \leq n \leq \frac{k-1}{2} \\ 0 & n = \frac{k+1}{2} \end{cases}. \quad (6.218)$$

The contribution from branch i to the current-like form of rule k is

$${}^k I^i = \sum_{n=1}^{\frac{k+1}{2}} \left(-\frac{c_{2n}^i}{c_{s(2n-1)}^i} {}^k \alpha_n^i + \frac{c_{2n-1}^i}{c_{s(2n-1)}^i} {}^k \beta_n^i \right) {}^k F_n^i. \quad (6.219)$$

If $k = 3$ then

$${}^3 F_1^i = 1 \quad \text{and} \quad {}^3 F_2^i = 0. \quad (6.220)$$

Otherwise, $k \geq 5$ and

$${}^k F_n^i = \begin{cases} -[{}^{k-1} E_1^i] & n = 1 \\ -[{}^{k-1} E_n^i] + [{}^{k-1} E_{n-1}^i] & 2 \leq n \leq \frac{k-1}{2} \\ 0 & n = \frac{k+1}{2} \end{cases}. \quad (6.221)$$

Remember that ${}^k \beta_{\frac{k+1}{2}}^i = 0$.

C. Pre-terminal Conditions: $k \leq m_i + 1$ and k is even

The contribution from branch i to the voltage-like form of rule k is

$${}^k V^i = \sum_{n=1}^{\frac{k}{2}} \left({}^k p_n^i + {}^k q_n^i \right) {}^k E_n^i. \quad (6.222)$$

If $k \geq 4$, then

$${}^k E_n^i = \begin{cases} [{}^{k-1} E_{n+1}^i] \frac{c_{2n+1}^i}{c_{s(2n)}^i} + [{}^{k-1} E_n^i] \frac{c_{2n}^i}{c_{s(2n)}^i} & 1 \leq n \leq \frac{k-2}{2} \\ 0 & n = \frac{k}{2} \end{cases}. \quad (6.223)$$

Note that the coefficients of the two components that meet at the origin are not involved in this expression. The isolation condition has already ensured that ${}^k q_0^L = -{}^k q_0^R$ so these two components will automatically satisfy a cut terminal at $x = l$.

The contribution from branch i to the current-like form of rule k is

$${}^k \mathcal{I}^i = \sum_{n=1}^{\frac{k}{2}} \left(-\frac{c_{2n+1}^i}{c_{s(2n)}^i} {}^k p_n^i + \frac{c_{2n}^i}{c_{s(2n)}^i} {}^k q_n^i \right) {}^k F_n^i + {}^k q_0^i {}^k F_0^i. \quad (6.224)$$

If $k \geq 4$, then

$${}^k F_n^i = \begin{cases} -[{}^{k-1} E_1^i] & n = 0 \\ [{}^{k-1} E_n^i] - [{}^{k-1} E_{n+1}^i] & 1 \leq n \leq \frac{k-2}{2} \\ 0 & n = \frac{k}{2} \end{cases}. \quad (6.225)$$

Note that the coefficients of the two components that meet at the origin do contribute to this expression. The isolation condition has already ensured that ${}^k q_0^L = -{}^k q_0^R$ so that these two components can only satisfy a cut terminal at $x = l$. The only way in which a current injection condition could be satisfied when k is even is if ${}^k q_0^L = {}^k q_0^R = 0$.

Remember that ${}^k q_{\frac{k}{2}}^i = 0$.

D. Post-terminal Conditions: m_i is odd and k is odd, $k \geq m_i + 2$

The contribution from branch i to the voltage-like form of rule k is

$${}^k \mathcal{V}^i = \sum_{n=1}^{\frac{m_i+1}{2}} \left({}^k \alpha_n^i + {}^k \beta_n^i \right) {}^k E_n^i. \quad (6.226)$$

If $m_i = 3$ then

$${}^k E_n^i = \begin{cases} [{}^{k-1} E_1^i] \frac{c_2^i}{c_{s1}^i} & n = 1 \\ [{}^{k-1} E_1^i] & n = 2, \quad T_i = S \\ 0 & n = 2, \quad T_i = C \end{cases}. \quad (6.227)$$

Otherwise, $m_i \geq 5$ and

$${}^k E_n^i = \begin{cases} [{}^{k-1} E_1^i] \frac{c_2^i}{c_{s1}^i} & n = 1 \\ [{}^{k-1} E_n^i] \frac{c_{2n}^i}{c_{s(2n-1)}^i} + [{}^{k-1} E_{n-1}^i] \frac{c_{2n-1}^i}{c_{s(2n-1)}^i} & 2 \leq n \leq \frac{m_i-1}{2} \\ [{}^{k-1} E_{\frac{m_i-1}{2}}^i] & n = \frac{m_i+1}{2}, \quad T_i = S \\ 0 & n = \frac{m_i+1}{2}, \quad T_i = C \end{cases}. \quad (6.228)$$

The contribution from branch i to the current-like form of rule k is

$${}^k \mathcal{I}^i = \sum_{n=1}^{\frac{m_i+1}{2}} \left(-\frac{c_{2n}^i}{c_{s(2n-1)}^i} {}^k \alpha_n^i + \frac{c_{2n-1}^i}{c_{s(2n-1)}^i} {}^k \beta_n^i \right) {}^k F_n^i. \quad (6.229)$$

If $m_i = 3$, then

$${}^k F_n^i = \begin{cases} -[{}^{k-1} E_1^i] & n = 1 \\ [{}^{k-1} E_1^i] & n = 2, \quad T_L = C \\ 0 & n = 2, \quad T_L = S \end{cases}. \quad (6.230)$$

Otherwise, $m_i \geq 5$ and

$${}^k F_n^i = \begin{cases} -[{}^{k-1} E_1^i] & n = 1 \\ -[{}^{k-1} E_n^i] + [{}^{k-1} E_{n-1}^i] & 2 \leq n \leq \frac{m_i-1}{2} \\ [{}^{k-1} E_{\frac{m_i+1}{2}}^i] & n = \frac{m_i+1}{2}, \quad T_L = C \\ 0 & n = \frac{m_i+1}{2}, \quad T_L = S \end{cases}. \quad (6.231)$$

Remember that ${}^k \beta_{\frac{m_i+1}{2}}^i = 0$.

E. Post-terminal Conditions: m_i is odd and k is even, $k \geq m_i + 1$

The contribution from branch i to the voltage-like rule is

$${}^k V^i = \sum_{n=1}^{\frac{m_i-1}{2}} \left({}^k p_n^i + {}^k q_n^i \right) {}^k E_n^i. \quad (6.232)$$

If $m \geq 3$ then

$${}^k E_n^i = [{}^{k-1} E_{n+1}^i] \frac{c_{2n+1}^i}{c_{s(2n)}^i} + [{}^{k-1} E_n^i] \frac{c_{2n}^i}{c_{s(2n)}^i} \quad 1 \leq n \leq \frac{m_i-1}{2}. \quad (6.233)$$

The contribution from branch i to the current-like rule is

$${}^k I^i = \sum_{n=1}^{\frac{m_i-1}{2}} \left(-\frac{c_{2n+1}^i}{c_{s(2n)}^i} {}^k p_n^i + \frac{c_{2n}^i}{c_{s(2n)}^i} {}^k q_n^i \right) {}^k F_n^i + {}^k q_0^i {}^k F_0^i. \quad (6.234)$$

If $m_i \geq 3$, then

$${}^k F_n^i = \begin{cases} -[{}^{k-1} E_1^i] & n = 0 \\ [{}^{k-1} E_n^i] - [{}^{k-1} E_{n+1}^i] & 1 \leq n \leq \frac{m_i-1}{2} \end{cases}. \quad (6.235)$$

F. Post-terminal Conditions: m_i is even and k is odd, $k \geq m_i + 1$

The contribution from branch i to the voltage-like rule is

$${}^k V^i = \sum_{n=1}^{\frac{m_i}{2}} \left({}^k \alpha_n^i + {}^k \beta_n^i \right) {}^k E_n^i. \quad (6.236)$$

If $m_i = 2$, then

$${}^k E_1^i = \left[{}^{k-1} E_1^i \right] \frac{c_{s1}^i}{c_{s1}^i}. \quad (6.237)$$

Otherwise, $m_i \geq 4$ and

$${}^k E_n^i = \begin{cases} \left[{}^{k-1} E_1^i \right] \frac{c_{s1}^i}{c_{s1}^i} & n = 1 \\ \left[{}^{k-1} E_n^i \right] \frac{c_{s(2n-1)}^i}{c_{s(2n-1)}^i} + \left[{}^{k-1} E_{n-1}^i \right] \frac{c_{s(2n-1)}^i}{c_{s(2n-1)}^i} & 2 \leq n \leq \frac{m_i}{2} \end{cases} \quad (6.238)$$

The contribution from branch i to the current-like form of rule k is

$${}^k \mathcal{I}^i = \sum_{n=1}^{\frac{m_i}{2}} \left(-\frac{c_{2n}^i}{c_{s(2n-1)}^i} {}^k \alpha_n^i + \frac{c_{2n-1}^i}{c_{s(2n-1)}^i} {}^k \beta_n^i \right) {}^k F_n^i. \quad (6.239)$$

If $m_i = 2$, then

$${}^k F_1^i = - \left[{}^{k-1} E_1^i \right]. \quad (6.240)$$

Otherwise, $m_i \geq 4$ and

$${}^k F_n^i = \begin{cases} - \left[{}^{k-1} E_1^i \right] & n = 1 \\ - \left[{}^{k-1} E_n^i \right] + \left[{}^{k-1} E_{n-1}^i \right] & 2 \leq n \leq \frac{m_i}{2} \end{cases} \quad (6.241)$$

G. Post-terminal Conditions: m_i is even and k is even, $k \geq m_i + 2$

The contribution from branch i to the voltage-like form of rule k is

$${}^k \mathcal{V}^R + \sum_{n=1}^{\frac{m_i}{2}} \left({}^k p_n^i + {}^k q_n^i \right) {}^k E_n^i = 0. \quad (6.242)$$

If $m_i = 2$, then

$${}^k E_n^i = \begin{cases} \left[{}^{k-1} E_1^i \right] & n = 1, \quad T_i = S \\ 0 & n = 1, \quad T_i = C \end{cases} \quad (6.243)$$

Otherwise, $m_i \geq 4$ and

$${}^k E_n^i = \begin{cases} \left[{}^{k-1} E_{n-1}^i \right] \frac{c_{s(2n)}^i}{c_{s(2n)}^i} + \left[{}^{k-1} E_n^i \right] \frac{c_{s(2n)}^i}{c_{s(2n)}^i} & 1 \leq n \leq \frac{m_i-2}{2} \\ \left[{}^{k-1} E_{\frac{m_i}{2}}^i \right] & n = \frac{m_i}{2}, \quad T_i = S \\ 0 & n = \frac{m_i}{2}, \quad T_i = C \end{cases} \quad (6.244)$$

The current-like rule is

$${}^k \mathcal{I}^R + \sum_{n=1}^{\frac{m_i}{2}} \left(-\frac{c_{2n-1}^i}{c_{s(2n)}^i} {}^k p_n^i + \frac{c_{2n}^i}{c_{s(2n)}^i} {}^k q_n^i \right) {}^k F_n^i + {}^k q_0^i {}^k F_0^i = 0, \quad (6.245)$$

If $m_i = 2$, then

$${}^k F_n^i = \begin{cases} -[{}^{k-1} E_1^i] & n = 0 \\ [{}^{k-1} E_1^i] & n = 1, \quad T_L = C \\ 0 & n = 1, \quad T_L = S \end{cases} . \quad (6.246)$$

Otherwise, $m \geq 4$ and

$${}^k F_n^i = \begin{cases} -[{}^{k-1} E_1^i] & n = 0 \\ [{}^{k-1} E_n^i] - [{}^{k-1} E_{n+1}^i] & 1 \leq n \leq \frac{m_i-2}{2} \\ [{}^{k-1} E_{\frac{m_i}{2}}^i] & n = \frac{m_i}{2}, \quad T_i = C \\ 0 & n = \frac{m_i}{2}, \quad T_i = S \end{cases} . \quad (6.247)$$

Remember that ${}^k q_{\frac{m_i}{2}}^i = 0$.

6.4.8 Termination and Disconnected Sections

With the rules that have been developed so far one can construct, cylinder by cylinder, the fully equivalent cable for a general Y-junction. Apply the electrical continuity rules to generate a framework potential, then apply the isolation-termination rules to determine cylinder c-values and fix the potential function.

If one does this, then eventually the process terminates at the end of a cable cylinder, n say, and the connected section is produced, simply because eventually the component weights for potential function ϕ_n turn out to be just right for termination. Basically, for each component pair, the two components will have the same magnitude but opposite sign (for satisfying an overall cut end) or their ratio will equal the ratio of their respective cylinder c-values (so that an overall current condition can be satisfied). Of course, an additional requirement for proper overall termination is that non-zero single components cannot end on a cut terminal when the overall terminal condition is sealed, and vice-versa; it has previously been noted that a sealed terminal could never be achieved when k is even unless the two components ending at the origin have zero coefficient.

How, though, do the isolation-termination rules guarantee this termination, and how are disconnected sections determined for degenerate Y-junctions. The key lies in a further examination of the structure of the voltage-like and current-like rules.

Counting Rules and Components — Cable Predictions

As the number, k say, of generated potential functions increases, then for both the odd-numbered and even-numbered rules the number of components involved in potential k increases until both left and right terminals have been reached. Once the terminals have

been reached (when $k = m_R$ in fact), however, subsequent potentials cannot involve any more than $m_L + m_R$ components. Consequently, the number of components involved in the voltage- and current-like rules must reach a maximum. Consider the structure of post-terminal potential functions, as already illustrated in Figure 6.13. For a specific m_L and m_R , all even-numbered potential functions will have the same general component structure, as will all odd-numbered potential functions. Of course, component weights will vary between two structurally similar, but different numbered, potential functions.

Meanwhile, as k increases beyond m_R , the number of rules that describe the structure of the components will still increase. Recall that all odd-numbered rules from 3 to k apply to the component coefficients of odd-numbered potential k , while all even-numbered rules from 2 to k apply to the component coefficients of even-numbered potential k . It is simple enough to count them, revealing that k -odd potential functions satisfy $(k - 1)/2$ rules, while k -even potential functions satisfy $k/2$ rules, including the isolation condition.

Now consider once again the form of the voltage-like (6.226, 6.232, 6.236, 6.242) and current-like rules (6.229, 6.234, 6.239, 6.245). Each voltage-like rule is essentially a linear combination of component pairs sums plus the occasional single component (or two). Each current-like rule takes a similar form, but is a linear combination of weighted component differences, again with the occasional single component (or two), and also possibly a pair of components that meet at the origin. (In the forms given for the rules, the terminal components are actually paired with zero components for convenience.)

It is straightforward to determine from the construction rules (voltage and current), that *for each branch i* the following number of components pairs and singles are involved

in the rules for post-terminal potential function k ,

$$\begin{aligned}
 & \text{component pairs (voltage)} \quad = \quad \begin{cases} \frac{m_i-1}{2} & m_i \text{ odd, } k \text{ odd or even} \\ \frac{m_i}{2} & m_i \text{ even, } k \text{ odd} \\ \frac{m_i-2}{2} & m_i \text{ even, } k \text{ even} \end{cases} \\
 & \text{or component differences (current)} \\
 & \text{origin components} \quad = \quad \begin{cases} 0 & k \text{ odd} \\ 1 & k \text{ even,} \end{cases} \\
 & \text{for current-like rules} \\
 & \text{(always zero for voltage-like)} \\
 & \text{number of} \quad = \quad \begin{cases} 0 & T_i=C \\ 1 & T_i=S, m_i \text{ odd, } k \text{ odd} \\ 1 & T_i=S, m_i \text{ even, } k \text{ even} \\ 0 & T_i=S, m_i \text{ even, } k \text{ odd} \\ 0 & T_i=S, m_i \text{ odd, } k \text{ even} \end{cases} \\
 & \text{terminal components} \\
 & \text{in voltage-like rules} \\
 & \text{number of} \quad = \quad \begin{cases} 0 & T_i=S \\ 1 & T_i=C, m_i \text{ odd, } k \text{ odd} \\ 1 & T_i=C, m_i \text{ even, } k \text{ even} \\ 0 & T_i=C, m_i \text{ even, } k \text{ odd} \\ 0 & T_i=C, m_i \text{ odd, } k \text{ even} \end{cases} \\
 & \text{terminal components} \\
 & \text{in current-like rules} \tag{6.248}
 \end{aligned}$$

Note that only the number of origin and terminal components differs between voltage-like and current-like rules.

Each rule can be regarded as a linear equation in a number of unknowns. Each component pair, single terminal component, and single origin component is regarded as an unknown, while the ${}^k E_n^i$ and ${}^k F_n^i$ are the linear coefficients. The set of odd rules and the set of even rules may each be regarded as a set of linear homogeneous equations.

Using equation (6.248), Table 6.1 summarise the total numbers of paired components and single components (referred to collectively as unknowns) on the left and right Y-junction branches for all configurations of m_L odd/even, m_R odd/even, and k odd/even. Note that the results for m_L even and m_R odd are essentially the same as for m_L odd, m_R even, since it does not matter really which branch is longer, and so they are not included to avoid repetition. It must be emphasized that different sets of rules apply depending on whether k is odd or even. For convenience, the total number of left and right branch cylinders is denoted m_T , so

$$m_T = m_L + m_R. \tag{6.249}$$

For each combination of m_L , m_R , T_L , T_R , k odd and k even, and for both voltage-like

	m_L odd and m_R odd		m_T even and m_R even		m_L odd and m_R even	
rules \rightarrow	k odd	k even	k odd	k even	k odd	k even
$T_L=C, T_R=C$ unknowns \rightarrow (voltage rule) match $k =$	$\frac{m_T - 2}{2}$	$\frac{m_T}{2}$	$\frac{m_T}{2}$	$\frac{m_T - 2}{2}$	$\frac{m_T - 1}{2}$	$\frac{m_T - 1}{2}$
	$^*m_T - 1$	$^{\dagger}m_T$	$m_T + 1$	$^{\ddagger}m_T - 2$	$^{\dagger}m_T$	$^*m_T - 1$
	$\frac{m_T + 2}{2}$	$\frac{m_T + 2}{2}$	$\frac{m_T}{2}$	$\frac{m_T + 4}{2}$	$\frac{m_T + 1}{2}$	$\frac{m_T + 3}{2}$
	$m_T + 3$	$m_T + 2$	$m_T + 1$	$m_T + 4$	$m_T + 2$	$m_T + 3$
$T_L=S, T_R=S$ unknowns \rightarrow (voltage rule) match $k =$	$\frac{m_T + 2}{2}$	$\frac{m_T}{2}$	$\frac{m_T}{2}$	$\frac{m_T + 2}{2}$	$\frac{m_T + 1}{2}$	$\frac{m_T + 1}{2}$
	$m_T + 3$	$^{\dagger}m_T$	$m_T + 1$	$m_T + 2$	$m_T + 2$	$m_T + 1$
	$\frac{m_T - 2}{2}$	$\frac{m_T + 2}{2}$	$\frac{m_T}{2}$	$\frac{m_T}{2}$	$\frac{m_T - 1}{2}$	$\frac{m_T + 1}{2}$
	$^*m_T - 1$	$m_T + 2$	$m_T + 1$	*m_T	*m_T	$m_T + 1$
$T_L=S, T_R=C$ unknowns \rightarrow (voltage rule) match $k =$	$\frac{m_T}{2}$	$\frac{m_T}{2}$	$\frac{m_T}{2}$	$\frac{m_T}{2}$	$\frac{m_T + 1}{2}$	$\frac{m_T - 1}{2}$
	$m_T + 1$	*m_T	$m_T + 1$	*m_T	$m_T + 2$	$^{\dagger}m_T - 1$
	$\frac{m_T}{2}$	$\frac{m_T + 2}{2}$	$\frac{m_T}{2}$	$\frac{m_T + 2}{2}$	$\frac{m_T - 1}{2}$	$\frac{m_T + 3}{2}$
	$m_T + 1$	$m_T + 2$	$m_T + 1$	$m_T + 2$	$^{\dagger}m_T$	$m_T + 3$
$T_L=C, T_R=S$ unknowns \rightarrow (voltage rule) match $k =$	$\frac{m_T}{2}$	$\frac{m_T}{2}$	$\frac{m_T}{2}$	$\frac{m_T}{2}$	$\frac{m_T - 1}{2}$	$\frac{m_T + 1}{2}$
	$m_T + 1$	*m_T	$m_T + 1$	*m_T	*m_T	$m_T + 1$
	$\frac{m_T}{2}$	$\frac{m_T + 2}{2}$	$\frac{m_T}{2}$	$\frac{m_T + 2}{2}$	$\frac{m_T + 1}{2}$	$\frac{m_T + 1}{2}$
	$m_T + 1$	$m_T + 2$	$m_T + 1$	$m_T + 2$	$m_T + 2$	$m_T + 1$

Table 6.1: Predictions for fully equivalent cable structure for the general Y-junction.
Notation: $m_T = m_L + m_R$. A * indicates at what length and with what boundary condition the connected section terminates. A † indicates where a unit-length disconnected section occurs. A ‡ indicates where a two-length disconnected section occurs. See text for more details.

and current-like rules, the total number of unknowns is tallied, and we determine the value of k for which the total number of rules that are valid for the components of ϕ_k equals the total number of unknowns in rule k . Using the resulting information, it is possible to predict the lengths of connected and disconnected sections for all possible combinations of branch lengths and terminal conditions.

Suppose the odd rules and even rules each form a set of linearly independent homogeneous equations. If we have n such equations (the rules) in n unknowns (component pairs or weighted differences, and singles) then there is no non-trivial solution and the unknowns must therefore be zero. For voltage-like rules, this leads to every pair of component coefficients summing to zero, i.e. the two coefficients have the same magnitude but opposite sign and so can satisfy a cut condition; in addition, any component that might end on a sealed terminal would have to be zero. On the other hand, for current-like rules this leads to each weighted difference of two components being equal to zero, i.e. the ratio of the two coefficients equals the ratio of the corresponding c-values, and so the component pair can satisfy a sealed condition where they meet; in addition, the coefficients of any components ending at the origin or at a cut terminal must become zero.

Connected Sections

To predict cable structure for each combination of m_L , m_R , t_L , and t_R (there are twelve distinct possibilities given in the Table 6.1), search for acceptable values of k , i.e. k must be less than or equal to $m_L + m_R$, since total Y-junction electrotonic length is preserved in the cable. The lowest value of k , i.e. the first instance, for which equations match unknowns is indicated by a *. If this value is $k = m_T = m_L + m_R$ then the Y-junction is non-degenerate and the connected section is the full equivalent cable.

Note that, although there are apparently seven types of non-degenerate Y-junction from the Table 6.1, there are really only five actual fundamentally different situations. There are two pairs of equivalent situations due to the fact that when both branches have odd length or even-length, the same result applies if one swaps around the two different terminal conditions.

An example of this situation occurs when m_L is odd, m_R is even, and both terminals are sealed. Only one of the four possible combinations of rule-type (voltage or current) and k odd/even is acceptable (all the other evaluate to $k > m_L + m_R$). It is the current-like rule/ k odd combination, i.e. the number of current-like rules equals the number of unknowns involved in the current-like rules when $k = m_L + m_R$ (k odd). The connected section therefore terminates with a sealed terminal.

Figure 6.14 illustrates one component diagram for each of the five non-degenerate cases. Each component diagram describes the potential function structure in the final

terminating cylinder.

It is also possible that equations and unknowns are matched when $k < m_L + m_R$ (the remaining five situations from Table 6.1). In such cases the connected section is less than the total equivalent cable length, and a disconnected section remains to be found. For example when m_L and m_R are both odd, and both terminals are cut. The number of voltage-like rules matches the number of unknowns involved in the voltage-like rules when $k = m_L + m_R - 1$ (k odd).

Disconnected Sections

From the predictions made in Table 6.1, there are five classes of degenerate Y-junctions. The cables for four of these have a unit length disconnected section, i.e. $k = m_L + m_R - 1$ (one off maximum) is the lowest value of k where equations match unknowns. In each of these four cases, there also happens to be a rule-unknown match when $k = m_L + m_R$ (indicated by a †), i.e. if the connected section ends with a k -odd rule then the k -even rules can subsequently be satisfied by the disconnected section. Similarly, if the connected section ends with a k -even rule then the k -odd rules can subsequently be satisfied by the disconnected section.

Proceeding as before, we would just apply the electrical continuity rules once more to get the appropriate framework potential function. Unfortunately this cannot be done in the conventional manner because c-value ratios between connected and disconnected cylinders are effectively either zero or infinity.

Consider first the case where the connected section terminates with a cut end, and consider the final potential function, k say (less than $m_L + m_R$), of the connected section. Two components on the same branch which meet to satisfy a cut terminal must have the form

$$A(v_i((j-1)l+x) - v_i((j+1)l-x)). \quad (6.250)$$

The are similarities here to the isolation condition, i.e. the two component coefficients sum to zero. Applying the electrical continuity rules now produces,

$$-\frac{c_k^G}{c_{k+1}^G}(v_i(jl-x) - v_i((jl+x))). \quad (6.251)$$

Since the c-value c_{k+1}^G is effectively infinity as far as the connected section is concerned, this expression is not acceptable as it stands.

Similarly, consider the final potential function, k , of a connected section terminated with a sealed end. Observe that two components on the same branch which meet to satisfy a sealed terminal have the form

$$A(c_j^i v_i((j-1)l+x) + c_{j+1}^i v_i((j+1)l-x)). \quad (6.252)$$

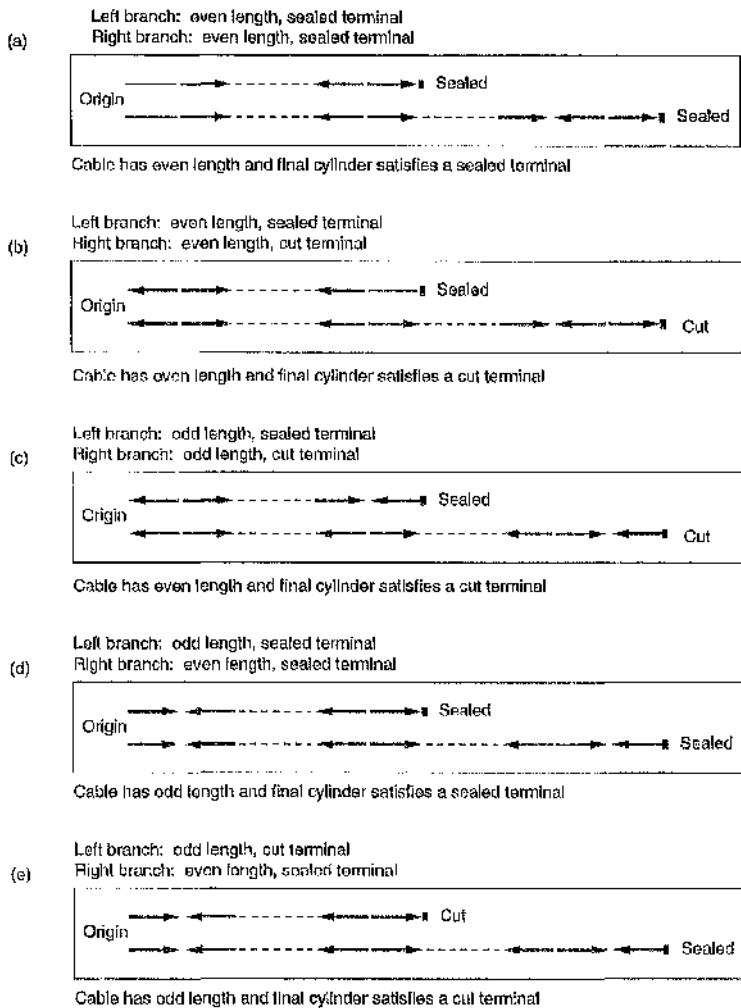


Figure 6.14: The component structure for the final cylinder of the connected section for all non-degenerate Y-junctions. The right branch need be the longer branch. (a) Left and right branches both have even lengths and sealed terminals. The connected section has even length, and terminates with a sealed end, so the two components that meet at the origin must each have zero coefficient, as must the two that end at the cut terminals. (b) Left and right branches both have even lengths, one with a sealed terminal and one with a cut terminal. The connected section has even length, and terminates with a cut end end, so only the component that reaches the sealed end must be zero. (c) Left and right branches both have odd lengths, one with a sealed terminal and one with a cut terminal. The connected section has even length and terminates with a cut end, so no components need be zero. (d) Left branch has odd length, right branch has even length. Both terminate with a sealed end. The connected section has odd length and terminates with a sealed end. No components need be zero. (d) Left branch has odd length, with a sealed end. Right branch has even length, with a cut end. The connected section has odd length and terminates with a cut end. No components need be zero.

Applying the electrical continuity rules to this produces

$$A(c_j^i v_i(jl - x) + c_{j+1}^i v_i(jl + x)) , \quad (6.253)$$

so the components coefficients have clearly been conserved. There is no obvious problem with cable c-values at this point since the zero c-value c_{k+1}^G representing the boundary condition doesn't appear, however, applying the normal reflection rule simply doesn't produce the correct result.

Components in ϕ_k that end on a cut or a sealed end are not actually involved in the voltage-like and current-like rules respectively. They do not need to be because they automatically satisfy the appropriate terminal condition. When they are next reflected to produce a contribution to the next cable potential, the reflected component may take any value and still satisfy the same condition at $x = 0$. We therefore have some flexibility in our choice of such reflected components.

So, if the connected section is cut, we apply the reflection rules to all pairs of components, except those ending at the origin or at cut terminals. This will ensure a cut terminal is satisfied at $x = 0$ in the new potential. The components must be divided through by the reflection coefficient to remove the problem of an infinite cable diameter, and then we can fix any "free" components so that the next rule ($k = m_T$) is satisfied (there will be only one choice for each reflected component if the entire potential is to satisfy a terminal condition at $x = l$). The process is similar if the connected section is sealed, except that no rescaling is necessary, and the new potential satisfies a sealed (or current injection) condition at $x = 0$.

Although this approach works, fortunately, in all circumstances where the disconnected has unit length, the structure of the potential is easily determined without having to make any effort to re-apply the electrical continuity rules. There is actually little choice over the potential function for a unit length cable segment which is terminated at each end. Only two boundary condition configurations arise — either both ends are cut, or one is cut and one is sealed.

If both terminals are cut then the components for the disconnected section potential (ϕ_{m_T}) must all have coefficients of the same magnitude but arranged such that components on adjacent cylinder have opposite sign. Figure 6.15a illustrates the configuration. One simply chooses one component at random and assigns it a non-zero coefficient; the remaining component coefficients are therefore fixed automatically.

If one terminal is sealed and the other is cut, the arrangement is only slightly more complicated. All component pairs that meet with a cut terminal must have coefficients with the same magnitude but different sign. The different component pairs which meet at a the sealed terminal must have a coefficient ratio equal to the corresponding cylinder

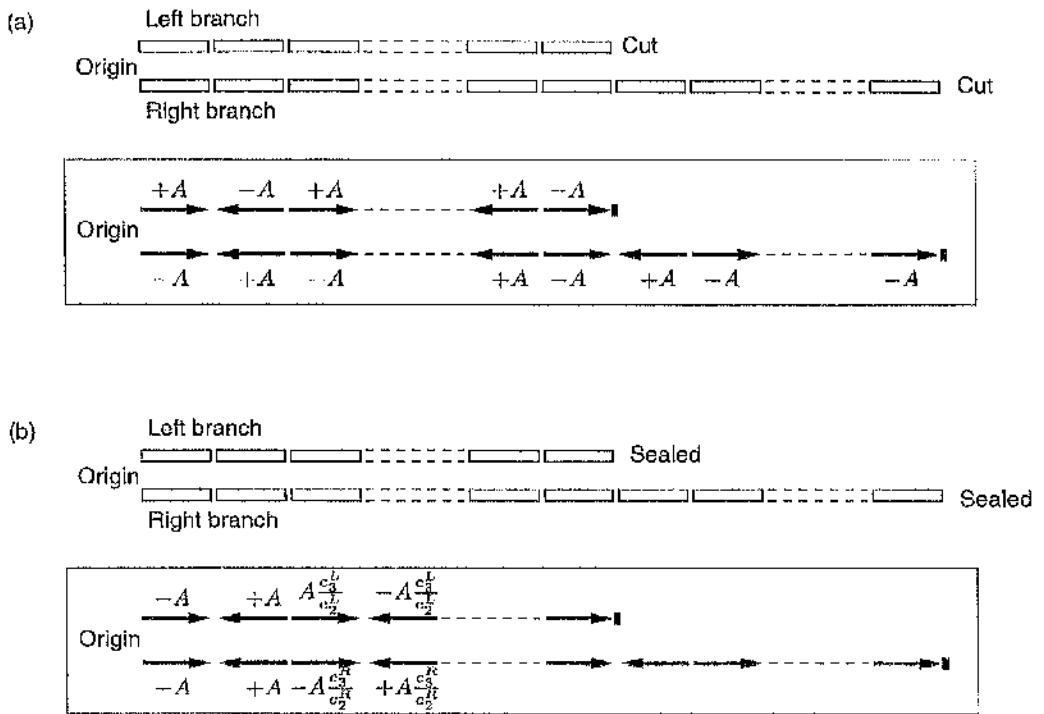


Figure 6.15: Unit length disconnected section component structure. (a) A unit length disconnected section with two cut terminals. (b) A unit length disconnected section with one cut and one sealed terminal. See text for details.

c -value ratio. This configuration is illustrated in Figure 6.15b.

Both types of component structure trivially satisfy the relevant (k -odd or k -even, voltage-like or current-like) construction rule.

There is one final degenerate Y-junction to be considered, i.e. that indicated in Table 6.1 by a ‡. Here, both m_L and m_R are even, and a voltage condition can be satisfied when $k = m_L + m_R - 2$ (k even), i.e. two unit lengths short of the full equivalent cable. There doesn't appear, however, to be a larger k for which equation and unknowns are matched. This is because the disconnected section has a length of two units and satisfies another cut condition when $k = m_L + m_R$ (k even again).

Simply use the method described above to reflect the components of the final connected section potential, and rescale by the cut reflection factor ($-c_{k-2}^G/c_{k-1}^G$ in this case). The $k = m_L + m_R - 1$ current-like and voltage-like rules (as well as all previous odd numbered rules) must be satisfied by the first cylinder of the disconnected section, and this fixes the coefficients of the components reflected from the origin and terminals. The electrical continuity rules and the isolation-termination rules then determine the final cylinder.

The full set of predictions are illustrated in Figures 6.16, 6.17 and 6.18. There are ten in total. These predictions don't actually depend on which branch is the longer, just on

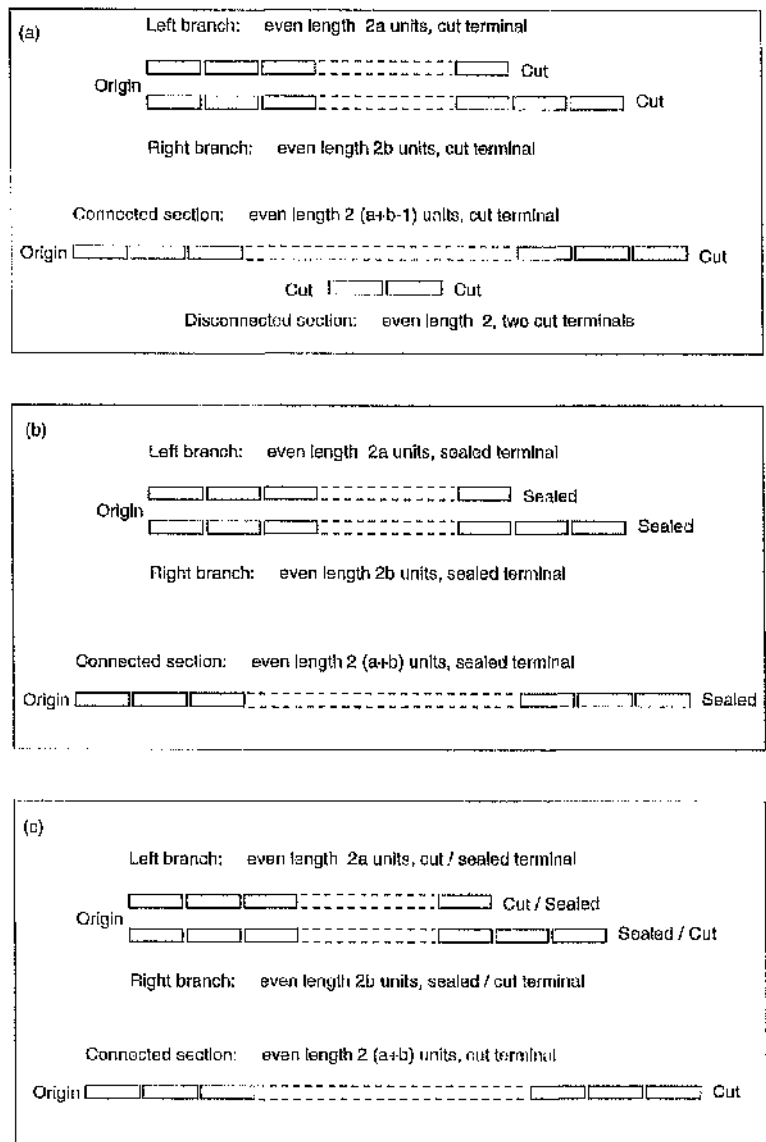


Figure 6.16: Predicted Equivalent cable structure when each Y-junction limb is an even number of basic length units.

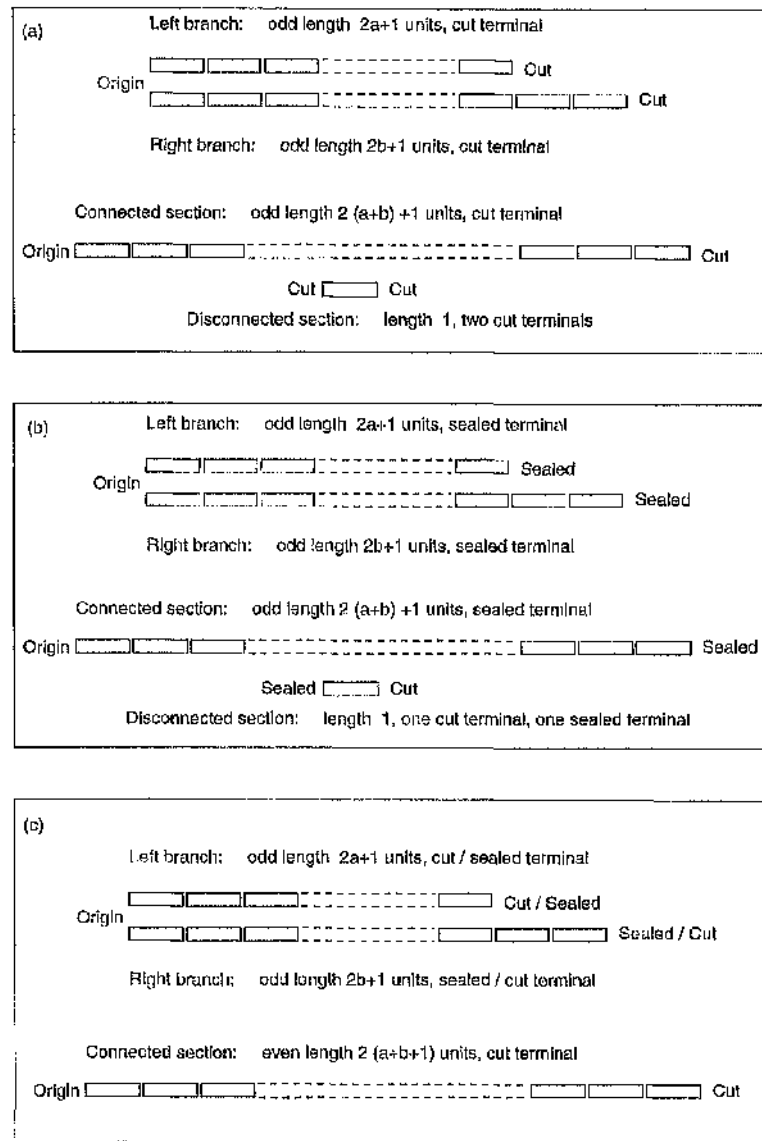


Figure 6.17: Predicted Equivalent cable structure when each Y-junction limb is an odd number of basic length units.

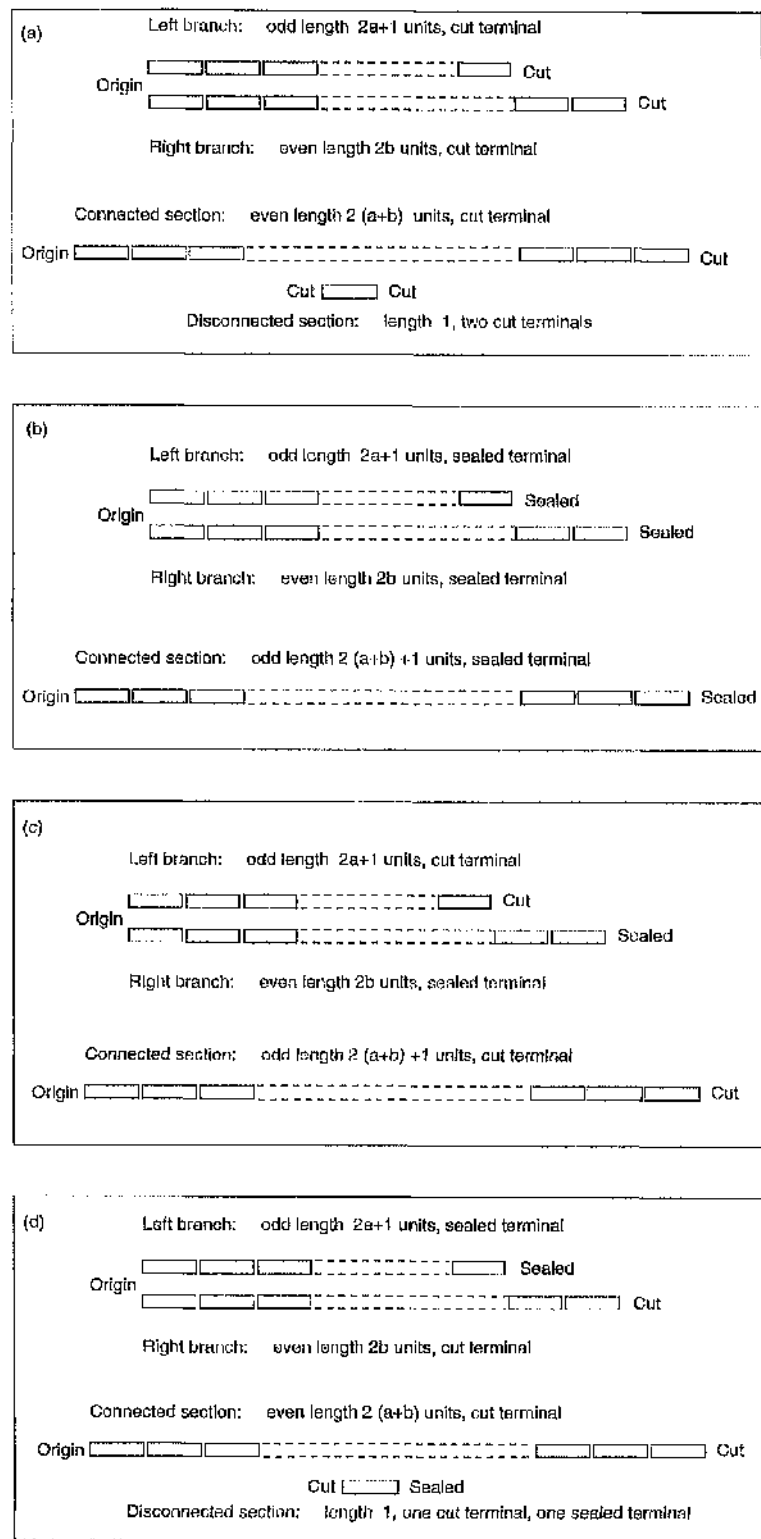


Figure 6.18: Predicted Equivalent cable structure when one Y-junction limb is an even number of basic length units, and the other is an odd number of basic length units.

oddness and evenness, and boundary condition types. The predictions can also be used as a guide for determining electrical degeneracy and cable section length in advance of using the matrix methods of cable construction (Chapter 4). This can be an advantage when numerical errors prevent the generation of the exact subspaces in the matrix methods. The implications of these results, when constructing fully equivalent cables using real tree data, are discussed in Chapter 8.

The only situations in which the predictions are not accurate are when a Y-junction is a Rall-tree or the generalisation of this result for non-uniform diameter profiles. In these situations, there are never any reflected components and the connected section will terminate as soon as the terminals are reached, as shown in section 6.4.2.

6.5 A Matrix Formalism for Analytical Results

The continuous electrical mapping between a tree and its fully equivalent cable can be represented in a matrix form. For this purpose, we define vectors of potential functions,

$$\mathbf{V} = [v_1^L(x, t), v_2^L(l - x, t), \dots, v_1^R(x, t), v_2^R(l - x, t), \dots] \quad (6.254)$$

and

$$\Psi = [\phi_1(x, t), \phi_2(l - x, t), \phi_3(x, t) \dots]. \quad (6.255)$$

Note how the even numbered tree and cable potentials are written so that both odd and even cable potentials can be expressed in terms of the same basic tree potentials. It is also necessary to define vectors of Y-junction and equivalent cable c-values,

$$\mathcal{D}_T = \text{diag} \left(c_1^L, c_2^L, \dots, \dots, c_{m_L+m_{R-1}}^L, c_{m_L+m_R}^L \right), \quad (6.256)$$

and

$$\mathcal{D}_C = \text{diag} \left(c_1^G, c_2^G, \dots, c_{m_L+m_{R-1}}^G, c_{m_L+m_R}^G \right). \quad (6.257)$$

The relationship between Y-junction and cable can then be expressed in the notation similar to that in Chapter 4.

$$\Psi = \mathcal{M}_V V, \quad (6.258)$$

where \mathcal{M} is a matrix of potential function component coefficients, referred to as the *voltage EGP-matrix* (Electro-Geometric Projection matrix). The initial structure of \mathcal{M} takes the form

$$\mathcal{M} = \begin{bmatrix} {}^1\alpha_1^L & 0 & 0 & 0 & 0 & \dots & 0 & {}^1\alpha_1^R & 0 & 0 & 0 & 0 & \dots & 0 \\ {}^2q_0^L & {}^2p_1^L & 0 & 0 & 0 & \dots & 0 & {}^2q_0^R & {}^2p_1^R & 0 & 0 & 0 & \dots & 0 \\ {}^3\alpha_1^L & {}^3\beta_1^L & {}^3\alpha_2^L & 0 & 0 & \dots & 0 & {}^3\alpha_1^R & {}^3\beta_1^R & {}^3\alpha_2^R & 0 & 0 & \dots & 0 \\ {}^4q_0^L & {}^4p_1^L & {}^4q_1^L & {}^4p_2^L & 0 & \dots & 0 & {}^4q_0^R & {}^4p_1^R & {}^4q_1^R & {}^4p_2^R & 0 & \dots & 0 \\ \vdots & \vdots & \vdots & \vdots & \vdots & \dots & \vdots & \vdots & \vdots & \vdots & \vdots & \vdots & \dots & \vdots \end{bmatrix} \quad (6.259)$$

and it is fairly easy to see how it continues in the same manner.

Along the same lines, there is a *current EGP-matrix*,

$$\mathcal{M}_I = \mathcal{D}_C \mathcal{M}_V \mathcal{D}_T^{-1}, \quad (6.260)$$

which relates the current injected along cable and Y-junction cylinders.

Extracting the Continuous Mapping from the Discrete Mapping

This continuous mapping can be identified with the internal node of a matrix representation when every tree cylinder is represented by three nodes ($z=2$). Once a cable has been constructed using a matrix method, the continuous mapping can be inferred by observing, from a simple understanding of the electrical continuity reflection-transmission procedure, the direction of the corresponding component.

6.6 Future Analytical Work

Although much insight into why and how cables exist has been gained simply through deriving the rules, there are still results that have not yet been explained. Application of the analytical rules will produce a cable that properly terminates, along with any disconnected sections. However, it has not been shown explicitly that c-values are guaranteed to be positive. Also, in the case of a completely sealed tree, how does the procedure ensure surface area is preserved, and input current is conserved — these features are undoubtably related to the coefficient conservation that is always guaranteed in sealed trees. Physical arguments show that these properties must be conserved.

The rule development hints at much deeper mathematical structure that is not yet fully understood (though work completed so far suggests approaches to the problem that are likely to reveal this structure). For example, we had to move to potential function ϕ_{k+1} to determine the right form of rule k . Yet despite this, the rules are conveniently independent of tree structure beyond the k^{th} cylinder on each branch. There is also the fact that the rules generally involve component coefficients that have already been arranged, although in quite a complex fashion, and the rules as presented don't take direct advantage of this. The branch-shifting operations in Chapter 7 shed some additional light on simple Y-junction structure and hint that a more complicated procedure involving a "folding in" of branch potentials.

Deriving the Matrix Procedures Using Analytical Results

Work has been done in deriving the matrix method from the analytical results, but it is incomplete and requires further investigation. Again, an proper derivation of the matrix

methods will likely follow once the analytical theory is fully understood (the matrix methods, in particular the scaling/rescaling transformations, are important considerations in developing the deeper analytical rules). In overview, the odd and even numbered potential functions are analogous to the odd and even numbered orthogonal vectors that form T , the tri-diagonalising matrix. This matrix relates scaled tree and cable potentials. The potential functions relate the actual potentials. The idea is to derive the orthogonality of the scaled potential functions, and show how this can lead to a matrix formulation of the problem.

Chapter 7

An Analysis of Cable Structure Using Branch-shifting

7.1 Introduction

The general analytical rules (Chapter 6) for constructing fully equivalent cables are complicated, and difficult to analyse to determine the deeper mathematical structure that we believe exists. Fortunately, a start can be made with simple Y-junctions since they always have fairly simple equivalent cables and electrical mappings. This simplicity isn't immediately obvious, but manifests itself as the ability to generate equivalent cables rapidly and highly efficiently by using a *branch-shifting* method.

Branch-shifting is a procedure whereby a simple Y-junction may be reduced to its equivalent cable by way of a number of intermediate steps which involve a partial collapse of the tree, producing a portion of the equivalent cable connected section to which another, shorter (in terms of total child limb lengths) Y-junction is attached. Total electrotonic length is preserved at each stage, and only at the final branch-shifting step is any disconnected section produced. Essentially the method generates an intermediate set of fully equivalent singly branched trees¹.

The results in this chapter include analytical expression for equivalent cable c-values and potential functions that clearly indicate how the electrotonic lengths of a tree's branches, as well as boundary conditions, shape the fine structure of an equivalent cable. Observations concerning the trends in cable structure obtained from these results are

¹The derivation of the general analytical rules in Chapter 6 hints at an deeper mathematical framework for cable construction which has yet to be determined. Branch-shifting may be a manifestation of this underlying structure. Thus, the deeper mathematical framework for general Y-junctions may also be an iterative collapsing procedure, although mathematical structures generated at intermediate stage may not always have a physical interpretation.

equally valid for general Y-junction.

As in previous chapters, a Y-junction consists of left and right branches, with the left being the shorter (electrotonically) of the two. For simple Y-junctions, the left and right branch cylinders have electrotonic lengths ml and $(m+n)l$ respectively, where $m \geq 1$ and $n \geq 0$. The total electrotonic length of the Y-junction is therefore $(2m+n)l$. Left and right boundary conditions are denoted T_L and T_R , and are either cut (c) or sealed (s). (Of course, the general current injection condition is also valid, but the additional applied current is merely mapped to applied currents on the cable without influencing cable structure. From results in Chapter 6, i.e. equation (6.42), the current mapping follows from a slight modification of the voltage mapping.)

Length and boundary condition configurations can be divided into five distinct classes which cover all possible simple Y-junctions.

- Symmetric Y-junctions ($n = 0$).
- Short branch has a cut end ($T_L=c$, $n > 0$).
- Short branch has a sealed end; long branch is over twice the length of the short branch ($T_L=s$, $n > m$).
- Short branch has a sealed end; long branch has a sealed end; long branch no greater than twice the length of the short branch ($T_L=s$, $T_R=s$, $0 < n \leq m$).
- Short branch has a sealed end; long branch has a cut end; long branch is no greater than twice the length of the short branch ($T_L=s$, $T_R=c$, $0 < n \leq m$).

For each case, rules are given for determining cable c-values and an electrical mapping between the Y-junction and its branch-shifted equivalent. At any point during the iterative procedure, the Y-junction in the current equivalent structure will fit into one of these classes and so, with all five possibilities accounted for, any simple Y-junction can be branch-shifted until the final equivalent cable is generated. Up to four Y-junction classes may be encountered when the branch-shifting procedure is applied to a particular simple Y-junction. As usual, time dependence in all expressions will be suppressed.

All branch-shifting results follow straightforwardly from the analytical construction rules. The fact that voltage continuity and current conservation holds in the each new Y-junction structure, electrotonic length is preserved, and a bijective electrical mapping is established, may be regarded as proof of the validity of the results. However, to indicate the methods by which these results were originally obtained, full derivations are given for the two Y-junction classes listed second and third.

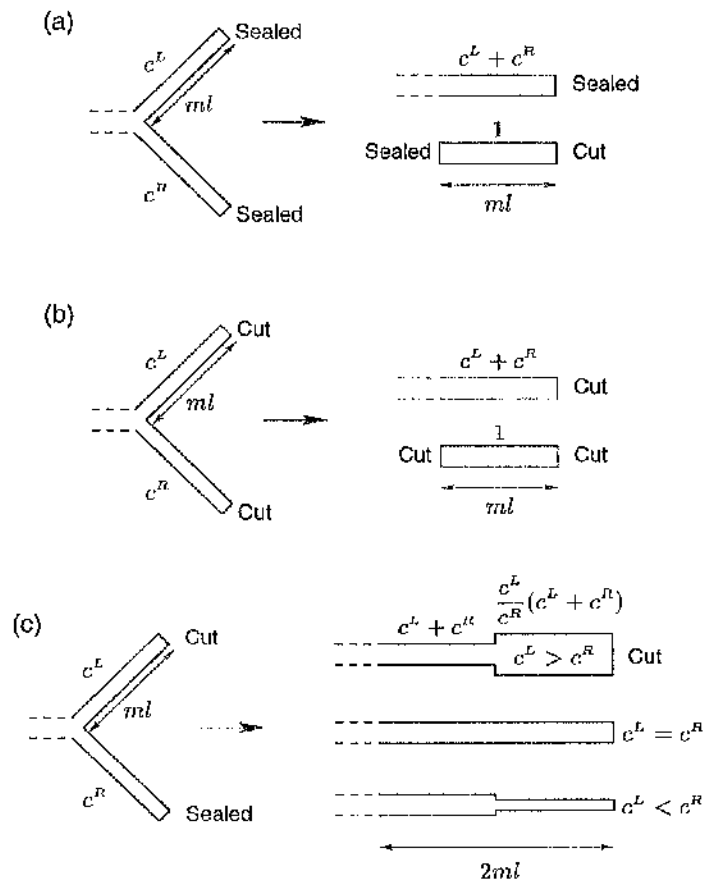


Figure 7.1: The branch-shifting operations for symmetric Y-junctions. Cylinder lengths and c -values are given. (a) Rall Y-junction with two sealed terminals. (b) Rall Y-junction with two cut terminals. (c) Non-Rall Y-junction with one cut and one sealed terminal.

7.2 The Symmetric Y-junction

The Y-junction is regarded as *electrotonically symmetric* when $n = 0$. This very simple condition encapsulates three of the situations that can mark the final stage in a branch-shifting sequence. These junctions collapse directly to unbranched structures, and are illustrated in Figure 7.1.

7.2.1 Rall Symmetric Y-junction

Provided $T_L = T_R$, the Y-junction is a simple, degenerate Rall tree and collapses to an equivalent cable consisting of the cylinder (connected section) with c -value

$$c_1^G = c^L + c^R, \quad (7.1)$$

and potential

$$\phi_1(x) = \frac{c^L}{c^L + c^R} v_L(x) + \frac{c^R}{c^L + c^R} v_R(x), \quad 0 \leq x \leq ml, \quad (7.2)$$

plus a disconnected section,

$$\phi_2(x) = v_L(l - x) - v_R(l - x), \quad 0 \leq x \leq ml, \quad (7.3)$$

which may be arbitrarily assigned a non-zero c-value.

If both Y-junction cylinders are sealed, the connected section is sealed, while the disconnected section has a sealed terminal at $x = 0$ and a cut terminal at $x = l$. If both Y-junction cylinders are cut, the connected section is cut, while the disconnected section has a cut terminal at both $x = 0$ and $x = l$. The form of the first cylinder in any reduced structure is Rall-like (its c-value is the sum of the connecting Y-junction cylinders), so equations (7.1) and (7.2) are repeatedly encountered.

7.2.2 Non-Rall Symmetric Y-junction

Now suppose that the Y-junction has one cut limb (assumed to be the left cylinder) while the other (the right cylinder) is sealed. The connected section has length $2ml$, terminates with a cut end, and is the complete equivalent cable, i.e. such Y-junctions are non-degenerate. This time the second cylinder is not disconnected and its potential function components are obtained by elementary application of the isolation condition, so

$$\phi_2(x) = \frac{c^L}{c^L + c^R} (v_L(l - x) - v_R(l - x)), \quad 0 \leq x \leq ml, \quad (7.4)$$

while the c-value is

$$c_2^G = \frac{c^L}{c^R} (c^L + c^R). \quad (7.5)$$

The electrical continuity rules ensure that current conservation and voltage continuity are guaranteed, i.e. $\phi_1(l) = \phi_2(0)$ and $c_1^G \partial \phi_1(l) / \partial x = c_2^G \partial \phi_2(0) / \partial x$.

7.3 Short Cylinder has a Cut Terminal

This is the simplest actual branch shifting operation, and involves shifting the short branch length ml along the right branch by moving the branch point, redefining potentials and rescaling certain c-values. Despite its simplicity, this case illustrates the general approach used to determine the new equivalent structure.

Applying the electrical continuity rules to potential function (7.2), and then ensuring that the isolation condition holds, yields

$$\phi_2(x) = -\frac{c^R c^L}{c_1^G (c^R + 2c^L)} (v_L(ml - x) - v_R(ml - x)) + \frac{c^R}{(c^R + 2c^L)} v_R(ml + x), \quad (7.6)$$

valid for length ml , and

$$c_2^G = \frac{c_1^G(c^R + 2c^L)}{c^R}. \quad (7.7)$$

At this point we ask whether it is possible to choose two properly terminated branches that form a Y-junction which, when connected to the initial cable cylinder, forms a new tree with the same total electrotonic length as the original Y-junction. Voltage continuity and current conservation must hold at the new branch point, and an electrical mapping between the Y-junction and new tree must be produced. If this is possible, the new structure must be equivalent to the original Y-junction.

Denote the potentials in the new left and right branches by $\xi_L(x)$ and $\xi_R(x)$, and their c -values by c_ξ^L and c_ξ^R . The only reasonable choice for the potentials, since we must be prepared for arbitrary structure beyond $x = l$ on the right branch, is to set

$$\xi_L(x) = \alpha(v_R(ml - x) - v_L(ml - x)) \quad \text{and} \quad \xi_R(x) = \beta v_R(ml + x). \quad (7.8)$$

where α and β are yet to be determined. The new left potential can only be valid for length ml , while the new right potential must be valid for nl , i.e. the length of the section of the right branch which has yet to be collapsed. Since these new limbs connect to the initial cable segment, which has length ml , total electrotonic length is preserved. Potential ξ_L terminates properly at $x = l$ with a cut terminal, while ξ_R terminates with the right branch condition at $x = nl$.

Voltage continuity requires that, at the new branch point,

$$\xi_L(0) = \xi_R(0) = \phi_1(l), \quad (7.9)$$

thus $\alpha = \beta = c^R/c_1^G$, and the potentials may be written

$$\xi_L(x) = \frac{c^R}{c_1^G}(v_R(ml - x) - v_L(ml - x)), \quad 0 \leq x \leq ml, \quad (7.10)$$

and

$$\xi_R(x) = \frac{c^R}{c_1^G} v_R(ml + x), \quad 0 \leq x \leq nl. \quad (7.11)$$

Since the new Y-junction, when collapsed, must have an initial cylinder corresponding to the second fully equivalent cable cylinder, the two new branch potentials must be related to ϕ_2 by the simple Rall sum,

$$\phi_2(x) = \frac{c_\xi^L}{c_2^G}\xi_L(x) + \frac{c_\xi^R}{c_2^G}\xi_R(x), \quad (7.12)$$

where $c_2^G = c_\xi^L + c_\xi^R$. It therefore follows that

$$\phi_2(x) = \frac{c_\xi^L c^R}{c_1^G c_2^G} (v_R(ml - x) - v_L(ml - x)) + \frac{c_\xi^R c^R}{c_1^G c_2^G} v_R(l + x). \quad (7.13)$$

Matching this up with the known expression for ϕ_2 (7.6) gives

$$\frac{c_\xi^L c^R}{c_1^C c_2^C} = \frac{c^R c^L}{c_1^C (c^R + 2c^L)}, \quad \text{and} \quad \frac{c_\xi^R c^R}{c_1^C c_2^C} = \frac{c^R}{(c^R + 2c^L)}, \quad (7.14)$$

so that

$$c_\xi^L = \frac{c_1^C c^L}{c^R}, \quad c_\xi^R = \frac{(c_1^C)^2}{c^R}. \quad (7.15)$$

Checking current conservation shows that

$$c_1^C \frac{\partial \phi_1}{\partial x} \Big|_{x=0} = c_\xi^L \frac{\partial \xi_L}{\partial x} \Big|_{x=0} + c_\xi^R \frac{\partial \xi_R}{\partial x} \Big|_{x=0}, \quad (7.16)$$

and the branch-shifting operation illustrated in Figure 7.2, has been established.

Note that the c-value for the new left branch is the same as that for the second cylinder on the non-Rall symmetric Y-junction. If $n = 0$, i.e. the right branch disappears, then we can obtain two of the symmetric results by observing how the right branch condition influences the point where the cable stem and left branch meet. If the right branch condition is cut, then the cable stem and left branch must essentially both leak current into the cut terminal. The fact that they are each connected to the other cylinder of finite diameter is irrelevant considering the effectively infinite diameter of the cut terminal. The two branches are electrically isolated from each other, hence the disconnection. If the right branch is sealed, however, no disconnection occurs because current flows between cable stem and left branch as if there were no right branch at all.

It is useful to perform a brief analysis of the magnitudes of the new limb c-values and the implications of this. Observing that

$$c_\xi^L > c^L, \quad \text{and} \quad c_\xi^R > c^R + c^L, \quad (7.17)$$

it is clear that, in order to obtain equivalence, the new Y-junction limbs are wider than those of the original Y-junction. If the right branch of the original Y-junction is long enough, it is possible to repeat this same operation perhaps several times. Using the above c-values, it is straightforward to determine that, in general, after j such shifting operations, the j^{th} cable cylinder is given by

$$c_j^C = \frac{(c^R + jc^L)(c^R + (j-1)c^L)}{c^R}. \quad (7.18)$$

The left and right Y-junction limbs after j such operations are

$$\begin{aligned} c_{\xi,j}^L &= \frac{c^L}{c^R} (jc^L + c^R) \\ c_{\xi,j}^R &= \frac{(jc^L + c^R)^2}{c^R}. \end{aligned} \quad (7.19)$$

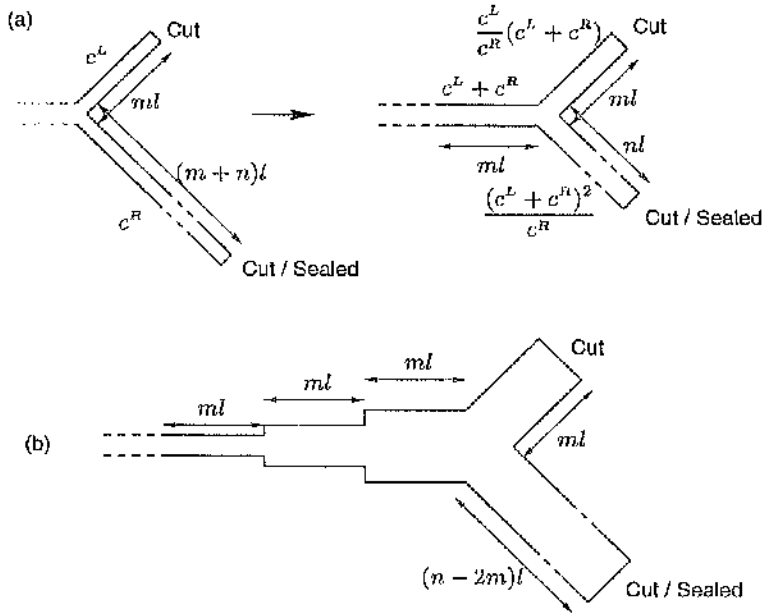


Figure 7.2: The branch-shifting operation when the short branch has a cut terminal. (a) The single operation. (b) Typical structure when three such operations are applied, i.e. $n > 2m$.

Cable cylinder c -values are clearly increasing, i.e. $c_j^G > c_{j-1}^G$. Note also, that the quantity

$$\frac{c_{\xi,j}^R}{(c_{\xi,j}^L)^2} = \frac{c^R}{(c^L)^2} \quad (7.20)$$

is preserved over j . Figure 7.2b illustrates the equivalent structure after three such operations. Eventually, a point is reached where the new Y-junction must be reassessed to determine the class it falls into.

7.4 Short Cylinder has a Sealed Terminal

When the short cylinder has a sealed terminal, it is necessary to construct length $2ml$ of the cable before attaching the new Y-junction. There are three distinct cases to be considered. When $n > m$, the rules are not much more complicated than those for the cut short branch. If $n \leq m$, however, the long cylinder boundary condition must also be taken into account and it is necessary to express m in terms of n ,

$$m = kn + z, \quad (7.21)$$

where $k \geq 1$ is an integer and $0 \leq z < n$ is an integer that makes up any deficit length. Clearly, if $z = 0$ then m is an exact multiple of n , and so are both Y-junction cylinders —

such situations actually lead to unbranched structure and so are possible final stages of a branch-shifting process. Together with the symmetric trees, such situations complete the set of final shifting operations.

7.4.1 Long Branch is at Least Twice as Long as Short Branch ($n > m$)

In this case, the electrical continuity rules and the isolation condition, when applied to potential function (7.2), give

$$\phi_2(x) = \frac{c^L}{c_1^G} (v_L(ml - x) - v_R(ml - x)) + v_R(ml + x), \quad (7.22)$$

valid for length ml , and

$$c_2^G = \frac{c_1^G c^R}{(c^R + 2c^L)}. \quad (7.23)$$

At this point, it turns out that it is not possible to branch shift just length ml . Voltage continuity and current conservation simply cannot be achieved at the new branch point.

Applying analytical construction rules once more yields

$$\phi_3(x) = \frac{c^L}{c^R + 3c^L} (v_R(x) - v_L(x)) + \frac{c^L}{c^R + 3c^L} v_R(2ml - x) + \frac{c^R + 2c^L}{c^R + 3c^L} v_R(2ml + x), \quad (7.24)$$

and

$$c_3^G = \frac{c^R(c^R + 3c^L)}{(c^R + 2c^L)}. \quad (7.25)$$

This time we assume there is a new Y-junction connected at the end of the second cable section. The new left and right potentials are again denoted ξ_L , ξ_R , with c-values c_ξ^L , c_ξ^R . To allow for arbitrary right branch structure, it is necessary to choose

$$\xi_L(x) = \alpha [v_R(x) - v_L(x) + v_R(2ml - x)] \quad \text{and} \quad \xi_R(x) = \beta v_R(2ml + x). \quad (7.26)$$

where α and β must again be determined. The new left branch has length ml and terminates with a scaled end, while the new right branch has length $(n - m)l$ and terminates with the original right branch condition.

Voltage continuity demands that

$$\phi_2(ml) = \xi_L(0) = \xi_R(0), \quad (7.27)$$

so $\alpha = \beta = 1$, and the new potentials may be written

$$\begin{aligned} \xi_L(x) &= v_R(x) - v_L(x) + v_R(2ml - x), & 0 \leq x \leq ml \\ \xi_R(x) &= v_R(2ml + x), & 0 \leq x \leq (n - m)l. \end{aligned} \quad (7.28)$$

Since ϕ_3 must be a simple Rall combination of the two new potentials, then

$$\phi_3(x) = \frac{c_\xi^L}{c_3^G} \xi_L(x) + \frac{c_\xi^R}{c_3^G} \xi_R(x). \quad (7.29)$$

Consequently,

$$\phi_3(x) = \frac{c_\xi^L}{c_3^C} (v_R(x) - v_L(x) + v_R(2ml - x)) + \frac{c_\xi^R}{c_3^C} v_R(2ml + x), \quad (7.30)$$

and, by matching up coefficients from potential function (7.24), we obtain

$$c_\xi^L = \frac{c^R c^L}{c^R + 2c^L}, \quad c_\xi^R = c^R. \quad (7.31)$$

Current conservation at the new branch point can be checked as before, showing

$$c_2^C \frac{\partial \phi_2}{\partial x} \Big|_{x=0} = c_\xi^L \frac{\partial \xi_L}{\partial x} \Big|_{x=0} + c_\xi^R \frac{\partial \xi_R}{\partial x} \Big|_{x=0}. \quad (7.32)$$

Interestingly in this situation, the right branch c -value is not scaled. Since the original Y-junction structure beyond $2ml$ on the right branch may take any form, this must be the case if total surface area is to be preserved — it is easily shown that $c_1^C + c_2^C + c_\xi^L = 2c^R + c^L$ (recalling that the c -value is effectively a measure of surface area for a unit electrotonic length of cylinder). The branch-shifting operations must maintain surface area until a cut terminal is encountered.

Again, an analysis of new cable c -values can be performed, so note initially that

$$c_1^C > c_3^C > c_2^C. \quad (7.33)$$

Also, while the right branch maintains the same c -value, the left c -value narrows, i.e.

$$c_\xi^L < c^L. \quad (7.34)$$

In fact, it can be proven using a simple induction argument that, if j is odd then

$$c_j^C = c^R \left[1 + \frac{c^L}{c^R + (j-1)c^L} \right], \quad (7.35)$$

while if j is even,

$$c_j^C = c^R \left[1 - \frac{c^L}{c^R + jc^L} \right]. \quad (7.36)$$

As $j \rightarrow \infty$, clearly $c_j^C \rightarrow c^R$.

So, if the right branch is long enough for multiple shifting operations the general trend for the cable c -values is to tend towards the right branch c -value, but with a castellated diameter profile oscillating above and below c^R , as illustrated in Figure 7.3b.

The new left branch limb after a operations is connected to the $(2a)^{th}$ cable cylinder, and has c -value

$$c_{\xi,2a}^L = \frac{c^R c^L}{c^R + (2a)c^L}. \quad (7.37)$$

which clearly decreases as a increases.

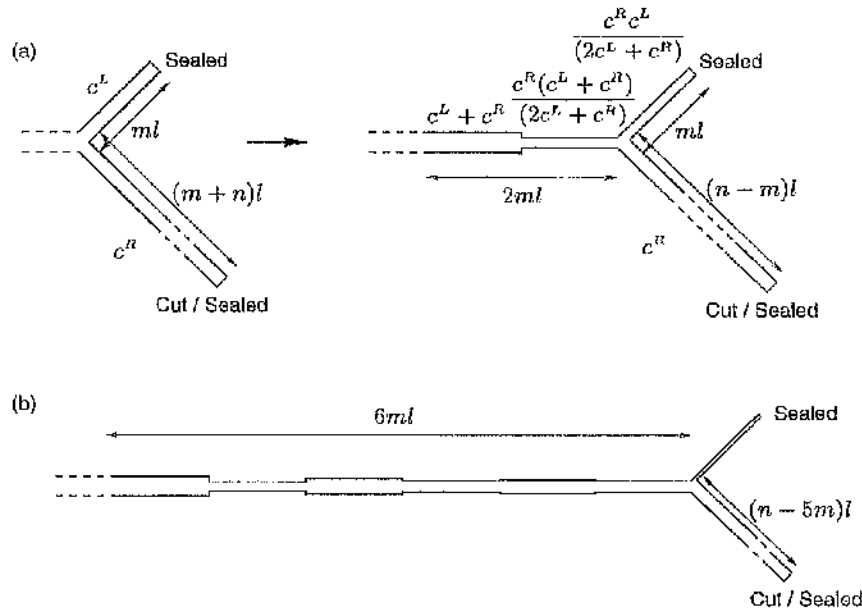


Figure 7.3: The branch-shifting operation when the short branch has a sealed terminal and $n > m$. (a) The single operation, with new c -value. (b) If right branch is long enough, the operation can be repeated multiple times.

7.4.2 Long Cylinder Has a Sealed End and is Less Than Twice the Length of the Short Cylinder ($n \leq m$).

The c -values and potential function expressions now start to get more complex, with the equivalent trees having stems consisting of more than two cylinders. A full derivation is not given since it is similar to the previous case².

Recall that $m = kn + z$. The part of the equivalent cable that is generated (i.e. the stem to which the new Y-junction will be connected) is formed from $(k+2)$ cylinders. The first cable segment is the usual one, with length ml . Connected to this cylinder are k cylinders each of length nl , and then a final cylinder of length zl , at the end of which a new Y-junction is connected. One of the two new Y-junction cylinders has length zl , while the other has length $(n-z)l$.

The first two stem c -values, c_1^G and c_2^G , are identical to those of the previous Y-junction class, as are the potential functions except that ϕ_2 is only valid for length nl . The remaining c -values are given iteratively, for $3 \leq i \leq (k+2)$ by

$$c_j^G = c_{j-1}^G \left[1 - \frac{2c_1^G}{(j-1)c_1^G + c^L} \right]. \quad (7.38)$$

²Though with an inductive extension to the argument.

It is then easily shown that

$$c_j^C = \frac{c_1^C c^L c^R}{[(j-1)c_1^C + c^L][(j-2)c_1^C + c^L]}, \quad (7.39)$$

which is also valid for $j = 2$. Clearly the c-values decrease as j increase.

The new Y-junction cylinders have c-values

$$c_\xi^L = c_{k+2}^C \left[\frac{kc_1^C + c^L}{c_1^C} \right], \quad c_\xi^R = c_{k+2}^C \left[\frac{(k+1)c_1^C + c^L}{c_1^C} \right]. \quad (7.40)$$

which may also be written as

$$c_\xi^L = \frac{c^L c^R}{(k+1)c_1^C + c^L}, \quad c_\xi^R = \frac{c^L c^R}{kc_1^C + c^L}. \quad (7.41)$$

Clearly, for large k at least, the new Y-junction c-values are small, yet they will still be significantly bigger than the c_{k+2}^C . After length $2ml$, then, the cable c-values are pumped up slightly before they continue narrowing when the new Y-junction is reduced.

To simplify the corresponding potential functions, it is convenient to write

$$\psi(x) = v_R(x) - v_L(x). \quad (7.42)$$

Now, if j is odd and $3 \leq j \leq k+2$ then

$$\begin{aligned} \phi_j(x) &= \psi((m - (j-2)n)l + x) - \frac{(j-2)c_1^C + c^L}{c_1^C} \psi((m - (j-2)n)l - x) \\ &+ \sum_{a=0}^{\frac{j-5}{2}} \psi((m - (2a+1)n)l + x) + \psi((m - (2a+1)n)l - x) \\ &+ v_R((ml + x)). \end{aligned} \quad (7.43)$$

(Note that the sum goes to zero for $j = 3$.) Otherwise, for j even and $2 \leq j \leq k+2$,

$$\begin{aligned} \phi_j(x) &= \frac{(j-2)c_1^C + c^L}{c_1^C} \psi((m - (j-2)n)l - x) + v_R((ml + x)) \\ &+ \sum_{a=0}^{\frac{j-4}{2}} \psi((m - 2(a+1)n)l + x) + \psi((m - 2an)l - x). \end{aligned} \quad (7.44)$$

(This formula also produces the correct potential for $j = 2$).

Each stem potential from ϕ_2 to ϕ_{k+1} is valid for $0 \leq x \leq nl$. The final stem potential ϕ_{k+2} is valid for $0 \leq x \leq zl$. Each pair of components with the same destination satisfies a local sealed condition (i.e. their coefficients have the same sign and magnitude).

If k is odd then the potentials in the new Y-junction are

$$\begin{aligned} \xi_L(x) &= \psi(x) + \psi(2zl - x) \\ &+ \sum_{a=0}^{\frac{k-3}{2}} \psi((m - (1+2a)n + z)l - x) + \psi((m - (1+2a)n - z)l + x) \\ &+ v_R((n + m - z)l + x), \quad 0 \leq x \leq zl. \end{aligned} \quad (7.45)$$

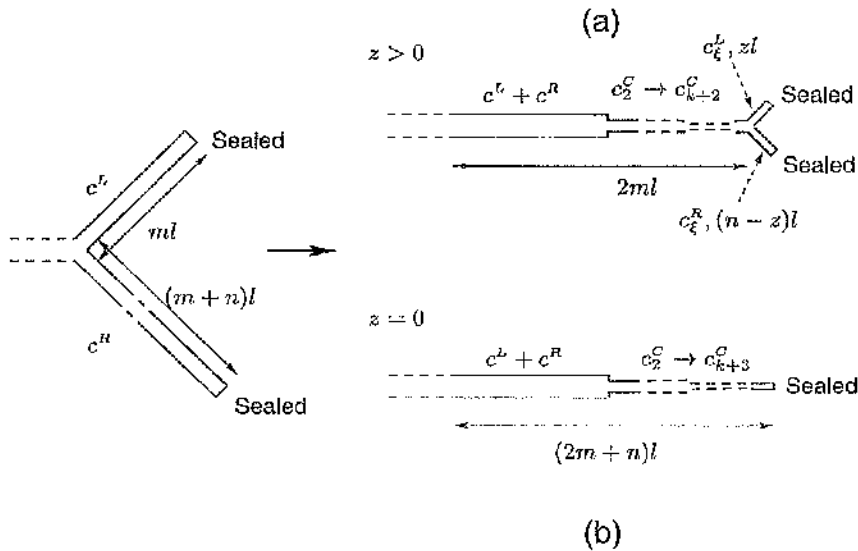


Figure 7.4: The branch-shifting operation when both Y-junction terminals are sealed and $n < m$. (a) A new Y-junction is formed when $0 < z < n$ (b) This is a final shifting operation when $z = 0$, and the original Y-junction is non-degenerate. See text for full details of c -value expressions.

$$\begin{aligned}\xi_R(x) &= \psi(2zl + x) \\ &+ \sum_{a=0}^{\frac{k-3}{2}} \psi((m - (1+2a)n + z)l + x) + \psi((m - (1+2a)n - z)l - x) \\ &+ v_R((n+m-z)l - x), \quad 0 \leq x \leq (n-z)l.\end{aligned}\quad (7.46)$$

(Note that the sum goes to zero when $k = 1$.) Otherwise k is even and

$$\begin{aligned}\xi_L(x) &= \psi(x) \\ &+ \sum_{a=0}^{\frac{k-2}{2}} \psi((m - 2(a+1)n + z)l - x) + \psi((m - 2an - z)l + x) \\ &+ v_R((m+z)l - x), \quad 0 \leq x \leq zl.\end{aligned}\quad (7.47)$$

$$\begin{aligned}\xi_R(x) &= \sum_{a=0}^{\frac{k-3}{2}} \psi((m - 2(a+1)n + z)l + x) + \psi((m - 2an - z)l - x) \\ &+ v_R((m+z)l + x), \quad 0 \leq x \leq (n-z)l.\end{aligned}\quad (7.48)$$

Both child cylinders terminate with a sealed condition.

Consider now the special case where $z = 0$. The right cylinder of the new Y-junction has length nl , while the left disappears. Both terminals, but in particular the left, are sealed and so the new right limb becomes the final segment of an equivalent unbranched

structure, i.e. there is no disconnected section. Since one limb of the original Y-junction has length equal to an odd number of nl while the other is an even number, analytical results in Chapter 5 have already predicted this non-degeneracy. We can write $c_{k+3}^C = c_k^R$. Figure 7.4 illustrates this operation for both $z \neq 0$ and $z = 0$.

It is important to note that, as j increases, and cylinder c-values decrease, the potential function component coefficients become large. Basically, the voltage electrical mapping from tree to narrow cylinders is strong. Recalling from Chapter 6 that injected current divided by c-value is mapped in the same way as the potential, then, since the cable c-values become much smaller than tree c-value, the current mapping from tree to narrow cable sections is weak.

7.4.3 Long Cylinder Has a Cut End and is Less Than Twice the Length of the Short Cylinder ($n \leq m$).

This situation is the most complicated encountered when dealing with simple Y-junctions. The first two cable cylinders and potentials take forms identical to those in the previous case where the long branch is sealed. This is not surprising since at this stage no components have reflected from the cut terminal. Again the stem is formed from $(k+2)$ cylinders, with the same lengths as in the previous case (i.e. m , k times n , and z), then the stem splits into a new Y-junction, with one child length zl , the other length $(n-z)l$.

When j is odd and $3 \leq j \leq k+2$,

$$c_j^C = c_{j-1}^C \left[1 + \frac{2c_1^C}{(j-3)c_1^C + c^L} \right]. \quad (7.49)$$

Otherwise, for j even and $2 \leq j \leq k+2$,

$$c_j^C = c_{j-1}^C \left[1 - \frac{2c_1^C}{(j-1)c_1^C + c^L} \right]. \quad (7.50)$$

It can be subsequently be shown quite easily that when j is odd and $j \geq 3$ then

$$c_j^C = \frac{c^R c_1^C}{c^L} \left[\frac{(j-1)c_1^C + c^L}{(j-2)c_1^C + c^L} \right], \quad (7.51)$$

while if $j \geq 2$ is even, then

$$c_j^C = \frac{c^R c_1^C}{c^L} \left[\frac{(j-2)c_1^C + c^L}{(j-1)c_1^C + c^L} \right]. \quad (7.52)$$

Clearly, then, the cable c-values exhibit a castellated diameter profile, and as $j \rightarrow \infty$, they tend to c-value $c^R c_1^C / c^L$, i.e. the c-value of the second cable cylinder for the symmetric non-Rall Y-junction. This is because the large j (high k) are only possible when the right branch is only slightly longer than the short branch, i.e. tree structure does not deviate too much from the symmetric case.

The new Y-junction c-values are, for both k even and k odd,

$$c_\xi^L = c_{k+2}^C \left[k + \frac{c^L}{c_1^C} \right], \quad c_\xi^R = c_{k+2}^C \left[k + 1 + \frac{c^L}{c_1^C} \right]. \quad (7.53)$$

The larger the value of k , the bigger the c-values in the new Y-junction.

If j is odd and $3 \leq j \leq k+2$ the potential functions are

$$\begin{aligned} \left[\frac{(j-1)c_1^C + c^L}{c^L} \right] \phi_j(x) &= -\frac{(j-2)c_1^C + c^L}{c_1^C} \psi((m-(j-2)n)l-x) \\ &+ (-1)^{\frac{j-1}{2}} \psi((m-(j-2)n)l+x) \\ &+ (-1)^{\frac{j-1}{2}} \sum_{a=0}^{\frac{j-5}{2}} (-1)^a [\psi((m-(1+2a)n)l+x) - \psi((m-(1+2a)n)l-x)] \\ &+ (-1)^{\frac{j-1}{2}} v_R((m+n)l-x). \end{aligned} \quad (7.54)$$

(The sum is zero when $j=3$.) Observe that where two components on the same branch meet their coefficients ensure a local current condition.

Otherwise, if j is even and $2 \leq j \leq k+2$,

$$\begin{aligned} \left[\frac{(j-1)c_1^C + c^L}{c^L} \right] \phi_j(x) &= -\frac{(j-2)c_1^C + c^L}{c_1^C} \psi((m-(j-2)n)l-x) \\ &+ (-1)^{\frac{j}{2}} \sum_{a=0}^{\frac{j-4}{2}} (-1)^a [\psi((m-2(a+1)n)l+x) - \psi((m-2an)l-x)] \\ &+ (-1)^{\frac{j-1}{2}} v_R(ml+x). \end{aligned} \quad (7.55)$$

Observe that where two components on the same branch meet their coefficients ensure a local cut condition.

The new child cylinder potential functions are, if k is odd

$$\begin{aligned} \left[\frac{(k+1)c_1^C + c^L}{c^L} \right] \xi_L(x) &= \psi(x) + \sum_{a=0}^{\frac{k-1}{2}} (-1)^{a+1} \psi(2(z+an)l+x) \\ &+ \sum_{a=0}^{\frac{k-3}{2}} (-1)^{a+1} \psi(2(a+1)nl-x) \\ &+ (-1)^{\frac{k+1}{2}} v_R(knl+x), \quad 0 \leq x \leq zl. \end{aligned} \quad (7.56)$$

$$\begin{aligned} \left[\frac{(k+1)c_1^C + c^L}{c^L} \right] \xi_R(x) &= \sum_{a=0}^{\frac{k-1}{2}} (-1)^a \psi(2(z+an)l+x) \\ &+ \sum_{a=0}^{\frac{k-3}{2}} (-1)^{a+1} \psi(2(a+1)nl-x) \\ &+ (-1)^{\frac{k+1}{2}} v_R((k+1)nl-x), \quad 0 \leq x \leq (n-z)l. \end{aligned} \quad (7.57)$$

In this case, the new left branch satisfies a sealed condition, while the right branch satisfies a cut condition. Otherwise, k is even and

$$\left[\frac{kc_1^C + c^L}{c^L} \right] \xi_L(x) = \psi(x) + \sum_{a=0}^{a=\frac{k-2}{2}} (-1)^a \psi(2(z+an)l - x) \\ + \sum_{a=0}^{a=\frac{k-2}{2}} (-1)^{a+1} \psi(2(a+1)nl + x) \\ + (-1)^{\frac{k}{2}} v_R((m+z)l - x), \quad 0 \leq x \leq zl. \quad (7.58)$$

$$\left[\frac{kc_1^C + c^L}{c^L} \right] \xi_R(x) = \sum_{a=0}^{a=\frac{k-2}{2}} (-1)^a \psi(2(z+an)l + x) \\ + \sum_{a=0}^{a=\frac{k-2}{2}} (-1)^{a+1} \psi(2(a+1)nl - x) \\ + (-1)^{\frac{k}{2}} v_R((m+z)l + x), \quad 0 \leq x \leq (n-z)l. \quad (7.59)$$

In this case, the new left branch satisfies a cut condition, while the right branch satisfies a sealed condition.

If $z = 0$, then m is an integral multiple of n , and the left branch disappears. In this case we have a final branch-shifting operation. However, the existence of a disconnected section depends on whether k is odd or even.

Consider k odd, where the left branch has a sealed terminal. When $z = 0$, this condition is essentially shifted to the connection between right branch and cable, but as has been noted previously, the sealed terminal does not interfere with current flow between the right branch and cable. Thus when k is odd, the original Y-junction is non-degenerate. The right branch simply extends the cable by length nl , and we may write $\phi_{k+3}(x) = \xi_R(x)$.

If k is even, however, the left branch has a cut terminal. Shifting the cut terminal to the point where right branch and cable meet effectively isolates them electrically, and the right branch, with length nl , forms a disconnected section.

Figure 7.5 illustrates all cases for this class of Y-junction.

In contrast to the situation where both terminals are sealed, when j increases, and cylinder c -values increase, the potential function component coefficients become small. The voltage electrical mapping from tree to wide cylinders is weak. Again recalling that injected current divided by c -value is mapped in the same way as the potential, then the current mapping from tree to wide cable is strong.

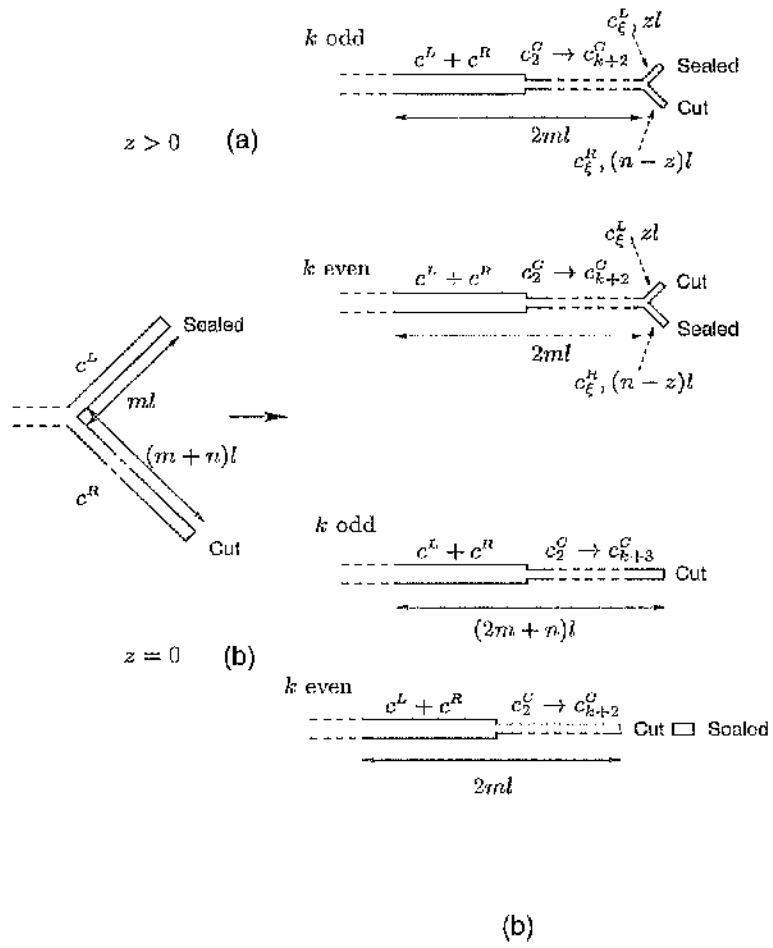


Figure 7.5: The branch-shifting operation when the short cylinder terminal is sealed, the long terminal is cut and $n < m$. (a) A new Y-junction is formed when $0 < z < n$. (b) This is a final shifting operation when $z = 0$, and the original Y-junction is non-degenerate if k is odd, and degenerate if k is even. See text for full details of c-value expressions.

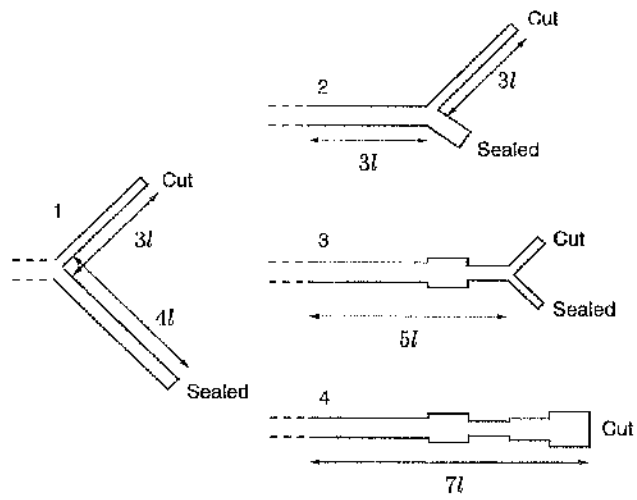


Figure 7.6: Example 1, illustrating the branch-shifting process. (1) The original tree, consisting of one cylinder length $3l$ with a cut terminal, and one cylinder length $4l$ with a sealed terminal. (2) The equivalent tree generated after shifting the short cut cylinder length $3l$ along the long branch. (3) The equivalent tree after shifting the new Y-junction's short sealed cylinder by length $2l$ along the new Y-junction's long cut terminal. (4) The non-degenerate fully equivalent cable obtained after collapsing the non-Rall symmetric Y-junction.

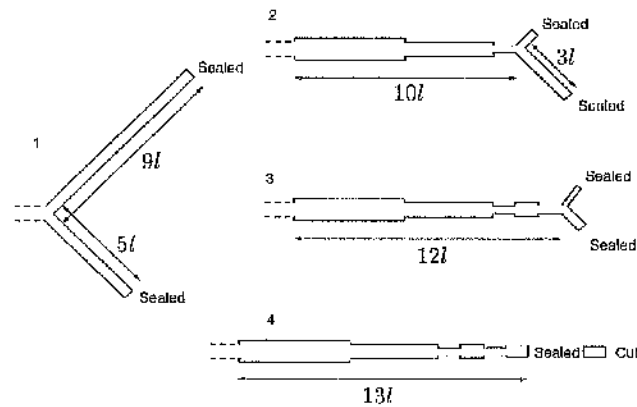


Figure 7.7: Example 2, illustrating the branch-shifting process. (1) The original tree, consisting of one cylinder length $9l$ and one cylinder length $5l$, both with sealed terminals. (2) The equivalent tree generated after shifting the short sealed cylinder by length $10l$. Since $5 = 1 \times 4 + 1$, three cylinders of the equivalent cable are produced, with lengths $5l$, $4l$ and l in order. The new Y-junction has one branch with length $3l$ and one with length l , both with sealed terminals. (3) The equivalent tree generated after shifting the new short sealed cylinder by length $2l$. (4) The fully equivalent cable after collapsing the Rall symmetric Y-junction. The original Y-junction is therefore degenerate.

7.5 Discussion

Branch-shifting operations can be applied to generate fully equivalent cables for simple Y-junctions, as illustrated in Figures 7.6 and 7.7. They may also be used to partially collapse Y-junctions that have suitable (i.e. uniform) structure up to a certain distance from the junction. For example, the short branch may consist of one cut cylinder of length $4l$ while the right branch consists of one cylinder of length $5l$ connected to a further two l -length cylinders the second of which terminates with a sealed condition. The short cut branch may be shifted once, but none of the given shifting operations are valid after this.

Attempts have been made to extend the branch-shifting process to general Y-junctions, however, shifting of multi-cylinder short branches has proven problematic. Therefore, it has not been possible to derive general branch-shifting operations that apply to trees with order higher orders of branching because the fully equivalent cable for a uniform Y-junction is not usually uniform itself. Basically, it seems that in these more complex structures, the analytical rules don't ensure that simple sub-sets of potential function components can satisfy boundary conditions. However, branch-shifting is possible if the left branch consists of one cylinder length ml , while the right cylinder consists of a chain of cylinders of length ml . The derivation of these results takes only a little more effort than for the simple Y-junction, and is not repeated.

Despite this current lack of obvious extensibility, the analytical results produced by the branch-shifting method clearly indicate how cable structure is shaped by length and boundary conditions, and how the electrical mapping is obtained by a repeated nesting of simpler potentials. Formulae for equivalent cables c-values for general Y-junctions are much more complicated, but this is only because the cable fine structure is more complicated. The general trend is for c-values to (1) increase in size when a cut terminal is encountered, (2) castellate when a single sealed terminal has been encountered, or castellate and/or increase when both a cut and sealed terminal have been encountered, (3) narrow when two sealed terminals have been encountered, and (4) increase rapidly in size if two cut terminals have been encountered.

Further discussion, from a physiological point of view, of why cable structure follows these trends is given in Chapter 8.

Chapter 8

Discussion, Conclusions, and Future Work

8.1 Introduction

Beyond their general role as integrators of distributed electrical activity, the full implications of complicated dendritic morphologies for neuronal signal processing are not known. Fully equivalent cables are a novel approach to the geometrical analysis of passive dendrites that allows one to extract information about their signal processing capabilities that is otherwise obscured by physical complexity.

This chapter summarises and discusses the main results of this thesis. Included is a brief comparison of the fully equivalent cable construction methods and a thorough discussion, in physiological terms, of cable structure as revealed through the analytical results in Chapters 5, 6 and 7. To link the theory with reality, several cables are constructed from morphological data for real motoneuron dendrites. We consider how equivalent cable structure is robust under small changes in dendritic structure; this is an important consideration given inevitable uncertainties in any experimentally obtained data.

The novelty and generality of the approach used makes fully equivalent cables far more suitable than either numerical simulation or previous cable models as a tool for analysing passive dendritic tree geometry and signal integration within such structures. We discuss the physiological implications of fully equivalent cables for understanding the relationship between structure and function in passive tree models, in particular the geometry-determined local and global signal processing capabilities of complicated dendrites. The implications for models with active membrane are also considered.

We also consider briefly the subject of parameter estimation, commonly associated with the quasi-equivalent cables models that were outlined in Chapter 3. Fully equivalent

cables have several implications in this area.

Finally, we consider possible applications of fully equivalent cables, and outline future work that might employ or extend the equivalent cable theory.

8.2 Fully Equivalent Cable Construction

The passive tree model (Chapter 2) is formed from linked neuronal cylinders subject to joining (current conservation, voltage continuity) and terminal boundary conditions. Terminals may either be of the cut (zero voltage) or current injection (specified voltage gradient) types. For simplicity, only the sealed end (zero voltage gradient) special case of the latter will be considered, since the specific value of the gradient has no bearing on cable structure and only enters the problem through the electrical mapping.

The existence of fully equivalent cables follows, without restrictions, from the passive model, and they are obtained on application of a suitable mathematical transformation. Also formed from linked cylinders, though without branching, a fully equivalent cable is electrically identical, with respect to a point of origin, to its associated tree. A fully equivalent cable consists of one connected section that is attached to the origin, and possibly several isolated disconnected sections. The (electrotonic) length-preserving mapping which relates electrical activity between tree and cable ensures that fully equivalent cables satisfy the mathematical definition of equivalence given in Chapter 3. None of the previous restrictive or empirical quasi-equivalent cable models meet the requirements for mathematical equivalence.

Several mathematical procedures for transforming multiple uniform segment (in particular multi-cylinder) passive dendritic tree models into their fully equivalent cables have been presented. These comprise two matrix methods (Chapter 4) and an analytically derived method (Chapters 5 and 6), each of which is suitable for transforming passive tree models of arbitrary morphology. In addition, a branch-shifting process (Chapter 7) will reduce simple Y-junctions (two uniform limbs) to their equivalent cables via an intermediate set of equivalent Y-junctions. Figure 8.1 summarises cable construction and general features of cable structure. Each construction method can be implemented effectively as a computer algorithm.

In order to generate disconnected sections, the construction methods must transform a tree in a Y-junction by Y-junction fashion, gradually removing branch-points, transforming more and more structure, and accumulating any disconnected sections associated with specific sub-trees, until the fully equivalent cable is generated. If a (binary) tree has N branch points, a set of $N + 1$ equivalent structures (equivalent structures include the original tree, the intermediate trees with disconnected sections associated with transformed

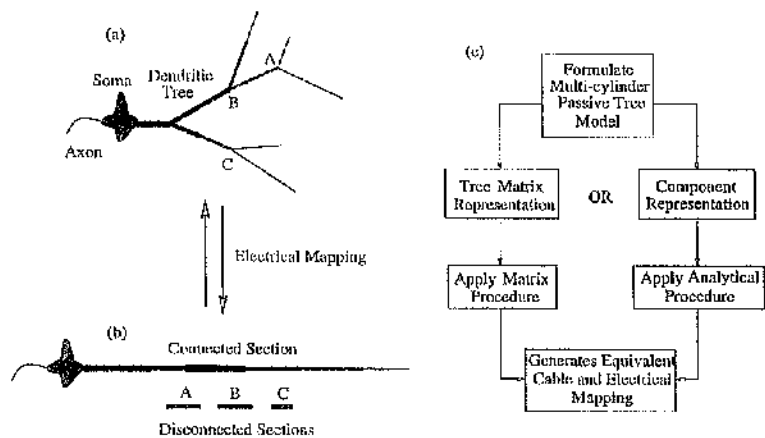


Figure 8.1: Features of fully equivalent cable structure and the construction methods. (a) An electrically passive multi-cylinder dendritic tree model may be transformed to (b) its fully equivalent cable, using (c) either a matrix or analytically derived construction algorithm. A connected section is attached to the cell body instead of the original tree. Disconnected sections (A, B, and C) are associated with local activity over specific dendritic sub-trees (stemming from points A, B, and C).

sub-structure, and also the final equivalent cable) will be generated in the process. This does not constitute the full set of equivalent structures, however, since one can usually transform certain Y-junctions in a different order, and additional intermediate trees may be found if any Y-junctions can be branch-shifted. Note that the order in which its sub-trees are reduced does not affect the structure of the the final equivalent cable.

The derivation of the analytical method of cable construction (consisting of two sets of construction rules) gives great insight into why the cables can actually exist at all. The electrical continuity rules, which follow straightforwardly from a first-principles construction algorithm (Chapter 5), show that it is possible to guarantee voltage continuity and current conservation in a new unbranched structure, but without uniquely defining this structure. By insisting that Y-junctions may be transformed in isolation from the rest of the tree, a set of isolation-termination rules may be formulated which ensure that the cable will eventually terminate, and is uniquely defined. The isolation-termination rules simplify substantially for simple Y-junctions. There are indications that an even deeper mathematical structure, and a more fundamental set of construction rules probably exists.

The analytically derived construction algorithm is reasonably effective, although, in the form given, cannot compete with the matrix methods for raw speed. If any simple Y-junctions are encountered during the transformation of a tree, then by far the most efficient way to rapidly produce their equivalent cables is to use the analytical expressions obtained from the branch-shifting method (Chapter 7).

Of the two matrix methods, the Householder is the preferred approach since it naturally generates disconnected sections, and is established as a highly stable procedure. The Lanczos method is the fastest and most memory-efficient way to construct fully equivalent cable structure provided the connected section is all that is required, i.e. information concerning disconnected sections and the electrical mapping is not retained. It is not as numerically stable as the Householder method, but this instability is only likely to emerge where the tail of a sealed connected section narrows rapidly. Fortunately, analytical results allow cable structure, and the existence of disconnected sections in particular, to be predicted prior to construction, and this enables checks to be made as the matrix algorithms progress.

The construction methods all ensure that important properties of a tree are conserved in its fully equivalent cable. The total electrotonic length of a tree equals the total electrotonic length of its fully equivalent cable. The steady-state input conductance of the tree equals the steady-state input conductance of the cable connected section. In addition, if the tree terminals are sealed (or subject to current injection boundary conditions), total surface area and injected current are preserved in the equivalent cable's connected section.

The assumptions for the passive multi-cylinder model ensure that cable results are independent of specific electrical parameters, i.e. membrane capacitance per unit area, membrane conductance per unit area, and cytoplasmic resistivity, which have been taken to be constant for the tree¹.

8.3 Fully Equivalent Cable Structure and Tree Function

Electrical activity on a multi-cylinder passive dendritic tree model either must (if all Y-junctions encountered during reduction are non-degenerate) or may (if any Y-junctions are degenerate) induce a resultant disturbance in the potential at the origin. Fully equivalent cable cylinders must have just the right electrotonic lengths, diameters and boundary conditions such that the corresponding activity over the equivalent cable, as defined by the electrical mapping, will generate exactly the same effect at the origin. An input current (or the membrane potential) at one point on a dendritic tree will typically map to many inputs (or a distribution of membrane potentials) on the equivalent cable, and vice-versa.

The analytical results in Chapter 6 have shown that the electrotonic lengths of each separate cable section can be determined prior to construction (see Figures 6.16, 6.17 and 6.18). In addition, the branch-shifting results of Chapter 7 clearly describe trends in the

¹Recall from Chapter 2 that there is actually more flexibility than this, i.e. in the choice of cross-sectional profile (A and P) and the electrical parameters (ρ_i , g_M , C_M) in each uniform segment of dendrite, provided that the ratio C_M/g_M is a constant throughout the tree.

connected section fine structure which are determined primarily by boundary conditions, and also by relative electrotonic lengths of branches. Disconnected sections are generally short (compared to the total electrotonic length), most often consisting of a single cylinder of basic unit length. They are long only when the original Y-junction exhibits a high level of symmetry, i.e. Rall trees and the non-uniform generalisation given in section 6.4.2 (where the left and right branches have the same electrotonic length and boundary condition, and a constant c-value ratio from origin to tips). In such cases, the disconnected section structure is similar to that of the connected section, except that one end terminates with a cut end rather than being attached to the junction (recall Figure 6.7).

8.3.1 The Influence of Boundary Conditions

Boundary conditions dominate in determining whether there is a tendency for an increasing, decreasing, or roughly uniform (castellating) trend in the diameter profile of an equivalent cable's connected section (moving away from the origin towards the terminal). These trends are clear from the analytical expressions obtained in Chapter 7 for simple Y-junctions. As one moves from junction to branch tips of a Y-junction, constructing a fully equivalent cable cylinder by cylinder, c-values tend to

1. Increase in size once a single cut terminal is encountered.
2. Castellate, or oscillate, when a single sealed terminal has been encountered.
3. Narrow when two sealed terminals have been encountered, possibly with the occasional distinct jump in diameter.
4. Increase rapidly in size if two cut terminals have been encountered.
5. Castellate, or oscillate, and/or increase in size, once both a cut and sealed terminal have been encountered.

The connected section terminates with a cut terminal unless both Y-junction terminals are sealed, in which case it terminates with a sealed end.

Recalling that the current injection boundary condition is equivalent to a sudden drop in diameter to zero, while a cut boundary condition is equivalent to a sudden jump to infinite diameter, then it can be seen that a boundary condition tends to impose itself on cable structure by shifting c-values towards the particular extreme diameter that the terminal condition represents.

Tree structure at an electrotonic distance x from the origin can only influence cable structure beyond a distance x from the origin. Although there exist symmetric trees (Rall trees and the generalisations given in Chapter 3) where boundary conditions don't have a

chance to exert their influence on cable structure before the connected section terminates (tree boundary conditions only determine cable boundary conditions), in general the length of the connected section is longer than the maximum origin-to-tip electrotonic length, enabling a boundary condition at electrotonic length l to influence subsequent equivalent cable connected section structure.

Figure 8.2 illustrates a set of equivalent cables for Y-junctions where each branch has the same c -value, as well as sealed terminals. Total electrotonic length, and consequently surface area, is the same in each Y-junction — they are distinguished only by the relative electrotonic lengths of the two branches, indicated to the left of the connected section. The sealed boundary conditions ensure that cable structure tends to experience castellating and/or narrowing, while relative lengths determine how far from the origin significant (if any) narrowing takes place. Clearly, the smaller the difference in branch lengths (i.e. the closer the Y-junction is to satisfying conditions for a Rall tree) then the shorter the connected section length before either termination or distinct narrowing occurs. In fact this length corresponds to the length of the longer Y-junction limb. In most cases, the narrower structure is clearly not negligible. Note that the construction methods for empirical cable models (Chapter 3) would terminate when the long limb terminal was reached, unable to approximate important tail sections in the fully equivalent structure.

It is not practical to illustrate cables for the same trees but with both terminals cut, since diameters, from origin to terminal, often range over several orders of magnitude — c -values are always increasing. Except for the Rall Y-junction, the surface area of the connected section is very much greater than that of the tree.

A selection of cables for Y-junctions, where one terminal is cut and the other is sealed, are illustrated in Figure 8.3. Ratios of sealed branch length to cut branch length range from 39:1 to 3:37. For the length of the sealed branch, the equivalent cables have identical structure to the corresponding cables in Figure 8.2. Beyond this point, the cut terminal comes into play and the diameters are generally increasing. The closer the cut terminal to the junction, the more dramatic the influence it has on cable structure, increasing surface area considerably. The non-Rall symmetric Y-junction (20:20) is merely a uniform cylinder, but with electrotonic length twice that the origin-to-tip length.

8.3.2 Signal Loss and Signal Reflection

The fact that two boundary condition types have extreme and opposite effects on equivalent cable diameters, can be understood in terms of signal loss and signal reflection at the dendritic tree terminals. Recall from Chapter 2 that no charge may leak from a sealed terminal (this is regarded as signal reflection, since charge flow is redirected back towards the cell body), while charge leaks directly from a cut terminal (this is regarded as signal

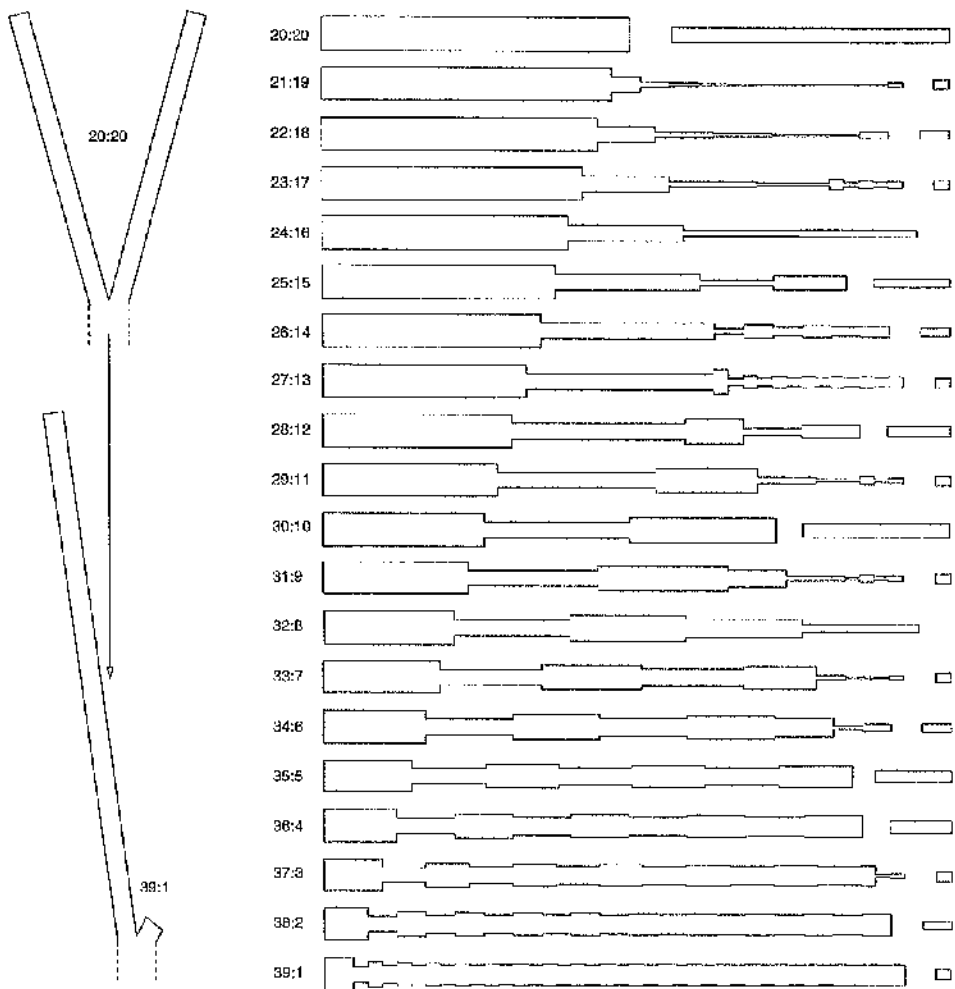


Figure 8.2: A selection of cables for simple Y-junctions with the same surface area but different left and right branch lengths; both tree terminals are sealed. Both branches have the same diameter so that all trees have the same total electrotonic length (40 basic units). The cable origin is at the left in each case. Moving from top to bottom, the tree branch length ratio progresses from 20:20 (the Rall Y-junction) to 39:1. The quantum length for a particular is the largest common factor of the two branch lengths, which in many cases is larger than 1, in the units given. See text for discussion.

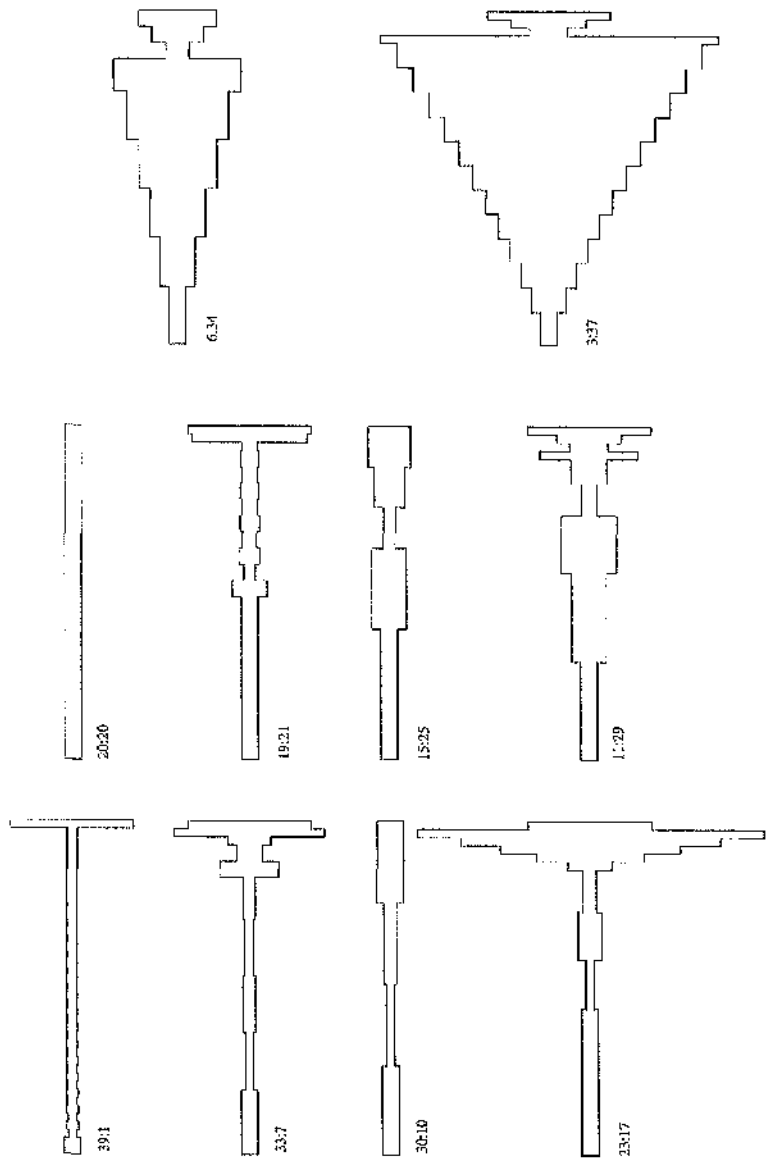


Figure 8.3: A selection of cables for simple Y-junctions with the same surface area but different left and right branch lengths; one tree terminal is sealed, while the other is cut. Both branches have the same diameter so that all trees have the same total electrotonic length (40 basic units). The cable origin is at the left in each case. branch length ratios are given in the form (sealed branch length):(cut branch length). See text for discussion.

loss). We must consider cable structure in conjunction with the nature of the electrical mapping to this structure.

As the analytical expression derived from the branch-shifting method have already indicated (Chapter 7), there is a clear relationship between equivalent cable cylinder diameter and the relative magnitude of the electrical mapping from any point on the tree to that cylinder. Since trends in cable structure are determined primarily by boundary conditions, then so is mapping strength. Basically, sealed terminals promote strong voltage mappings and weak injected current mappings, while cut terminals promote weak voltage mappings and strong injected current mappings.

This can now been seen in Figures 8.4a–c. A unit potential is mapping from each tree to its equivalent cable. The potential at electrotonic distance X on the dendritic tree will map to a scaled potential at distance X on the cable connected section, plus multiple positive and negative potentials further down the cable. These additional potentials are necessary to compensate for the non-Rall nature of the Y-junction, i.e. they account for the modulation of electrical activity in unsymmetric dendritic structure.

For a unit potential input on a branch of the dendritic tree, at distance X , say, from the origin, then beyond distance X along the equivalent cable there is generally a large mapping to cylinders with small diameters and a small mapping onto cylinders with large diameters. The current mapping follows straightforwardly — recall that the ratio of applied current to c -value is mapped in the same way as voltage. Where there is a large membrane surface area (large diameter), a large current will be required to depolarise it a small amount, while only small currents are required to produce a significant depolarisation across the membrane of thin cylinders.

The promotion of large diameters by cut ends is consistent with the fact that accumulated charge leaks from cut terminals. Since the greater amount of current flows in the direction of lower impedance (i.e. larger diameters), within these large cylinders a greater amount of charge is channelled away from the origin towards the cut end. The large current mapping describes this lost current. The corresponding small voltage mapping mimics the fact that there is minimal signal reflection within the tree.

The promotion of small diameters by a completely sealed tree is consistent with the fact that there is no signal loss from such a terminal. The decreasing cylinder diameters channel the greater amount of charge back towards the equivalent cable origin, a result of full reflection at sealed terminals in the original tree. The strong voltage mapping describes the strong reflected component of the signal, while the corresponding weaker current mapping mimics the zero current loss from terminals.

Two different boundary conditions on a Y-junction (one cut and one sealed) results in an equivalent cable connected section with a cut terminal. This ensures that accumulated

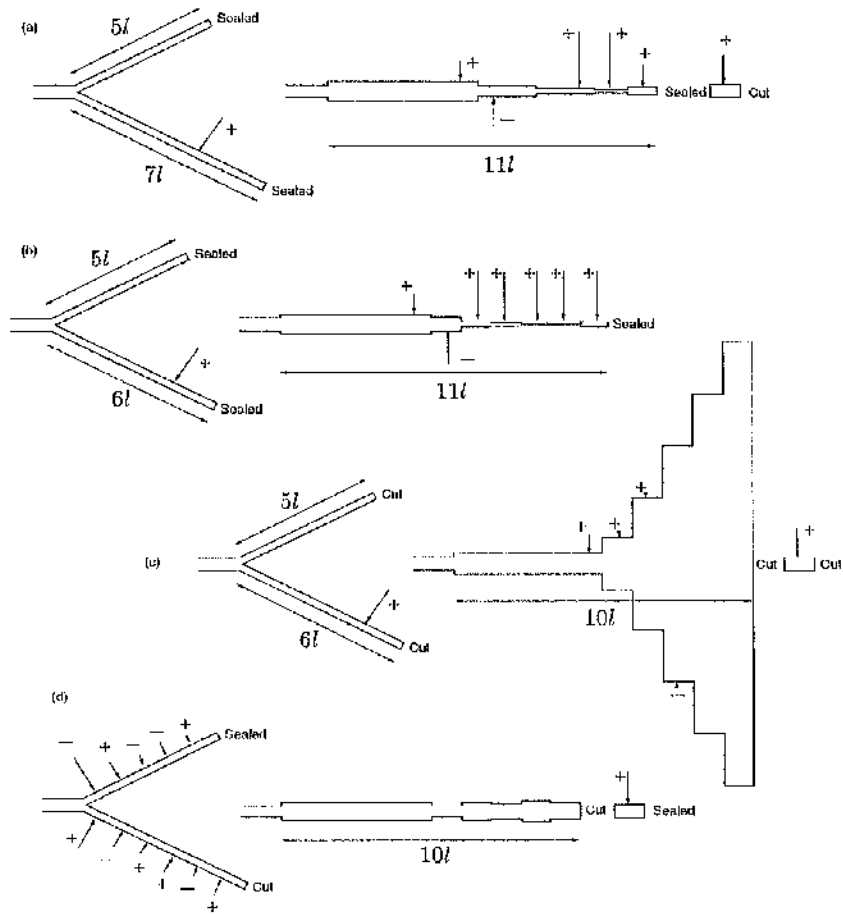


Figure 8.4: Examples of electrical mappings in Y-junction dendritic trees where the electrotonic lengths of child branches are unequal. The sizes of the arrows indicate the strength of the mapping at each point.

charge may still leak from the system (other than through the membrane).

8.3.3 Implications of “Fuzzy” Tree Data

The trees that are used for cable construction must be formed from cylinders whose lengths are multiples of a common basic length, however small this might be. As discussed in Chapter 2, real tree morphological data has some measure of uncertainty associated with it. For example, it is possible that two Y-junction representations, one degenerate and one non-degenerate, are equally valid models of real data for a Y-junction. The point is that fully equivalent cables are equivalent to the tree model, not the data.

It is important to note that, except in the unlikely case of the non-uniform generalisations of a Rall tree, the length of a disconnected section is typically one basic unit, but possibly two units (if both terminals are cut). Clearly, then, by decreasing the basic unit of electrotonic length in order to increase model resolution, one is likely to increase the electrotonic length of the connected section, and decrease the length of disconnected sections by the corresponding amount (in certain cases so that disconnected sections may disappear completely). Exactly disconnected sections, and therefore exact electrical degeneracy, are features of the multi-cylinder model, not necessarily of the original tree data.

This is where approximate degeneracy must be considered. It is possible that sections of the connected section that are near the end of the connected section are so narrow (in the case of a sealed end), or so wide (in the case of a cut end), as to be regarded as effectively disconnected, and having negligible influence at the origin. The corresponding electrical mappings describe activity that is, for all intents and purposes, ineffective at the origin in comparison to similar activity mapped from cable cylinders that are closer to the origin. Fully equivalent cables are robust objects, as discussed in Chapter 3.

8.3.4 Complicated Dendritic Geometry

Equivalent cable results for Y-junctions generally extend naturally to more complicated trees — after all, any tree can be turned into a Y-junction by successive reduction of its sub-trees. The major differences are in the number of disconnected sections, and the subtlety in the fine structure of the cable, while the influence of boundary conditions is more pronounced, i.e. cut terminals promote extremely large diameters, while sealed terminals promote more significant narrowing of a cable. Of course, these things depend on the level of complexity in the dendritic tree being transformed.

As more structure is transformed, the ratio of basic electrotonic length to total electrotonic length becomes smaller. This tends to produce cables that are less obviously discontinuous, and have a smoother diameter profile.

For example, suppose the Y-junctions at the tips of a sealed tree (with n orders of branching) are transformed, producing narrowing cables that are reattached at the corresponding branch points. The Y-junctions at the tips of the new tree (with $n - 1$ orders of branching) must then have, in general, distinctly narrowing limbs. These new Y-junctions are transformed in turn, producing cables that have even more pronounced narrowing. The process continues until the final fully equivalent cable is generated. An even more striking effect is seen with cut terminals, with extreme increases in diameter, as more and more Y-junctions are transformed — large diameters in equivalent cables for sub-trees promote even larger diameter in the final equivalent cable.

Eleven dendrites from an alpha motoneuron (identified as M43/5) have been discretised and transformed (thanks to Dr. R.E. Burke, NINDS, NIH, for supplying morphological data for motoneuron dendrites. See Burke *et al.* (1988) and Cullheim *et al.* (1987a, 1987b) for additional details of this cell). The equivalent cables (connected sections) are illustrated in Figure 8.5 (in physical space). In addition, the eleven trees (regarded as attached to a point-like lumped soma) are collapsed into one equivalent cable, also illustrated.

All terminals are treated as sealed, and the consequent narrowing of the cables is clear. Because of the small basic unit of electrotonic length used, the large combined cable appears as an effectively continuous structure.

8.3.5 Consequences for Parameter Estimation

Fully equivalent cable structure has several implications for parameter estimation methods that use quasi-equivalent cable models. As well as being a possible replacement for the quasi-equivalent cables, fully equivalent cables can serve as guide to interpretation of results obtained using these previous methods, i.e. to determine when it is reasonable to use quasi-equivalent cables, and to warn against their use when it is not appropriate.

Parameter estimation for real neurons is inherently prone to uncertainty, relying on several geometrical and electrical assumptions about properties of a neuron's dendritic trees and cell body. The use of fully equivalent cables instead of, say, lambda cables, may not remove much of the uncertainty in estimates obtained in this way. However, by comparing a lambda cable to the fully equivalent cable connected section for the same tree, one can observe how close a match the two are, and consider whether the differences are significant enough to cause concern.

One must also beware of interpreting data where the assumption of sealed dendritic terminals may not be valid. It is possible that experimental conditions under which transient voltage responses are recorded at the soma cause some dendritic branches to be physically cut, and a cut condition may be more realistic than a sealed condition because of significant current leakage. The assumption of empirical cable models (in particular the

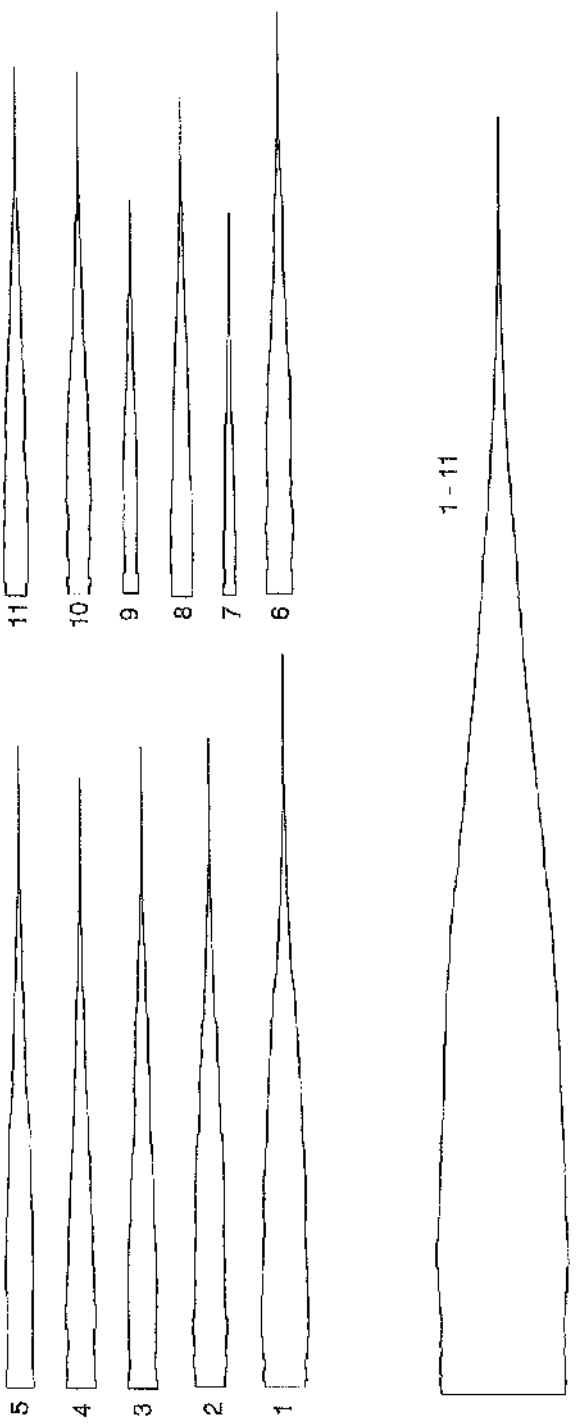


Figure 8.5: Equivalent cables generated from data for motoneuron cell M43/5. Eleven dendrites have been transformed individually, and also combined together. See text for discussion.

lambda cables) that surface area is conserved in the replacement structure, is no longer valid. It can be seen from Figures 8.2 and 8.3 that the same tree structure subject to different boundary conditions yields markedly different fully equivalent cables.

The structure of fully equivalent cables also raises questions as to what is meant by “effective electrotonic length” (Rall, 1969a; see also Holmes and Rall, 1992a,b; Holmes *et al.*, 1992) of a tree, which is often used as a measure of the electrical compactness of a tree. While this concept is certainly valid for Rall trees, for less symmetric trees it is a less well defined quantity. In Figure 8.5, the total electrotonic length of the cable is essentially the total electrotonic length of all the tree limbs, and so significantly greater than the electrotonic length of quasi-equivalent cable models. Of course, a tail portion of this is clearly very narrow. The tapering is gradual, however, and there is often no clear decision as to where the cut-off point lies. The idea of effective electrotonic length is therefore not very meaningful unless discussed in conjunction with the fully equivalent cable’s geometry — for example, one might define a measure of electrotonic length as that length from the origin at which the cable diameter has fallen to some proportion of the initial diameter.

8.3.6 Local and Global Processing

Fully equivalent cables allow one to completely classify the geometry-dependent signal processing properties of a passive dendritic tree model with arbitrary geometry.

Electrical activity over a tree is mapped into activity over cable cylinders. Each cable cylinder can be regarded as representing a characteristic configuration of activity over the tree — i.e. a configuration that acts like it is generated in just one cable cylinder of an unbranched structure. Any activity over the tree is a combination of such characteristic “modes” of electrical activity. Disconnected sections define configurations, or modes, of activity that interact entirely locally. The connected section defines configurations, or modes, of activity that have global influence on the tree. When considering real trees, narrow cylinders or extremely wide cylinders at the end of a connected section can be regarded as representing modes of activity that are negligible at the origin.

It is interesting that the electrical mapping from specific cable cylinders back to the tree usually maps a single input on the cable to many inputs on the tree. It would be even more interesting if, for certain neurons, excitatory and inhibitory synapses are arranged over dendritic sub-tree in such a way that the resulting activity decays passively in corresponding configurations (though this is possibly overoptimistic). In particular, if such an input configuration equates to activity mapped from a disconnected section, then it may be that synapses are arranged to take advantage of the local processing capabilities of geometry. Sub-sets of the local configuration may be activated simultaneously — the passive coincidence of configurations of activity discussed in Chapter 3.

8.3.7 Tree Classification

While two different dendritic trees may have entirely different local properties, it is possible that they have very similar global properties. One implication of fully equivalent cables is that observably different dendritic trees may transform to equivalent cables that will have the same, or approximately the same, connected section. Similarities in connected sections can form the basis for a classification of neuronal types (in terms of their passive properties). Electrical mappings and disconnected sections will be different, of course (unless the two trees are morphologically identical!). Recall Figure 3.15.

8.4 Concluding Remarks and Future Perspectives

While some areas still need further mathematical clarification, the foundations of equivalent cable construction have now been laid. However, the full implications of the fully equivalent cables has yet to be determined for real neurons. In the present model the membrane time constant must be uniform over the tree, a factor which prevents the current techniques being used for the construction of dynamic cables with active membrane. Synaptic inputs must be simulated by current injection (rather than conductance change), so transmembrane depolarisations and hyperpolarisations are assumed to interact linearly. Observations made using fully equivalent cables should have significance for classes of neuron where passive electrotonic structure dominates the spread of membrane potential (or where active properties have been pharmacologically blocked). Sub-threshold voltage disturbances can behave passively, and equivalent cables describe how geometry shapes this activity.

The present cables will not account for non-linear effects due to active membrane conductance changes, and so will not naturally reproduce observed phenomena such as action potentials, or other phenomena involving signal regeneration by the voltage-gated opening of ion channels.

It has often been recognised that the simpler case of passive tree geometry must be fully understood before one can even begin to understand the interaction between geometry and active membrane properties (e.g. Rapp *et al.*, 1994). At this stage, we sacrifice full realism in an attempt to get a handle on the function of complicated dendritic tree geometry. One cannot hope to understand geometry in the active model beforehand. The passive model describes a fundamental layer of geometry determined signal processing capability that is probably enhanced enormously by non-linear effects associated with voltage-dependent conductance changes.

The apparent power of equivalent cables which satisfy the demands of a rigorous mathematical definition of equivalence suggests that, if these techniques can be adapted for tree

models where the membrane is active, one may gain further insights into the role of geometry in signal processing. Though extensive work has been done to investigate the properties of passive geometry, they have almost invariably involved an analysis of solutions, rather than the describing equations themselves.

If the fully equivalent cable concept cannot be extended to active membrane, then at least it may prove useful to investigate configurations of inputs and voltage distributions mapped from connected and disconnected sections in an attempt to determine a significant role for passive coincidence detection in shaping sub-threshold activity.

Significantly, for the first time it is possible to overcome geometrical complexity to perform a thorough quantitative analysis of the role of passive geometry. Concepts such as electrical degeneracy, and layers of coincident configurations of activity associated with tree sub-structure, show that a neuron can take full advantage of the spatial structure of trees to process signals. It is highly likely that more complicated electrical degeneracies, or redundancies, exist in real neurons — an ability for the same signal processing operation to be performed by many different input configurations is possibly a highly desirable feature. These results also suggest that an understanding of singly branched dendritic trees with active membrane may transfer quite easily to highly branched structure.

Many analytical and numerical tools are available to solve cable equations. Recorded transients can be analysed in several ways, electrotonic structure of the tree can be visualised, and parameters can be estimated. Fully equivalent cables define clear properties of tree geometry in a novel and physiologically intuitive way. Together, all these tools allow a complete understanding of the properties of the passive tree model. The move to gain similar insights into the non-linear models can be made more confidently.

Bibliography

- Abbot, L.F. (1992) Simple diagrammatic rules for solving dendritic cable problems. *Physica A.*, 185:343–356.
- Abbot, L.F., Farhi, E. and Gutmann, S. (1991) The path integral for dendritic trees. *Biol. Cybern.*, 66:49–60.
- Abeles, M. (1982) Role of the cortical neuron: integrator or coincidence detector. *Israel J. Med. Sci.*, 18:83–92.
- Agmon-Snir, H. and Segev, I. (1993) Signal delay and input synchronization in passive dendritic structures. *J. Neurophysiol.*, 70:2066–85.
- Bernander, O., Douglas, R., Martin, K. and Koch, C. (1991) Synaptic background activity influences spatiotemporal integration in single pyramidal cells. *Natl. Acad. Sci. U.S.A.*, 88:11569–11573.
- Bernander, O., Koch, C. and Usher, M. (1994) The effects of synchronized inputs at the single neuron level. *Neural Comp.*, 6:622–641.
- Brown, T.H., Zador, A.M., Mainen, Z. and Claiborne, B.J. (1992) Hebbian modifications in hippocampal dendrites and spines. In T. McKenna, J. Davis, and S.F. Zornetzer, editors, *Single Neuron Computation*, pages 88–116. Academic Press, Boston.
- Burke, R.E. (1997) Equivalent cable representations of dendritic trees: Variations on a theme. *Soc. Neurosci. Abstr.*, 23:654.
- Burke, R.E., Fleshman, J.W. and Segev, I. (1988) Factors that control efficacy of group Ia synapses in alpha-motoneurons. *J. Physiol., Paris*, 83:133–140.
- Burke, R.E., Fyffe, R.E.W. and Moschovakis, A.K. (1994) Electrotomographic architecture of cat gamma motoneurons. *J. Neurophysiol.*, 72(5):2302–2316.
- Butz, E.G. and Cowan, J.D. (1974) Transient potentials in dendritic systems of arbitrary geometry. *Biophys. J.*, 14:661–689.

- Canuto, C., Hussaini, M.Y., Quarteroni, A. and Zang, T.A. (1990) *Spectral Methods in Fluid Dynamics*. Springer-Verlag, Berlin.
- Cao, B.J. and Abbot, L.F. (1993) A new computational theory for cable theory problems. *Biophys. J.*, 64:303–313.
- Clements, J.D. and Redman, S.J. (1989) Cable properties of cat spinal motoneurones measured by combining voltage clamp, current clamp and intra-cellular staining. *J. Physiol., Lond.*, 409:63–87.
- Cullheim, S., Fleshman, J.W., Glenn, L.L. and Burke, R.E. (1987a) Membrane area and dendritic structure in type-identified triceps surae alpha motoneurons. *J. Comp. Neurol.*, 255:68–81.
- Cullheim, S., Fleshman, J.W., Glenn, L.L. and Burke, R.E. (1987b) Three-dimensional architecture of dendritic trees in type-identified alpha-motoneurons. *J. Comp. Neurol.*, 255:82–96.
- DeSchutter, E. (1992) A consumer guide to neuronal modeling software. *TINS*, 15(11):462–464.
- Edwards, D.H. and Mulloney, B. (1984) Compartmental models of electrotonic structure and synaptic integration in an identified neurone. *J. Physiol.*, 348:89–113.
- Eisenberg, R.S. and Johnson, E.A. (1970) Three dimensional electric field problems in physiology. *Prog. Biophys. Mol. Biol.*, 20:1–65.
- Evans, J.D. and Kember, G.C. (1998) Analytical solutions to a tapering multi-cylinder somatic shunt cable model for passive neurons. *Mathematical Biosci.*, 149(2):137–165.
- Evans, J.D., Kember, G.C. and Major, G. (1992) Techniques for obtaining analytical solutions to the multicylinder somatic shunt cable model for passive neurons. *Biophys. J.*, 63:350–365.
- Evans, J.D., Major, G., and Kember, G.C. (1995) Techniques for the application of the analytical solution to the multicylinder somatic shunt cable model for passive neurons. *Mathematical Biosci.*, 125(1):1–50.
- Fleshman, J.W., Segev, I. and Burke, R.E. (1988) Electrotonic architecture of type-identified α -motoneurons in the cat spinal cord. *J. of Neurophysiology*, 60(1):60–85.
- Goldman, D.E. (1943) Potential, impedance and rectification in membranes. *J. Gen. Physiol.*, 27:37–60.

- Goldstein, S.S. and Rall, W. (1974) Changes in action potential shape and velocity for changing core conductor geometry. *Biophys. J.*, 14:731-757.
- Golub, G.H. and Van Loan, C.F. (1990) *Matrix Computations*, second edition. John Hopkins University Press, Baltimore, Maryland.
- Halliday, D.M. (1995) Effects of electrotonic spread of epsps on synaptic transmission in motoneurones: A simulation study. In A. Taylor, M.H. Gladden, and R. Durbaba, editors, *Alpha and Gamma motor systems*, pages 337-339. Plenum Press.
- Hamill, O.P., Marty, A., Neher, E., Sakmann, B. and Sigworth, F.J. (1981) Improved patch-clamp techniques for high-resolution current recording from cells and cell-free membrane patches. *Pflügers Arch.*, 391:85-100.
- Hille, B. (1984) *Ionic channels of excitable membranes*. Sinauer, Sunderland, Massachusetts.
- Hines, M. (1984) Efficient computation of branched nerve equations. *Int. J. Bio-Med. Comp.*, 15:69-76.
- Hodgkin, A.L. and Huxley, A.F. (1952) A quantitative description of membrane current and its application to conduction and excitation in nerve. *J. Physiol.*, 117:500-544.
- Holmes, W.R. (1986) A continuous cable method for determining the transient potential in passive trees of known geometry. *J. Neurophysiol.*, 55:115-124.
- Holmes, W.R. and Rall, W. (1992a) Electrotonic length estimates in neurons with dendritic tapering or somatic shunt. *J. Neurophysiol.*, 68:1421-1437.
- Holmes, W.R. and Rall, W. (1992b) Estimating the electrotonic structure of neurons with compartmental models. *J. Neurophysiol.*, 68:1438-1452.
- Holmes, W.R., Segev, I. and Rall, W. (1992) Interpretation of time constant and electrotonic length estimates in multicylinder or branched neuronal structures. *J. Neurophysiol.*, 68:1401-1420.
- Holmes, W.R. and Woody, C.D. (1989) Effects of uniform and non-uniform synaptic 'activation distributions' on the cable properties of modeled cortical pyramidal neurons. *Brain Research*, 505:12-22.
- Horwitz, B. (1981) An analytical method for investigating transient potentials in neurons with branching dendritic trees. *Biophys. J.*, 36:155-192.

- Horwitz, B. (1983) Unequal diameters and their effects on time-varying voltages in branched neurons. *Biophys. J.*, 41:51–66.
- Iansek, R. and Redman, S.J. (1973) An analysis of the cable properties of spinal motoneurons using a brief intracellular current pulse. *J. Physiol.*, 234:613–636.
- Jack, J.J.B., Noble, D. and Tsien, R.W. (1983) *Electric Current flow in excitable cells*. Oxford University Press, second edition.
- Jack, J.J.B. and Redman, S.J. (1971a) The propagation of transient potentials in some linear cable structures. *J. Physiol.*, 215:283–320.
- Jack, J.J.B. and Redman, S.J. (1971b) An electrical description of the moroneurone and its application to the analysis of synaptic potentials. *J. Physiol.*, 215:321–352.
- Jackson, M.B. (1992) Cable analysis with the whole-cell patch clamp — theory and experiment. *Biophys. J.*, 61:756–766.
- Kandel, E.R., Schwartz, J.H. and Jessel, T.M. (1991) *Principles of Neural Science*. Appleton and Lange, East Norwalk, Connecticut, third edition.
- Kawato, M. and Tsukahara, N. (1983) Theoretical studies on electrical properties of dendritic spines. *J. Theoret. Biol.*, 103:507–22.
- Kelvin, W.T. (1855) On the theory of the electric telegraph. *Proc. Roy. Soc.*, 7:382–399.
- Kember, G.C. and Evans, J.D. (1995) Analytical solutions to a multicylinder somatic shunt cable model for passive neurons with spines. *IMA J. Math. Applied in Medicine and Biology*, 12(2):137–157.
- Koch, C. (1997) Computation and the single neuron. *Nature*, 385:207–210.
- Koch, C., Poggio, T. and Torre, V. (1982) Retinal ganglion cells: a functional interpretation of dendritic morphology. *Phil. Trans. R. Soc. Lond.*, B298:227–264.
- Koch, C. and Segev, I. editors. (1989) *Methods in Neuronal Modeling: From Synapses to Networks*. MIT Press, Cambridge, Massachusetts.
- Lanczos, C. (1950) An iteration method for the solution of the problem of linear differential and integral operators. *J. Res. Natn. Bur. Stand.*, 45:255–282.
- Lindsay, K.A., Ogden, J.M., Halliday, D.M. and Rosenberg, J.R. (in press) An introduction to the principles of neuronal modeling. In *Modern Techniques in Neuroscience Research*, U. Windhorst and H. Johannson, editors. Springer-Verlag, Berlin.

- Major, G. (1993) Solutions for transients in arbitrarily branching cables: III. Voltage clamp problems. *Biophys. J.*, 65:469–491.
- Major, G., Evans, D. and Jack, J.J.B. (1993a) Solutions for transients in arbitrarily branching cables: I. Voltage recording with a somatic shunt. *Biophys. J.*, 65:423–449.
- Major, G., Evans, D. and Jack, J.J.B. (1993b) Solutions for transients in arbitrarily branching cables: II. Voltage clamp theory. *Biophys. J.*, 65:450–468.
- Major, G. and Evans, J.D. (1994) Solutions for transients in arbitrarily branching cables: IV. Non-uniform electrical parameters. *Biophys. J.*, 66:615–634.
- Manor, Y., Gonczarowski, J. and Segev, I. (1991) Propagation of action potentials along complex axonal trees: model and implementation. *Biophys. J.*, 60:1411–1423.
- Mascagni, M.V. (1989) Numerical Methods for Neuronal Modeling. In C. Koch and I. Segev, editors, *Methods in Neuronal Modeling*, pages 255–282. MIT Press, Cambridge, Massachusetts.
- McCormick, D.A. (1990) Membrane properties and neurotransmitter actions. In G.M. Shepherd, editor, *The Synaptic Organisation of the Brain*, pages 32–66. Oxford University Press, Oxford.
- McKenna, T., Davis, J. and Zornetzer, S.F. editors. (1992) *Single Neuron Computation*. Academic Press, Boston.
- Mel, B.W. (1994) Information processing in dendritic trees. *Neural Computation*, 6:1031–1085.
- Ogden, J.M., Lindsay, K.A. and Rosenberg, J.R. (1997) Construction of complete equivalent cables for passive dendritic trees of arbitrary geometry and their application to the analysis of voltage transients. *J. Physiol.*, 501:32P.
- Ogden, J.M., Rosenberg, J.R. and Whitehead, R.R. (1999) The Lanczos procedure for generating equivalent cables. In R.R. Poznanski, editor, *Modeling in the Neurosciences: From Ion channels to Neural Networks*, Harwood Academic.
- Ohme, M. and Schierwagen, A. (1998) An equivalent cable model for neuronal trees with active membrane. *Biol. Cybern.*, 78(3):227–243.
- Paige, C.C. (1972) Computational variants of the Lanczos method for the eigenproblem. *J. Inst. Maths Applies.*, 10:373–381.

- Paige, C.C. (1976) Error analysis of the Lanczos algorithm for tri-diagonalising a symmetric matrix. *J. Inst. Maths Applies.*, 18:341–349.
- Paige, C.C. (1980) Accuracy and effectiveness of the Lanczos algorithm for the symmetric eigenproblem. *Linear Algebra and Appl.*, 34:235–258.
- Perkel, D.H. and Mulloney, B. (1978a) Calibrating compartmental models of neurons. *Am. J. Physiol.*, 235:R93–R98.
- Perkel, D.H. and Mulloney, B. (1978b) Electrotropic properties of neurons: steady-state compartmental model. *J. Neurophysiol.*, 41:621–639.
- Poznanski, R.R. (1988) Membrane voltage changes in passive dendritic trees — a tapering equivalent cylinder model. *IMA J. Math. appl. Med. and Biol.*, 5(2):113–145.
- Poznanski, R.R. (1991) A generalized tapering equivalent cable model for dendritic neurons. *Bull. Math. Biol.*, 53:457–467.
- Poznanski, R.R. (1994) Electrotropic length estimates of CA3 hippocampal pyramidal neurons. *Neurosci. res. comm.*, 14(2):93–100.
- Poznanski, R.R., editor. (1999) *Modeling in the neurosciences: from ionic channels to neural networks*. Harwood Academic, Amsterdam.
- Poznanski, R.R. and Glenn, L.L. (1994) Estimating the effective electrotropic length of dendritic neurons with reduced equivalent cable models. *Neurosci. res. comm.*, 15(1):69–76.
- Rall, W. (1959) Branching dendritic trees and motoneuron membrane resistivity. *Exp. Neurol.*, 1:491–527.
- Rall, W. (1960) Membrane potential transients and membrane time constant of motoneurons. *Exp. Neurol.*, 2:503–532.
- Rall, W. (1962a) Theory of physiological properties of dendrites. *Ann. NY Acad. Sci.*, 96:1071–1092.
- Rall, W. (1962b) Electrophysiology of a dendritic neuron model. *Biophys. J.*, 2(2):145–167.
- Rall, W. (1964) Theoretical significance of dendritic trees for neuronal input-output relations. In R. Reiss, editor, *Neural theory and modeling*, pages 73–97. Stanford University Press, Stanford, California.

- Rall, W. (1969a) Time constants and electrotonic length of cylinders and neurons. *Biophys. J.*, 9:1483–1508.
- Rall, W. (1969b) Distributions of potential in cylindrical coordinates for a membrane cylinder. *Biophys. J.*, 9:1509–1541.
- Rall, W. (1977) Core conductor theory and cable properties of neurones. In E.R. Kandel, J.M. Brookhardt, and V.B. Mountcastle, editors, *Handbook of Physiology : the Nervous System*, volume one, pages 39–98. Williams and Wilkinson, Baltimore, Maryland.
- Rall, W., Burke, R.E., Holmes, W.R., Jack, J.J.B., Redman, S.J. and Segev, I. (1992) Matching dendritic neuron models to experimental data. *Physiol. Rev.*, 72(4):S159–S186.
- Rall, W. and Rinzel, J. (1973) Branch input resistance and steady attenuation for input to one branch of a dendritic neuron model. *Biophys. J.*, 13:648–688.
- Rall, W. and Segev, I. (1990) Dendritic branches, spines, and excitable spine clusters. In E.L. Schwartz, editor, *Computational Neuroscience*, pages 69–81. MIT Press, Cambridge, Massachusetts.
- Ramon y Cajal, S. (1911) *Histologie du Système Nerveux de l'Homme et des Vertébrés*. Maloine, Paris.
- Rapp, M., Segev, I. and Yarom, Y. (1994) Physiology, morphology, and detailed passive models of guinea-pig cerebellar purkinje cells. *J. Physiol.*, 474(1):101–118.
- Rapp, M., Yarom, Y. and Segov, I. (1992) The impact of parallel fiber background activity on the cable properties of cerebellar purkinje cells. *Neural Comp.*, 4:518–533.
- Rinzel, J. and Rall, W. (1974) Transient response in a dendritic neuron model for current injected at one branch. *Biophys. J.*, 14:759–790.
- Rugg, M.D. editor. *Cognitive Neuroscience*. Psychology Press, Hove.
- Sakmann, B. and Neher, E. (1983) *Single Channel Recording*. Plenum Press, New York.
- Schwartz, E.L., editor. (1990) *Computational Neuroscience*. MIT Press, Cambridge, Massachusetts.
- Segev, I., Fleshman, J.W. and Burke, R.E. (1989) Compartmental models of complex neurons. In C. Koch and I. Segev, editors, *Methods in Neuronal Modelling*, pages 63–96. MIT Press, Cambridge, Massachusetts.
- Segev, I. and Rall, W. (1998) Excitable dendrites and spines: earlier theoretical insights elucidate recent direct observations. *Trends in Neuroscience*, 21(11):453–460.

- Segev, I., Rinzel, J. and Shepherd, G.M., editors. (1995) *The theoretical foundation of dendritic function — Selected papers of Wilfred Rall with Commentaries*. The MIT press, Cambridge, Massachusetts.
- Sejnowski, T.J. (1997) The year of the dendrite. *Science*, 275:178–179.
- Shepherd, G.M., editor. (1990) *The synaptic organisation of the brain*. Oxford University Press, Oxford.
- Softky, W.R. (1993) Submillisecond coincidence detection in active dendritic trees. *Neuroscience*, 58:13–41.
- Softky, W.R. and Koch, C. (1994) The highly irregular firing of cortical cells is inconsistent with temporal integration of random epsps. *J. Neurosci.*, 13:334–350.
- Stratford, K., Mason, A., Larkman, A., Major, G. and Jack, J.J.B. (1989) The modeling of pyramidal neurones in the visual cortex. In R. Durbin, C. Miall, and G. Mitchison, editors, *The computing neuron*, pages 296–321. Addison-Wesley, Reading, Massachusetts.
- Toth, T.I. and Crunelli, V. (1998) Effects of tapering geometry and inhomogeneous ion channel distribution in a neuron model. *Neuroscience*, 84(4):1223–1232.
- Tuckwell, H.C. (1988a) *Introduction to Theoretical Neurobiology Volume 1 — Linear cable theory and dendritic structure*. Cambridge University Press, Cambridge.
- Tuckwell, H.C. (1988b) *Introduction to Theoretical Neurobiology Volume 2 — Nonlinear and stochastic theories*. Cambridge University Press, Cambridge.
- Ulrich, D., Quadroni, R. and Lüscher, H.R. (1994) Electrot tonic structure of motoneurons in spinal-cord slice cultures — a comparison of compartmental and equivalent cylinder models. *J. Neurophysiol.*, 72(2):861–871.
- Walsh, J.B. and Tuckwell, H.C. (1985) Determination of the electrical potential over dendritic trees by mapping onto a nerve cylinder. *J. Theor. Neurobiol.*, 4:27–46.
- Whithead, R.R. and Rosenberg, J.R. (1993) On trees as equivalent cables. *Proc. R. Soc. Lond. B.*, 252:103–108.
- Whitehead, R.R., Watt, A., Cole, B.J. and Morrison, I. (1977) Computational methods for shell model calculations. *Adv. Nucl. Phys.*, 9:123–176.
- Woolf, T.B., Shepherd, G.M. and Greer, C.A. (1991) Local information processing in dendritic trees: Subsets of spines in granule cells of the mammalian olfactory bulb. *J. Neurosci.*, 11(6):1837–1854.